SCIENCE
Serial Dept.
MAR 1 3 1961

AEROSPACE ENGINEERING

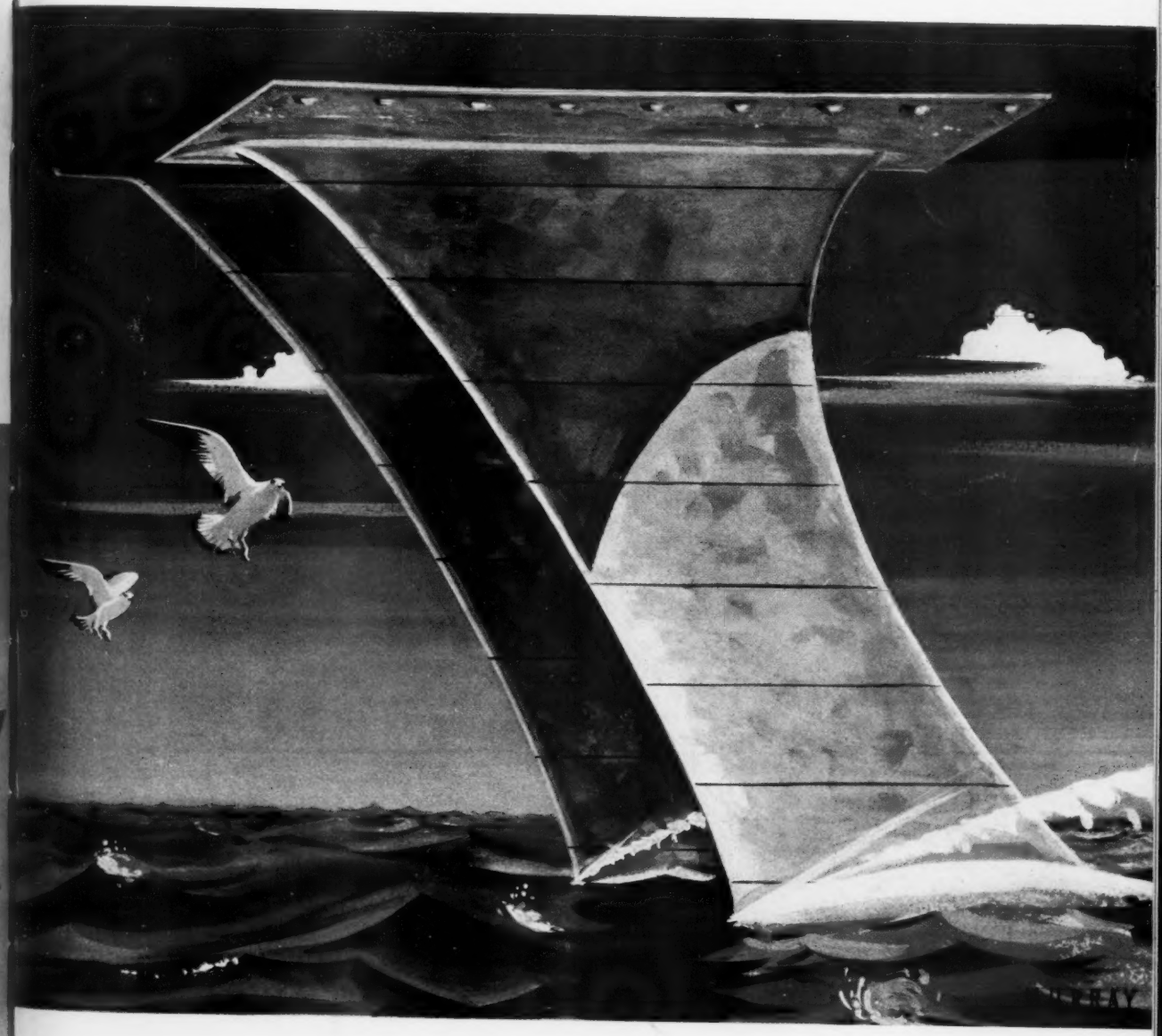

MARCH / 1961

The first six years of **S**pace **T**echnology **L**eadership

Since 1954, when the Air Force ballistic missile program was accorded top national priority, Space Technology Laboratories has been engaged in virtually every major phase of research, development, testing and technical management of missile and space systems • STL's contributions have hastened the day of operational capability for Air Force ballistic missiles, and have been applied as well in satellite projects and space probes • Today, as STL's activities expand in significance and scope, STL offers exceptional opportunity to the outstanding scientist and engineer whose talents and training will add to, and benefit from, the accumulated experience that has enabled STL to conceive and accomplish major advances in the state-of-the-art • STL's creative flexibility, anticipating and responding to the demands of space progress, ranges in application from abstract analysis to complex hardware fabrication for military and civilian space projects • STL invites scientists and engineers to consider career opportunities in the atmosphere of Space Technology Leadership. Resume and inquiries will receive meticulous attention.

SPACE TECHNOLOGY LABORATORIES, INC. P.O. BOX 95005E, LOS ANGELES 45, CALIFORNIA

a subsidiary of Thompson Ramo Wooldridge Inc.

Los Angeles • Santa Maria • Edwards Rocket Base • Canoga Park

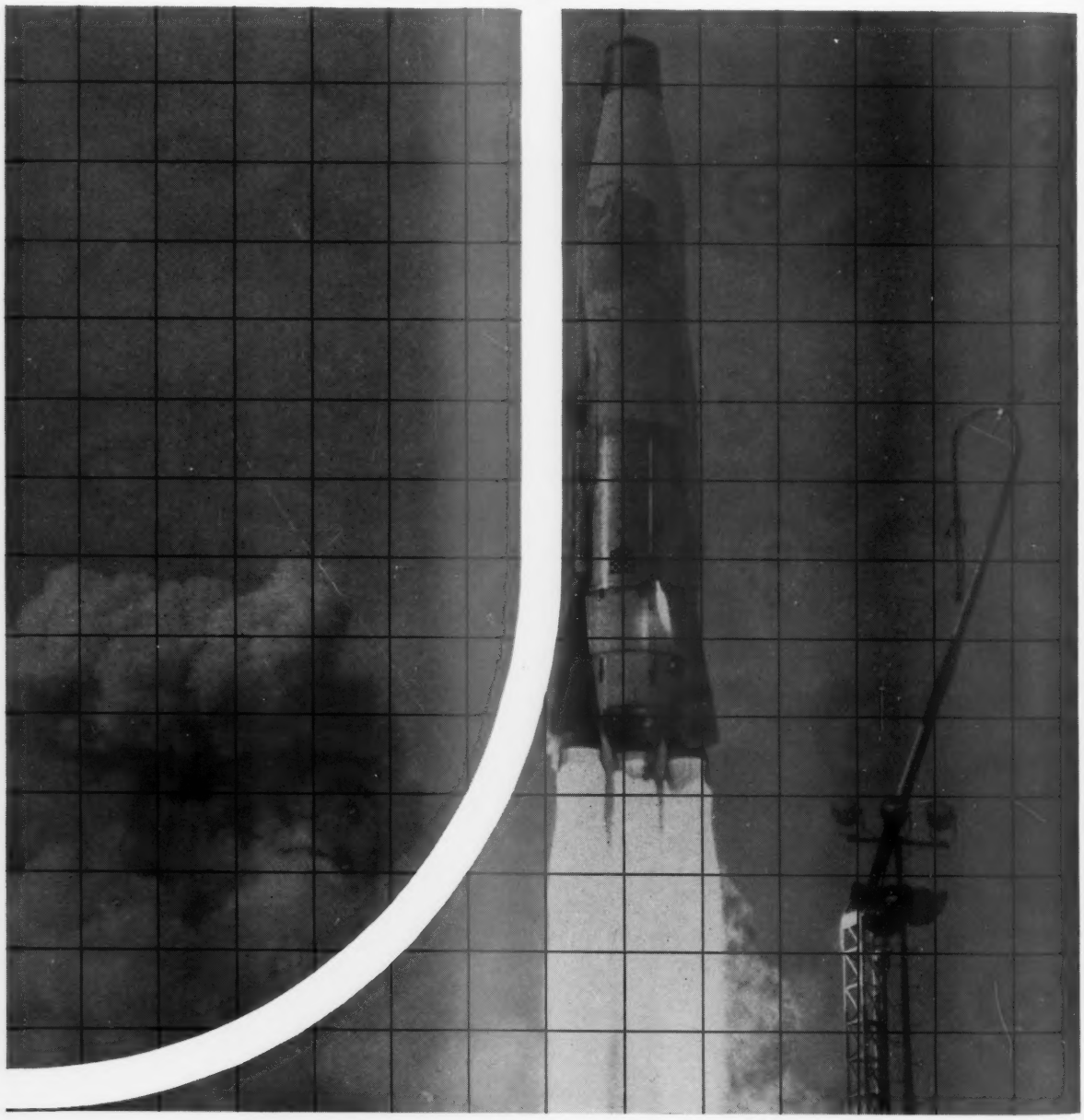

Cape Canaveral • Manchester, England • Singapore • Hawaii

Those attending the International Convention of the IRE are invited to visit STL at Booth Number 1435.

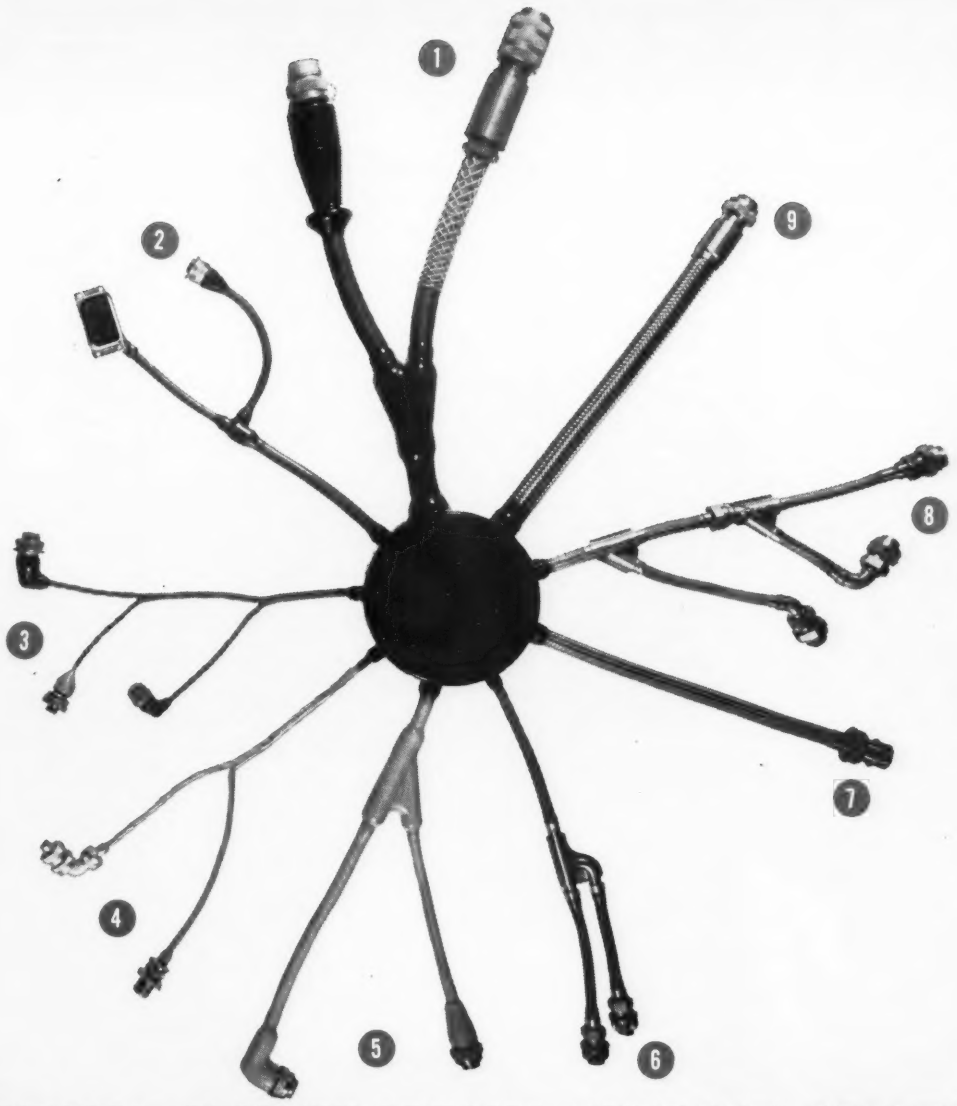

TYPICAL BENDIX® SPECIAL-PURPOSE CABLES THAT SOLVE CRITICAL ENVIRONMENTAL PROBLEMS

1 Heavy Duty—Ground Support Cable
2 Benseal® Missile Control Cable
3 Fabric Braided—Aircraft and Missile Control Cable
4 Metal Braid—Aircraft Nacelle Cable
5 High Temperature—Radiation Resistant Cable
6 High Temperature—Lightweight—Missile Cable
7 "Wet Wing" Aircraft Fuel Cell Cable
8 Rewirable—Jet Engine Control Cable
9 High Temperature—1500°F.—Thermocouple Cable

Bendix cables—products of over a quarter-century of design and manufacturing experience—are proving their complete reliability in a countless variety of applications involving critical environmental conditions.

BENDIX CABLES • BENDIX CONNECTORS

Designed together to work best together

For complete information, write:

Scintilla Division
SIDNEY, NEW YORK

THE Bendix CORPORATION

PIONEERING IN SPACE RESEARCH

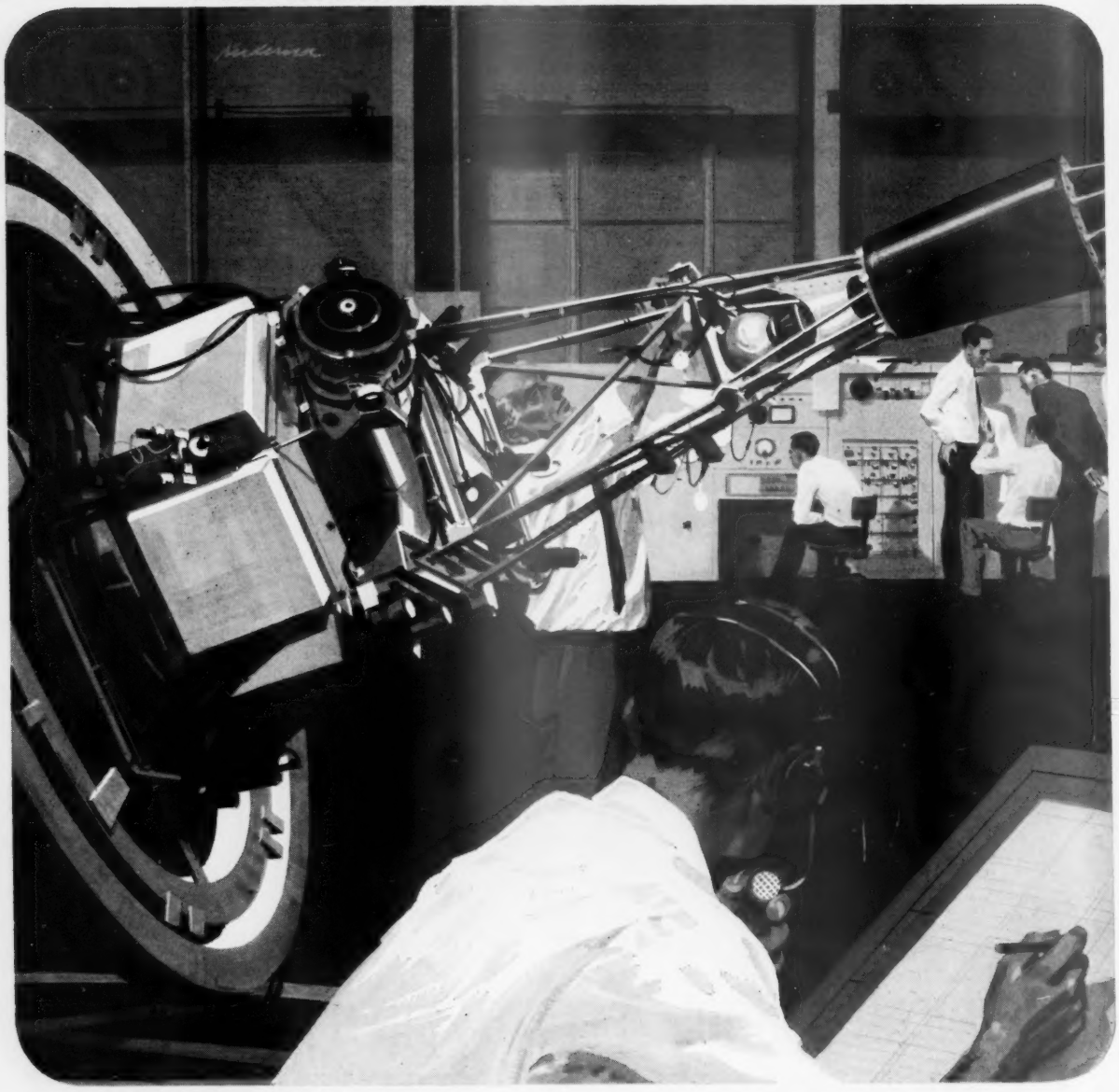

DEVELOPMENT OF LUNAR SPACECRAFT

The "Ranger" series of spacecraft, designed first to explore the environment and later to land instrument capsules on the Moon, are now being developed and tested at Jet Propulsion Laboratory.

Illustrated is a "Ranger" proof-test model undergoing design verification testing at the Laboratory. Here design features are tested and proved, operational procedures developed and handling experience gained for the actual construction of the initial flight spacecraft.

This is one phase of JPL's current assignment from the National Aeronautics and Space Administration—to be responsible for the Nation's unmanned lunar, planetary and interplanetary exploration.

An advanced program such as this provides numerous objectives and incentives for qualified engineers and scientists who are eager to help solve the complex problems of deep space exploration.

Such men are welcome at JPL.

jpl

JET PROPULSION LABORATORY

Operated by the California Institute of Technology under contract with the National Aeronautics and Space Administration

PASADENA, CALIFORNIA

Employment opportunities for Engineers and Scientists interested in basic and applied research in these fields:

COMMUNICATIONS • INSTRUMENTATION • INFRARED • ASTROPHYSICS • GEOPHYSICS • GEOCHEMISTRY • ASTRONOMY • PROPULSION • MASER • STRUCTURES • PHYSICS •

Send professional resume, with full qualifications and experience, for our immediate consideration

AEROSPACE ENGINEERING

"Written Exclusively By Engineers—For Engineers"

Established 1934

VOLUME 20 / NUMBER 3 **March 1961**

Featured in this issue

Guest Editorial	9	The IAS Looks Ahead
J. J. Stilwell, P. W. Nelson, and W. R. Porter	10	Hydrofoils at the Crossroads
Norman R. Garner, D. E. Hartvigsen, and Richard W. Vail, Jr.	12	Experimental Designs for Rocket Motors
Mell D. Cassidy and Phillip J. Sullivan	14	Supersonic Ejectable-Nose Escape Capsule
Eric E. Ungar	16	Response of Plates to Moving Shocks
Henry E. Payne III, Frank R. Carter, and Wayne J. Harrison	18	The Navy's Flying Wind Tunnel
M. C. Kurbjun, R. F. Brissenden, E. C. Foudriat, and B. B. Burton	20	Pilot Control of Rendezvous
F. W. Reichelderfer	22	Meteorological Satellite Systems in Weather Research and Services
Lewis A. Rodert	24	Whither Aerospace Industry Research Management?
Ivan Rattinger and Joseph Padlog	26	Design Implications of Creep in Pressurized Cylindrical Shells
B. H. Goethert	28	Base Flow Characteristics of Missiles With Cluster-Rocket Exhausts
V. R. Boulton	30	Economics of Instrumentation Precision for Space Vehicle Development
Departments	118	IAS Papers
	119	Personnel Opportunities
	120	Index to Advertisers

On our cover

As put by a triumvirate of authors writing exclusively in this issue, "Hydrofoil development requires contributions from the aircraft and shipbuilding industries, the aeronautical engineer, and the naval architect. Future development rests on continued successful welding of the two arts and sciences" into a "hydronautic" discipline. Such a welding is interpreted on our cover, and taken up in "Hydrofoils at the Crossroads," beginning on page 10. The article, first comprehensive work of its kind in almost a decade, includes a full description of the first operational military hydrofoil craft designed and being built for the Navy by Boeing Airplane Co. Authors are Capt. James J. Stilwell and Lt. Comdrs. Perry W. Nelson and William R. Porter of the Navy's Bureau of Ships. Discussions have been invited by the authors and publication plans initiated by Aerospace Engineering.

AEROSPACE ENGINEERING

PUBLICATION STAFF

Publisher: Welman A. Shrader

Editor: Allan Bernhardt

Managing Editor: Rita J. Turino

Editorial Assistants: Helen S. Goldman
Carol A. Schau
Vehig S. Tavitian

Technical Advisers:
Paul J. Burr, Robert R. Dexter,
S. Paul Johnston, W. R. Sears

Business Staff:

Advertising Director: John R. Cockerell

Business Mgr. & Adv. Production:
John Phillips

National Advertising Representatives:
John Cockerell, Inc., Chicago, Ill.

Regional Advertising Offices:

New York 17
380 Lexington Ave.
OXford 7-9048

Miami 32
141 N.E. Third
FRanklin 1-9941

Cleveland 15
1501 Euclid Ave.
TOwer 1-8338

Chicago 1
360 N. Michigan Ave.
ANdover 3-6929

St. Louis 1
915 Olive Street
GArfield 1-0907

Los Angeles 5
3757 Wilshire Blvd.
DUnkirk 3-1135

IAS AEROSPACE TECHNOLOGY PANELS

Paul J. Burr, Technical Services Director, Coordinator

The members of the IAS Aerospace Technology Panels shown here are to be available, collectively or as individuals, to assist and advise IAS committees, Sections, and staff members as to currently interesting and important technical topics related to their specialties and as to people most qualified to speak or write on such topics. The panels will also stimulate thought and scientific papers of potential value for the future, and they should be sensitive to technical activity of other professional groups, seeking through joint action the enlightenment of all having professional aerospace interests. Panel chairmen are indicated with an asterisk (*).

Aerodynamics and Fluid Mechanics

Lester Lees*
Dean R. Chapman
Antonio Ferri
Paul Germain
Wayland C. Griffith
Hans W. Liepmann
C. C. Lin
W. R. Sears
John R. Sellars
R. T. Whitcomb
Hideo Yoshihara

Aeroelasticity

R. L. Bisplinghoff*
Y. C. Fung
I. E. Garrick
Martin Goland
Kurt H. Hohenemser
J. C. Houbolt
W. P. Jones
W. J. Mykytow
Robert F. Speaker

Biomedical Sciences

Brig. Gen. Don Flickinger, USAF*
W. Ross Adey
Capt. William Augerson, USA
Stuart Bondurant
A. Scott Crossfield
Cdr. J. H. Ebersole, USN
W. R. Lovelace, II
Capt. Bruce Pinc, USAF
Stanley C. Roscoe
Foreign Correspondent,
Hilding Bjurstedt

Communication

P. C. Sandretto*
James M. Bridges
Leonard Jaffe
David S. Little
Cdr. D. O. Mann, USN
William Sen
Arnold Shostack
Teck A. Wilson

Control, Guidance, & Navigation

C. S. Draper*
R. C. Berendsen
B. Paul Blasingame
Robert N. Brown
S. F. Eyestone
Percy Halpert
B. J. O'Connor
Robert L. Roderick
S. F. Schmidt
O. Hugo Schuck
H. Philip Whitaker

Energy Conversion

David Altman*
Robert Bromberg
M. U. Clauser
J. Preston Layton
Frank Marble
G. H. Markstein
A. M. Rothrock
Milton M. Slawsky
Martin Summerfield
T. Y. Toong

Flight Mechanics

H. J. Kelley*
Malcom J. Abzug
H. Julian Allen
A. E. Bryson, Jr.
T. N. Edelbaum
William C. House
Angelo Miele
John D. Nicolaides
Charles B. Westbrook

Instrumentation

R. H. Tripp*
Paul F. Bechberger
J. M. Hungerford
Mac Lowy
Walter McKay
M. David Prince
Charles P. Sonett
George I. Toumanoff
William A. Wildhack

Meteorology

Thomas F. Malone*
Robert D. Fletcher
Henry T. Harrison
Joseph Kaplan
Donald T. Perkins
Herbert Riehl
Morris Tepper
Harry Wexler

Nuclear Applications

J. Donald Rauth*
Jack L. Armstrong
Robert W. Bussard
H. M. Dieckamp
Capt. R. L. Duncan, USN
Harold B. Finger
Donald J. Keirn
Frank E. Rom
Raymer E. Schreiber
D. Ray Shoults
T. B. Taylor

Operations

Benjamin S. Kelsey*
Maj. Gen. Otis Benson, USAF (MC)
Ernest A. Cutrell
Capt. E. E. Fawkes, USN
Melvin N. Gough
Franklin W. Kolk
Col. J. L. Marinelli, USA
Richard V. Rhode
W. E. Rhodes
M. B. Spaulding, Jr.
Maj. Gen. D. N. Yates, USAF

Propulsion Systems

Bruce T. Lundin*
Robert H. Boden
George W. Brady
David Cochran
Elliot Mitchell
Perry W. Pratt
C. C. Ross
John G. Wilder, Jr.
Maurice J. Zucrow

Space Physics

H. G. Stever*
John C. Evvard
Herbert Friedmann
Leo Goldberg
C. F. Hansen
Arthur Kantrowitz
Bruno Rossi
S. F. Singer
Leo Steg
Fred L. Whipple

Structures and Materials

Nicholas J. Hoff*
Samuel B. Batdorf
Bruno A. Boley
Pol Duwez
R. R. Heldenfels
Samuel Levy
George N. Mangurian
S. S. Manson
Nathan E. Promisel
Ernest E. Sechler

Support

Ernest G. Stout*
Albert D. Brown
Edward I. Brown
Col. Paul T. Cooper, USAF
Cdr. P. J. Daniel, USN
Paul Hartline
Donald R. Hill
Capt. H. D. Hodson, USN
Lt. Col. George L. Lovett
R. R. Malik
John McKenna
Gilbert Rolan
Richard A. Schmidt
William R. Owens

Vehicle Design

C. E. Pappas*
Ralph Alex
Adolph Burstein
C. H. Christenson
A. J. Eggers, Jr.
E. V. Marshall
Rene H. Miller
John R. Ragazzini
George S. Schairer
George S. Trimble, Jr.

AEROSPACE ENGINEERING

...is published monthly by the Institute of the Aerospace Sciences, Inc., at 20th and Northampton Streets, Easton, Pa. Headquarters and Editorial Offices: 2 East 64th Street, New York 21, N.Y. (TEmpleton 8-3800). Western Office: 7660 Beverly Blvd., Los Angeles 36, Calif.

Subscription rates: United States and possessions, 1 year, $5.00; single copies, $0.50. Foreign countries including Canada (American currency rates), 1 year, $6.00; single copies, $0.50.

Second-class mail privileges authorized at Easton, Pa. This publication is authorized to be mailed at the special rates of postage prescribed by Section 132.122.

Notices of change of address should be sent to the Circulation Department, Institute of the Aerospace Sciences, Inc., 2 East 64th Street, New York 21, N.Y., at least 30 days prior to actual change of address.

© Copyright, 1961, by the Institute of the Aerospace Sciences, Inc.

Statements and opinions expressed in *Aerospace Engineering* are to be understood as individual expressions and not those of the Institute.

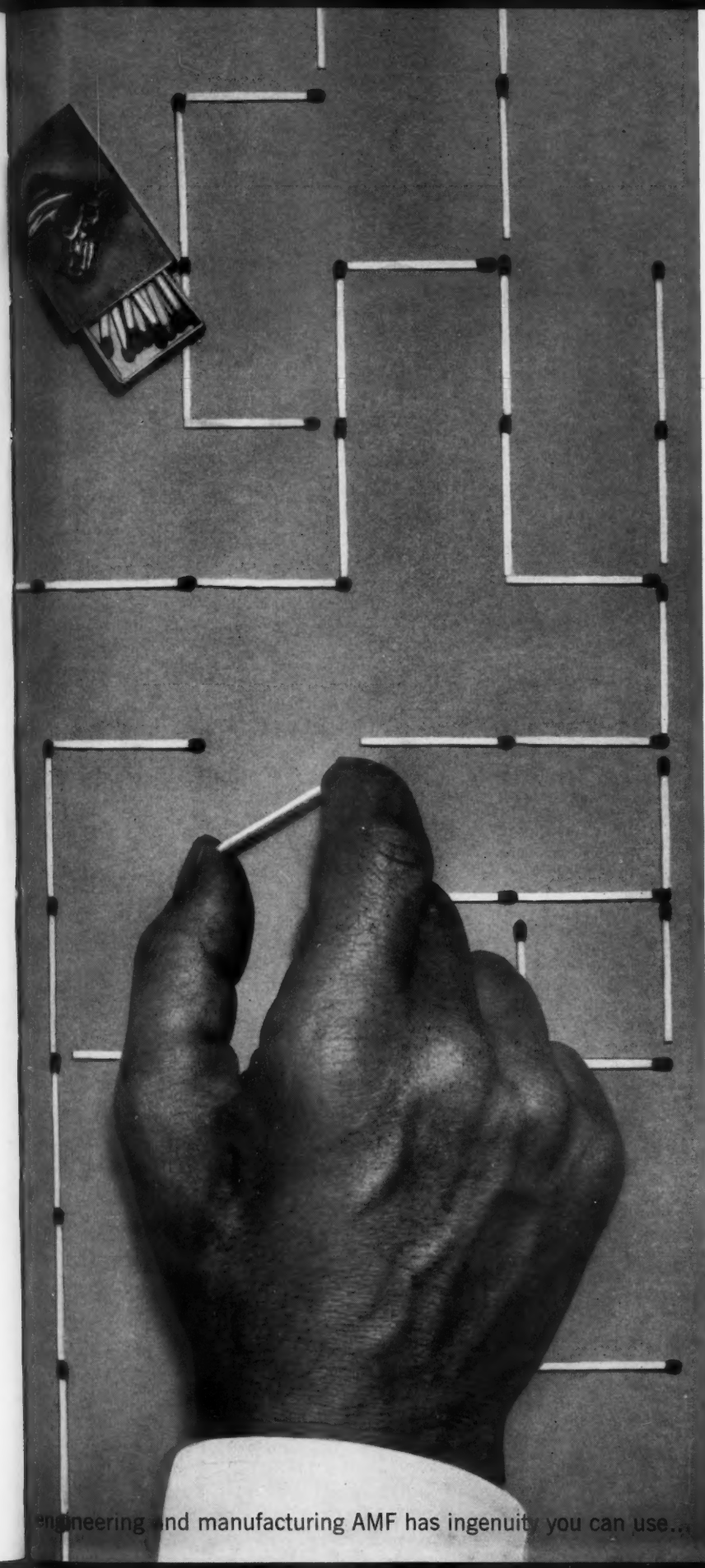

He designed a new interchange for radio traffic

This AMF engineer, part of an AMF-U.S. Army team, solved the problem of traffic delays and personal danger in manual re-connection of jumpers when interchanging R.F. transmitters and antennas.

His solution is a push-button-operated, coaxial crossbar switching system, using vacuum switches for circuit selection. A typical system consists of 4 transmitter inputs, 7 antenna outputs plus a dummy load, in a 4 x 8 matrix that can be mounted in a 19″ rack. It can be controlled locally or remotely over any type of communication network having a bandwidth of at least 200 cycles.

AMF's coaxial crossbar switching system provides 100% flexibility in circuit path selection and accommodates power levels as high as 500,000 watts and frequencies up to 30 megacycles. It allows 100% utilization of all transmitting equipment. Stubs are automatically eliminated.

To insure fail-safe operation, power is required for the vacuum switches *only* during change of condition. Selection rate: 1 per second. Operating transmitters are safety-interlocked to insure a load. There are no hazards from open wires or inadvertent application of power to dead-lined antennas.

Single Command Concept

AMF's imagination and skills are organized in a *single operational unit* offering a wide range of engineering and production capabilities. Its purpose: to accept assignments at any stage from concept through development, production, and service training...and to complete them faster...in

- *Ground Support Equipment*
- *Weapon Systems*
- *Undersea Warfare*
- *Radar*
- *Automatic Handling & Processing*
- *Range Instrumentation*
- *Space Environment Equipment*
- *Nuclear Research & Development*

GOVERNMENT PRODUCTS GROUP,
AMF Building, 261 Madison Avenue,
New York 16, N. Y.

AMF

AMERICAN MACHINE & FOUNDRY COMPANY

engineering and manufacturing AMF has ingenuity you can use...

LUNAR PROBE

The moon — lacking an erosive atmosphere — may hold the key to the history of the solar system. Because of this lack of atmosphere, oceans, and wind, lunar explorations may help solve fundamental, universal questions.

Logically, the moon will be the first objective in the exploration of space. Initially the moon itself will be photographed and instrumented; then manned observation stations will be established for astronomical and meteorological purposes. In time, the moon will serve as an intermediate station enroute to other planets — step by step into infinite space.

The National Aeronautics and Space Administration's Lunar Program will utilize Lockheed's AGENA B satellite to play a significant part in forthcoming lunar explorations — as well as a host of other scientific space missions. The NASA lunar launch in 1961-62 will utilize the highly reliable Lockheed AGENA as second stage to carry the RANGER spacecraft. The AGENA will provide the extremely critical guidance and controls necessary to place the RANGER on the required lunar impact trajectory.

The lunar probe application demonstrates the versatility, reliability and success of the AGENA vehicle in Lockheed's satellite and spacecraft programs. Developed for the Air Force for use in the DISCOVERER program, the AGENA also is utilized in the MIDAS missile defense alarm system. Noted for a record of outstanding accomplishments, the AGENA is credited with being the first to be placed on a polar orbit; first to achieve a precise, predicted and nearly circular orbit; first to attain attitude control on orbit; first to eject a reentry capsule which was successfully recovered. The AGENA can be modified for a variety of missions such as navigation, geophysical investigations, long-range communications and deep space probes.

Lockheed's capability in satellites and spacecraft, manifested by such an achievement as the AGENA, encompasses the entire field. It includes current and long-range programs such as interplanetary probes, global and space communication systems, and manned space travel.

Engineers and Scientists: The accomplishment of such programs offers challenging opportunities to engineers and scientists in the research, design, development, test and operation phases of these programs. If you are experienced in work related to any of the above areas, you are invited to write: Research and Development Staff, Dept. M-29A, 962 W. El Camino Real, Sunnyvale, California. U.S. citizenship or existing Department of Defense industrial security clearance required.

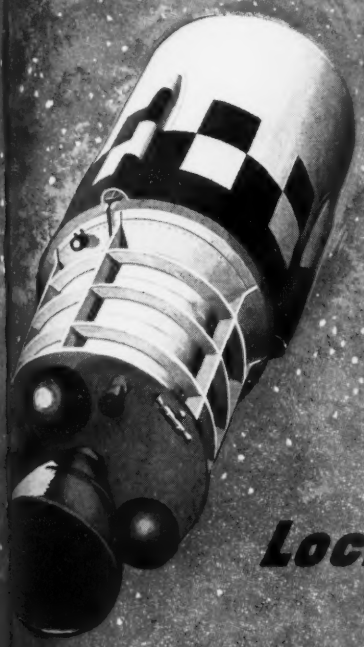

Lockheed / **MISSILES AND SPACE DIVISION**

Systems Manager for the Navy POLARIS FBM and the Air Force AGENA Satellite in the DISCOVERER and MIDAS Programs

SUNNYVALE, PALO ALTO, VAN NUYS, SANTA CRUZ, SANTA MARIA, CALIFORNIA • CAPE CANAVERAL, FLORIDA • HAWAII

Building block concept for very large solid boosters successfully demonstrated

United Technology Corporation has successfully completed the firing of a series of flight-weight conical, segmented solid propellant rockets – one phase of a study being conducted for NASA.

The use of conical segments makes possible the fabrication of very large solid rockets at lower cost, significantly reduces handling and manufacturing problems.

With the successful demonstration of UTC's building block concept, current technology can now provide solid booster thrusts exceeding any known to exist in the world.

UNITED TECHNOLOGY CORPORATION

A subsidiary of United Aircraft Corporation

Capability backed by four decades of propulsion experience

P. O. Box 358, Sunnyvale, California

Conical, segmented solid propellant rocket pictured during one of a series of successful firings at UTC's multi-million-dollar Development Center in the San Francisco Bay Area. The UTC rocket, with minor adaptation, is ready for immediate use as an operational vehicle.

THE IAS LOOKS AHEAD

Guest Editorial

Excerpts from address by Dr. H. Guyford Stever, IAS President, 1961 at the Honors Night Dinner—Hotel Astor, January 24, 1961

"These are exciting and challenging times for our country, our profession, and the Institute. The more senior members of this Institute have brought aeronautics from its pioneering days to a mature technology upon which the world's business and pleasure daily depend, and upon which the defense of the free world is largely based . . . . On top of the continuing challenges of aeronautics, there are new challenges in space for those members of our Institute who will continue the pioneering ventures in technology which from the beginning have marked this Institute.

✦ ✦ ✦

"The rapid expansion of missile and space activities has caused all of us in our profession to expand our technical horizons. Our Institute has led in the move to ensure complete coverage of the flight sciences over the entire speed range and throughout all regions of the flight media, from the dense lower atmosphere to rarified outer space. This has been done in the forums and publications we provide for our members. I consider the Institute now poised to cover the flight spectrum with a proper balance to deal with the technical interests of all of its members. In technical coverage, the phrase from zero to infinity has been put into effect.

"The people who will carry out the new space programs which our country wants are, by and large, our own IAS members, for our members are the ones who are dedicated to seeing new things in flight from zero to infinity successfully started and completed.

"The country today is experiencing a vast wave of self-searching and re-evaluation which has led to an upsurge of interest in progress and change. For the most part, it is a heartening and healthy trend brought about by many causes, none more significant, however, than the sudden steps into space exploration with all its ramifications. All this has given new importance to the fields represented by the IAS.

"The IAS has also conducted some self-examination. Already, as a result of it, we have reorganized the society to bring our individual members, the local Sections, and the Regions into positions of more influence in our affairs. More recently, as many of you know, we had a consultant conduct a series of lengthy depth interviews with many of our members, as well as selected outsiders, from one end of the country to the other, to delineate more sharply the new aspirations of our members for enlarging activities within the framework of IAS goals. The Council has already begun to implement this report.

"In these self-studies of the IAS, we have above all discovered that we have truly immense resources in interested and capable professionals who are the members of our society. Our unifying theme of flight of all kinds is a potent one. Under its banner, we have a professional society made up of individuals with widely divergent capabilities, responsibilities, and interests, each with the same dedication to the aerospace field—teachers and students, researchers, components and systems engineers, technical managers, and administrators from colleges, industry, and government. Because of this interlocking of skills, because of this cross-fertilization of disciplines, the sum total output of the IAS in aerospace progress is much more than could come from independent and isolated activities for basic science, for engineering design, for technical administration on the one hand, or for component disciplines of flight on the other.

"We have also discovered that each segment of our Institute wants us to improve the quality of work in its own particular field, not only for its own sake but also to contribute to the general advancement of the aerospace sciences. I believe that we must respond to this with renewed vigor, paying attention this year to another kind of spectrum—that of the broadening professional interests of our members—as in the recent past we addressed our efforts to their broadening technical interests.

"On one extreme of the interest spectrum, the research-minded members want a deeper coverage of the new sciences of importance emerging in aerospace. To this end we will continue and improve the fine new activities in meetings and publications which have been started in the recent past. At the other end of the spectrum, our more senior people want to delve into the complex interrelationships which aerospace in general, and the Institute in particular, have with other facets of our society—military, governmental, educational, industrial, together with community and public affairs concerns—and to explore the impact of our advancing technology upon our national security, our economic growth, and our ability as a people to defend and extend all the frontiers of freedom." ✦✦✦

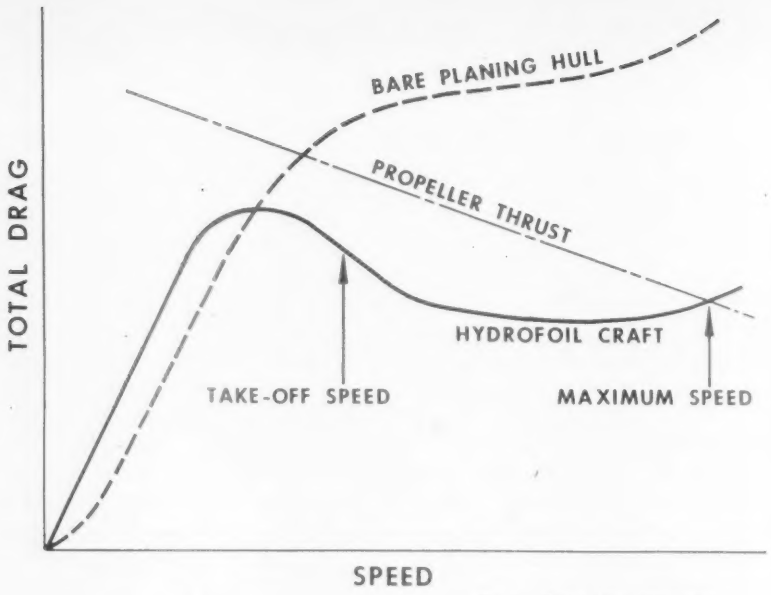

Fig. 1. Thrust-drag comparison.

THROUGH THE YEARS, improvements have been made in providing the surface ship with ways and means of greater speed. However, basic natural laws have limited the effectiveness of our efforts, especially with regard to improved performance in heavy seas. Some improvement has been due to the mere addition of power to existing ships. Unfortunately, the propulsion power required by conventional hull increases as a power of the speed, and the brute-force approach is not satisfactory.

This problem has not gone unchallenged, and, since the turn of the century, various inventors have attempted to overcome the barriers to higher speeds. The hydrofoil approach has been to avoid the barrier of costly wave-making resistance by lifting the hull of a boat or ship out of the water. This has been accomplished by the use of lifting surfaces or hydrofoils which fly just under or penetrate the water surface and generate enough lift to hold the hull clear of the water. It has been shown experimentally that the hydrofoil has several potential advantages which all show promise of providing the high-speed capability. These are a reduced resistance that permits a greater maximum

---

The assertions and opinions expressed by the authors are not necessarily official views of the Navy Dept. or the Bureau of Ships.

The authors wish to acknowledge that credit for much of the work reported here is due their colleagues in the Bureau of Ships and its contractors, and particularly Owen H. Oakley, Technical Director, Preliminary Design Branch of the Bureau of Ships.

Captain Stilwell (*left*) graduated from the U.S. Naval Academy in 1938 and, after duty at sea, from the Massachusetts Institute of Technology in 1943 where he had majored in Marine Engineering and Naval Architecture. After further duty at sea and in naval shipyards, he was designated Project Officer for hydrofoil research in the Bureau of Ships, 1950–1953. In 1953 he coauthored the paper, "An Appraisal of Hydrofoil Supported Craft," presented at the 1953 annual meeting of the Society of Naval Architects and Marine Engineers and reprinted abroad. He maintained personal interest in hydrofoil matters during assignment to other duties and resumed active leadership in the Navy's program upon his reassignment to the Bureau of Ships in 1958. He is presently Head of the Hull Design Branch.

Commander Nelson (*center*) graduated from the U.S. Naval Academy with the accelerated Class of 1948 in 1947 and, after duty at sea, from the Webb Institute of Naval Architecture in 1955. There he majored in Marine Engineering and Naval Architecture. After duty in the Puget Sound Naval Shipyard, he was assigned Head, Ship Protection Section of the Bureau of Ships. Subsequently he was reassigned to the Preliminary Design Branch and became Project Officer for hydrofoil development.

Commander Porter (*right*) graduated from the U.S. Naval Academy with the accelerated Class of 1947 in 1946 and, after duty at sea, from the Massachusetts Institute of Technology in 1948. After serving at sea again, he returned to M.I.T. for further study and graduated in 1955. Following duty in naval shipyards, he was assigned to the Preliminary Design Branch of the Bureau of Ships. In 1958 he was selected to continue advanced studies in naval hydromechanics at the University of California, Berkeley, and achieved his doctorate there. He is presently assigned in the Hull Design Branch of the Bureau of Ships.

Hydrofoils at the Crossroads

"One direction is toward limited, small-craft application, and the other leads toward larger, high-speed ships." The naval architect and the aeronautical engineer will determine what this future will be.

Capt. J. J. Stilwell, Lt. Comdr. P. W. Nelson, and Lt. Comdr. W. R. Porter

United States Navy

speed for a given power, a more comfortable ride, and seakeeping characteristics that permit maintaining speed in a severe sea condition.

Fig. 1 illustrates why there is such an active interest in the hydrofoil principle. In this figure, speed is plotted against total drag. As the hydrofoil ship builds up speed, the resistance of the hull and foils also increases rather rapidly to a maximum. Once the lift generated on the foils exceeds the weight of the ship, the hull is lifted clear of the water and the total resistance decreases to that of drag of the foils and struts alone. The resistance is approximately constant for some speed range but eventually increases again. The maximum speed is reached at the limit of the installed power. Fig. 1 also plots the drag curve for a planing hull, the best high-speed competitor to a hydrofoil ship. It can be seen that at lower speeds the hydrofoil might require 25–30 per cent more power than a conventional ship. However, this is a cheap way to obtain high-speed performance.

To emphasize that hydrofoil craft are not without competition, Fig. 2 shows what might be called the efficiency of transporting payload or providing a military capability as a function of speed for three design forms. The ordinate is a measure of transportation efficiency, which is payload multiplied by speed and divided by installed power. The abscissa is the speed-length ratio, a convenient base for comparing different ships at varying speeds based on the Froude number. It can be seen that, at the

(*Continued on page 68*)

Fig. 2.

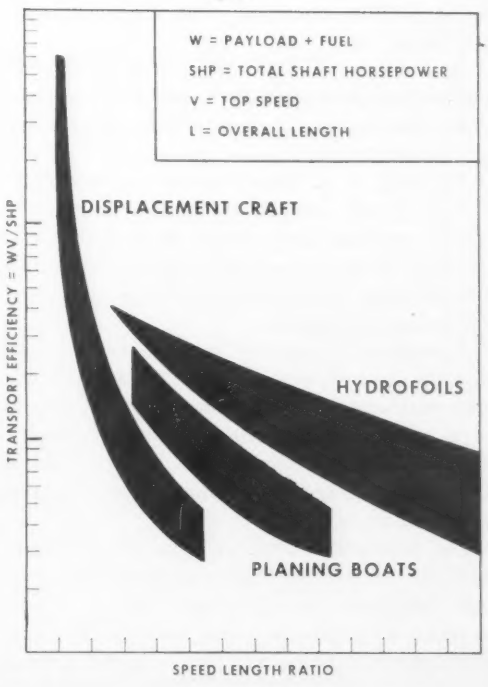

Experimental Designs for Rocket Motors

Norman R. Garner, D. E. Hartvigsen, and Richard W. Vail, Jr.

Aerojet-General Corporation

THE RATE at which a rocket motor progresses through its developmental program and the capability of the final engineering design to meet customer requirements are dependent upon many of the following factors:

(a) Severity of the usage environment.

(b) Performance and reliability requirements established by the customer.

(c) How well the initial engineering design is conceived.

(d) Quality of material used in rocket fabrication.

(e) Manufacturing skills and facilities.

(f) Effectiveness of the quality control program.

(g) Adequacy of test facilities.

(h) Validity, adequacy, and effectiveness of test programs.

(i) Abilities of cognizant personnel to interpret test data objectively and to make associated decisions affecting the future direction of the rocket development program.

Although all of these factors are extremely important to the success and rate of progress of the rocket program, and are to some degree interdependent, this paper is restricted to a discussion of ways and means of making the most effective use of the various test programs.

A program is proposed for maximizing assurances that the final engineering rocket design will comply fully with customer requirements when produced in large quantities and that both the cost and total program time for development will be minimized. The program makes use of the concept of continuous development.

The procedure advanced is predicated upon the scientific method and utilizes the principles of statistical test design to crystallize program objectives; to relate development, proof, and qualification test programs so that they will form a unified package of information; and, finally, to present an objective procedure for analyzing test information to monitor the growth of the rocket motor.

The procedure reflects the fact that tests are made for the express purpose of obtaining data for use in determining the future course of action—for example, to ascertain when a rocket design is ready to enter its next phase of development. If the action is to be

Mr. Garner (*left*), a member of Aerojet-General's Reliability Assurance Staff, has been associated with the Corporation since 1957 as a technical specialist in the application of statistics to research reliability and quality control programs, and has had many reports published showing use of statistics in all phases of industrial enterprise. He received his B.A. degree in mathematics from the University of Rochester in 1949, and his M.S. in statistics from North Carolina State in 1951.

Mr. Hartvigsen (*center*) is Associate Manager of Corporate Reliability Assurance. Although applied statistics is his chosen field, he worked from 1942 to 1947 as a Navy physicist—first in the degaussing program at Bayonne, N.J., and later in the aerodynamic testing of rocket models at U.S. NOTS China Lake. During 8 years at NOTS, and from 1955 to the present at Aerojet-General, Mr. Hartvigsen has specialized in the application of statistical concepts to weapons development and testing programs. He received his B.S. degree in mathematics in 1938 from Utah State Agricultural College, and his M.S. in mathematics in 1941 from Iowa State College.

The third member of this author team, whose principal interests lie in the fields of experimental design and regression analysis, is a statistical consultant assigned to the Corporate Reliability Assurance Staffs. Mr. Vail (*right*) became associated with Aerojet-General in 1958 after receiving his M.S. degree in statistics from V.P.I. He was graduated in 1956 from the University of Florida with a B.A. degree in mathematics.

Development • Proof • Qualification Testing

Description of an experimental procedure that utilizes the minimum number of test specimens required to obtain information necessary to make decisions for any continuous developmental program.

proper, the data upon which the decision is based must be adequate in quantity, valid—i.e., truly pertinent to the problem at hand—and of an acceptable level of accuracy and precision.

There are many things that must be done to provide assurance that test information has these properties. Some of the more important tasks are to:

(1) Design the experimental program scientifically, using appropriate statistical concepts to provide pertinent and adequate data amenable to objective analysis.

(2) Employ the principle of randomization to the order of conduct of the experiment and allocation of test material. This is necessary to implement the laws of probability and prevent biased results.

(3) Establish suitable end measurements; select instrumentation with known and adequate levels of accuracy and precision.

(4) Refine experimental techniques to prevent gross errors and secure uniformity in the application of treatments. This requires sufficient control of external influences so that every treatment produces effects under comparable and desired conditions to obtain unbiased measures of the effects of treatments. (When satisfactory methods of measurement are not available, they must be developed.)

(5) Improve the handling of experimental material. A serious effort should be made to determine the characteristics of the material to be used. Group the experimental material in such a way that the material to which one treatment is applied is closely comparable with that to which another treatment is applied.

These five tasks or requirements were considered in developing the program outlined in this report.

Concept of Continuous Development

It is generally conceded that engineering development is a continuous iterative process. The cycle—theorize, design, experiment, (*Continued on page 32*)

Fig. 1. A continuous development program.

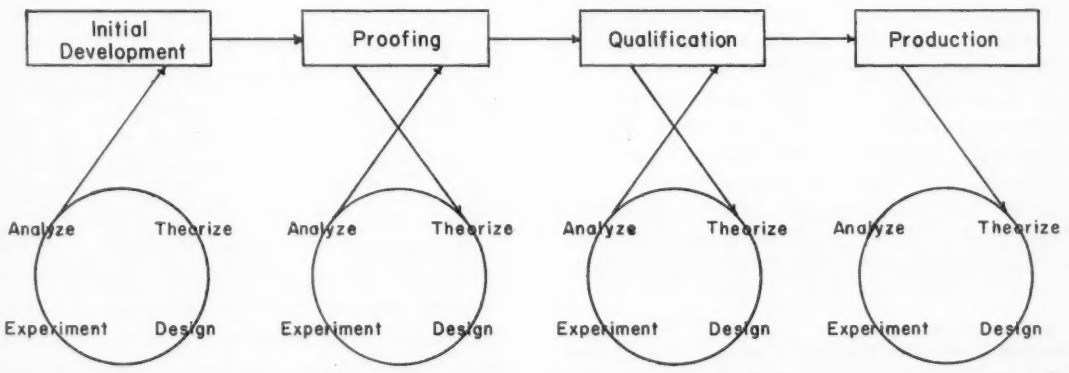

High-performance aircraft (and eventually spacecraft) call for more than successful escape—the need is for protection from environment, not with cumbersome clothing, but with a capsule equipped for survival.

FROM WORLD WAR I until World War II, airplanes were relatively slow as compared with today's high-speed, high-performance vehicles and did not produce forces or difficulties which the pilot's muscular power could not overcome in order to escape from the machine and employ his parachute. During and since World War II, however, the picture has changed radically. Aircraft speed and performance have increased to such an extent that pilot escape by conventional bail-out methods is almost impossible because of the large aerodynamic and inertia forces generated at the high speeds. The Germans, who were the first to put a parachute into service near the end of World War I, were also the first to improve escape capability significantly by placing ejection seats in service near the end of World War II. These concepts have remained the basic means for escape until now. The advent of the rocket catapult, improved seat stability, increased automation, and developments in protective clothing for the pilot have increased the capability of ejection seats for escape from high-performance aircraft. These improvements, however, have not allowed ejection seat performance to keep pace with airplane performance. The pilot has become more and more encumbered with bulky protective clothing and equipment resulting in reduced efficiency and effectiveness during the performance of a mission. Even after a successful escape, survival is, at best, a difficult problem due to lack of shelter and ability to carry survival equipment.

The trend toward greater speeds and higher altitudes will increase the disparity between ejection seat performance and airplane performance. Environments will be such that men may be subjected to fatal burns due to aerodynamic heating during escape at high Mach numbers, frost bite, freezing and decompression during high-altitude descent and to crushing air loads during high-speed, low-altitude escape. It appears that many of these problems may be solved by capsulation. For a typical high-speed fighter/interceptor airplane the cockpit section, which constitutes the nose of the aircraft, appears to present the obvious and logical geometric shape for an ejectable escape capsule. It is along these lines that the design study presented in this paper is developed. Other capsulation techniques are also being investigated under U.S. Air Force and Navy sponsorship. All capsules must be able to withstand the maximum dynamic pressure loads and skin friction temperatures which the new high-performance airplanes will encounter. They must furnish protection when landing on all types of terrain and water, even if the pilot is unconscious, and they must serve as shelter against the elements after landing. If the capsule pressure structure and related equipment are properly designed, it will not be necessary for the pilot to wear all the currently necessary items of cumbersome protective clothing and he can more nearly approach the concept of "shirt sleeve" flying and the improved efficiency derived therefrom.

The study presented in this paper is based on investigations made at Lockheed Aircraft Corp. under USAF Contract No. AF 33(600)-35430.

Supersonic Ejectable-Nose Escape Capsule

Mell D. Cassidy, MIAS, and Phillip J. Sullivan, AIAS

Lockheed Aircraft Corporation

The purpose of this paper is to present the more important results and findings of an ejectable-nose escape capsule study performed at Lockheed under Air Force sponsorship, and to highlight the more significant problems which must be faced in the development of such a capsule. Many of the problems, principles, and solutions may be utilized in the design of other capsule-type escape systems. Complete documentation of the study is beyond the scope of this paper. However, WADC Report No. TR 59-493, entitled *Development of an Ejectable-Nose Escape Capsule*, presents the results of the analyses and test data in detail. The final capsule configuration resulting from this investigation is shown in Fig. 1 (artist's rendition, see headpiece).

Mr. Cassidy is a member of the Advanced Research and Applications Staff at Lockheed's California Division. He was awarded a B.S. (1952) and an M.S. (1954) in aeronautical engineering by the California Institute of Technology. His experience with escape systems is a direct outgrowth of aerodynamic work in connection with the development of the F-104 Starfighter. Mr. Cassidy was a major participant in the design, development, and testing of a stabilized, high-performance ejection seat. During the preliminary design of the nose capsule study, he was assigned technical responsibility for the program. His design and aerodynamic experience also includes work on space and re-entry vehicle designs, space vehicle escape systems, and a wide range of advanced aircraft concepts.

Mr. Sullivan is a Senior Aerodynamics Engineer on the staff of the Advanced Research and Applications Division at Lockheed. He has been engaged primarily in hypersonic aerodynamic research of both a theoretical and an experimental nature on aerodynamic interference, lifting re-entry configurations, boost-glide and cruise vehicles, and high-speed escape systems. He holds B.A.E. and M.S. in M.E. degrees from the Georgia Institute of Technology. Prior to studying engineering, Mr. Sullivan was on duty with the U.S. Navy as a pilot of various categories of combat and transport aircraft.

System Requirements

For the purpose of this investigation, numerous performance criteria and design ground rules were stipulated by the Air Force These include the following:

(1) The performance shall be 900 knots E.A.S. from sea level to an altitude of 50,000 ft., and Mach 4.0 from an altitude of 50,000 to 100,000 ft. The capsule will be statically and dynamically stable throughout the entire performance range. Fig. 2 presents the required performance for the capsule. It can be seen that the performance boundary conditions present tremendous problems. For example, a speed of 900 knots E.A.S. produces a dynamic air pressure of approximately 2,750 lbs./sq.ft. At a Mach number of 4 at 50,000 ft. altitude, the skin temperature is approximately 900°F.; while at 100,000 ft. altitude, the atmospheric pressure is about 1/100 of that at sea level. The capability of the C-2 upward ejection seat currently being utilized in the F-104A aircraft is included in Fig. 2 for comparison purposes.

(2) A typical flight duration of 4 hours is to be assumed.

(3) The pilot will not be (*Continued on page 38*)

Response of Plates to Moving Shocks

Eric E. Ungar, MIAS, *Bolt Beranek and Newman Inc.*

IT IS WELL-KNOWN that most shock waves observed in wind tunnels and in flight oscillate to some extent. For oblique waves whose positions are anchored by the flow geometry the oscillations generally remain of small amplitude, but when certain flow instabilities occur shock oscillations of large amplitude may be set up.[1–4] Further, the normal shock waves occurring on transonic wings and control surfaces are often found to oscillate severely and thus to cause severe buffeting and control problems.[1]

Since shocks are essentially pressure discontinuities, the motion of a shock relative to a structure constitutes a nonsteady airload which may cause the structure to vibrate, possibly quite severely. Such structural oscillations are at the very least annoying because of the noise radiated by them into an aircraft.[2] More seriously, continued oscillations may lead to fatigue of a structural member and to failure of a flight vehicle's mission.

The intent of the present paper is to provide some insight into the mechanisms by means of which moving shocks can set up large structural oscillations and to outline calculation methods for these structural responses in some rather idealized cases.

In the following pages the analyses are presented first in as much generality as possible, thereafter they are specialized to simply supported plates. Responses of these structures to uniformly moving shocks (as might be experienced by one vehicle passing through the shock created by another[5, 6]) and to sinusoidally oscillating shocks are discussed in detail.

The results presented herein were obtained in the course of studies sponsored by WADD under Contract AF 33(616)-6217 and were presented to the sponsor in extended form in reference 13.

The many helpful comments by Drs. Ira Dyer, Peter A. Franken, and Günther Kurtze, all of the author's company, are greatly appreciated.

As Senior Engineering Scientist, Dr. Ungar since 1958 has been engaged in a series of research and consulting programs, primarily dealing with structural dynamics and viscoelastic damping. Before joining BBN he devoted two years to atomic weapons development at Sandia Corp., then served on the faculty and research staff of N.Y.U. for five years. He was educated at Washington University (B.S.M.E., 1951), the University of New Mexico (M.S., 1954), and N.Y.U. (Eng.Sc.D, 1957). In addition to IAS, he holds membership in ASME, Sigma Xi, and Tau Beta Pi.

Throughout the following analyses the effect of a shock on a structure is represented by an abrupt change in pressure. Since compression shocks have thicknesses of the order of magnitude of the mean free path of the fluid molecules,[7] this assumption appears reasonable, even though the presence of a boundary layer tends to smoothen the pressure discontinuity experienced by a rigid surface.[8] This smoothing will not affect the utility of the present results in bringing out the mechanisms of energy transfer, and it will affect the accuracy of the specific results significantly only for those cases where the pressure changes on the plate occur over distances which are not small compared to the shock excursions.

General Expression for Plate Responses to Determinate Pressures

Consider an elastic plate subject to a pressure $p(x, y, t)$, where x and y are convenient Cartesian coordinates and t denotes time. It is assumed that the plate obeys the classical equation of motion,

$$D\nabla^4 u + M(\partial^2 u/\partial t^2) = p(x, y, t) \qquad (1)$$

where u denotes plate deflection, M plate mass per unit area, and D flexural rigidity. Damping is neglected for the present for the sake of simplicity; its effect is introduced subsequently where necessary.

General expressions for plate responses to pressure variations are derived in terms of generalized coordinates associated with the plate normal-mode shapes. The expressions are then specialized for moving pressure discontinuities, which correspond to shocks. The responses of simply supported rectangular plates to uniformly moving and to sinusoidally oscillating shocks are determined in detail for shocks parallel to a pair of edges. The importance of the mechanisms of trace-matching, force-resonance, and moment-resonance, is established.

In order to obtain a solution for Eq. (1), one may first solve the corresponding homogeneous equation. By postulating[11] $u = u(x, y)e^{i\omega t}$ the latter reduces to

$$(\nabla^4 - k^4)u = 0 \qquad k^4 \equiv (M/D)\omega^2 \qquad (2)$$

This has a doubly infinite set of solutions, namely, the set of eigenfunctions ψ_{mn} corresponding to the eigenvalues k_{mn} (which are associated with the natural frequencies ω_{mn}).

Possibly one of the most direct methods of solving the nonhomogeneous problem is that involving generalized coordinates based on the eigenfunctions. To apply this technique one expands a general deflection $u(x, y, t)$ in terms of the eigenfunctions,

$$u = \sum_{m=1}^{\infty} \sum_{n=1}^{\infty} q_{mn}(t)\ \psi_{mn}(x, y) \qquad (3)$$

and substitutes this into the well-known equations for the kinetic and potential energies of plates.[9] By substituting the results into Lagrange's equations[9] one then obtains a set of differential equations for q_{mn}. If the eigenfunctions are orthogonal (as they are for plates with simply supported and/or clamped boundaries, approximating practical conditions), then the differential equations are uncoupled and one obtains

$$(\omega_{mn}^2 + d^2/dt^2)\ q_{mn} = Q_{mn}/M\Phi_{mn} \qquad (4)$$

where the "modal masses" Φ_{mn} are defined as

$$\Phi_{mn} \equiv \iint_A \psi_{mn}^2\, dA \qquad (5)$$

and Q_{mn} denotes the generalized force corresponding to the series coefficient (or generalized coordinate) q_{mn}. A denotes the plate surface area, of course. The forcing function $Q_{mn}(t)$ may be found, for example by use of the principle of virtual displacement,[9] to be given by *(Continued on page 78)*

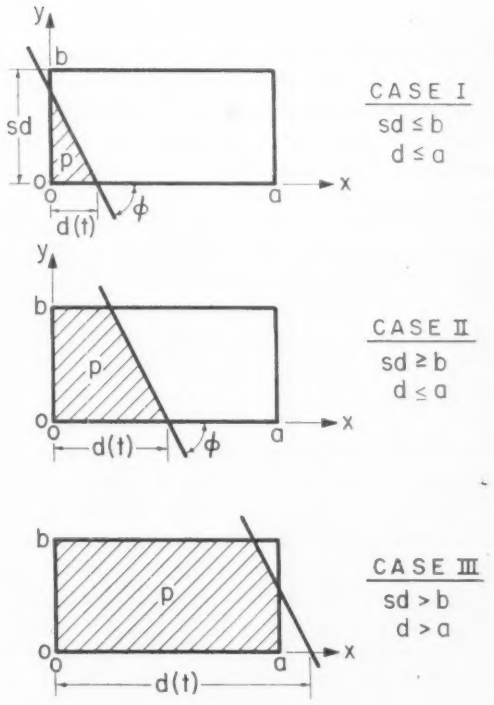

Fig. 1. Pressure discontinuities on rectangular plates.

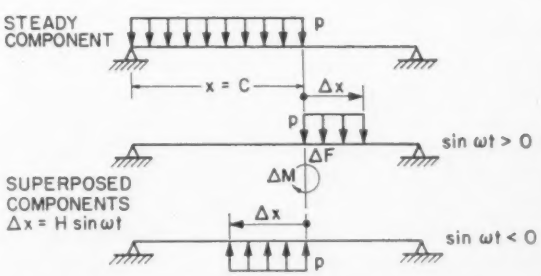

Fig. 2. Steady and varying pressure distributions associated with sinusoidally oscillating shocks.

The Navy's Flying Wind Tunnel

Henry E. Payne III (AIAS), *Princeton University*
Lt. Comdr. Frank R. Carter, USN (AIAS), Lt. Comdr. Wayne J. Harrison, USN

The airship as a flying wind tunnel

WITH THE ADVENT of VTOL/STOL aircraft, it has become increasingly necessary to expand our knowledge in the field of low-speed aerodynamics. At the present time there is an appalling lack of experimental test data applicable to this type of high power-to-weight ratio aircraft. As a result of this, analytical work on evaluating simple static stability derivatives is almost nonexistent, and most of what has been done has not been confirmed or correlated with test information. More effort must be devoted to obtaining reliable expressions for these derivatives, for the predictions of the various mathematical methods can be only as good as the empirical inputs.

In line with this thinking the Subsonic Aerodynamics Laboratory of Princeton University in searching for a means of gathering accurate test data has developed a flying wind tunnel utilizing a U.S. Navy airship as a stable model carriage.[2] Since most VTOL/STOL machines derive their lift primarily from their thrusting systems, the models tested must, necessarily, be powered. The simulation of propeller slipstreams, jet flaps, or direct jet lift, presents a series of problems in model design and fabrication as well as testing difficulties.

Since the models must be powered, there is a tendency to make them of a larger size than would be required for more conventional unpowered wind-tunnel models designed to obtain similar types of information. This larger size, of itself, causes these models to require large test sections, but when coupled with the desirability of avoiding the unknown wall correction factors arising from the impingement of the slipstreams or jets, the desirable test section size becomes very large indeed. Somewhat paradoxically, the lower the minimum speed investigated, the larger the test section required, since the turning effects of the free stream on the jets and slipstreams are greatly reduced.

Mr. Payne is Research Assistant in the Subsonic Aerodynamics Laboratory of the Forrestal Research Center of Princeton University, working under a contract for the Office of Naval Research. He is research engineer in charge of VTOL/STOL basic research. Mr. Payne graduated from Yale University in 1957 with a B.S. degree in mechanical engineering and from Princeton University in 1960 with a Master's degree in aeronautical engineering. He is an IAS Associate Member, and member of ARS and Sigma Xi.

Commander Carter was commissioned and received his B.S. degree from the U.S. Naval Academy in June of 1950. He was designated an HTA and LTA aviator in 1952. After three years of operational duty in an airship ASW squadron, he studied at the U.S. Naval Postgraduate School in Monterey, Calif., where he graduated with a B.S. degree in aeronautical engineering. In 1958 he received his M.S. degree in aeronautical engineering from M.I.T. Currently he is the Aeronautical Engineering Officer of the Airship Test and Development Department at Lakehurst where he has been engaged in the Bureau of Naval Weapons R&D project work associated with airships. Commander Carter is an Associate of the IAS.

Commander Harrison received his HTA wings and was commissioned an ensign in the U.S. Navy in May of 1944. He saw action in World War II and Korea, and has flown PB2Y's, P4Y's, F6F's, TBM's, R7V's, WV's, R4D's, and pilotless drones accumulating over 4,000 pilot hours. Commander Harrison was designated an LTA aviator in April of 1954, and since flown, 1,100 hours in ZP-3K's, ZSG-4's, and ZS2G-1's. He has attended the University of Idaho and the University of Pennsylvania where he majored in geology. Currently he is the Material Officer of the Airship Test and Development Department at Lakehurst and is Project Officer of the Navy's Flying Wind Tunnel.

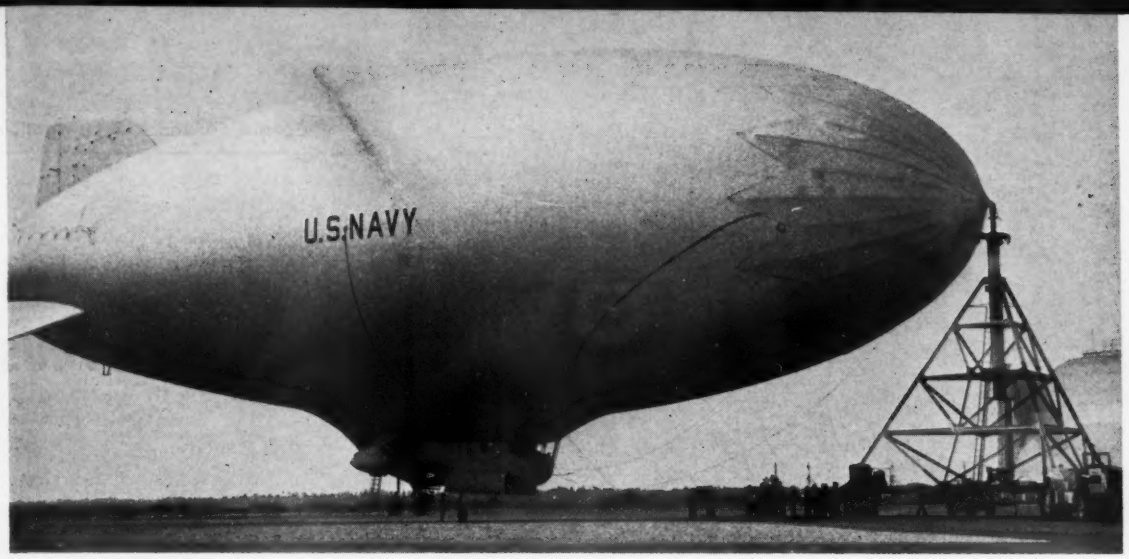

Fig. 1. ZS2G-1 airship.

is shown to give accurate, repeatable data for a variety of configurations.

At the present time there are few tunnels in the country large enough to provide the test environment required. The majority of these, having been built primarily in an attempt to obtain large scale Reynolds numbers, are not designed to provide the low speeds desired to simulate the landing and take-off conditions of typical VTOL/STOL configurations. As a consequence, designers have had to content themselves with data largely obtained under dubious test conditions in small tunnels, or in large tunnels that could not provide stabilized operation at low speeds. In many cases under such test conditions unacceptable velocity variations existed throughout the test section.

As a result of these conditions, there has in the last few years developed a tendency in many laboratories to attempt to modify either the diffuser or settling chamber of existing subsonic tunnels to produce a more adequate low speed testing facility. With a few exceptions, these modifications have been somewhat crude and not altogether satisfactory, but they have at least provided test sections of sufficient dimensions for minimum test programs.

Recently there have been a number of proposals for the construction of entirely new tunnels having very large test sections and capable of stabilized operation in the speed range between 0 and 100 to 150 ft. per sec. The major disadvantages of such tunnels are their physical size, their high initial cost and their operating expenses. Although a series of such proposals have been under study by the Subsonic Aerodynamics Labora- (*Continued on page 50*)

Fig. 2. (Official U.S. Navy Photo.)

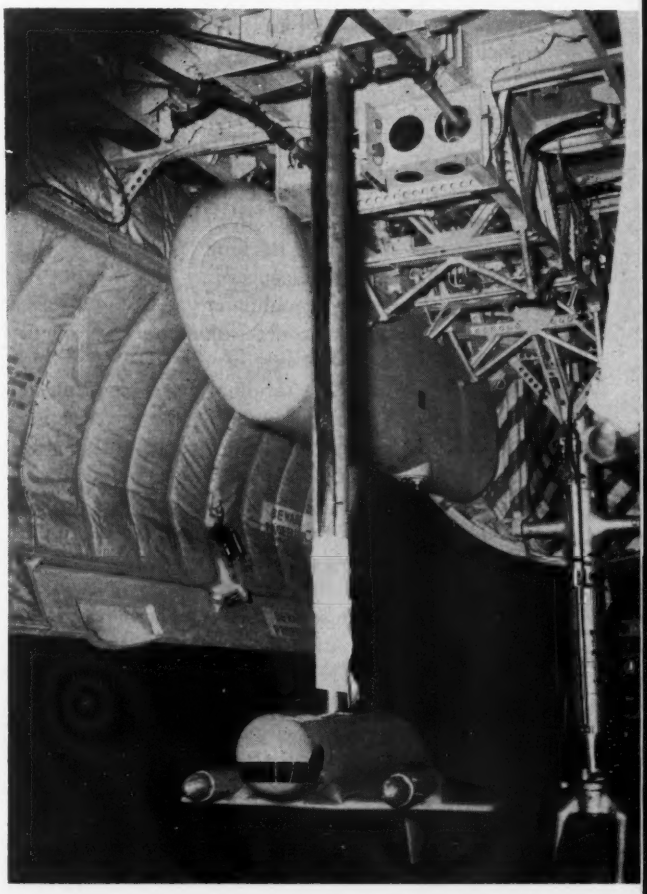

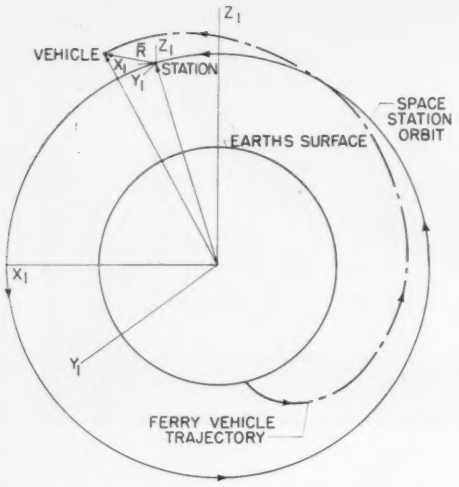

Fig. 1. Trajectory relations between the rendezvous vehicle and the space station.

Pilot Control of Rendezvous

M. C. Kurbjun, R. F. Brissenden, E. C. Foudriat, and B. B. Burton

NASA Langley Research Center

SPACE EXPLORATIONS will occur in the near future where man will be part of the mission. His abilities in these missions can, therefore, be utilized to simplify the equipment requirements and increase the overall system reliability. Rendezvous of space vehicles will play an important role in these future space missions. Rendezvous can be used for many purposes, such as supplying a space station or building up equipment in orbit for extended space missions.

Rendezvous may be divided into three separate phases; the launch phase, the closing or terminal phase, and the final docking phase. Previous studies have been made concerning all three phases. Reference 1 presents a preliminary analytical study which was conducted to determine boundary conditions for launching the interceptor into the proper position to initiate the terminal rendezvous phase. In reference 4 a static simulation of the terminal phase of rendezvous, made primarily within one-half mile and 60 ft./sec. closure rate, concluded that coplanar rendezvous is in the realm of human-pilot capability. Reference 3 concludes that the human pilot is superior to an automatic system in performing the highly accurate vernier corrections required for the docking phase, and is a valuable asset to override an automatic system during the closing phase.

A study of the terminal phase of the rendezvous of a manned ferry with a space station in an earth orbit has been made to determine a pilot's ability to control this phase and to minimize the equipment and instrumentation required for the task. The terminal phase of this study is assumed to begin at a relative range of 50 miles, the range within the capability of existing onboard radar equipment, and end at essentially zero range with zero relative velocity.

This study used a pilot in a closed simulation loop which included a fixed-base cockpit simulator having the required instruments, vehicle attitude and propulsion controls, and an analog computer to solve the six-degree-of-freedom equations.

Description of the Rendezvous Program

Equations of Motion

The geometric relation between the rendezvous vehicle and the space station is illustrated in Fig. 1

Symbols

b	=	distance from rocket nozzle to vehicle center of gravity, ft.
$\bar{F}$	=	sum of all forces other than that of gravity acting on the vehicle, lb.
g	=	acceleration due to earth's gravitational field, ft./sec.^{2}
G	=	universal gravitational constant
$\bar{\imath}, \bar{\jmath}, \bar{k}$	=	unit vectors
I	=	principal moment of inertia, slug-ft.^{2}
m	=	instantaneous mass of the vehicle, slugs
M	=	mass of the earth, slugs
$M_{1,2,3}$	=	control couple, ft.-lbs.
$\bar{R}$	=	position of ferry vehicle in a coordinate system with origin at space station center of mass and axes always parallel to lines fixed in an inertial frame, ft.
T	=	thrust, lb.
ΔV	=	velocity increment, ft./sec.
ΔW	=	fuel used by rocket, lb.
X, Y, Z	=	coordinates of vehicle from space station to vehicle along inertial axes
α	=	angle subtended by line of sight between space

Importance of pilot's abilities in space missions to simplify equipment requirements and increase system reliability especially in rendezvous of space vehicles.

for a typical launch trajectory. The space station is shown in a circular orbit moving in a counterclockwise direction, and the rendezvous ferry vehicle is coasting to apogee from a direct launch along an elliptic path to the station orbit. A set of inertial axes, whose origin is located at the center of the earth, form the basic coordinate system. A nonrotating axis system was selected to simplify the piloting technique used during the terminal rendezvous, as will be explained subsequently. The range vector $\bar{R}$ of the vehicle relative to the station is illustrated. Also shown are $\bar{\rho}$ and $\bar{\sigma}$, the position vectors

(*Continued on page 84*)

station and ferry vehicle and projection of line of sight on $X_I - Y_I$ plane, deg.

β = angle between X_I-axis and projection of line of sight on $X_I - Y_I$ plane, deg.

ϵ = angle of rocket thrust misalignment, deg.

ρ = distance from earth's center to orbiting space station, ft.

$\bar{\sigma}$ = position of ferry vehicle in a coordinate system with origin at earth's center and axes always parallel to lines fixed in an inertial frame, ft.

τ = time constant obtained by rate feedback, sec.

ψ, θ, ϕ = yaw, pitch, and roll angles, deg.

p, q, r = roll, pitch, and yaw rates, deg./sec.

Subscripts

I = relative to inertial axes

x, y, z = relative to body axes of vehicle

X, Y, Z = relative to coordinate axes

1, 2, 3 = referenced to reaction control for roll, pitch, and yaw

A bar over a quantity denotes a vector.

A dot over a quantity denotes a time derivative; two dots denote a second derivative with respect to time.

The senior author of this article is Head, Control and Simulation Section, Aero-Space Mechanics Division, at NASA's Langley Field facility. His government service began in 1946 (with NACA) and his contributions since have included findings in the fields of high speed aerodynamics, noise, and high speed propellers. He also conducted the initial recovery system tests for Project Mercury. Mr. Kurbjun received his B.S. in A.E. from VPI in 1944 and has done graduate work at the University of Minnesota. Prior to joining NACA, he was a U.S. Navy engineering officer.

Mr. Brissenden is on the staff of the Control and Simulation Section, Aero-Space Mechanics Division, at Langley Research Center, previously having done work on automatic tracking systems for piloted interceptors, and flight testing of variable-stability aircraft for the Stability and Control Branch, Flight Research Division. He joined NACA in June, 1955 following graduation from North Carolina State College with a B.S. degree in M.E. During the ensuing two years, he did graduate work at VPI. He was an Army pilot in World War II.

Mr. Foudriat is Head of the Systems Analysis Section, Guidance and Control Branch, Aero-Space Mechanics Division, at Langley Research Center. An active member of AIEE, he received a B.S. degree in E.E. from the University of Illinois in June, 1950, his M.S. degree in E.E. at Ohio State in March of 1956, and is working toward a Ph.D. at Ohio State. He joined Battelle Memorial Institute as an engineer in 1951, transferred to North American Aviation as Senior Research Engineer in the Flight Control Systems Analysis Section in 1955 and ater became Supervisor of the Servo Analysis Section. His government service began in Nov., 1957.

Now pursuing a Naval career, Mr. Burton was an engineer in the Aero-Space Mechanics Division of Langley Research Center from June, 1959 to Sept., last year, and contributed in significant degree toward solution of space rendezvous problems. His initial enlistment in the Navy was from 1951 to 1955, following which he studied at Louisiana State University and received a B.S. degree in M.E. in June, 1959.

Meteorological Satellite Systems in

F. W. Reichelderfer, FIAS
U.S. Weather Bureau

DURING THE 78 days immediately following its launching on April 1, 1960, meteorological satellite Tiros I provided some 23,000 photographs of earth and clouds, most of them for areas of 500,000 square miles or more as viewed from an orbit about 450 miles from earth's surface. Since then Tiros II has given many more photo cloud maps. Earlier (October 13, 1959), Explorer VII began telemetering the first long series of infrared data for much of the earth. The epochal significance of these successful meteorological satellites may best be seen by comparison of meteorological data now available with what is required to satisfy man's needs for weather information. The great disparity is often overlooked in view of the very large number of synoptic weather reports now received every day in national meteorological centers.

Usually, when one wants to know about the weather at a particular time and place the desired information can be stated in a few words. But weather reports and forecasts for an aircraft operator may be quite inapplicable for the agriculturalist, the engineer, the industrialist, the mariner, or the sportsman. The aviator wants to know about cloud ceilings, terminal airport visibility, clear air turbulence, jet streams many thousands of feet above the ground, icing in clouds, and so on. These conditions have little interest for the farmer engaged in harvesting or the horticulturalist seeking to protect his crop from frost damage.

For much of the information given in this paper the author is indebted to Dr. Harry Wexler, Dr. Sigmund Fritz, David S. Johnson, and others on the staff of the Meteorological Satellite Section, and to F. W. Burnett, as well as other members who worked on the plans summarized here.

The different combinations of physical conditions of the atmosphere near the ground and up to the heights now frequented by man are almost legion. The conditions usually change from hour to hour. Moreover, the many changes in weather and storm behavior from place to place compound the vagaries which the national weather reporting system must try to observe, report and analyze. The international weather code lists 99 different states of the weather referring primarily to hydrometeors, that is, cloudiness and precipitation. This number does not exhaust the list of significantly different states of weather. In addition, the air temperatures at different altitudes, the humidities, the winds with their endless fluctuations in direction, speed and gustiness, level by level, the barometric pressures and other atmospheric conditions must be included in the descriptions of weather required for various practical purposes.

Stated in brief, the requirements placed by modern society on national meteorological services include knowledge of practically *everything* with regard to the physical conditions of the atmosphere, almost *everywhere* from the surface up to 50,000 ft. or more. Questions of long-range weather forecasting—and perhaps modification or control of undesirable weather conditions and destructive storms—are outside the scope of this article, but for a complete list of ever-pressing meteorological "requirements" these would have to be considered.

Fragmentary Data

The point made here is that although millions of weather observations and reports are made each day, their world total represents only a fraction of what is needed—probably less than 20 per cent of

Weather Research and Services

Hurricane, cyclone, tornado, typhoon?

Tiros cloud photographs fill in many serious gaps in our observation and measurement of the atmosphere

requirements for purposes of general analysis and broad scale forecasting. For detailed local analysis and predictions of airport terminal weather or other specialized local weather forecasts for agriculture, boating, etc., the data coverage probably is only about 5 per cent of that required and in some parts of the atmosphere much less than this.

In their efforts to obtain much-needed measurements of atmospheric conditions, early meteorologists established observatories on mountain tops. Later, they sent simple instruments aloft on kites, balloons and airplanes. Eventually, they developed radiosondes, rockets, radar and other radio and sonic sounding devices. The latest means for telemetering atmospheric conditions is the meteorological satellite. It will supplement data obtained by several of the preceding methods and will not in general replace them. The significance of meteorological satellites in the national and international systems of synoptic weather reporting can be seen in the estimates that Tiros types can provide about 10 per cent of the total observations required for weather analysis and forecasting on the local scale and about 20 per cent of those required for very broad scale and extended period (5-day) forecasting. The comparable figures for satellites of advanced design operating at capabilities within present design knowledge are 60 per cent for local forecasting and about 90 per cent for very general-area and extended-time-range forecasting. These estimates are only indicative and approximate and since satellites give, for the most part, information not obtainable in other ways the percentages should be considered as going to reduce present data deficiencies represented in the 80 per cent or greater difference between data now available and total data required.

Dr. Reichelderfer started his career in science as a chemist, having graduated from Northwestern University in 1917. Incident to aviation training during World War I, he took further studies in meteorology, supplemented later by work in the Geophysical Institute, Berger, Norway, and other meteorological institutions. He completed aviation flight school in 1918 and received the Naval aviation pilot's certification. Later in airship operations in Lakehurst, N.J., he obtained the pilot's certificate for airships and free balloons also. In the early 1930's, he served as station Executive Officer at Lakehurst and on the U.S.S. "Utah," gunnery experimental battleship. Some 30 years of his career have been in active meteorological positions, among them President of World Meteorological Organization, 1951–1955, and he is now Chief, U.S. Weather Bureau.

Satellite Capabilities

For many regions, particularly over oceans, where weather observations are relatively sparse and upper air soundings very infrequent or in much of the southern hemisphere, practically unknown, the meteorological satellite appears to be the only likely means for obtaining information of the state of the atmosphere and its never-ending changes. As an instrument for achieving the comprehensive coverage in weather reporting that is recognized as a responsibility of the national meteorological service of every modern country, the satellite has unique and far-reaching applications for international exchange of weather information. This is illustrated in Fig. 1 which shows interrelated storm systems and associated air masses and fronts extending from Canada, Mexico, and the United States across the ocean to the western Pacific. The chart and photograph illustration are described in a later paragraph. International aspects of the output from satellites

(*Continued on page 91*)

Whither Aerospace Industry Research Management?

Lewis A. Rodert, FIAS, *Lockheed Aircraft Corporation*

THE ADVANCE of technology increasingly determines the course of human destiny, and research is the only known practical method of advancing technology. Yet, research in private industry is a strange activity. It requires long-range faith with large sums of money, and in the day-to-day events of industry pure research is often considered nonproductive and an overhead charge. Research at the basic level is not wholly accepted in America partly because of our strong frontier traditions and austere living of the early years. There still remains more than a trace of anti-intellectualism in our land today. Still we know that research means survival, and that the concept of research as an essential foundation for survival reaches into national and social, as well as industrial, areas of interest.

Some firms in our country have supported industrial research for many years and recognize the importance of *in-house* investigations as a prime factor in company growth. National Science Foundation statistics have shown that firms having the most rapid growth invest upwards of two per cent of gross sales value in research. Experience has also shown the wisdom of investment in basic research[1] even though the waiting period for recouping the investment may be somewhat longer than for development profits. Although the airplane industry leaned heavily on the fruits of research and expended large sums in development, evaluating, testing, and engineering, there has been a lack of familiarity in research.

An analysis of U.S. research by the Army[2] led to the view that "although the world's leader in technology, our contribution to pure science has not been impressive." Basic research in our industry has for a long time lagged behind that of other technologically oriented industries.[3] Basic research is needed because we are now working at the periphery of technical knowledge.[1] Some industrialists hope that university research will meet the nation's needs for the advance of science. Experienced industrial leaders have taken other views and concluded that the scope of university research is not sufficiently large to supply basic data needed for industrial growth.[4]

There is also the view that the government will fill the science gap. It is true that government R&D budgets have grown. The National Science Foundation reports that the Federal government funded about $7.7 billion for R&D in 1960. But only about six per cent of Federal R&D funds in 1960 went to basic research, and only about 1/10 of government funded basic research was done in private industry.

Analysis

Having stated the problem, some factors to be considered will be reviewed before going on to a discussion of aerospace industry research management. Stated simply,

$$\text{Research Ingredients} = \text{Personnel} + \text{Facilities} + \text{Support} + \text{Management}$$

Under suitable conditions research personnel are available and can be assigned to research work. A study of 1954 research personnel statistics[1] showed that private industry had 52,000 engaged in research compared to 16,534 in colleges and universities. A more efficient use of technical manpower would make even more personnel available for research in industry. When all other problems have been solved, the limitation in the number of persons who will become qualified for scientific research will be a critical problem.[5] In the view of this writer, we have not yet reached this point. Personnel, facilities, and support are today available to those able to make the investment and who have faith that the returns will ultimately be justified. The critical element in the equation above is the *research management* input. If the quality of research management is high and the owners continue to have faith in research (and re-

Competent research management is necessary to preserve and advance the concept of research as an essential foundation for the survival of national, social, as well as industrial, areas of interest.

search management), research results can cause the company to prosper. It is of interest to examine the ingredients of research management. Simply,

Research Management = Direction + Planning + Coordination + Environment

Research direction starts at the top with a policy that company funds will be expended for the purpose of extending technical knowledge on which the industry is based, with the faith that the investment will be returned. Direction is given strength by the responsibility, authority, capability, and support assigned.

Planning also starts at the top with the establishment of the company's long-range economic objectives spelled out in terms of sales goals and product areas (some of which may stand unidentified). Planning continues with all sub-plans in harmony with the gross sales long-range projection, including research plans. It is the responsibility of research management, in cooperation with the scientists, to interpret company economic plans in terms of research programs and to execute these programs in the research organization. Planning, therefore, is a continuous line from top management to the individual research scientist. Difficulty arises because of the divergence between the long-range nature of the research process and the necessity for top management to be concerned with today's business. Holding to the research plan requires steadfastness and continuous fiscal support for the long-range goals. The interweaving of research plans with fiscal plans just noted, and with market planning as basic guide lines, is indicative of the need for coordination at many points.

It is difficult to say just where coordination should stop. If research is as important as we believe, and if the national security is so critically involved in the advance of science, then the future may well bring an increase in research coordination, even between competitors, not presently contemplated. In the transient period, while research is growing to maturity, research coordination is essential among many company functions. As the scope of responsibility and authority of research management broadens, the necessity for coordination diminishes and the need for communication then becomes acute. However, there will always remain a minimum level of coordination required between research activities and other company activities along horizontal lines of communication.

Environment and organization are closely related. Without a climate in which creative work can prosper, the research investment will not produce contributions to science. The distinguishing feature of a scientist is his intellectual specialization. He is more apt to be oriented toward his profession[7] than the company. He desires an autonomy from company authority, but acquiesces to his scientific peers.

Another factor in environment is the staff size. Unless the size of the research organization is above a critical value, the magnitude of which is dependent on centralization, effective cross-breeding of ideas fails to materialize. The (*Continued on page 62*)

Mr. Rodert, Research Assistant to the Chief Scientist, is responsible for fundamental research planning at Lockheed (California Div.), and in this article draws freely upon a store of knowledge gained over almost three decades of aeronautical research work. His contributions in this field have brought him honors from the Institute of the Aerospace Sciences, American Meteorological Society, The Franklin Institute, Flight Safety Foundation, and the University of Minnesota. In 1947, he won the Collier Trophy, being cited for his "pioneering research and guidance in the development and practical application of a thermal ice-prevention system for aircraft." His electon as an IAS Fellow came in 1955. Mr. Rodert's professional associations include 19 years as a NACA (now NASA) Aeronautical Research Scientist and work on several NACA specialized groups. He is author of more than 40 NACA Reports, and many papers presented before IAS, ASME, and SAE assemblies. He is a native of Missouri, and was graduated from the Univ. of Minnesota with a B.A.E. degree.

Design Implications of
Creep in Pressurized Cylindrical Shells

Ivan Rattinger, AFIAS, *Aerospace Corporation*

Joseph Padlog, AIAS, *Bell Aerosystems Company*

RECENT TECHNOLOGICAL ADVANCES have permitted vehicle flight speeds and operational life to be increased. Accompanying these increases have been a parallel need to raise the operating stress and temperature and ever-greater demands for structures of higher efficiency and reliability. To meet these demands, many new temperature-resistant alloys are being developed, and older, more conventional materials are undergoing a re-examination in an effort to widen their range of application.

An additional factor demanding consideration is that of development cost and time. In the past, the cost of performing material evaluations has, to a large extent, been borne by other industries with similar needs. However, future vehicle requirements have extended the operational environment sufficiently beyond that encountered in these industries to demand solutions to future problems almost entirely from within the aircraft industry. Also, according to past experience, the time required to develop a new alloy is extensive, and likely to increase as a result, in part, of existing limitations on the availability of the necessary test facilities. Further, processing and fabrication techniques may be expensive and time consuming. Thus a dual criterion is brought into being. On the one hand, there is a need for evaluating materials separate from, yet anticipating their use in, advanced vehicles. On the other hand, attention should be limited to the more promising of these materials and only to those combinations of time and temperature for which these materials are efficient.

Additional complexities are introduced in future designs by the presence of new modes of failure, one of the more important of these being due to creep rupture. Many of the components subject to this failure phenomenon have not been previously

A portion of this work was sponsored by the Special Projects Branch, Aircraft Laboratory, Wright Air Development Center, Wright-Patterson AFB, Ohio.[1]

The authors wish to express their appreciation to Miss Mary Faron for performing the necessary calculations, and to their associates who contributed to the efforts of the subject study.

Mr. Rattinger received a B.Aero Eng. and M.Aero Eng. from the Polytechnic Institute of Brooklyn in 1950 and 1951, respectively. For the following 3 years he was employed as a structures research engineer at Bell Aircraft Corporation. He served as an aeronautical engineer in the U.S. Army from 1954 to 1956; he then returned to Bell Aircraft until 1959. In 1957 he received a M.S. in Engineering from the University of Buffalo where he was also a lecturer in engineering. From 1959 to 1960 he was a Member of the Technical Staff at the Space Technology Labs. Since September 1960 he has been employed at Aerospace Corporation, Los Angeles, specializing in structures analysis and research. Mr. Rattinger is an Associate Fellow of the IAS.

Symbols

a	=	cylinder radius (nominal or initial), in.
$\dot{a}$	=	instantaneous cylinder radius, in.
B	=	proportionality factor of true stress-true strain rate relation
C_{cp}	=	creep function
e	=	base of natural logarithms ($e = 2.71828\ldots$)
n	=	exponent of true stress in the true stress-true strain rate relation
p	=	tank internal pressure, psi
t	=	cylinder wall thickness (nominal or initial), in.
$\dot{t}$	=	instantaneous cylinder wall thickness, in.
T	=	temperature, °F.
β	=	constant of proportionality in the effective stress-effective strain relationship
$\epsilon_1, \epsilon_2, \epsilon_3$	=	principal strains at a point, in./in.

- *Estimates of creep deformations and time to failure of pressurized cylindrical shells are presented and compared with test results.*
- *Complexities introduced by time-varying stresses and temperatures are also hypothesized.*

Mr. Padlog is a Structures Research Engineer in the Aerospace Engineering Department of Bell Aerosystems, Buffalo. He received the Bachelor's and Master's degrees in Aeronautical Engineering from New York University in June 1949 and 1950, respectively, and a Master of Science in Engineering from the University of Buffalo in 1957. He has been with Bell Aerosystems (formerly Bell Aircraft) since June 1950, holding positions as static test engineer, structures analyst, research engineer, and project engineer for several WADC research contracts. For the past 6 years he has been associated with elevated temperature structural problems. Mr. Padlog is an Associate of the IAS.

analyzed or tested under current conditions or in the parameter range of current interest. Thus the benefit normally derived from past experience may be limited, and the applicability of previous work may be questionable.

One of the major components for which this state of affairs exists is that of a cylindrical, thin-walled, pressurized shell which generally serves as the main propellant tank in current and near-future high-speed vehicles. This problem is further aggravated by the fact that the allowable amount of creep in a pressurized shell is severely limited by the manner in which creep is experienced in a structure of this type. It is evident that any creep deformation results in an increase in the tank diameter and a reduction in wall thickness. Accompanying these changes is a rise in the operating stress level and, correspondingly, the rate at which creep progresses. Hence, in time, an unstable situation may develop. It is necessary, therefore, to be able to predict the time to failure by this mechanism.

Thus, this paper develops a method whereby estimates of the creep deformations and failure times of cylindrical shells operating at uniform elevated temperature and constant applied pressure may be rapidly made. Further, to permit maximum use of previous work, the solution presented allows these estimates to be made from conventional uniaxial creep data. Test-theory comparisons are then

(*Continued on page 97*)

ϵ	=	conventional strain, in./in.
$\bar{\epsilon}$	=	effective strain, in./in.
$\dot{\epsilon}$	=	true strain, in./in.
θ	=	time, hours
θ_{cr}	=	theoretical creep-rupture time, hours
σ	=	conventional stress, psi
$\sigma_1, \sigma_2, \sigma_3$	=	principal stresses at a point, psi
$\bar{\sigma}$	=	effective stress, psi
$\dot{\sigma}$	=	true stress, psi

Subscripts

c	=	circumferential
cp	=	creep
cr	=	critical
l	=	longitudinal
r	=	radial

Fig. 1. Cylinder geometry and coordinates.

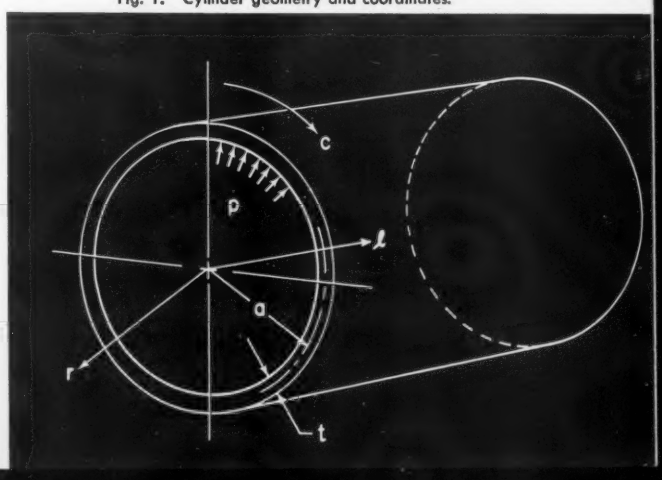

B. H. Goethert, AFIAS, ARO, Inc.

Characteristic altitudes for the change of the base flow pattern are determined—particularly the critical altitudes for flow reversal from atmospheric air flowing into the base to backflow of hot exhaust gases toward the base. Significant flow parameters—base pressure, heat flux, and base thrust increments—are calculated and presented in graphs.

Base Flow Characteristics of

MULTINOZZLE EXHAUSTS have recently been incorporated in the design of rocket-powered airplanes and missiles in an increasing number of applications. In some cases, such multinozzle arrangements have resulted from the installation of more than one rocket motor in the base of the vehicle because suitable rocket engines with a sufficiently large thrust were not available. In other cases, multinozzle exhausts were fitted to a single rocket chamber because such nozzles require a shorter exterior length and consequently save space and weight. Also, the multinozzle arrangement offers a number of advantages from the point of view of control because the nozzles may be used in pairs and deflected in opposite directions.

Because of the interaction of the individual exhaust jets with each other and with the external flow, a complex flow pattern occurs with multinozzle arrangements, leading frequently to intense recirculation in the base region and to backflow of exhaust gases into the missile base area. Experiments and theory show that extremely intense backflow can occur when the multinozzles are arranged in a circular pattern. Because the recirculation of hot exhaust gases can have serious effects on the heat flux and on the pressure distribution at the base of a missile, exploratory experiments and theoretical calculations were carried out to determine quantitatively the magnitude of these effects for some typical cluster-nozzle arrangements.

For cold-flow model tests, the similarity rule relating hot rocket exhausts to cold air exhausts is applied according to reference 1. According to this similarity rule, the chamber pressure of the cold air model is adjusted so that the nozzle exit pressure is

ARO, Inc., is the operating contractor of the USAF's Arnold Center, ARDC, at Tullahoma, Tenn.

The author wishes to acknowledge gratefully the assistance of the ARO staff in performing the experiments and calculations presented in this paper—in particular, Messrs. Williams, Towery, and Matz for the cold-flow model testing, and Mr. Sheraden for the calculations of the theoretical investigations

Symbols

A^*	=	nozzle throat area
A_e(or A)	=	nozzle exit area
A_R	=	total exit area of all rockets
A_V	=	total vent area
c_T	=	thrust coefficient = $T/p_R A^*$
d_c	=	diameter of circle through nozzle centers
d_e	=	nozzle exit diameter
d_m	=	effective interference diameter
G	=	mass flow per unit width
I_1	=	mass flow coefficient
I_{1j}	=	mass flow coefficient for jet boundary
L	=	length in circumferential direction
M	=	Mach number
m_R	=	total mass flow of all cluster rockets
p	=	static pressure
p_B	=	base pressure
p_R	=	rocket chamber pressure
q	=	heat flux per unit area
s	=	distance between centers of adjacent rockets
T_R	=	total thrust of all nozzles
u	=	velocity in mixing layer
u_1	=	velocity of exhaust jets

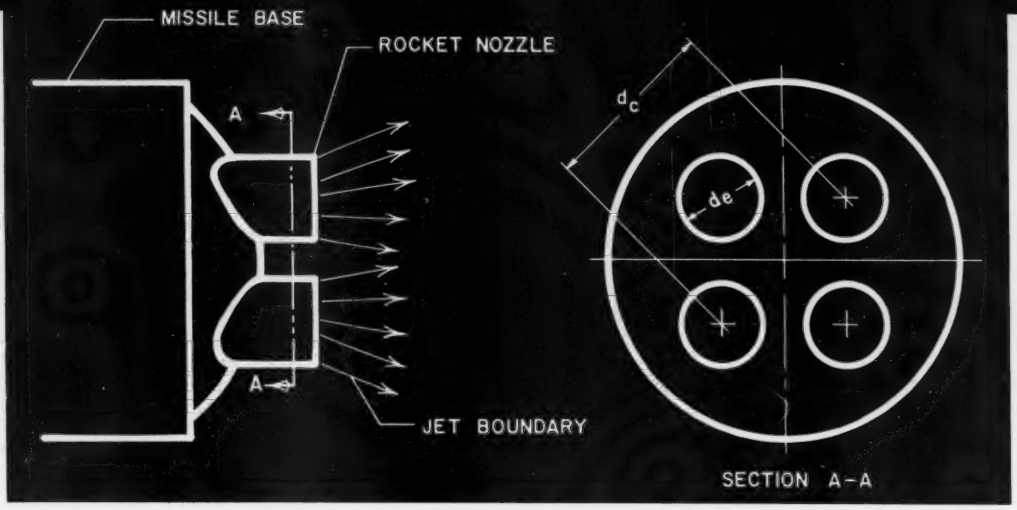

Missiles With Cluster-Rocket Exhausts

equal in both hot and cold flow. Furthermore, the nozzle area ratio is selected so that the pressure sensitivity of the exhaust flow with respect to the flow direction is kept equal for both hot and cold flow—that is,

$$(1/p)(dp/d\theta) = \text{constant}$$

or

$$\gamma\,(M^2/\sqrt{M^2 - 1}) = \text{constant}$$

It was shown in experiments that (see Fig. 7) this similarity rule correlates cold model data satisfactorily with hot rocket data.

---

u_{1max} = maximum velocity for $p \to 0$
w = shroud width
y, x = coordinates
γ = ratio of specific heats
Δm = bleed mass flow
ΔT = thrust increment
Δx = forward shift of x mixing layer origin
η = $\sigma x/y$ = parameter
θ = flow angle or nozzle exit half angle
ρ = density
σ = $(12 + 2.758)\,M$
ζ = flow coefficient

Subscripts

B = base
D = discriminating streamline
e = nozzle exit
R = rocket
SH = shroud
t = total pressure
1 = free jets
2 = conditions downstream of interference shock
∞ = ambient static conditions

(I) Characteristics of Four-Nozzle Clusters

(1) *Qualitative Results*

Some cold air experiments were conducted for a four-nozzle cluster designed to simulate hot rocket exhaust for $\gamma = 1.20$, an expansion ratio of each nozzle of $A/A^* = 11$, nozzle spacing corresponding to $d_c/d_e = 1.9$, and a nozzle exit angle of 17.5 deg. or half-angle (Fig. 1, headpiece). Each individual nozzle had an exit diameter of approximately $d_e = 1.0$ in. The flow pattern in the base region of the model was made visible by means of small dust particles which were ejected as a tracer through a hole in the model base center. (*Continued on page 108*)

Dr. Goethert has a B.S. in mechanical engineering from the Techn. University, Hanover, Germany; an M.S. in aeronautical engineering from the T.U. in Danzig; and a Doctor of Engineering degree in aeronautical engineering from the T.U. in Berlin. Before coming to this country in 1945, Dr. Goethert was Chief, High-Speed Aerodynamics, in the DVL Research Institute for Aerodynamics in Berlin. Prior to joining ARO, Inc., in 1952 as Chief of the Propulsion Wind Tunnel, he was consultant and section chief for wind-tunnel testing at WADC. He was named Chief of the Engine Test Facility in 1956 and held that position until he was named Director of Engineering in November 1959. As such, he is responsible for programs of research, development, and evaluation, utilizing the technical facilities of the Arnold Center at Tullahoma, Tenn. He is an Associate Fellow of the IAS and a Fellow of the ARS.

Economics of Instrumentation Precision for Space Vehicle Development

Some of the major ways that instrumentation precision affects testing costs, and three examples of cost savings resulting from accuracy improvements.

V. R. Boulton, AFIAS, *Aerojet-General Corporation*

THIS PAPER presents some observations resulting from our test experiences at Aerojet's Sacramento Plants on the effects of instrumentation precision on testing costs. This experience encompasses over 20,000 tests during the past 5 years on rocket propulsion systems, subassemblies, and components for application to more than 20 different weapon systems or space vehicles. The cost of testing is a major part of the development costs of large advanced weapon systems. In some cases it is as much as 70 per cent of the total cost when the cost of the test hardware and the analysis of the test data are included. Therefore, the potential savings to be made by reducing the costs of testing are tremendous. One of the factors that can have a significant effect on testing costs is the accuracy of the information obtained from the tests.

Within the Soviet Union considerable emphasis on a national scale is being accorded the area of improved measurements. In an address to the 21st Congress of the Communist Party of the Soviet Union on the "Development of the National Economy of the U.S.S.R. in 1959–1965," Nikita Khrushchev spent more than 10 min. discussing the need for increased efforts and results in the fields of standards and metrology. In a Soviet publication discussing this address the following statement was made: "...It is known that the uniformity, correctness, and correct employment of measures and measuring devices is a matter of great importance for the national economy, since the use of incorrect measures and measuring devices causes unproductive losses, leads to an increase in production rejects, and to an incorrect assessment of material values; it also fails to ensure the interchangeability of components and subassemblies of mechanisms, and gives rise to a number of other difficulties and losses in the national economy." [1] The fact that measurement accuracy is being given attention and emphasis at this level in the Soviet Government indicates the importance which they feel it warrants. It is surprising that so little has been said in the literature of this country on this subject. It is a subject that warrants a considerable increase in attention.

Some of the major ways that instrumentation precision affects testing costs will be discussed, and three examples are presented wherein the cost savings resulting from accuracy improvements are analyzed.

Primary Considerations

The primary effect of instrumentation precision on test costs is that the number of tests required is a sensitive function of the accuracy of the test results. This is clear when we examine the reasons for which tests are conducted. Tests are conducted in order to obtain the information necessary to determine if a system performs in the manner predicted by the designer, and to obtain information on functional relationships required to refine the designs. Tests are conducted to determine the limits over which the design assumptions are valid. Tests are conducted to determine the reliability of the materials, components, and systems which are produced.

Ideally, a measuring system should be an order of magnitude more repeatable and accurate than the

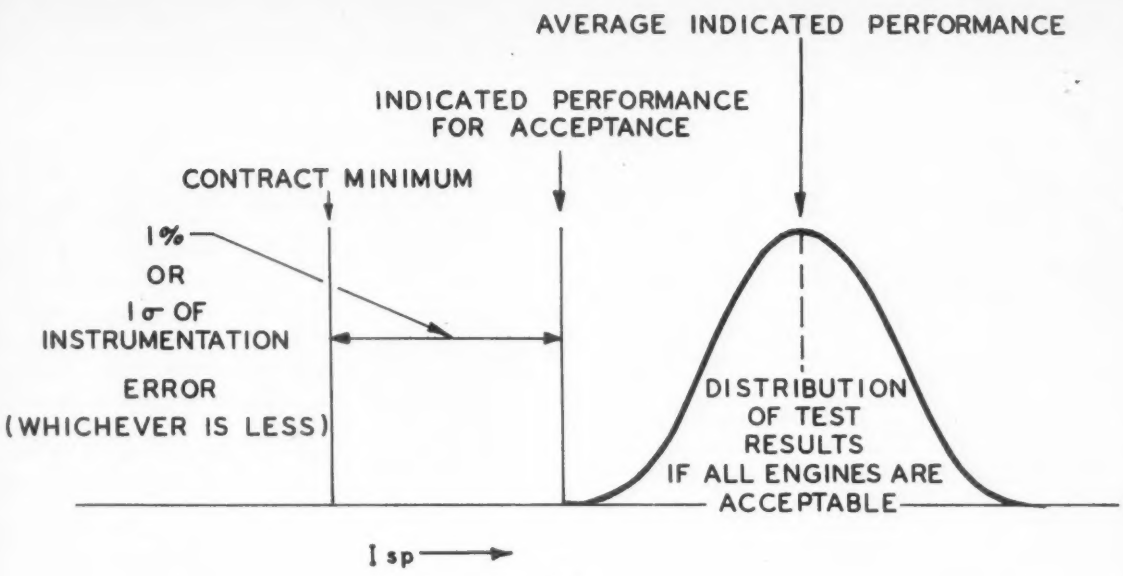

Fig. 1.

system under test so that test results can be accepted confidently as representing the performance of the test item under evaluation, and so that variations in the results from test to test represent primarily the variations in performance of the item being tested. Realistically, the repeatability of most measuring systems is hardly as good as that of the systems they are used to evaluate—at least this is true of present day rocket propulsion systems. Therefore, statistical techniques must frequently be used to evaluate performance against specifications with the test data obtainable. As the propulsion system designs have become more refined and as the requirements placed upon their performance have become more stringent, the number of tests required to adequately evaluate the designs and the reproducibility of the hardware has increased. The uncertainty in the evaluation results provided by the non-repeatability of the measuring system is, at present, much too large.

Increasing the number of tests required increases program costs by: (1) increasing the size of the test facilities required; (2) increasing the amount of hardware produced for testing purposes; and (3) increasing the total testing effort involved, including the planning, logistics, operating, and analyzing of results.

The money spent in increasing the test population to compensate for measurement error serves the needs of only the immediate program, whereas money spent to increase measurement accuracy results in improved equipment which will provide savings on a continuing basis.

Delays or wrong decisions caused by uncertainties due to insufficient precision in the information available can be very costly, particularly in a program which may be costing several million dollars a month.

Examples

Three examples drawn from rocket static testing experience illustrate the economic effects of instrumentation error.

(1) Economic Aspects of Demonstrating Minimum Allowable Performance

This example involves the problem of demonstrating the specific impulse of a large liquid rocket engine to be above a contractually required minimum. The requirement as stated (*Continued on page 64*)

The author is an electrical engineer who has specialized in rocket instrumentation systems, having direct technical responsibility for these at both Aerojet-General's Solid and Liquid Rocket Plants, and assisting in management of all testing activities. Now Assistant Manager, Test Division, Sacramento Plants, Mr. Boulton became associated with Aerojet in 1949, and was assigned to the Titan Program in 1955 with his firm's entry into the large liquid rocket engine field. He was given responsibility for design of instrumentation and control systems required for testing. Results were several state-of-the-art improvements, including development of a highly accurate stabilized DC amplifier, a standardized transducer system, and rapid digital data handling system. He received a B.S. degree in E.E. with honors at the State University of Iowa, and pursued advanced studies in physics at C.I.T. He is former chairman of the AIEE Technical Committee on Aircraft and Flight Test Instrumentation.

analyze—will usually lead to a new cycle. This process is applied to at least four phases (Geckler[8]) of a rocket's life cycle (Fig. 1):

Initial development phase: During this phase, certified evidence is to be obtained to assure performance feasibility and to demonstrate that the basic design is capable of meeting proposed specification requirements.

Proof phase: These tests are performed to establish the reliability and reproducibility of performance. The results of the development and proof tests should be analyzed together to pinpoint potential trouble areas or to indicate readiness to enter qualification tests.

Qualification phase: This is the last stage prior to mass production. It is the qualification of the rocket for unlimited use within an applicable environmental envelope, as well as qualification of the complete manufacturing process. After this phase, all tests should be analyzed to obtain the best estimate of reliability and performance. The overall statistical design should pinpoint trouble spots exactly if such exist.

Production phase: This is the phase of mass production.

It is obvious that these phases are interdependent. However, historical records indicate, unfortunately, that the test programs associated with these phases are frequently planned independently and the data obtained therefrom are analyzed independently of the other. The fact that they are not independent strongly suggests that the experimental design utilized should consider the amalgamation of the data from all of the first three phases—that is, those phases prior to mass production. To pinpoint potential trouble areas accurately and to obtain the best estimates of reliability and reproducibility, all data generated should be analyzed together when possible. Changes in engineering design might complicate and limit the amount of data that can be amalgamated. However, unless a major engineering modification is effected, data obtained can at least be composited for analysis to detect gross differences. Another important aspect of continuous development is that tests are performed sequentially so that the results of early tests may be available before undertaking later tests.

In the initial stages of a complete development program, interest lies mainly in locating large differences of environmental effects. Large differences will usually require substantial design modifications and therefore should be discovered as early as possible. Small differences will usually require only minor alterations and consequently are not of major importance in the early stages of development programs. These differences, however, become important as the program progresses. This philosophy is adopted because of the tremendous economic savings.

Environmental Envelope for Experimentation

Since development, proof, and qualification testing should be compatible with requirements established for the end item, it should be emphasized that the end item must be acceptable for unlimited use within an applicable environmental envelope. Thus, in establishing the overall experimental program, it is necessary to establish test limits which adequately describe the operational environmental envelope. An appraisal of potential environmental factors affecting most rockets indicates that these factors can be categorized into the following groups:

Effects due to

(a) Firing temperature, F.
(b) Aging, A.
(c) Environmental temperature cycling, T.
(d) Motion or vibration, V.
(e) Shock, dropping, or rough handling, H.
(f) Inclement weather, W.

Table 1. Six environmental factors at two levels.

			F_0				F_1			
			A_0		A_1		A_0		A_1	
			T_0	T_1	T_0	T_1	T_0	T_1	T_0	T_1
V_0	H_0	W_0	D	Q	Q	P	Q	P	D	Q
		W_1	Q	P	D	Q	D	Q	Q	P
	H_1	W_0	Q	D	P	Q	P	Q	Q	D
		W_1	P	Q	Q	D	Q	D	P	Q
V_1	H_0	W_0	Q	D	P	Q	P	Q	Q	D
		W_1	P	Q	Q	D	Q	D	P	Q
	H_1	W_0	D	Q	Q	P	Q	P	D	Q
		W_1	Q	P	D	Q	D	Q	Q	P

Table 2. Tabulation of 15 Effect-Contrasts and Their Aliases for Development Tests.

1	F, -AW, -FTVH, AWTVH
2	A, -FW, -ATVH, FWTVH
3	T, -VH, -FAWT, FAWVH
4	V, -HT, -FAWV, FAWTH
5	H, -TV, -FAWH, FAWTV
6	W, -FA, -WTVH, FATVH
7	FT, -AWT, -FVH, AWVH
8	FV, -AWV, -FTH, AWTH
9	FH, -AWH, -FTV, AWTV
10	AT, -FWT, -AVH, FWVH
11	AV, -FWV, -ATH, FWTH
12	AH, -FWH, -ATV, FWTV
13	TW, -FAT, -WVH, FAVH
14	WV, -FAV, -WTW, FATH
15	WH, -FAH, -WTV, FATV

This seems to be an exhaustive set of environmental conditions. The next decision is to determine the number of levels for each environmental effect. It is noted that usually the experimental program is not required to describe a complete response surface. Interest is primarily in determining feasibility, reliability, reproducibility, etc., within the boundary of the environmental envelope and with minimum amount of testing. Unless there is some danger of destroying the test vehicle, it is suggested that each environment be applied only at its peripheral values. If there is a risk of the vehicle being destroyed by the test, the values of each environmental factor should be backed away sufficiently from the boundary of the environmental envelope to place losses of test specimens at an acceptable minimum. It is noted that, if testing is done at the boundary of the environmental envelope, an estimate of minimum reliability is obtained—that is, the reliability of the rocket will be better than that indicated by the test program. This might be considered as some type of safety margin.

Proposed Test Plan

A design based upon the concept of continuous development is shown in Table 1. The subscript 0 refers to either the absence of that environment or its lower level, whereas the subscript 1 refers to its presence or higher level. For example, F_0 refers to the cold firing temperature, and F_1 refers to the hot firing temperature. Similarly, V_0 represents no vibration, whereas V_1 represents a peripheral vibration.

This design is a factorial experiment consisting of three blocks of fractional replicates. The first block is a quarter-replicate, the second block is another quarter-replicate which is orthogonal to the first, and the third block is a

Total cryogenic control systems capability *for missiles and spacecraft...*

AIRESEARCH designs, develops, manufactures and tests a *complete* line of cryogenic valves and controls in individual packages or complete systems for missiles, space vehicles and related ground support equipment.

The superior reliability of AiResearch cryogenic systems and components is backed up by more than 20 years of experience as the largest producer of valves and controls in the aircraft and missile industries. This capability includes liquid and gaseous fuel and oxidizer components and systems operating at temperatures ranging from −420°F. to more than 2000°F.

AiResearch leadership in all of these fields is supported by the most complete cryogenic testing and manufacturing facilities available. All AiResearch missile components are designed and qualified to meet or exceed requirements of military specifications.

Inquiries should be directed to Control Systems, AiResearch Phoenix Division.

1. *Airborne pressure regulator and shutoff valves for propellant tank.*
2. *Airborne check valves.*
3. *Ground-to-missile fill and drain systems for fuels and oxidizers.*
4. *Airborne pressure relief regulator and vent valves for propellant tank.*
5. *Airborne turbo-pump speed sensors.*
6. *Airborne liquid propellant shutoff valves.*
7. *Ground support pressure regulator and shutoff valves.*

THE GARRETT CORPORATION

AiResearch Manufacturing Divisions

Los Angeles 45, California • Phoenix, Arizona

Systems and Components for: AIRCRAFT, MISSILE, SPACECRAFT, ELECTRONIC, NUCLEAR AND INDUSTRIAL APPLICATIONS

Table 3. Coded chamber pressure results (psia).

			F_0				F_1			
			A_0		A_1		A_0		A_1	
			T_0	T_1	T_0	T_1	T_0	T_1	T_0	T_1
V_0	H_0	W_0	7.7	9.8	13.9	(13.4)	18.4	(17.0)	19.1	22.8
		W_1	9.5	(9.0)	9.5	15.4	16.6	18.2	22.5	(18.8)
	H_1	W_0	9.3	9.9	(11.1)	13.1	(16.6)	16.9	22.4	18.2
		W_1	(8.9)	11.3	13.3	12.9	18.0	15.1	(19.4)	22.4
V_1	H_0	W_0	9.6	9.7	(12.9)	14.6	(16.2)	18.3	23.2	18.4
		W_1	(8.8)	9.2	13.0	11.5	17.5	14.6	(19.9)	22.8
	H_1	W_0	8.0	8.9	13.4	(13.4)	19.3	(16.5)	19.6	22.7
		W_1	9.2	(8.5)	12.2	14.1	16.6	16.5	21.3	(21.1)

half-replicate which is orthogonal to the half-replicate obtained by adding together the two quarter-replicates. These blocks are performed sequentially, and, as the program progresses, information obtained from preceding blocks can be pooled to provide more precise estimates of treatment effects and experimental variation. Upon the completion of the program, all potential trouble areas are investigated.

The experiment was fractionated in such a way that all main effects and two-factor interactions in the first half-replicate are clear. This was done by using $FAWTVH$ as the defining contrast to split the factorial into half-replicates. The $+ FAWTVH$ half-replicate was further split into quarter-replicates by using $-FAW$ and $-TVH$ as the defining contrasts. This type of fractionation has the disadvantage that main effects are confounded with two-factor interactions in quarter-replicates. However, since during the development phase (wherein the first quarter-replicate will be tested) interest lies mainly in detecting large differences, this disadvantage is not critical.

The operational procedure is:

Development firings: Fire a motor designated by D (Table 1) under the environmental conditions specified. Continue firing until a motor has been tested under each of the 16 developmental environments indicated. If a gross defect occurs, the cause or causes should be identified and corrected. Begin pattern testing anew. When a complete pattern or 16 satisfactory firings have been obtained, analyze, make engineering changes indicated, and proceed to the proof testing phase.

Proof testing: Fire the 16 motors designated by P under the environmental conditions specified. These motors are, of course, fired one at a time sequentially. If a gross defect occurs, return to development work if necessary. If all 16 motors are successful, analyze the combined results of developmental and proof tests, make engineering changes indicated, and proceed to qualification testing.

It is of interest to point out that the second quarter-replicate is similar to the first in that all levels are reversed. The results obtained from each block may be added together to obtain a half-replicate which has all main effects and two-factor interactions clear. This, of course, is one of the major advantages in planning a program in this manner. All data can be amalgamated for an improved and efficient analysis. The blocking effect—that is, the effect of development tests versus proof tests—is confounded with the three-factor interactions $-FAW = -TVH$ and can be eliminated from the experimental error. Blocking in no way affects the estimates of the main effects and two-factor interactions when all results are combined for one overall analysis.

Qualification testing: Fire the 32 motors designated by Q under the environmental conditions specified. Again, these motors are fired one at a time sequentially, and, if a gross defect occurs, resort back to development work if necessary. If all motors are successful, qualification testing is complete and the motor is adjudged ready for mass production.

The 32 treatment combinations tested during the qualification phase constitute a half-replicate which is orthogonal to the half-replicate formed by combining the results from the first two blocks. Upon completion of the qualification testing, the results from all of the three blocks are pooled to form a complete factorial experiment. Again, it should be mentioned that any possible differences between development, proof, and qualification tests are blocked out and in no way affect the estimates of main effects, two-factor interactions or experimental variation.

There are several benefits to this approach. One is that with each phase of testing, motors are tested over a systematic region of the usage environment, and consequently, if the motor has any weakness in a particular region of the environmental envelope, the systematic testing will most likely discover this weakness. Second, by having tests in each phase of the motor life cycle complete a selected fraction of the total program, a complete package of information is obtained which can be used for analysis. These benefits are accomplished by utilizing the minimum number of motors to obtain the necessary information.

Normally, the order in which test motors are fired for each phase is determined by choosing both the motors and the environments for test at random. However, it is recommended that the motor firings for the development phase begin with the milder environments and proceed toward the more potentially hazardous environmental conditions. Initial firings under the milder environments give a measure of feasibility of the motor design. If the motor will not perform satisfactorily under the mild environments, it must be redesigned before other tests are applied. As soon as feasibility is demonstrated, other tests should be made as indicated above. Gradually increasing the severity of the test environments should provide trend information as to the susceptibility to hazardous malfunction and therefore minimize human hazards and damage to the test facility.

It is also recommended that the sequence in which the environmental factors are applied to the motor be compatible with the sequence encountered during the actual life cycle.

Analytical Procedure

After the completion of the development firings, a preliminary analysis can be made. Any conclusions, though, should be regarded as tentative since the estimates of all main effects con-

Table 4. Tabulation for Statistical Analysis of Development Plus Proof Firings.

Effect-Contrasts and Aliases	Total Effect	Rank i	Cumulative Percent P_i
FH, AWTV	0.1		
VW, FATH	0.1	2	4.8
FV, AWTH	0.5		
FAH, WTV	0.5	4	11.3
FAT, WVH	0.9	5	14.5
FA, WTVH	1.1	6	17.7
FAV, WTH	1.3	7	21.0
TH, FAWV	1.5	8	24.2
FTH, AWV	1.9	9	27.4
AW, FTVH	2.7		
AVH, FWT	2.7	11	33.8
W, FATVH	2.9		
VH, FAWT	2.9		
ATV, FWH	2.9	14	43.5
AT, FWVH	3.1	15	46.8
ATH, FWV	3.7	16	50.0
AH, FWTV	3.9	17	53.2
V, FAWTH	4.7	18	56.4
H, FAWTV	4.9		
T, FAWVH	4.9	20	62.9
FW, ATVH	5.3	21	66.1
HW, FATV	5.7		
TW, FAVH	5.7	23	72.6
TV, FAWH	5.9	24	75.8
FTV, AWH	7.7	25	79.0
AV, FWTH	8.5	26	82.2
FVH, ATW	10.9	27	85.5
TVH, FAW (BLOCKS)	11.9	28	88.7
FT, AWVH	13.5	29	91.9
A, FWTVH	51.7	30	95.1
F, AWTVH	116.3	31	98.4

Defining Contrast: I = +FAWTVH

tain confounded two-factor interactions. Table 2 shows the 15 orthogonal effect-contrasts and their aliases for developmental firings. The estimated experimental variation, however, can at least be used to determine some sort of upper limit on reliability of the rocket motor when compared with some standard requirement. It should be noted, at this point, that each main effect is estimated by eight firings at each level. This is true for all six main effects although only sixteen motors have been tested. This is called hidden replication by statisticians and is a result of planned experimentation. The estimated experimental variation applies to all main effects.

Upon completion of the proof firings, a more objective analysis of the observed results can be accomplished. This is done by pooling the results of the development and proof firings to obtain a full half-replicate of the experiment. Assuming all higher order interactions (three-factor and greater) to be negligible, the experiment now provides unbiased estimates of all main effects, two-factor interactions, and experimental variation. Statistical significance tests can be made to determine the existence or nonexistence of environmental effects, as well as any difference between development and proof results. Confidence limits on true environmental effects and reliability predictions can also be obtained.

The assumption that the higher order interactions are negligible can be tested at the conclusion of qualification testing. At this point the results from each phase are massed to obtain a complete factorial experiment from which all effects and interactions can be independently estimated. A test of this assumption can easily be made by using Daniel's[4,5] half-normal plotting technique. Hence, any trouble spots can be pinpointed and there will remain sufficient contrasts to yield a good estimate of experimental variation. As previously mentioned, any differences between development, proof, and qualification firings can be ascertained and in no way influence the estimates of main effects, two-factor interactions, or experimental variation.

Example

Coded average chamber pressure results (hypothetical) obtained during development, proof, and qualification testing of a particular rocket program are tabulated in Table 3. The six environmental factors and the manner of accumulation of data are in accordance with the discussion outlined above. The underlined observations are the results of the development tests, the parenthesized observations are the results of the proof tests, and the remaining observations are the results of the qualification tests.

In actual practice, the results of development tests would be analyzed before proceeding to proof tests, and the results of the proof tests would be analyzed before proceeding to qualification tests. Further, proof tests would not be started until all the development motors identified in Table 1 had test fired successfully. Similarly, qualification tests would not be started until all the proof test motors identified in Table 1 had fired successfully.

Since the analytical procedures are virtually identical for each stage of the program, only the results of the development plus proof firings will be analyzed here. A complete analysis of this example is given in reference 7. The statistical analysis of test results can be accomplished by utilizing standard analysis of variance techniques which can be found in any good statistical text. However, an alternative method of analysis for singly replicated 2^{p-q} factorial experiments suggested by Daniel,[4,5] commonly called "half-normal plotting," has certain advantages over standard analysis of variance techniques. This procedure will be utilized here.

In order to employ this procedure for the analysis of the development plus proof firings, we first calculate the 31 orthogonal effect-contrasts. These contrasts can be easily obtained by using a method given by Yates.[11] Details of this method are presented in Davies,[6] Bennett and Franklin,[1] and Cochran and Cox.[3] The 31 effect-contrasts (total effects) and their aliases are shown in Table 4. The contrasts are arranged in ascending order according to their absolute values. The ranks i are converted into cumulative per cents, $P_i = 100[i - (1/2)]/df$, where df indicates the total number of degrees of freedom (31 in this example). The contrasts are then plotted on the upper half of arithmetic probability paper, with the probability scale rewritten as $100 - 2P$, where P is the printed probability in per cent (Fig. 2). Omitting obviously discrepant points, a best-fitting straight line is drawn through these points and the origin. If the experiment is a null one—that is, if all the effects are equal to zero—then the standard error of the contrast sums σ_e is estimated by the 68 per cent point on the fitted line.

In this example, three contrasts—F, A, and FT—fall well to the right of the fitted line. Hence the experiment is certainly not null. The next largest contrast to FT is FAW, TVH which is confounded with blocks (development firings versus proof firings). Since blocks may well be significant, it seems appropriate to omit this contrast from error estimation. Omitting

NEW KODAK

METAL-ETCH RESIST

opens new chemical-milling applications

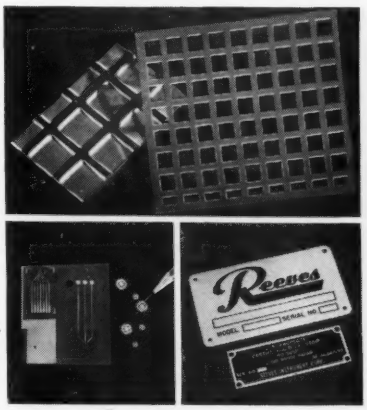

Speeds up, simplifies deep *etch* weight reduction and parts manufacture. Reproduces fine-line detail as in plating, dial and name-plate making. This new photographic process ends time-consuming handwork, results in high accuracy. Kodak Metal-Etch *Resist* withstands acids, alkalies, electrolytic fluids . . . adheres well to aluminum, titanium, magnesium, stainless and other alloy steels. High stability and strict uniformity simplify volume production. Send today for a detailed 16-page brochure that gives all the facts.

Text for this advertisement was set photographically.

No statement or suggestion is to be considered a recommendation or inducement of any use, manufacture or sale that may infringe on any patents now or hereafter in existence.

Graphic Reproduction Sales Division
EASTMAN KODAK COMPANY
Rochester 4, N. Y.
Please send me a copy of the booklet, "Etching, Chemical Milling and Plating with Kodak Metal-Etch Resist" (P-36).

Name _____
Company _____
Street _____
City _____
Zone ____ State _____

3-251

Kodak
TRADE MARK

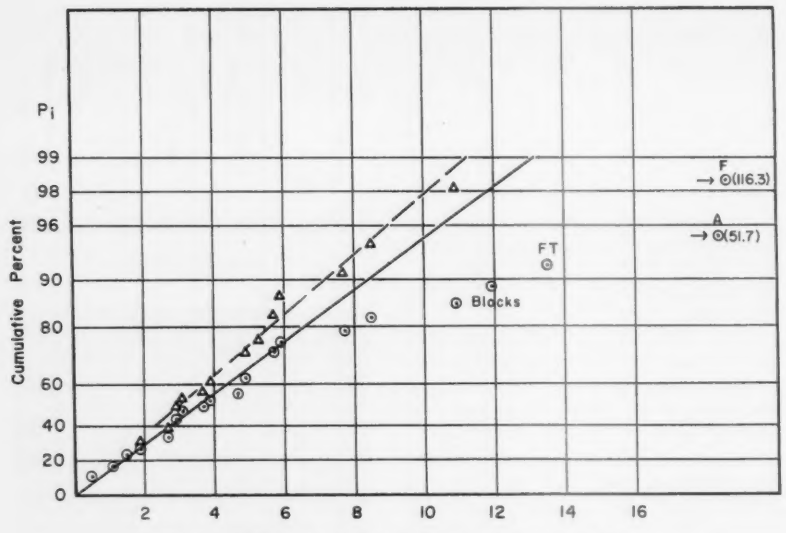

Fig. 2. Half-normal plot of development plus proof results.

these four contrasts, each P_i is recalculated using 27 degrees of freedom, and these points are replotted on Fig. 2. The Δ's represent the new points, and the dashed line the line fitted to these points. Since all of the Δ's fall very close to the new line, it is justifiable to assume that none of these contrasts are significant. Based on 27 degrees of freedom, the standard error of the contrast sums is estimated as 4.4. The estimate of the standard error of the contrast means is given by

$$\sigma = \hat{\sigma}_c/\sqrt{df + 1} = 0.831$$

To test the suspected contrasts for significance, use the test statistic

$$t' = y_k/\hat{\sigma}_c$$

where y_k is the smallest of the k contrasts it is desired to test, and $\hat{\sigma}_c$ is the estimated standard error of the contrast sums. The symbol t' is used to distinguish this statistic from the ordinary t-statistic commonly used in statistics. A detailed discussion of this statistic is given in references 5 and 2. For an experiment with 31 orthogonal contrasts, of which four are subject to test, the critical value of t' is 1.79 at the 0.05 significance level. In this example a t' of 2.70 is calculated, and therefore it is necessary to infer that all four of the effect-contrasts are significantly different from zero.

Since the *FT* interaction was significant, further investigation is advantageous in order to determine exactly how this interaction affects chamber pressure. By interaction is meant the differential response to one factor in combination with varying levels of a second factor applied simultaneously. Table 5 shows the average response of the *FT* interaction at the various levels. Statistical tests indicated that the interaction is caused by a difference due to temperature cycling at cold firing temperatures.

Table 5. Averages of *FT* Interaction

Levels	F_0	F_1
T_0	9.89	18.00
T_1	11.04	17.46

The estimated standard error of the contrast means can be used to place tolerance limits on chamber pressures. For example, for hot firing temperature for which the mean chamber pressure is 17.73 psi, 95 per cent of the time, 95 per cent of the motors will have a chamber pressure lower than 19.60 psi.[9]

The conclusions, summarized, are:

(1) The motor is sensitive to the firing temperature. The chamber pressure increases as the firing temperature increases.

(2) Aging increases the chamber pressure.

(3) The motor is sensitive to temperature cycling at cold firing temperatures.

(4) The chamber pressure of the proof motors has increased slightly over the development motors.

(5) An estimate of experimental variation is 0.831 psia.

(6) If all motors were fired at F_1, the upper tolerance limit is 19.60 psia—that is, 95 per cent of the time, 95 per cent of the rocket motors will have a chamber pressure less than 19.60 psia.

With these facts, a decision must be made to determine whether the motor is ready for qualification testing.

Conclusion

The experimental procedure presented in this paper provides an objective method for combining the test results from each phase of a continuous developmental program. This procedure is based upon the sequential application of orthogonal fractional replicates of factorial experiments. Although the procedure was discussed with respect to environmental testing of rocket motors, it is applicable to any continuous developmental program. A competent statistician would be able to determine the required experimental design to fit any particular program. It should be emphasized that this procedure utilizes the minimum number of test specimens required to obtain the information necessary to make decisions for progressive development.

References

[1] Bennett, C. A, and Franklin, N. L., *Statistical Analysis in Chemistry and the Chemical Industry*, John Wiley & Sons, New York, 1954.

[2] Birnbaum, A., *On the Analysis of Factorial Experiments Without Replication*, Technometrics, Vol. 1, No. 4, pp. 343–357, Nov. 1959.

[3] Cochran, W. G., and Cox, G. M., *Experimental Designs*, 2nd Ed.; John Wiley & Sons, New York, 1957.

[4] Daniel, C., *Fractional Replication in Industrial Research*, Proc. of Third Berkeley Symposium on Mathematical Statistics and Probability, Vol. 5, Univ. of California Press, Berkeley and Los Angeles, pp. 87–98, 1956.

[5] Daniel, C., *Use of Half-Normal Plots in Interpreting Factorial Two-Level Experiments*, Technometrics, Vol. 1, No. 4, pp. 311–341, Nov. 1959.

[6] Davies, O. L. (Ed.), *Design and Analysis of Industrial Experiments*, 2nd Ed.; Oliver and Boyd, London, and Hafner, New York, 1956.

[7] Garner, N. R., and Hartvigsen, D. E., *Experimental Designs in Development, Proof, and Qualification Testing of Rocket Motors*, Aerojet-General TR No. AQC58-1, Feb. 27, 1958.

[8] Geckler, R. D., *The Principles of Developing Solid Propellant Rockets*, Aerojet-General TM 220, June 1953 (main document classified).

[9] Lieberman, G. J., *Tables for One-Sided Statistical Tolerance Limits*, Industrial Quality Control, Vol. 14, No. 10, pp. 7–9, April 1958.

[10] Mood, A., *The Heart of a Reliability Program*, IRE Trans. on Reliability and Quality Control, June 15, 1960.

[11] Yates, F., *Design and Analysis of Factorial Experiments*, Harpenden, England, Imperial Bureau of Soil Science, Technical Communication No. 35, 1937.

Notices of all change of address should be sent to the Circulation Department, Institute of the Aerospace Sciences, Inc., 2 East 64th Street, New York 21, N.Y., at least 30 days prior to change of address.

One of a series of advertisements showing the breadth of Douglas experience being devoted to commercial, military and space-exploration projects.

DC-8
DOUGLAS DC-8
DC-8 can cross the country in 4¾ hours, flies the Pacific in 8½ hours, the Atlantic in 6½.
DC-7 was the first airliner to provide scheduled non-stop service coast-to-coast.
DC-6 appeared in 1946. By 1953 the "6's" were flying more than 500,000 route miles daily for 27 airlines.
DC-4 pioneered transocean flight. This 4-engine aircraft carried the brunt of the Berlin airlift.
DC-3 — Douglas built almost 11,000 of these famous 21-passenger airliners. Thousands are still in service.

Five big steps to a smaller world

How narrow the oceans have become! How small the world! And how quickly the shrinking has occurred!

Within a generation, man has stopped wondering if he would ever fly, and now asks how soon he will land on the moon.

Douglas, builder of the 5 great "DC" airliners that did so much to shrink the world you live in, is now at work on the great rockets and rocket ships which will shrink the solar system.

DOUGLAS

MISSILE AND SPACE SYSTEMS • MILITARY AIRCRAFT • DC-8 JETLINERS • TRANSPORT AIRCRAFT • ANTI-SUBMARINE SYSTEMS • AIRCOMB® • GROUND SUPPORT EQUIPMENT

Escape Capsule (Continued from page 15)

required to wear special protective clothing such as a pressure suit, ventilated suit, life vest, or parachute. His attire will consist normally of a standard-type anti-g suit, lightweight boots, and crash helmet.

(4) The accelerations on the pilot must, at all times, be within the limits of human tolerance as established by the Air Force Aero Medical Laboratory.

(5) An oxygen mask shall be available for emergencies, but shall not be required under normal aircraft operation.

(6) The capsule shall provide suitable shelter for the pilot after alighting on either land or water, even under extreme weather conditions.

(7) The pilot shall not be required to perform any functions, such as manipulation of controls or levers during the escape sequence, except the action which initiates the sequence.

(8) In order to obtain a realistic end item, the nose capsule is to be designed for use in an "F-104 type aircraft." It is not intended, however, that the capsule design presented herein be incorporated into the F-104. Instead, it is intended that the problem areas explored and the conclusions reached in this study will serve as a source of design data for designers of escape systems of new and different aircraft.

(9) "Off the deck" escape capability shall be provided. Although not specified in the initial design requirements from the Air Force, it was felt that safe escape should be provided throughout the entire low-speed range, and particularly for the case of low- or zero-velocity ground level ejection. Accordingly, this stipulation was included as a system requirement.

Escape Considerations

In its most general form, the purpose of an aircraft escape system is to remove a crew member from some perilous situation aboard an aircraft and to return him to safe surroundings in a condition such that he can carry out his duties and functions in a normal manner. For the purpose of this study, the escape sequence shall be considered to encompass that portion of time which elapses between the time the crew member decides to escape and when he is on the ground with sufficient protection and provisions to await rescue.

Within these limits, a typical escape may be broken down into the sequence of events outlined in Diagram A. This sequence holds for the complete range of escape conditions, with each event being critical to greater or lesser extent, depending upon the conditions at the time of escape. It also holds for the complete range of aircraft escape systems starting with the simple bail-out procedure, and extending through seat ejection, capsules and to devices for escape from space vehicles. The increase in complexity in going from the simple bail-out system to capsulation arises from the increased protection from environment and increased automation required for the crew member. In the simple bail-out, the crew member was physically capable of performing the separation and withstanding the aerodynamic forces, temperatures, and ambient pressures. This however is not true for present and future high-performance aircraft.

Discussion and Solution of Problems During Escape Sequence

Escape Problem

In the following paragraphs, the potential problems to be found during escape will be described along with their origin when necessary. A discussion will be made of methods to attack the problems followed by the proposed solutions for the capsule under consideration. The general escape sequence shown in the previous section will be used as an outline for discussing the problems.

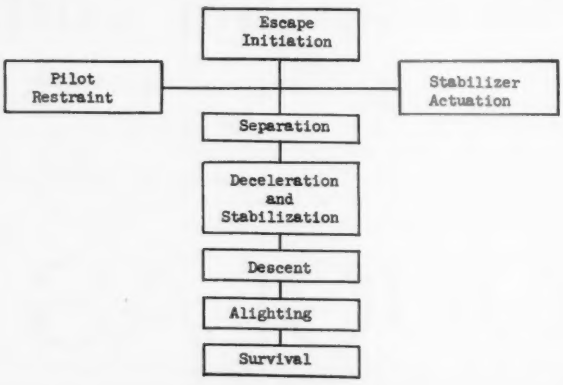

Diagram A.

(1) Escape Initiation

Although the initiation of the sequence is not one of the major design problems, it does require considerable thought if the required capability of the system is to be fully realized. The problem is to maximize the ability of initiating the system and to minimize the possibility of inadvertent initiation. The philosophy adopted in this design study is that escape is initiated only by *positive* action on the part of the pilot. Other approaches have been investigated such as automatic initiation, wherein sensors react to certain equipment or system malfunctions; and involuntary initiation wherein initiation is automatic if the pilot does not perform some task such as grasping the control stick, within a given length of time. Such methods may have merit in view of possible pilot incapacitation; however, at the present time it is felt that such a system is likely to be more of a hazard than a safety factor due to lack of reliability for automatic systems.

The action required of the pilot for initiation is very important since he must be able to perform such action while subjected to severe inertia forces and, upon completion of this action, must have his body in a position such that he may safely absorb the ensuing decelerative forces. Hand-grips, "D"-rings, and face curtains are used in current escape systems with the pilot physically supplying the power which fires pyrotechnic initiators. The hand-grip method of sequence initiation was preferred for the system in this study. There are two hand-grips at the forward end of the seat arm rests, either of which when raised initiates the escape sequence. The arm rest and grips then offer excellent support to the arms to help unload the spine during the rocket boost and to prevent arm flailing during the deceleration phase.

(2) Pilot Restraint and Stabilizer Actuation

Several functions must be performed prior to ignition of the separation rocket. To preclude the possibility of severe injury to the pilot under the high inertia forces, he must be properly restrained. All forces on the pilot, from all directions, must be sustained by the seat and harness system. In the proposed system, the harness is pulled tight for torso support. The arms are supported by the arm rest and hand-grip. The head is centered and restrained by guards that swing

into position from the sides. The legs are snatched back by a strap system normally stored under the instrument panel. These restraints are all pyrotechnically powered and tightly hold the pilot throughout the deceleration process and dynamic oscillations immediately after ejection.

The major pre-separation function involves the positioning of the stabilizers. Due to the large design aerodynamic pressures (2750 psf), and the high degree of instability of a basic nose capsule, the assurance of a stabilized configuration prior to separation is imperative. It would take only a fraction of a second to develop intolerable and fatal tumbling if stabilization were attempted during or after separation.

(3) Separation

Satisfactory separation and stabilization are probably the most difficult and important problems of escape under conditions of high aerodynamic loads. For the capsule under consideration which is mounted on the nose of the aircraft, very large forces are generated in the process of moving the capsule away from the basic airplane at high speeds; and the "off-the-deck" escape requirement dictates that the capsule move upward and gain sufficient altitude for parachute deployment. Some of the more important problems which develop in the separation process are as follows:

(a) Severing structural and communication connections with the remainder of the aircraft.

(b) Maintaining the integrity of separable structure and communication connections during normal aircraft operation.

(c) Providing positive movement away from the airplane under all conditions.

(d) Launching the capsule in the proper attitude and with a minimum of perturbations.

(e) Producing capsule dynamic motions and resultant decelerations safely within the limits of human tolerance.

(f) Minimizing reliance upon basic airplane for satisfactory separation.

(g) Precluding the possibility of collision with aircraft afterbody.

The net result of these requirements and design experience is that the attachment of the capsule to aircraft should be as simple as possible, and separation should be accomplished as rapidly and as positively as possible.

The "off-the-deck" escape essentially establishes the requirement for rocket propulsion during the separation. It would not, however, necessarily provide for getting the capsule away from the immediate vicinity of the aircraft at high speeds. Numerous methods were investigated for solving the problem of

Who is this man?

First, you should know a few things about him: He's responsible, as a man who leads others through new frontiers must be; he's a specialist . . . but a specialist with time for creative reverie; he welcomes new challenges and grows in learning and stature with whatever he faces; he's mature, dedicated, and inquisitive—traits of a true man of science. Who is he? He's the indispensable human element in the operations of one of the Navy's laboratories in California. Could he be you?

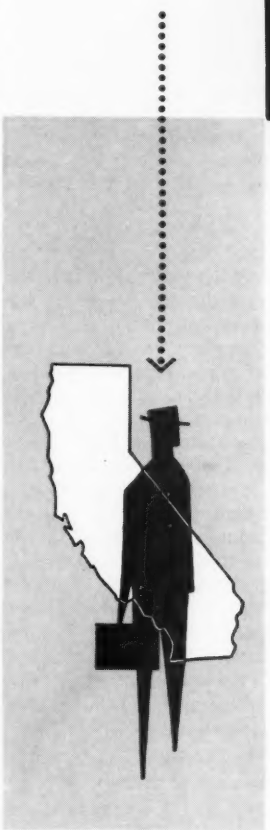

U. S. NAVAL ORDNANCE TEST STATION at China Lake and Pasadena: Research, development, testing, and evaluation of missiles, advanced propulsion systems, and torpedoes and other undersea weapons.

U. S. NAVAL ORDNANCE LABORATORY at Corona: Development of guidance and telemetry systems and missile components. Research in IR spectroscopy, magnetism and semiconductors, etc.

U. S. NAVAL RADIOLOGICAL DEFENSE LABORATORY at San Francisco: One of the nation's major research centers on nuclear effects and countermeasures.

U. S. NAVY ELECTRONICS LABORATORY at San Diego: One of the Navy's largest organizations engaged in the research and development of radar, sonar, radio, and acoustics.

PACIFIC MISSILE RANGE and U. S. NAVAL MISSILE CENTER at Point Mugu: National launching and instrumentation complex, guided missile test and evaluation; astronautics; satellite and space vehicle research and development.

U. S. NAVAL CIVIL ENGINEERING LABORATORY at Port Hueneme: Research, development, and evaluation of processes, materials, equipment, and structures necessary to the design, construction, and maintenance of the Navy's shore bases.

Openings for Aeronautical Engineers, Chemists, Civil Engineers, Electronic Engineers, Electronic Engineers (Digital Circuitry & Electro-Acoustic), Mathematicians (Test Data Processing & Analysis), Mechanical Engineers, Operations Research Analysts, Physicists.

The man we want must have an advanced degree, or a Bachelor's degree with at least three years' solid experience. He should contact . . .

Personnel Coordinator, Dept. E
U. S. Naval Laboratories in California
1030 East Green Street
Pasadena, California

U. S. NAVAL LABORATORIES
IN CALIFORNIA

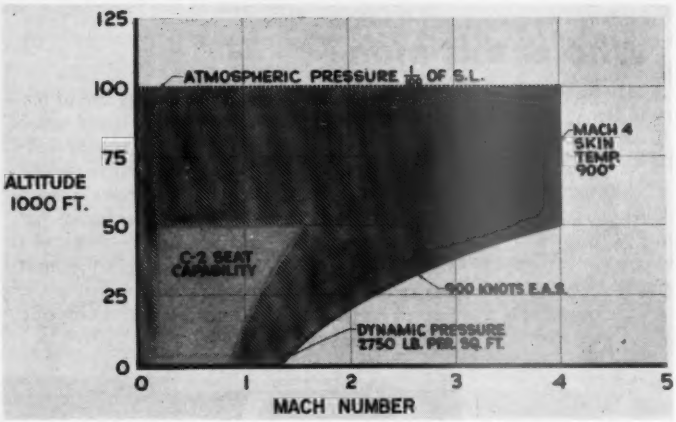

Fig. 2. Performance envelope.

the first few feet of capsule motion. Some of these were: rail systems similar to ejection seat mechanisms, pivot arms, bar linkages, and piston cylinder pushers. The first few feet of capsule travel during separation was a serious problem in the early preliminary design stages. The final proposed system which resulted from the study was evolved by tailoring the escape rocket thrust, thrust angle, and capsule drag to values which would allow essentially zero length launching with sufficient vehicle clearance at high air loads, but which would not impose accelerations beyond human tolerance at zero air loads. With no air loads, the acceleration due to rocket thrust peaks at about 20g and tapers off within the limits of human tolerance with a total duration of approximately 0.5 sec. The separation rocket thrust coupled with the aerodynamic lift and drag forces are such that the accelerations applied to the pilot do not exceed accepted limits anywhere within the performance envelope. Under maximum air-load conditions, the capsule moves forward and upward from the aircraft to perform clean separation. Analyses indicate that trajectories following rocket burnout are such as to preclude collision of the capsule with the aircraft afterbody.

Details of the actual structural and equipment disconnection present many design problems which are discussed in ensuring portions of this paper. Reliable operation of the various aircraft systems is a must during normal aircraft operation; yet a clean, rapid, and complete disconnection of these systems is imperative such that no binding or tip-off forces and moments are allowed to foul the separation sequence and capsule trajectory. A detailed discussion of these problems will not be attempted in this paper but may be found in reference 1.

The first two inches of capsule motion are guided by a nonbinding roller system, integral with the four structural attachments. This allows for one inch of motion to disconnect controls, electrical leads, air-conditioning ducts, etc. This short-guided portion of the ejection operation prevents tip-off problems, while at the same time insuring proper disconnection of equipment.

(4) Deceleration and Stabilization

The basic problem during this phase is to decelerate the capsule within the pilot's physical limitations but at a sufficiently high g level so as to minimize the distance traveled after ejection. The distance traveled after ejection is particularly important for the case of high-speed/low-altitude escapes wherein the speed, dive angle and altitude from which escapes can be made successfully are dependent upon decelerating to parachute deployment speed. It is fortunate that the limits of human tolerance allow high deceleration initially such that the distance traveled for a given speed loss is minimized.

An important factor in utilizing the high allowable deceleration is to take maximum advantage of the pilot's physical capabilities. This is done by stabilizing the capsule to preclude extraneous rotary excursions and resultant poorly orientated accelerations. It is well known that the deceleration levels which would be developed on an unstable capsule greatly exceed human tolerances. Other important mechanisms such as parachute deployment and speed-altitude sensors require a stable capsule.

The basic nose escape capsule used in this study is highly unstable aerodynamically. The instability arises from the fact that the nose of an F-104 type aircraft serves primarily as an aerodynamic fairing for the cockpit area where most of the mass is concentrated, and usually consists of an essentially empty radome necessary for radar viewing. Fig. 3 (*left*) indicates the measure of instability of the basic capsule in that the aerodynamic center is shown to be well forward of the center of gravity. This situation exists throughout the Mach number range from $M = 0$ to $M = 4.0$. In order to assure static and dynamic stability, the aerodynamic center must be moved to a position aft of the center of gravity, and this is essentially the task to be performed by the stabilizing surfaces. There are, of course, compromises to be made. Adding the rear-attached stabilizing surfaces and their attendant mechanisms, along with the separation rocket and other equipment at the rear of the capsule move the center of gravity further aft, necessitating larger or more powerful stabilizers, which in turn move the center of gravity even further aft. The final satisfactory arrangement is shown in Fig. 3 (*right*).

The capsule stability problem may be broken down into the following main categories:

(a) Adequate static and dynamic stability must be provided throughout the range from $M = 0$ to $M = 4$.

(b) The drag increase caused by the stabilizers and the trim attitudes caused by their aerodynamic characteristics must be such that the decelerations on the pilot are well within the limits of human tolerance for the entire performance range.

(c) The weight of the stabilizing system and its stowage and interference volume must be minimized.

(d) The operation of the system must be simple and reliable.

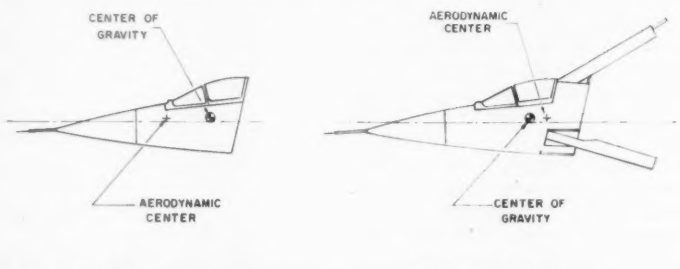

Fig. 3. Stabilization problem; basic nose (*left*) and stabilized capsule (*right*).

(e) During the separation of the capsule from the aircraft, the stabilizing surfaces must clear the aircraft afterbody with a satisfactory margin of safety throughout the entire performance range.

These problem areas required a comprehensive configuration investigation including extensive analytical studies followed by wind-tunnel tests in order to arrive at a satisfactory solution. Included in the analyses were approximately 50 different configurations which were investigated experimentally. Although analytical studies indicated that a flared-base capsule might be attractive from the aerodynamic, structural, and reliability viewpoints, experiments indicated that, in order to achieve sufficient aerodynamic stability, the size of the flare was excessively large and the drag increment added by this type of stabilizer was prohibitive. Also, such devices provided negligible roll damping, even with cut-outs in the flared base.

The utilization of fuselage contour fins, portions of the aft fuselage skin, yielded complex trim problems as well as being excessively large and complicated. They too provided no roll damping. Thin airfoils experience a loss in lift curve slope at high Mach numbers such that they also become excessively large. The thick wedges as stabilizing surfaces are unique in that they maintain stabilizing effectiveness at the high Mach numbers as well as allow increased tail length since the thick wedge sections which are very strong structurally allow higher aspect ratio surfaces than are possible with thin sections. After considering all the problems, the thick, symmetrically located wedges appeared to offer the best solution and, thus, attention was focused primarily on this type of stabilizing surface.

An analytical and wind-tunnel parametric study was carried out on the wedges to optimize their shape. The effects of wedge angle, sweep angle, wedge peripheral position and aspect ratio were investigated, and a satisfactory combination was achieved which attained the desired stability at the desired drag level. The symmetric arrangement was selected to preclude possible dynamic stability difficulties. The particular orientation allows adequate clearance of the aircraft afterbody during separation.

The effect of the wedge stabilizers on the capsule stability throughout the Mach number range is shown in Fig. 4. The figure clearly indicates the trim and stability problems which exist at the higher Mach numbers for a body such as the proposed capsule configuration. The stability curves in pitch are very nonlinear, with the nonlinearities becoming more pronounced in negative pitch and at the higher Mach numbers. A glance at this figure indicates that the general character and slope of the stability curves throughout the entire Mach number range remain essentially unchanged, but that the curves are displaced to the right of the axis origin as the Mach number is increased. This trim shift causes large normal forces to act on the capsule when the capsule is at its trim angle of attack. At $M = 4.0$ the configuration with wedges alone trims at an angle of attack of approximately -7 deg. and at a trim lift coefficient of approximately -0.72. At 50,000 ft. and at $M = 4.0$, which is within the required design performance of the capsule, this normal force coefficient would cause a downward acceleration on the capsule of approximately 15g. Such an acceleration would be directed against the upward component of the separation rocket thrust of approximately 12g and would cause incomplete separation and subsequent collision of the capsule with the airplane afterbody. In order to alleviate this problem, the trim angle of the configuration had to be altered in such a way that the normal force on the capsule at its trim point

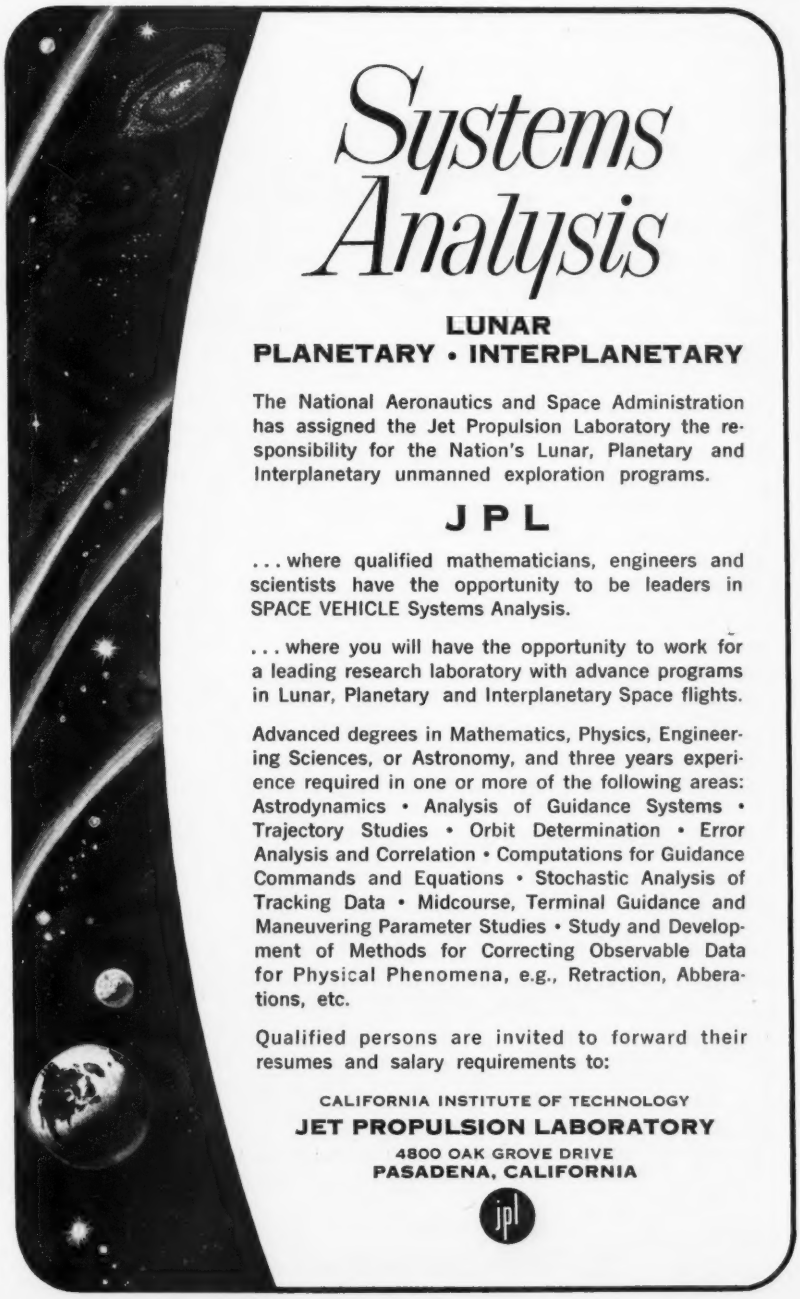

Systems Analysis

LUNAR
PLANETARY • INTERPLANETARY

The National Aeronautics and Space Administration has assigned the Jet Propulsion Laboratory the responsibility for the Nation's Lunar, Planetary and Interplanetary unmanned exploration programs.

JPL

... where qualified mathematicians, engineers and scientists have the opportunity to be leaders in SPACE VEHICLE Systems Analysis.

... where you will have the opportunity to work for a leading research laboratory with advance programs in Lunar, Planetary and Interplanetary Space flights.

Advanced degrees in Mathematics, Physics, Engineering Sciences, or Astronomy, and three years experience required in one or more of the following areas: Astrodynamics • Analysis of Guidance Systems • Trajectory Studies • Orbit Determination • Error Analysis and Correlation • Computations for Guidance Commands and Equations • Stochastic Analysis of Tracking Data • Midcourse, Terminal Guidance and Maneuvering Parameter Studies • Study and Development of Methods for Correcting Observable Data for Physical Phenomena, e.g., Retraction, Abberations, etc.

Qualified persons are invited to forward their resumes and salary requirements to:

CALIFORNIA INSTITUTE OF TECHNOLOGY
JET PROPULSION LABORATORY
4800 OAK GROVE DRIVE
PASADENA, CALIFORNIA

jpl

throughout the maximum q range of flight ($M = 1.36$ to $M = 4.0$) was within acceptable limits. The required trim shift was accomplished by the addition of a small flat-plate trimmer attached to the tip of the upper wedge stabilizer surface.

Dynamic model tests were conducted to verify that no dynamic problems would exist. These were performed by launching 1/10-scale, dynamically similar models under scale conditions and adjusting the stability margin to correspond to various Mach number conditions. The models were caused to roll beyond acceptable roll rates without exhibiting roll coupling problems.

As noted previously, decelerative forces on the pilot were adjusted to desired levels. Actually higher levels of deceleration would be tolerable to the pilot, however they had to be reduced somewhat due to the separation rocket characteristics. The rocket was limited by the zero air load acceleration noted in the separation section. Fig. 5 illustrates the acceleration history on the pilot for the critical case. This is shown as acceleration g vs. time. Superimposed on this chart are the human tolerance limits to acceleration established by WADD. It is seen that the longitudinal g limit is reached during rocket burning, and that the transverse g are well below the maximum limit. For the purpose of this study, it was assumed that the total decelerative load was established by the vector sum of the vertical and horizontal g, and that this vector sum must at all times be within the ellipse the major and minor axes of which are determined by the WADD established maximum limits of human tolerance. For example, the inset in the upper right-hand corner of Fig. 5 gives an account of the actual decelerative loads as compared to maximum allowable loads at

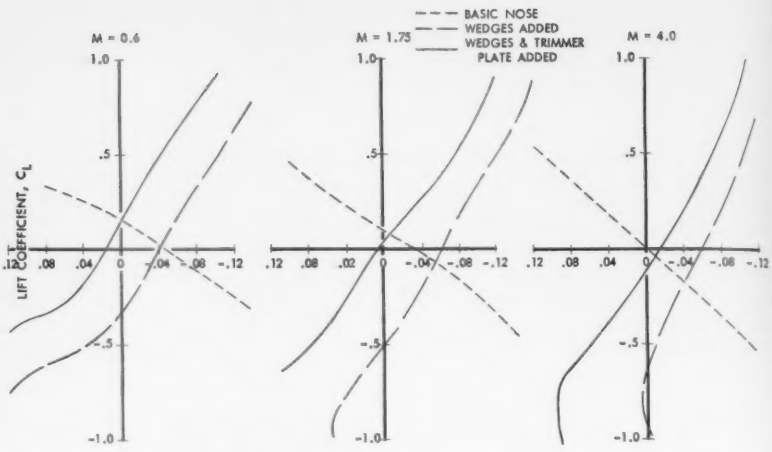

Fig. 4. Stability of capsule in pitch.

0.9 sec. after escape initiation for one particular case.

(5) Descent

There are two major problem areas associated with the descent phase—maintaining the pilot's environment within acceptable limits and deploying the parachute system for the final descent. After the capsule has separated from the aircraft, it will also be separated from the cooling system. The resulting capsule air and wall temperatures will then be a function of the transient heat transfer during the escape trajectory. Since the highest skin temperatures in normal flight are expected to occur at a Mach number of 4.0 at 50,000 ft., it is of interest to examine the cockpit environmental conditions for an ejection under these conditions. A transient analysis of the capsule inside wall and air temperature has been made for this case without intra-wall cooling. This results in the most severe thermal environment during any escape and descent. The results indicate that the wall and air temperature rise are quite moderate (145° and 125°F., respectively) and result in tolerable conditions for the pilot during the descent. With the added heat shield afforded by the intra-wall cooling air passage, the maximum temperatures will be considerably lower than these values.

The basic cockpit pressurization schedule is established so that the maximum cabin altitude during cruise will be 8,000 ft. Under normal flight conditions, it is estimated that the leakage at design differential pressure of 10.8 psi can be limited to 0.8 lbs. per min. However, for the escape, leakage in excess of 0.8 lbs. per min. must be considered. Since weight is a primary consideration, oxygen alone will be used directly to supplement the cabin air which leaks overboard. In this manner, the cabin pressure can be allowed to fall as long as an enriched oxygen atmosphere is maintained. The proposed pressure control system valves oxygen into the capsule at a rate which will limit the minimum cabin pressure to an equivalent altitude of 20,000 ft. The oxygen flood system will be actuated automatically by an aneroid sensor and pneumatic valve employing oxygen pressure for actuation.

The determination of when to deploy the parachute for the final descent phase presents a problem in compatibility between extremes in the escape envelope. From high altitudes, the parachute cannot be deployed immediately. From low altitudes, it is imperative to deploy the chute as soon as possible. The best compromise lies with highest possible speed deployment but not above a given altitude. To perform this operation reliably, the

Fig. 5. Predicted accelerations vs. human limits.

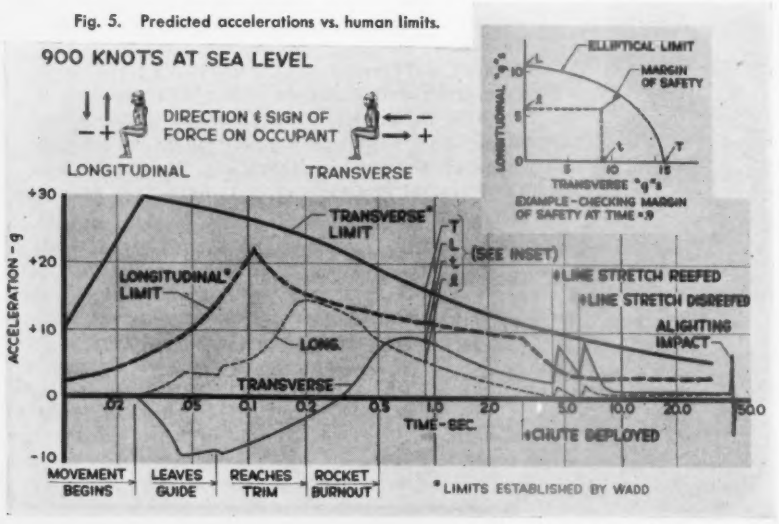

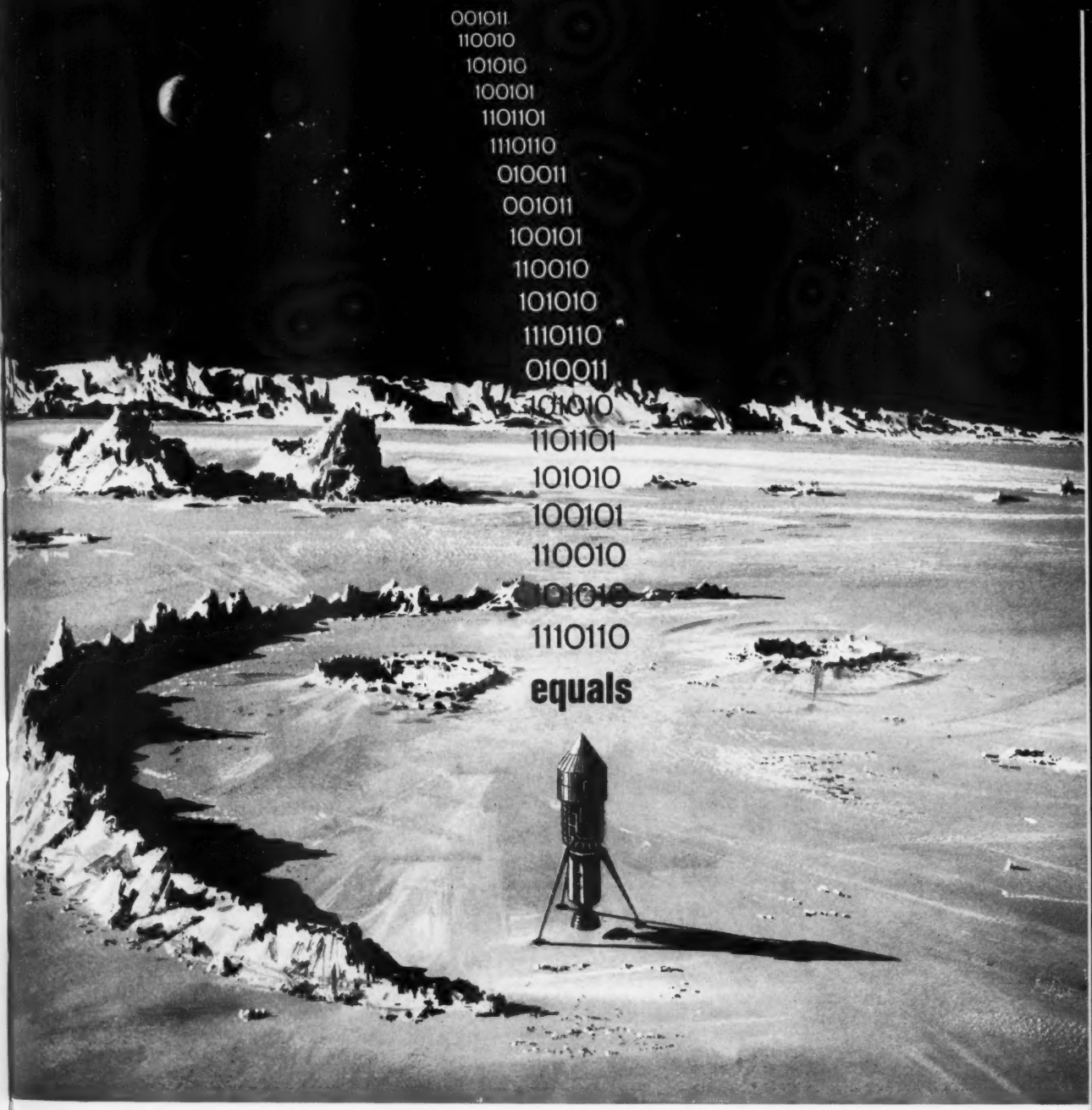

The more advanced our scientific ventures into space become, and the more sophisticated the weapons in our defense arsenal grow, the greater need there is for special purpose computers engineered to fit system requirements exactly. Serving as the nerve and intelligence center, the computer is playing an increasingly important role in system performance and reliability.

A prime Sperry capability is computer technology—both digital and analog. In the analog field, the B-58 bombing-navigation computer is outstanding. Airborne digital applications include a countermeasures computer which sorts out the enemy's "confusion" data, decides *logically* the best means of counteracting it. Another is a subminiaturized, radiation resistant, ultra-reliable computer for missile guidance. In component technology, Sperry memory drums, most advanced in the field, include an air-bearing floated-head type with extremely long life and high storage capacity. Other advanced techniques are incorporated in studies and designs for the future . . . for computers applicable to space vehicles.

On the surface, a small digital computer for ground support equipment checks out a complete airborne reconnaissance system. This "building block" computer is unique in its universal adaptability for reprogramming.

On the Polaris submarines, a digital "brain" collates, analyzes, decodes and distributes the widest variety of navigational data ever centered in a single operation. In an anti-submarine warfare program, a high speed digital computer accepts, operates on, stores and displays instantaneous data relating to the target under consideration.

In its computer work Sperry is often joined by Remington Rand Univac and Ford Instrument Company plus component divisions specializing in semiconductor and solid state devices. General Offices: Great Neck, N. Y.

SEA • SURFACE • AIR • SPACE

SPERRY

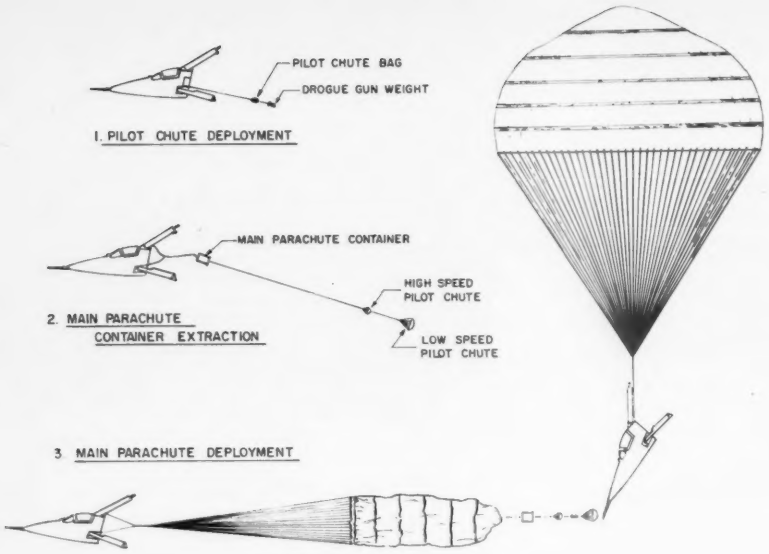

Fig. 6. Parachute deployment.

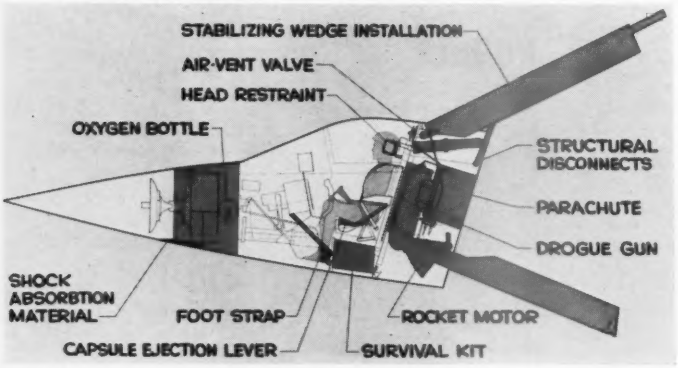

Fig. 7. Inboard profile.

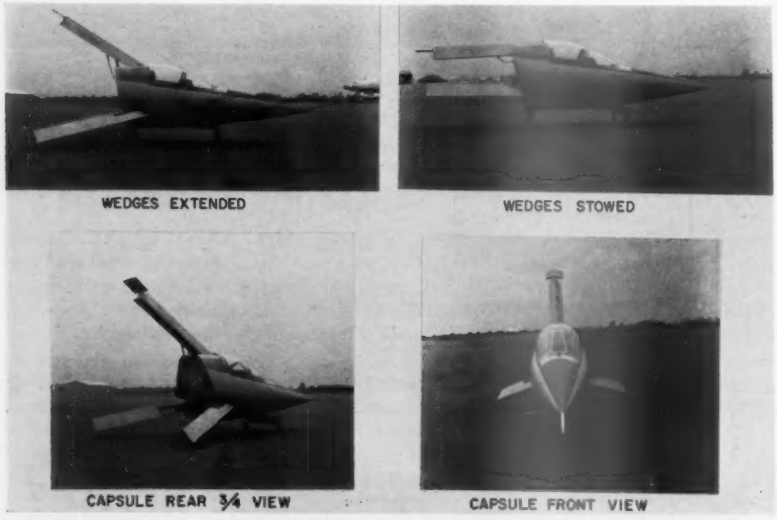

Fig. 8. Full-scale mockup of capsule.

parachute deployment mechanism is actuated by a simple speed-altitude sensor which balances static and pitot pressures against a spring mechanism to detect optimum and maximum opening conditions. The limiting opening speed and altitude are interdependent such that limit equivalent air speed at 15,000 ft. altitude is lower than limit equivalent air speed at sea level in order to take advantage of inherent parachute characteristics. The main canopy is deployed reefed to allow for high opening speeds, and disreefing is automatically accomplished by M-2 delay cutters.

"Off-the-deck" escape while at low or zero airspeeds requires parachute opening in minimum distance traveled. This is accomplished by using a secondary low-speed pilot chute which is much larger than the high-speed pilot chute. The low-speed chute fails at high speed. For a zero speed, zero altitude escape, the parachute deployment starts at rocket burnout. This allows maximum air distance to deploy the main canopy. The escape rocket has been designed with sufficient impulse to allow this type of escape.

The parachute deployment sequence is illustrated in Fig. 6. A drogue-gun weight pulls out the pilot chutes, which in turn extract the main canopy container. The main chute is deployed line-first from the container to assure maximum reliability.

(6) *Alighting*

The process of alighting extracts the final bit of velocity from the capsule which cannot be accomplished practically by the air. This amounts to approximately 30 ft./sec. In the simple "bail out" escape method this is accomplished by the man's legs. If the deceleration due to landing must be taken parallel to the pilot's spine, approximately two ft. of deceleration distance is required to preclude spinal damage. If the deceleration can be taken normal to the spine, higher g and significantly less deceleration distance can be tolerated.

The 30 ft./sec. velocity to be dissipated results from a practical balance between parachute size and decelerator capability. Reducing the terminal velocity reduces the decelerator requirements at the expense of increased parachute size.

Several methods of decelerating the capsule were investigated, including air bag deceleration, rotary arm shock absorbers, and paper cushions. A design ground rule established is that the capsule must remain in an upright position when alighting under all ground conditions, including rough terrain and severe cross winds.

The method chosen finally in this

study is a system which utilizes the higher physical capability of the man to take g normal to the spine coupled with the energy absorption capability of the nose structure. To accomplish this, the capsule is allowed to descend in an extreme nose-down attitude. The pyroceram nose cone is shattered after parachute deployment to allow initial ground contact on the forward metal structure which is modified to give desired crushing characteristics. The capsule then pivots so that the buckling of the two low wedge stabilizers absorbs the small remaining energy. The extreme nose-down descent attitude greatly simplifies the parachute attachment problem, as well as allowing an optimal deceleration sequence. Two small inflatable bags are extruded from the lower wedge stabilizers to provide roll stability when the capsule lands in the water.

(7) *Survival*

After alighting, the problem is one of surviving until rescue. A major advantage of the proposed capsule is that it may act as a shelter and lifeboat. Excellent insulation is already built in because the capsule is designed for high-speed flight. Conditions within the capsule may be easily controlled by adjusting a sun shade over the canopy and by the opening and closing of the canopy.

A large volume is available within the capsule for stowage of survival equipment such as radio, dye markers, food, clothing, fishing and hunting gear, etc. The contents of the pilot's survival kit will, of course, depend upon where he is flying; however, the large volume available will allow a greater selection and variety than is presently allowed in survival kits.

Considerations in Configuration Selection

Having introduced the problems and discussed their solutions step by step, it is felt that it would be beneficial to point out the factors which have had the *major* effect upon the final configuration design—separation, stabilization, and deceleration. These three factors also have the most significant effect on the important items of weight and reliability and are the factors which most likely vary from one capsule configuration to another or from one aircraft to another. The initiation, restraint, descent, alighting, and survival systems are relatively independent of the capsule configuration and normally may be optimized independently.

Capsule Description

In the preceding section, the various problems associated with the successful escape from a high-speed/high-performance aircraft have been discussed along with the proposed solutions thereto. The equipment and mechanisms which make up the final proposed escape capsule system have been briefly discussed. Fig. 7 presents a summary of the main items of equipment and shows their location within the capsule. The purpose of this section is to present a physical description of the proposed capsule, including some pertinent structural details, weight and volume requirements, and reliability considerations.

The full-scale mock-up of the final proposed capsule configuration is shown in Fig. 8. The stabilizing wedges are seen in the stowed position as they would normally be carried in the fueslage, and in the full-open position as they would appear upon ejection.

Structural Design

The escape capsule consists basically of an F-104 fuselage forebody suitably modified so as to withstand the high temperatures, bulkhead pressure differentials, inertia loads and aerodynamic forces associated with the required design performance envelope shown in Fig. 2. The structural modifications necessary were many and varied and are discussed in detail in reference 1. However, a discussion of the *primary* differences between the F-104 fuselage forebody and the basic unstabilized capsule, including a brief résumé of the proposed structural modifications, follows:

High Temperature and Pressure Structure

Skin and frames—In designing the structure, it was assumed that the life of the aircraft was 5,000 hours, of which 90 per cent is spent at $M = 4$ at an altitude of 100,000 ft., and approximately 10 per cent is spent at the maximum temperature condition, which occurs at $M = 4$ and at an altitude of 50,000 ft. A structural material capable of withstanding prolonged steady-state operation at a Mach number of 4 and the resultant skin temperatures of 900°F. is used instead of aluminum. Detailed analyses indicate that the lightest weight shell meeting the design requirements results from using a material such as MST 821 titanium, an alloy with excellent annealed properties under development by Mallory-Sharon Titanium Corporation. With a moderate additional weight penalty of 5 to 10 lbs., the shell could be fabricated from Inconel X.

With regard to pressure, the cockpit enclosure must be designed to withstand a pressure differential of approximately 11 psi limit at 900°F. A

MOTORS
ACTUATORS

BUILDING BLOCKS FOR THE SPACE AGE
by
ELECTRONIC SPECIALTY CO.

1 **MODEL D-1212—Designed for 2nd stage Minuteman guidance system**
Horsepower 3.95
Power ..... 26 vdc
Weight ..... 6.3 lbs.
Weight with filter ..... 8.8 lbs.
FEATURES:
Excellent h.p./wt. ratio • Reduced size • Advanced design • High history of reliability

2 **MODEL D-1115—Designed for F-104 pilot seat actuator (Mil-E-5272 A)**
Power ..... 26 vdc (or 400 ac)
Weight ..... 8.5 lbs.
Travel ..... 0.34 in/sec.
Stroke ..... 4.5 in.
Normal Load ..... 400 lbs. total
Compression Load ..... 4100 lbs.
Tension Load ..... 12,000 lbs.

3 **MODEL D-822—Designed for F-104 trailing edge slat actuator**
Normal Operating load .. 26,000 in.lbs.
Max. Operating load .. 52,000 in. lbs.
Ultimate Static load .. 75,000 in. lbs.
Travel ..... 45° at 0.625 rpm
Amperes
4 amps at 26,000 in. lbs. at 480 cps on 200 volts
Weight ..... 35 lbs.

4 **MODEL D-1029-1—Designed for pump applications, antenna drive systems, actuators and stabilizer applications**
Terminal voltage ..... 26.6 vdc
Horsepower ..... 6 hp
Speed ..... 7500 rpm
Duty cycle:
4.5 hp for 7.5 min.–6.0 hp for 20 sec.–2.0 hp for 30 min.
Weight ..... 20 lbs.

ES development engineers welcome the opportunity to furnish an engineering estimate on your specific requirement. Emergency circumstances given special consideration. Ask for the EEMCO DIVISION design folder.

EEMCO
DIVISION
ELECTRONIC SPECIALTY CO.
CORPORATE OFFICES:
5121 San Fernando Road
Los Angeles 39, California
CHapman 5-3771

The most proven large ballistic missiles, the Atlas (left) and Redstone (right), will launch America's Astronauts. Main-stage engines of both are by Rocketdyne.

AMERICA'S ASTRONAUTS WILL BE LAUNCHED INTO SPACE BY ROCKETDYNE ENGINES

America's man-in-space programs demand the ultimate in reliability. There is no room for error—that is why America's most experienced rocket engines have been chosen for the job.

And this means engines built by Rocketdyne.

A Redstone engine, whose performance over a decade of development includes 62 consecutive successful flights, will loft the first manned space craft high over the Atlantic in an exploratory ballistic arc.

Then an Atlas system of five engines, proven in more than 60 development and operational flights, will send a man soaring upward more than 100 miles to circle earth for four hours during man's first orbital flight in space.

To that dramatic moment, Redstone and Atlas will carry the heritage of more than 18,500 large engine tests at Rocketdyne's Propulsion Field Laboratory.

At every level of operation—from engineering to manufacturing to cost control—Rocketdyne has pioneered new concepts. Advanced management programs, combined with vast experience and the foremost high-thrust test facilities in the nation, give Rocketdyne the capability today to meet the challenges of tomorrow.

Rocketdyne engines have launched more than 250 missiles, satellites, and space probes.

FIRST WITH POWER FOR OUTER SPACE

ROCKETDYNE

DIVISION OF NORTH AMERICAN AVIATION

Canoga Park, California; Neosho, Missouri; McGregor, Texas

Table 1

Item	Weight, Lbs.	
Escape Capsule Weight Summary		
Mach 4 basic forebody	1,319	
Flotation equipment	12	
Ground contact structure	25	
Parachute recovery system	135	
Separation rocket installation	110	
Stabilization system	353	
Wedge door opening mechanism	9	
Separation joint structure	34	
Quick disconnects	10	
Controls	8	
Weight empty, escape capsule	2,015	
Pilot	215	
Survival kit	70	
Gun camera	4	
Gross weight, escape capsule	2,304	
Items not attached to capsule:		
Quick disconnects	20	
Separation joint bulkhead	37	
Cut outs fuselage for stabilizers	143	
Total weight with capsule system	2,504	
Comparison of Weight Penalties		
Total weight with capsule	2,504	
Less Mach 4 basic forebody	−1,608	
Weight increase due to capsule	896	
C-2 ejection seat:		896
Installed weight of C-2 type ejection seat	244	−244
Net weight increase of capsule over C-2 seat		652

material capable of sealing a structural joint at this temperature is not available and will probably not be available in the near future, and thus the basic shell must be seam welded at the joints and spot welded at the rings. Besides providing the lightest weight shell, MST 821 has the advantage of retaining its properties after welding since it is used in the annealed state. Its use thus simplifies the design of joints and the fabrication of the shell. Using the titanium shell also permits the use of relatively heavier sheet (0.032 titanium as compared with 0.016 Inconel X) with larger ring spacing (6.0 in. spacing for titanium as compared with 3.4 in. spacing for Inconel X), thus reducing the effect of thermal stresses due to differential expansion between skin and rings. Thermal buckling is not critical because of the tension stress in the skin due to cabin pressure acting with the temperature differential. Ordinarily, creep would be of primary significance, particularly in the cockpit region where the operating load due to pressure is a high percentage of limit load; however, with the recommended structure, permanent deformation due to creep is limited to 0.2 per cent during the lifetime of the airplane.

Windshield and canopy—Although it is entirely feasible that a direct-vision type canopy may not be required, and indeed may not even be useful for flight at the high-altitude/high-speed combinations under consideration, for conservatism a canopy of essentially conventional type was assumed to be an integral part of the capsule, and the aerothermodynamic problems arising therefrom were considered in some detail. In making a weight estimate, the canopy was assumed to be made of two sheets of a high-strength, heat-resistant, transparent material such as Corning Glass Company's Pyroceram, with the radome a single sheet of the same material.

Stabilizing wedges—The stabilizing wedges are fabricated from 6AL-4V, heat-treated titanium, which yields the lightest and most efficient structure under the temperature and load conditions. Although the external skin temperature is approximately 900°F., the maximum temperature of the wedges does not exceed 300°F. while in a stowed condition inside the fuselage. During the first few seconds after escape sequence initiation, and shortly after the wedges are extended, the skin temperature of the wedges is rapidly increased due to aerodynamic heating, but at the same time the capsule velocity decreases such that the maximum wedge skin temperature reached is of the order of 700°F. They may be fabricated from precipitation-hardenable stainless steels such as AM-350, 17-7PH or 15-7Mo, with only a moderate weight penalty.

Separation joint—Of the various problems associated with separation, structural disconnection is of *utmost* importance. A clean, reliable, and efficient separation of the capsule from from the aircraft afterbody is absolutely essential. The capsule is connected to the aircraft afterbody through machined fittings at the four longerons. These fittings serve a dual purpose in that they provide initial directional guidance at separation through short tracks which are integral with the fittings. Longeron loads are transmitted directly to the fittings through shear connectors, and from the forward fitting to the aft fitting through an explosive bolt. When these four bolts are fractured by the explosive charge initiated by the pilot, the capsule is structurally free to be propelled from the aircraft afterbody. This joint is designed so that shear is transferred from the shell to the four fittings by a forged titanium end bulkhead, and from the forward to the aft fitting by the bearing of the slide in the track of the guidance tracks. The end bulkhead supports the drag links of the three stabilizers.

Weight

In order to estimate the effect of the escape capsule on airplane weight, it was first necessary to design completely and determine the basic weight of the nose section of an F-104 type aircraft capable of achieving the required Mach number/altitude design criteria, and with *no* escape system provided. The equipment and accessories necessary for the installation of the capsule were then added and an all-up weight estimate made. A comparison of the relative weights was made and the results of this comparison are shown in Table 1. The total basic weight of the nose section of the Mach 4 aircraft is approximately 1,608 lbs. With the capsule installed, the weight is increased to 2,504 lbs., giving a weight difference of 896 lbs. If the basic nose or forebody contained an escape seat with the same capability as the F-104 C-2 seat, as shown in Fig. 2, the forebody weight would increase 244 lbs. The weight difference of the escape capsule over the airplane equipped with the C-2 ejection seat is then 652 lbs. As shown in Fig. 2, however, the capsule provides a vastly greater escape capability, and the installation of the C-2 type seat would provide protection in a very small part of the aircraft performance spectrum.

Fuselage Volume Effects

An increase in the volume as well as an increase in weight must be provided in the original aircraft design for the escape system. An idea of the potential problems involved in installing a capsule of this type may be attained by noting that the fuselage volume required for the proposed system, including all accessories and mechanisms, is more than 35 cu.ft.

Reliability

The system, as proposed, is a complicated one and, while not guaranteeing absolute reliability, its design offers

"MIDGET WITH A PUNCH"!

Bendix 16-lb. DC Starter Generator

Designed specifically to help the new lightweight gas-turbine engines get off to a quick start is the Bendix® type 30B56 DC Starter Generator. It provides 10 lb. ft. of torque at 3,000 rpm and will produce 30 volt/100 amp. DC power when driven between 7,000 and 12,000 rpm.

This "midget with a punch" requires a minimum envelope since it measures only 4.6" dia. x 8" long. It comes with round, square, or QAD flange and includes a fan to supply its own cooling air up to 20,000 feet.

If your needs are to start small gas turbines rated around 250 hp with a DC source, specify the Bendix type 30B56 and get 3 KW DC power, too. See us for details as related to your specific application.

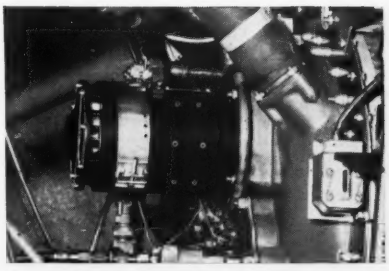

Its small size makes the 30B56 Starter Generator ideal for use on the new small gas-turbine engines.

GENERAL PRODUCTS DEPARTMENT

Red Bank Division

EATONTOWN, NEW JERSEY

THE Bendix CORPORATION

West Coast Office: 117 E. Providencia, Burbank, Calif. Export Sales & Service: Bendix International, 205 E. 42nd St., New York 17, N. Y.
Canadian Affiliate: Aviation Electric, Ltd., P.O. Box 6102, Montreal, Quebec

escape in flight regimes where none now exist and it enhances pilot survival for a reasonable time after landing in environments where previously he would have perished in a few minutes. It is impossible to calculate a definite numerical percentage for the reliability of such a complex system, and thus reliability may be discussed only qualitatively, at best. The designed overall reliability has been maximized as much as practicable by vigorously adhering to the following design fundamentals:

(1) The number of steps or phases in the escape sequence have been minimized.

(2) The number of mechanisms have been minimized and redundant mechanisms have been added to critical components.

(3) Time-proved initiation methods have been employed.

(4) Adequate maintenance accessibility has been insured.

Utility of the Capsule

In addition to providing a system for escape and survival from high speeds and altitudes, the ejectable nose capsule concept lends itself to other uses which could improve the economy and utility of the weapon system.

Interchangeable Maintenance Package

The nose sections, being removable and completely interchangeable, can be utilized as maintenance spare components capable of being repaired, overhauled, or modified, and then completely checked without holding the airplane on the ground. One or two spare capsules will provide the same off-line maintenance that is now available with power plants and will thus greatly improve the overall efficiency and utilization of a using command.

An incidental feature of the extra capsules is that they could be used as a source of parts during critical shortage and delays. Thus, at the relatively minor cost of a small percentage of spare nose capsules, aircraft availability can be improved.

Flight Simulator

In a similar fashion, a removable capsule can be used as the major portion of a flight simulator. In conjunction with a "black box" rear section and windshield covers, it will provide complete realism. The auxiliary devices necessary to permit operation of controls and instruments need not be nearly as complex or expensive as those which would be required in a completely separate training device.

This concept permits keeping the simulator completely up to date with the latest modifications to the actual airplanes without costly time consuming supplementary simulator modification programs and without interruption of a busy training schedule. Further, it permits utilization of a single basic simulator unit for training in different versions of the basic airplane by merely attaching the appropriate capsule. Obviously, it also offers maintenance benefits on the simulator equivalent to those on the airplanes.

Conclusions

As a result of the Air Force-sponsored studies summarized here, the following conclusions are drawn:

(1) An optimum ejectable-nose escape capsule has been designed to provide a safe and reliable escape throughout an altitude range of from sea level to 100,000 ft. and throughout the speed range from zero to 900 knots E.A.S. or a Mach number of 4, whichever is lower.

(2) The capsule may land safely on a variety of terrain ranging from concrete to the open sea without exceeding human physical limits to deceleration.

(3) The capsule will provide a suitable shelter from the elements under many conditions in which pilot survival would be impossible with a conventional escape system.

(4) The weight of the airplane with the capsule installed is 896 lbs. greater than with no escape system installed. The capsule equipped airplane would be 652 lbs. heavier than if it were equipped with the F-104 type escape system utilizing the C-2 ejection seat. However, as is shown in Fig. 2, the escape capability of the capsule is vastly greater than that of the C-2 seat.

(5) Fuselage volume requirements for the installed capsule are on the order of 35 cu. ft.

(6) Although the capsule was based on an F-104 nose, the principles and systems developed can be used on a wide variety of cockpit type capsules.

Reference

[1] Newquist, E. A., Cassidy, M. D., Lindblom, C. W., and Sullivan, P. J., *Development of an Ejectable-Nose Escape Capsule*, WADC TR 59-493, 1959.

✦ ✦ ✦

Navy's Flying Wind Tunnel (Continued from page 19)

tory at the Forrestal Research Center for the past two years, no satisfactory solution to the problem has as yet presented itself.

Numerous alternative proposals have also been studied and, in some cases, tried. In a sense, the dynamic model testing track at the Forrestal Research Center represents an attempt to overcome the lack of an adequate source of a steady free-stream velocity by accelerating the model to a given velocity. Once this velocity is achieved, the model is released and the perturbations to the steady state motion as it proceeds along the track are studied. Other attempts have taken the form of trucks or carts, sometimes moving along tracks, sometimes free to move along roads or runways.

A number of these solutions have been made to work and yield reliable data, but all have suffered from certain inherent difficulties and none has begun to approach the flexibility and convenience of a wind tunnel. The major limitation confronting such test vehicles is the restricted time over which steady test conditions can be maintained. Once the end of the track or runway is approached the test must be terminated. Thus it is seldom possible to examine more than one setting of a given variable before the test must be terminated and the test vehicle turned around or retracted. As a consequence, a series of tests that might require several hours to conduct in a wind tunnel may require as many weeks on a test vehicle.

A second problem of major proportions confronting such test vehicles is created by the difficulty of making and recording useful measurements. It is of course, necessary that the path along which the test vehicle travels be as smooth as possible to avoid extraneous accelerations leading to inertia forces that can mask the quantities it is desired to measure. It is also necessary that these data be recorded either on the test vehicle directly or at some remote station. Recording on the vehicle itself is simplest, but in many cases the recording instrumentation may be even more sensitive to accelerations than the measuring devices or may add unacceptable mass or volume to the vehicle. In such cases remote recording either by trailing wires or telemetering with all of the attendant instrumentation complications must be restored to.

As a result of an exploratory trip in an airship, provided by the Airship Test and Development Department based at the Lakehurst Naval Air Station, it was suggested that an investigation be made of the possibility of using an airship as an alternative to a ground supported test vehicle. The remarkable steadiness of flight obtainable in the stable

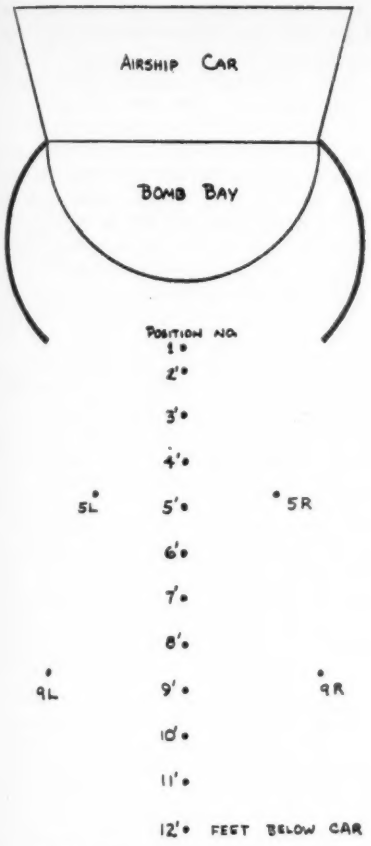

Fig. 3. ZS2G-1 airship velocity survey (1/4 in. = 1 ft.).

Pos. No.	V (fps)	
1	62	
2	62	
3	62	
4	60	
5	62	
5L	62	35
5R	62	knots
6	61	IAS
7	60	
8	60	
9	60	
10	60	
11	60	
12	60	
1	50	
2	51	
3	51	
4	48	
5	49	28
6	47	knots
7	48	IAS
8	49	
9	48	
10	48	
11	49	
12	49	
	8 2	
2	82	
3	82	
4	84	
5	88	
6	88	51
7	88	knots
8	88	IAS
9	88	
9L	88	
9R	88	
10	88	
11	88	
12	88	

Fig. 3. Addenda.

atmosphere over the water, the load carrying capacity, the lack of vibration, and the availability of space for instrumentation and test personnel coupled with the ability of making test runs of almost unlimited duration suggested that such an application might overcome the disadvantages of all other existing schemes.

This suggestion received enthusiastic support from Commander Walter D. Ashe and his staff of the Airship Test and Development Department. Thanks to their cooperation in making the ZS2G-1 airship available and performing the modifications required to provide a suitable retractable model mounting support, a test program aimed at exploring the potentialities and limitations of the use of an airship for such a purpose was conducted in a period of less than a month after the initial exploratory flight.

Description of Flying Wind Tunnel ZS2G-1 Airship

The ZS2G-1 airship used in the initial feasibility studies of a *flying wind tunnel* is shown in Fig. 1. It is a nonrigid airship formerly used by the Navy for antisubmarine warfare, but which has been replaced in the fleet service by the ZPG-2 airship. Its current assignment is in the research and development program of the Bureau of Naval Weapons. It measures 285 ft. in length and 68 ft. in diameter, contains 650,000 cu. ft. of helium, and has two R-1300-4 engines rated at 700 hp. capable of driving the airship at a V_{max} of 70 knots.

The airship has been demonstrated to fly stably at any speed from 0–60 knots with no difficulty under normal atmospheric conditions. Its 7 ft. × 15 ft. × 4 ft. bomb bay afforded access to the model in flight for adjustment and calibration by having the model mounted on a retractable strut (Fig. 2). Initial airspeed and flow field studies were made by extending a *Velometer** head below the airship car. It was found that the flow field was uniform at all points below the car and eminently suitable for model testing (see Fig. 3).

A retractable model mounting strut installed in supporting bearings in the car floor consisted of a 4-in. tube with a strain gage balance assembly bolted onto the lower end of the tube. The upper end was fitted with a flange scribed to show azimuth angle. The tube was able to be clamped to prevent its turning once the desired angle was set. A small hand winch enabled the strut to be lowered and raised with its limit being six ft. from the bottom of the car to the

* A commercial flow meter previously calibrated against a pitot tube.

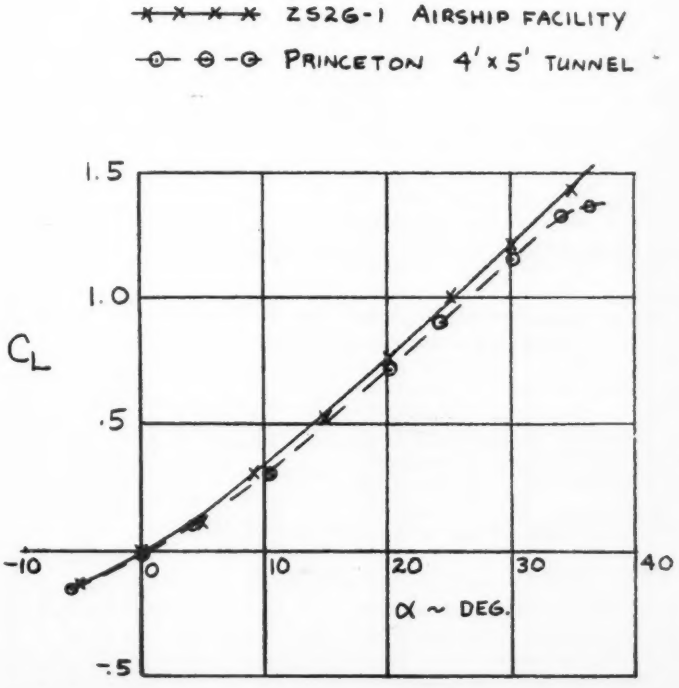

Fig. 4. C_L vs. α, 6 per cent delta wing. $N_R \sim 600{,}000$, $b = 1$ ft., $\mathcal{R} = 1$.

Fig. 5. (Official U.S. Navy Photo.)

top of the balance. Provisions were made in the tube to lead all the necessary strain gage cables directly from the balance up through the hollow tube so that no unnecessary wires were exposed to the airstream.

Balance System

To allow for raising and lowering the model from the free stream into the bomb bay and back again, a small, compact three-component strain gage balance was designed and built to fit inside the outer end of the strut. The model was attached directly to this balance in such a way that it could be rapidly removed in flight for further work or for exchange of models. The balance was designed to measure lift, drag and pitching moments of various powered or unpowered models. The basic design is described in reference 3. In place of the electric motor shown in Fig. 3 of reference 3, a steel spacer with suitable mounting points was machined and attached to the two flex beams. The entire assembly was slipped inside a $3^1/_2$-in. diameter steel sleeve and bolted in place. With the strain gage wires leading out of the rear of this sleeve, this assembly was affixed to the inside of the mounting strut. This results in the entire model and spacer being suspended, independently of the strut, solely by the two flex beams. The calibration and operation of this balance is covered in reference 3, but it should be mentioned that the flexible nature of the amplifier's read-out system for these strain gages eliminates the problem of designing a balance for various L/D ratios or model sizes. The balance measures three components accurately for models of any size and shape within the strength limitations of the supporting balance members.

The ZPG-2 Airship

Upon conclusion of these initial phases in the development of a satisfactory model testing technique, a Bureau of Naval Weapons task was assigned to prototype one of the large airships as a flying wind tunnel. This new airship, a ZPG-2 model has increased endurance and capability over the interim ZS2G-1 airship. It is of similar construction to the ZS2G-1 except that the car, or gondola, is considerably larger and more suited to this type of operation. The envelope measures 343 ft. in length, 75 ft. in diameter, and contains 1,011,000 cu. ft. of helium (Fig. 5). Its two R-1300-2A 700 (NRP) brake horsepower engines are capable of driving it at a top speed of 65 knots. It has been demonstrated that it can remain stable in flight at zero airspeed in an equilibrium condition with no pitching, rolling, or yawing perceptible. It has 8,000–10,000 lbs. of useful lift—i.e., capacity to lift 8,000–10,000 lbs. of crew, fuel, oil, instrumentation, etc., under normal operating conditions and maintain equilibrium flight. This lift figure varies with temperature and humidity.

Having a nonrigid envelope made of cotton impregnated with rubber, the airship has an air pressure system comprised of three ballonets, or small air bags, which control the airship trim and envelope pressure. The forward and the aft ballonets control the airship pitch and the center ballonet, the pressure. The center ballonet is actually made up of two interconnected ballonets which function as a large single ballonet. The total air capacity of these ballonets is approximately 25 per cent of the envelope volume and is the determining factor which limits the airship's ceiling. When the ballonets are empty, the ceiling has been reached for the condition of temperature and ballonet fullness at takeoff. Normal operating ceiling for the ZPG-2 is 5,000 ft.

Lift for the airship varies with temperature, helium purity and envelope fullness. For standard conditions (59° F., 95 per cent helium purity, and 97 per cent envelope inflation), static lift is 60,800 lbs. With the car (including instrumentation, strut assembly, and other project modifications), and the envelope weight of 15,862 lbs. for the flying wind tunnel airship, a 10,000-lb. useful lift is available for loading to meet project requirements with respect to personnel, fuel extra power units, and the like.

Clearance below the car and the space within the radome presently allows testing of models with wing spans of 10 ft., and fuselage lengths of 14 ft. Fig. 6 shows schematically car-ground distances, propeller spacing, etc.

The model mounting strut in the ZPG-2 has been enlarged to a 12-in. diameter to carry larger, heavier models with increased drag and thrust (for powered models). This strut is retractable within the helium chamber to permit landing and take-off and the adjusting of the model inflight from within the modified radome.

An inflight laboratory has been set up in the former ASW compartment. Fig. 7 shows the general layout and space

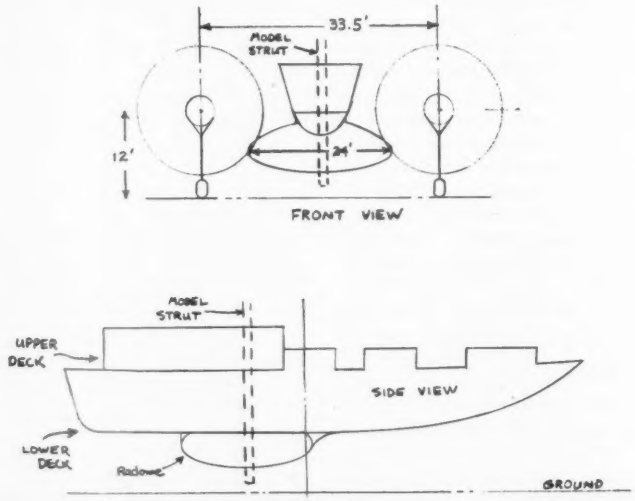

Fig. 6. ZPG-2.

available. The front section is the test center with the desired project instruments displayed as well as the necessary navigational instruments. Aft of this center are racks for recorder and amplifier instrumentation. For the present a planned capacity of 30 channels of information can be recorded simultaneously for analysis inflight or on the ground. On the port side of this compartment are the data boards, desks and observation stations for visually watching the models inflight. The model mounting strut passes through the utility compartment, the ward room topside, and into the helium chamber. Bearing surfaces in the upper and lower decks and an external cable to the forward section of the car take the moments created by the bag and/or thrust of the models when being flown.

Fig. 2 shows a VTOL model in the flying wind tunnel. The model is mounted in an inverted position to facilitate mounting and to reduce tail interferences.

Test Results

In developing any new and untried test facility it is essential that sources of error or difficulty be investigated to evaluate the performance of the facility in comparison with existing testing arrangements or techniques. In the case of the airship, major concern is centered on the following six items:

(1) Velocity Survey
(2) Vibration Level
(3) Adaptability of Mounting System
(4) Available Power Supply
(5) Ease of Calibration
(6) Access to Model and Ease of Testing

Velocity Survey

The first set of tests conducted were aimed at establishing the feasability of using the airship as a model testing platform. Accordingly, the information sought related to the steadiness and shape of the velocity profiles obtained in the test region below car, and to the suitability of the environment of the test instrumentation.

If the velocity was not relatively constant with time and the velocity profiles relatively free of distortion owing to the proximity of the airship's envelope, the test conditions represented no improvement over a wind-tunnel section since corrections of unknown magnitudes would be required. Equally, if the vibrations picked up either by the strain-gage balance or by the recording instrumentation itself were of such magnitude as to obscure the test results, there was no chance of successful data collection.

The velocity profiles were measured with a calibrated flow meter supported

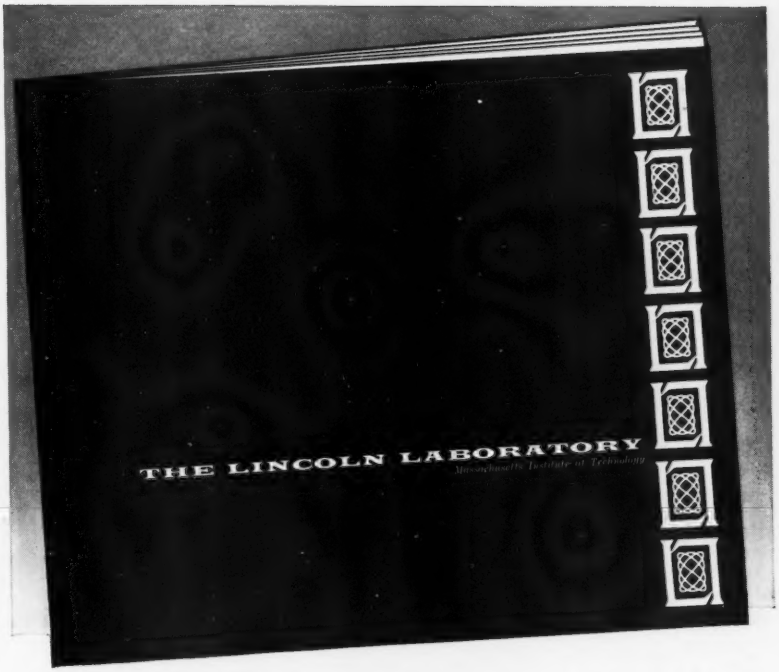

The Lincoln Laboratory, Massachusetts Institute of Technology, announces a major expansion in its program. We urgently request the participation of senior members of the scientific community in our programs in:

RADIO PHYSICS and ASTRONOMY
SYSTEMS:
Space Surveillance
Strategic Communications
Integrated Data Networks
NEW RADAR TECHNIQUES
SYSTEM ANALYSIS
COMMUNICATIONS:
Techniques
Psychology
Theory
INFORMATION PROCESSING
SOLID STATE Physics, Chemistry, and Metallurgy

- **A more complete description of the Laboratory's work will be sent to you upon request.**

Research and Development
LINCOLN LABORATORY
Massachusetts Institute of Technology
BOX 23
LEXINGTON 73, MASSACHUSETTS

Knowmanship in Action

BENDIX TRANSISTORIZED FLIGHT CONTROL SYSTEMS LOG OVER 1,500,000 COMMERCIAL FLIGHT HOURS

35 airlines plus 5 military services set new records daily

On the record, Bendix® automatic flight control systems qualify as the world's most experienced, most versatile for jet-age aircraft. Besides having flown more than 1,500,000 hours and over half a billion miles with the world's leading airlines, they have logged uncounted hours and miles on aircraft in the daily service of the U.S. and Canadian Air Forces and Navies.

In May 1957, the Bendix PB-20 became the first transistorized flight control system approved for airline use. Variations of it have since become operational on a great diversity of aircraft ranging from the world's first supersonic bomber—the Air Force's B-58 Hustler—to the world's tiniest jet-powered nuclear weapon carrier—the Navy's A4D-2N—and including the gigantic C-133A prop jet transport, the luxurious 707, 880 and Electra airliners, the RCN's deadly CL-28 submarine hunter and killer, and a host of other domestic and foreign aircraft.*

Dependability of these systems is underscored by the fact that many components have earned approval for an 8500-flight-hour overhaul schedule. Bendix flight

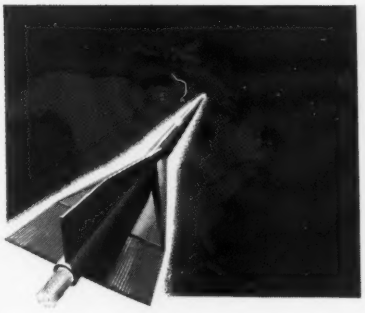

Another important current activity is a program to develop, build, and test hot gas systems for semi-orbital vehicles and missiles. Further proof that you can continue to look to E-P KNOWMANSHIP for major breakthroughs in flight controls, instrumentation, and components for aircraft, missiles, and space vehicles.

control experience extends across many fronts including successful performance on rotary winged aircraft and a completely solid state design that already has logged flight time. Our record in the field of flight controls is a direct result of more than 40 years of close association with the operating needs of all kinds of air vehicles.

**A complete list of the 40 operators and 15 aircraft types which employ Bendix transistorized automatic flight control systems is available on request.*

TECHNICAL KNOWLEDGE + EXPERIENCED MANAGEMENT + SPECIALIZED CRAFTSMANSHIP = **KNOWMANSHIP**

Eclipse-Pioneer Division

TETERBORO, N. J.

THE Bendix CORPORATION

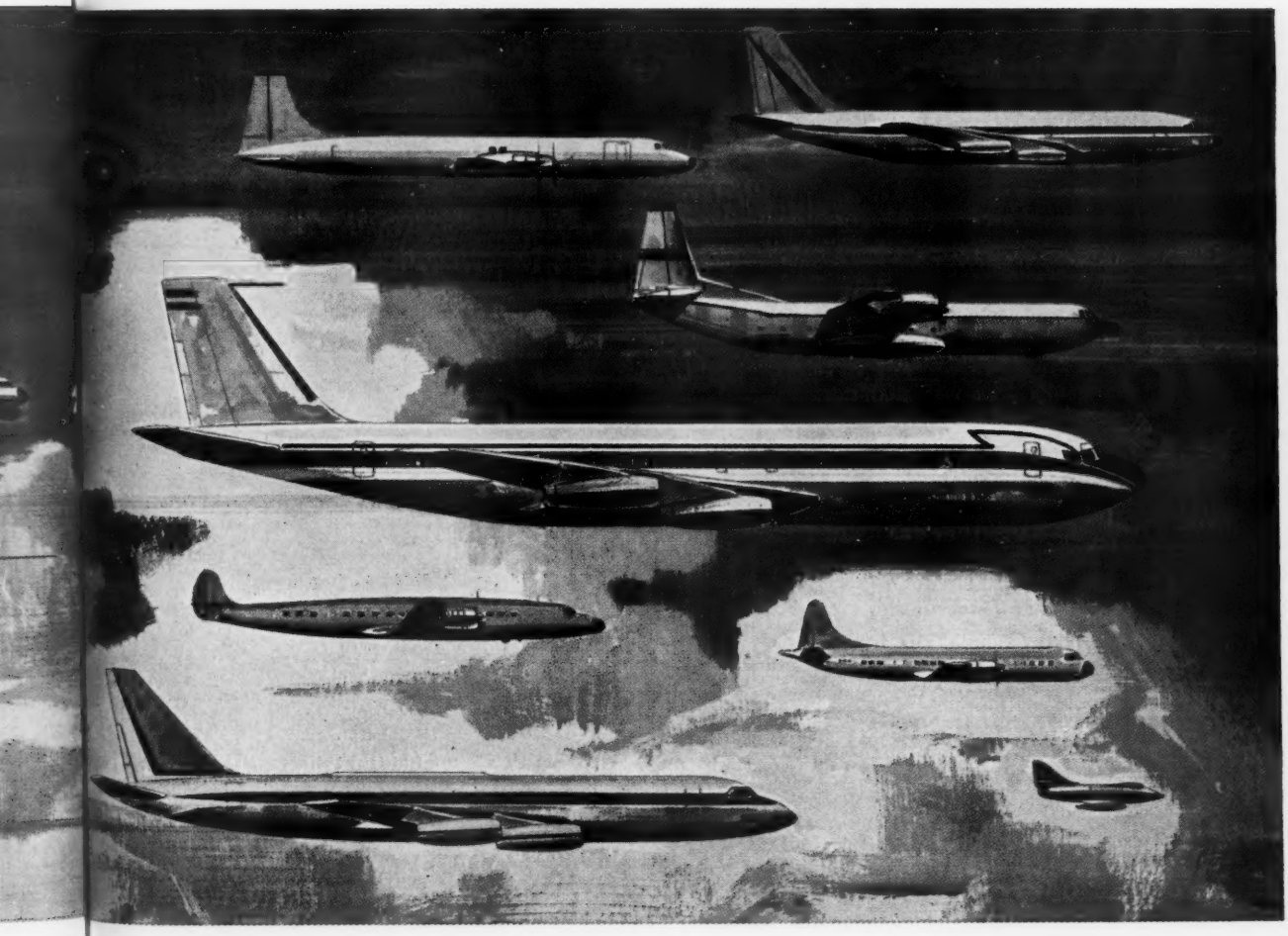

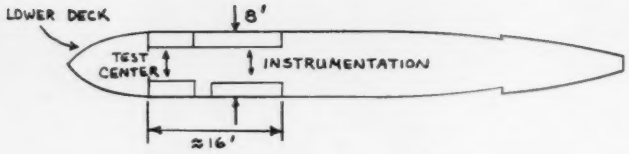

Fig. 7. Airship car layout ZPG-2.

at various positions below the car. Typical velocity profiles plotted for various airship speeds are shown in Fig. 3. Spot checks were made at various stations on either side of the center line which showed the entire flow field below the car to be uniform. The variation of velocity with time was also examined and found to be negligible for periods of 20 or more minutes.

The above tests were conducted on a relatively smooth day over water where prevailing conditions are generally less turbulent than over land. Subsequent tests have indicated that under conditions of rougher air, the time variation of velocity becomes greater; but even under those conditions, good test data are obtainable. Insufficient testing has yet taken place to enable the limits of acceptable turbulence to be established but such a limit will certainly be a function of the size and mass of the model, and the sensitivity of the balance elements, and the type of recording instrumentation employed. The indications to date are that such turbulence does not represent a serious limitation.

Vibration Level

The vibration level of the airship car was not measured as such, but was determined to be sufficiently low by observing the noise (or vibration) level as a percentage of full-scale reading (Table 1).

These results are considerably better than equivalent tests performed in Princeton wind tunnels. Apparently, the reason for this low vibration level in the car is the rather high damping provided by the envelope and car suspension arrangement.

Wind tunnels, driven by large rotating fans, suffer from machinery unbalance as well as air turbulence and minor flow separations (which are normally not felt by the structure of the airship car) with damping provided by the ground and

Large honeycomb panels are brazed between ceramic sections in this electric blanket brazing fixture.

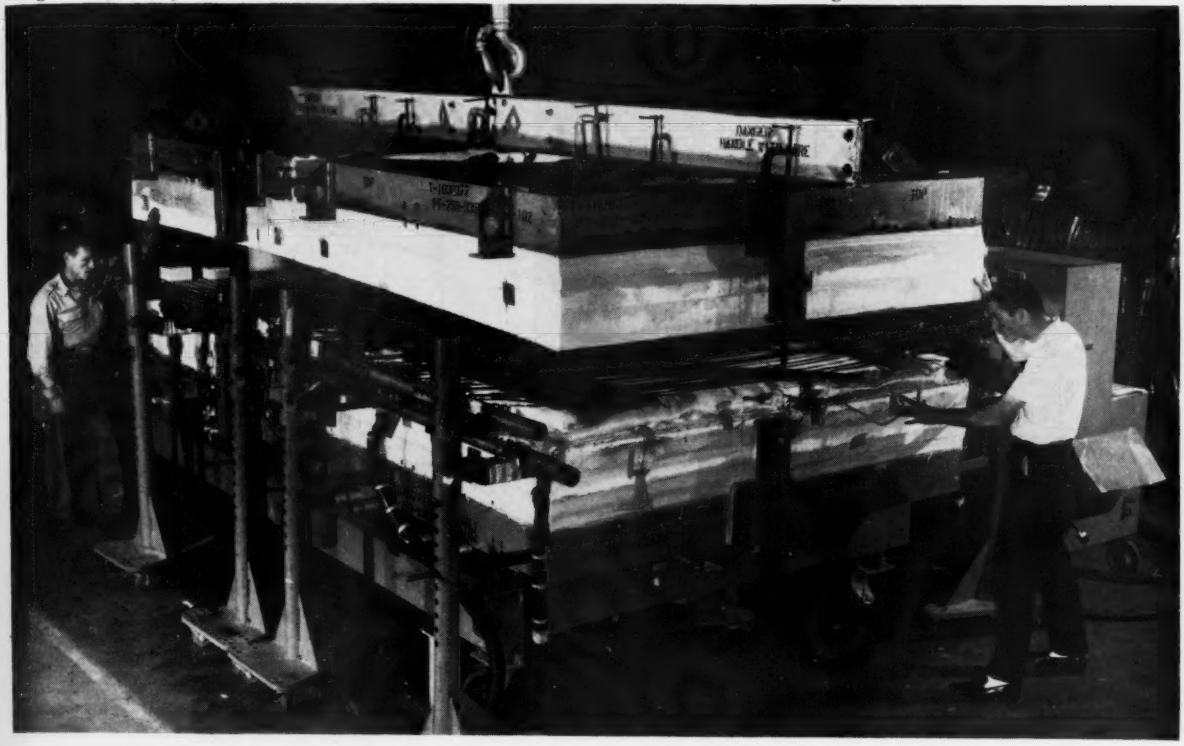

Mach 3 Manufacturing

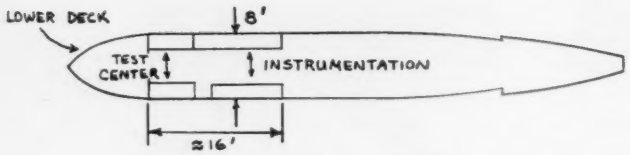

Fig. 7. Airship car layout ZPG-2.

at various positions below the car. Typical velocity profiles plotted for various airship speeds are shown in Fig. 3. Spot checks were made at various stations on either side of the center line which showed the entire flow field below the car to be uniform. The variation of velocity with time was also examined and found to be negligible for periods of 20 or more minutes.

The above tests were conducted on a relatively smooth day over water where prevailing conditions are generally less turbulent than over land. Subsequent tests have indicated that under conditions of rougher air, the time variation of velocity becomes greater; but even under those conditions, good test data are obtainable. Insufficient testing has yet taken place to enable the limits of acceptable turbulence to be established but such a limit will certainly be a function of the size and mass of the model, and the sensitivity of the balance elements, and the type of recording instrumentation employed. The indications to date are that such turbulence does not represent a serious limitation.

Additional test work has indicated that the uniformity of the flow field is not disturbed at speeds down to 0 knots (equivalent wind-off condition).

Fig. 8 shows the velocity and free stream angle measuring instruments used on the test strut. The indications of these instruments are continually recorded during a test run to monitor possible irregularities. These data have indicated that little or no variation in flow angle is present over a wide velocity range.

It is therefore expected that the velocity distribution and the flow angularity will be equal to the best conditions obtainable from wind tunnels with the added advantage of being maintained down to zero velocity.

Table 1.

Model	% Full Scale Caused by Vibratory Noise
Delta wing	Not measurable
Rotating propeller (14 in., 6,000 rpm, 10-gm. blades)	Not measurable
Rotating rotor (22 in., 4,000 rpm, 50-gm. blades)	3%

Vibration Level

The vibration level of the airship car was not measured as such, but was determined to be sufficiently low by observing the noise (or vibration) level as a percentage of full-scale reading (Table 1).

These results are considerably better than equivalent tests performed in Princeton wind tunnels. Apparently, the reason for this low vibration level in the car is the rather high damping provided by the envelope and car suspension arrangement.

Wind tunnels, driven by large rotating fans, suffer from machinery unbalance as well as air turbulence and minor flow separations (which are normally not felt by the structure of the airship car) with damping provided by the ground and

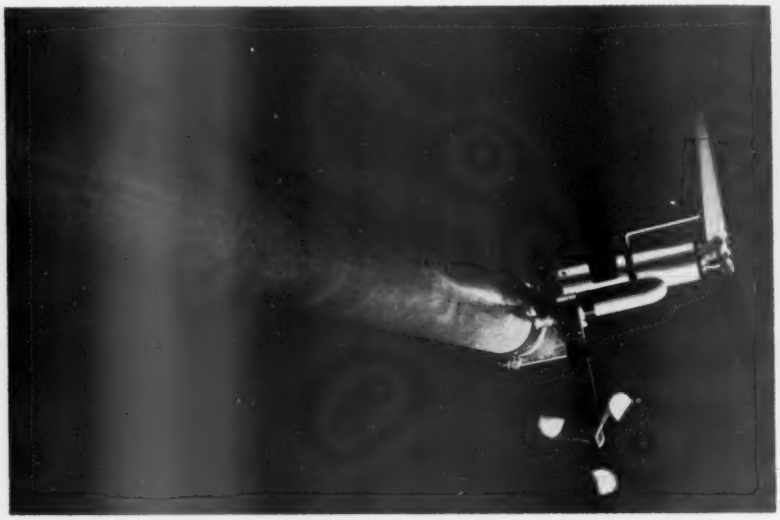

Fig. 8.

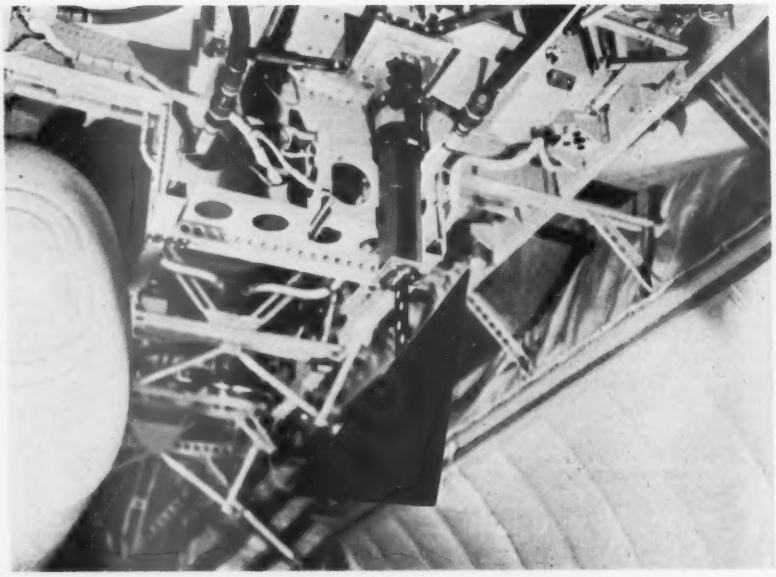

Fig. 9. Delta wing model.

Large honeycomb panels are brazed between ceramic sections in this electric blanket brazing fixture.

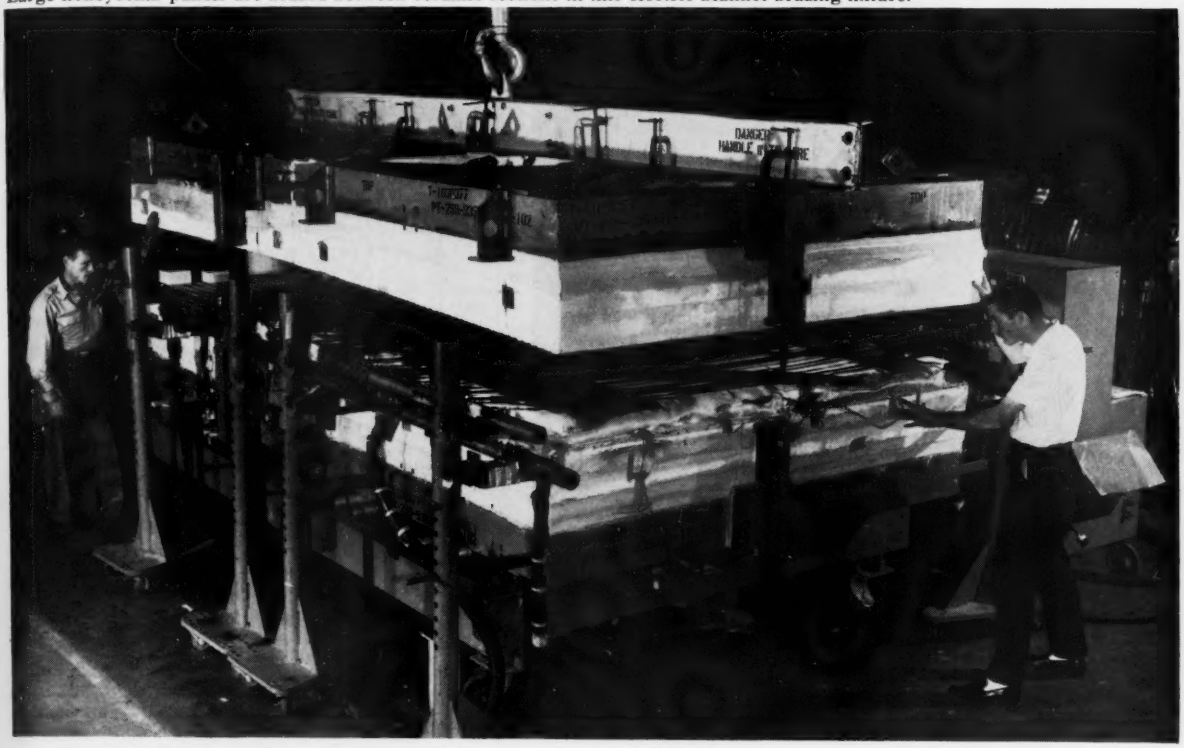

Mach 3 Manufacturing

Making an aircraft skin tough enough to withstand the heat barrier

To cope with the heat barrier and cruise at speeds in excess of 2000 miles an hour, an aircraft needs a skin unlike that of any plane in existence. Traditional covering methods were out of the question.

To solve this problem, the engineers and scientists at the Los Angeles Division of North American Aviation carried on further experiments with the techniques of manufacturing stainless steel honeycomb. They found that by sandwiching this honeycomb between two sheets of steel, sometimes only six thousandths of an inch thick, structural sections could be obtained with excellent insulating characteristics and stiffness approaching a solid slab of steel, yet would be far lighter.

The problem of brazing these honeycomb panels to meet the oven-hot temperatures of Mach 3 speed required an intensive development program. In conjunction with NAA's team of subcontractors, experiments were made with many kinds of brazing methods. One in particular would give high-quality results, with economy. This method utilizes a ceramic form to hold a honeycomb panel at controlled heats of over 1625 degrees.

As a result of this advanced development in the art of making aircraft coverings, a plane can now have a skin so tough it is well able to withstand thermantic speeds.

This technological breakthrough will help sustain America's leadership in aircraft and make possible the supersonic manned weapon systems and commercial aircraft of the future. Because of metallurgical achievements in supersonic fabrication, the American Society of Metals gave North American its 1959 Advancement of Research Award.

THE LOS ANGELES DIVISION OF **NORTH AMERICAN AVIATION, INC.**

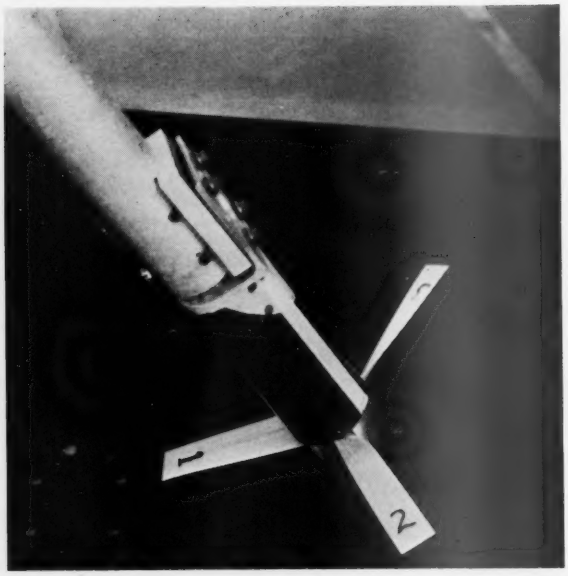

Fig. 10.

whatever vibration mounting that can be provided.

Adaptability of Mounting System

For VTOL/STOL testing procedure involving variable geometry wings and tails, it is felt that the best method of model mounting is by a single point center-of-gravity internal balance. This is attached to a tubular sleeve which attaches to the model-mounting strut. This installation permits build-up of the entire model and instrumentation system as a package away from Lakehurst so that it can be simply bolted to the mounting strut prior to take-off or inflight if necessary.

This is no different from any wind-tunnel installation except for the added complexity of allowing for extending and retracting the mounting strut. This has been of no consequence in tests performed to this date.

Available Power Supply

The present ZS2G-1 airship provides:

(a) 30 kva 120 volts 400 cycle a.c.
(b) 17 kva 28 volts d.c.
(c) 1 kva 120 volts 50 cycle a.c.

This is quite adequate for present test work; the addition of externally mounted gas turbine APU's (auxiliary power units) can provide up to 40 kva additional power or up to 200 lbs./min. of 52 psi compressed air for BLC (boundary layer control) work. A 10 kva variable frequency M-G set built for general wind tunnel use is being installed to allow a standard liquid-cooled 10-hp. motor to be used as a model power unit. These M.G. sets can be rolled into the rear compartment where their basic drive power is from the 400-cycle airship bus.

Generally, there appears to be no difficulty in obtaining sufficient electric or pneumatic power.

Ease of Calibration

In conjunction with the adaptability of the mounting system above, the model balance package can be calibrated remotely. The bomb-bay of the ZS2G-1 and the radome of the ZPG-2 provide sufficient room for check calibrations to be conducted in flight, when necessary.

Fig. 11.

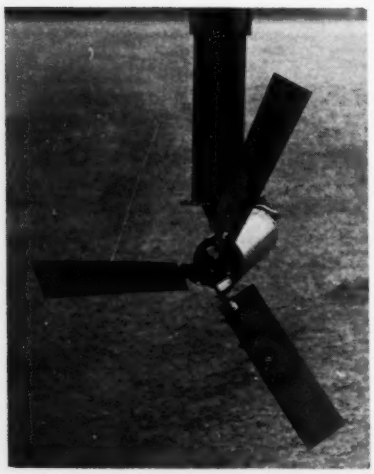

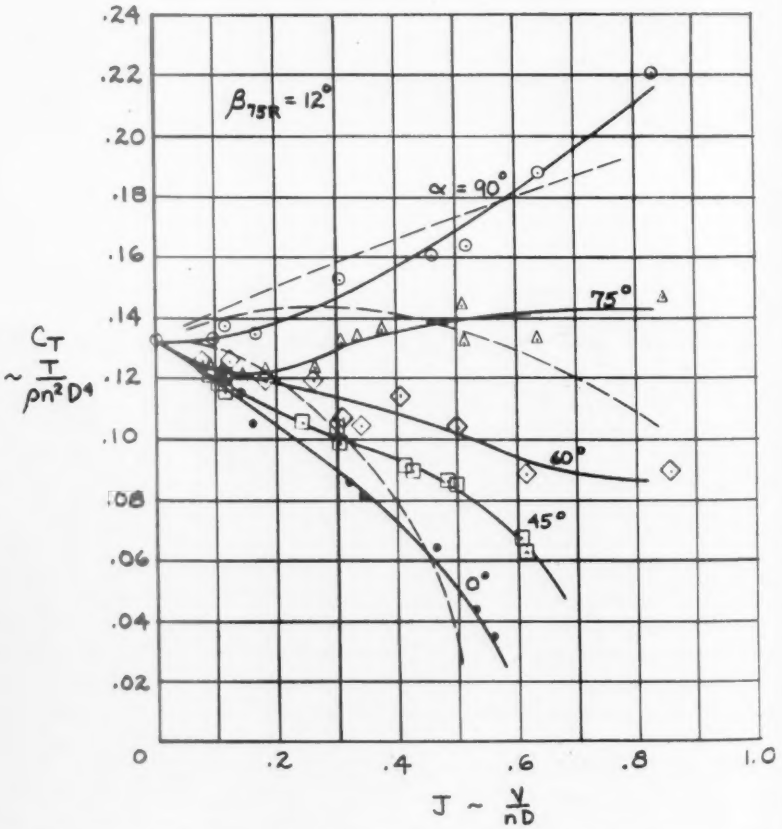

12. C_T vs. J airship data. 14-in. 3-blade paddle propeller. A.F. = 140, $C_{L_{DES}} = 0.5$, $\sigma = 0.1365$, $N_{R_{tip}} = 200{,}000 \rightarrow 300{,}000$. — — — — Forrestal 4- × 7-ft. tunnel data.

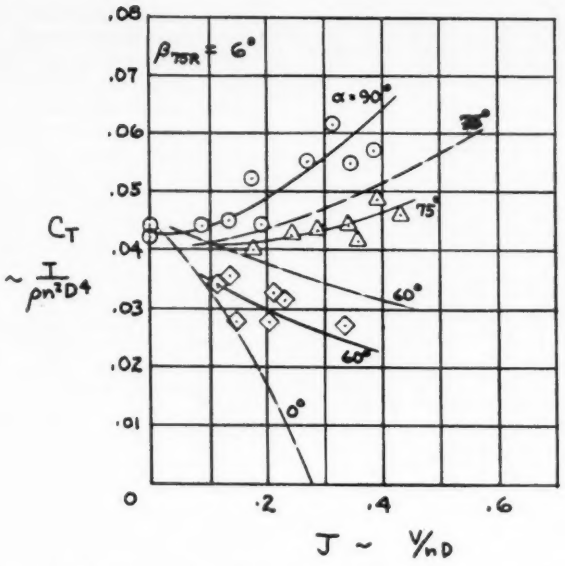

Fig. 13. C_T vs. J airship data. 22-in., 3-blade Vertol 76 rotor. A.F. = 180, $C_{L_{DES}} = 0$, $\sigma = 0.220$, $N_{R_{tip}} = 400{,}000 \rightarrow 600{,}000$. — — — — Ames 40- × 80-ft. tunnel.[5]

Access to Model and Test Conditions

Although the bomb-bay and/or radome area is somewhat restricted when compared to modern wind-tunnel access rooms, this has not proved to be a serious limitation since the model and instrumentation can be thoroughly prepared before being installed.

Wind-off balance readings are taken with the model retracted into the car by hovering the airship. The former is preferable for then the model may be extended and data taken on a series of pitch or yaw angles for a given stabilized air-speed. Air speeds from 65 knots down to 15 knots may be held indefinitely at a constant altitude. Velocities from 15 knots to 0 knots can be held for periods of approximately a half-hour allowing adequate time for any currently conceived set of tests.

As in most modern wind tunnels, all power settings, angle changes, and data recording is handled remotely from the airship test center.

It should be emphasized here that flights can be scheduled with little weather interference all year round. One of the most startling aspects of the airship flying wind tunnel to those unaccustomed to air ship operations is the regularity with which layers of smooth air can be located over water even when relatively gusty conditions prevail over land. In four months of continuous testing, there has never been any difficulty in scheduling flights as desired. Invariably, the airship is waiting for model and instrumentation modifications.

Force Data

At this time work has been accomplished on four model configurations:

(1) Generalized tilt-wing VTOL (Fig. 2)
(2) 6 per cent symmetrical delta wing (Fig. 9)
(3) 3-blade paddle propeller (Fig. 10)
(4) Vertol model 76 3-blade rotor (Fig. 11)

Configurations (1) and (2) were run primarily as check runs to correlate the airship data versus the known wind-tunnel characteristics of these models. Fig. 4 indicates close agreement between the two facilities with the exception that at high angles of attack, there appears to be a downwash restriction on the delta wing created by the presence of the tunnel floor. The C_L developed at 35° by the identical wing as tested from the airship is approximately 10 per cent greater than the corresponding point in a 4 ft. × 5 ft. tunnel.

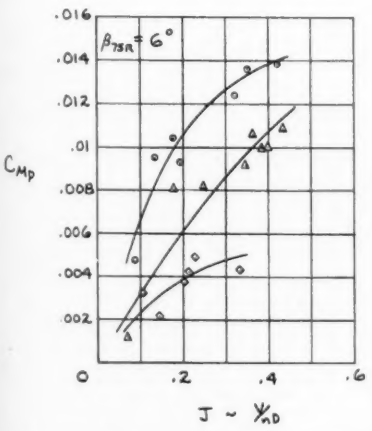

Fig. 15. C_{M_P} vs. J airship data. 22-in., 3-blade Vertol 76 rotor. Reference 5 indicates this moment equals zero.

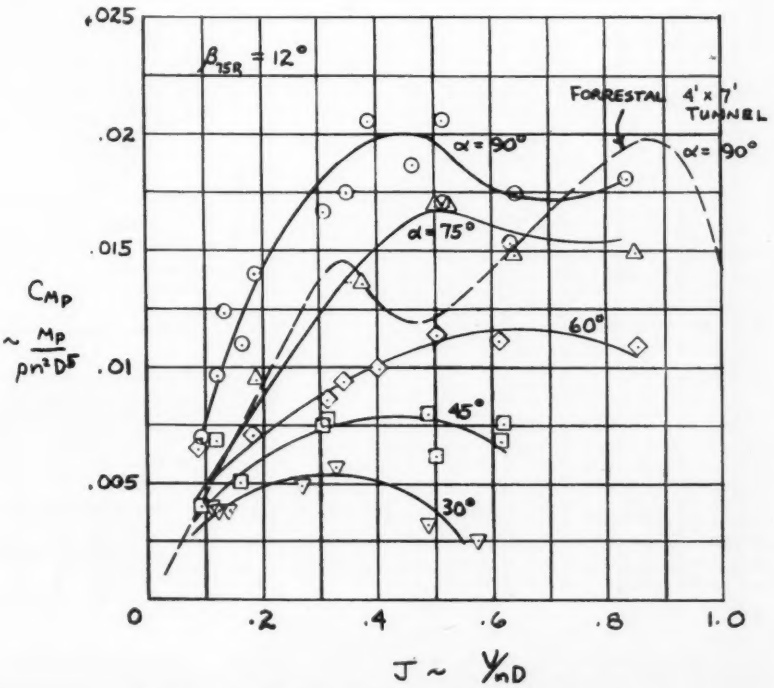

Fig. 14. C_{M_P} vs. J airship data. 14-in., 3-blade propeller.

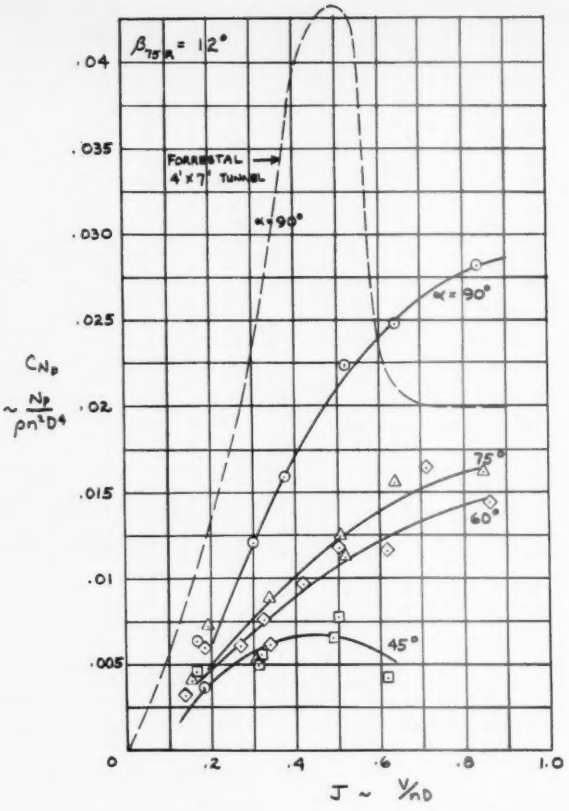

Fig. 16. C_{N_p} vs. J airship data. 14-in., 3-blade propeller.

The results of the propeller and rotor tests are presented in Figs. 12 through 17. This is a continuation of work begun in references 3 and 4. The actual data points taken from the flying wind tunnel are shown on these plots. The scatter is quite evident, yet not objectionable when one considers that these are the results obtained with pen recorders giving a maximum reading of only 30–40 mm. Repeatability is excellent and is considered to be the equal of Princeton wind-tunnel data. With the addition of a more sophisticated data acquisition system in the ZPG-2 airship, it is expected that this scatter will be considerably reduced and precise, accurate results can be obtained with no wall interference or nonuniformity of flow.

Figs. 12 and 13 are plots of thrust variation with forward speed for various angle of inclination to the free stream where $\alpha = 90°$ is the hover configuration and $\alpha = 0°$ is normal forward flight. Because of power limitations under the present relatively crude installation, the Vertol rotor was not able to be driven at a blade pitch angle greater than 6° at 85 per cent radius.

Figs. 14 and 15 represent hub-pitching moment versus forward speed and Figs. 16 and 17 propeller or rotor normal force variation with forward speed.

It is evident from comparison of the air ship free air data points with the dotted wind-tunnel results that a serious discrepancy exists.

The 3-bladed paddle propeller with a diameter of 1.167 ft. was previously tested quite extensively in the Subsonic Laboratory's 4 ft. × 7 ft. low-speed tunnel. It appears that the wind tunnel results differ primarily from the free air results at low values of J (or low-speed). Thrust and normal force data are considerably greater, whereas hub pitching moments seem to be smaller.

In the case of the tests with the Vertol rotor, a comparison was made with the identical rotor (9.5 ft.) as tested in the Ames 40 ft. × 80 ft. wind tunnel.[5] It is significant that here, too, the wind-tunnel data measures higher values for thrust and normal force. However, it should be realized that articulated rotors do not necessarily have a negligible pitching moment. In fact, the existing hub-pitching moment, as seen in Fig. 15, due to the hinge offset of the rotor reaches values of the same order of magnitude as that of the rigid propeller.

Experience with the Forrestal track facility has verified the suspicion that the mass flow field about a rotor is significantly influenced by the presence of wall restrictions. Here, in a 30 ft. × 30 ft. cross section, it was noticed that a considerable thrust change could be induced by varying the flow field restriction. From previous work in the Forrestal 4 ft. × 7 ft. tunnel with propellers alone and propellers fitted to a wing, it is immediately apparent that the presence of only the wing flow field causes great changes in the propeller forces and moments.[4]

In addition, it should be mentioned here that the propeller was mounted at approximately one diameter in front of the 4-in. mounting strut (Fig. 8). However, it is felt that this installation is considerably cleaner than most other propeller test stands. The strut interference on the propeller flow field may be appreciable and work is preceeding to investigate this phenomenon.

Considerable work is presently being done to further check the discrepancy between the free air test results and

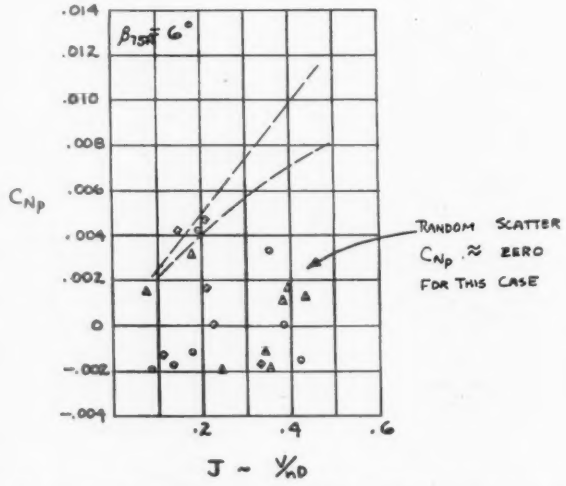

Fig. 17. C_{N_p} vs. J airship data. 22-in., 3-blade Vertol 76 rotor. ———— Ames 40- × 80-ft. tunnel.[5]

those of wind tunnels. Unfortunately, little or no flight-test information is available to provide an accurate correlation. It is possible that this may be rectified in the near future.

Conclusion

The airship as a flying wind tunnel has been shown to give accurate repeatable data for a variety of configurations with no difficulty.

The remarkable stability of the platform combined with the flexible nature of its operation provide an ideal facility for low-speed VTOL test work. Because these airships already exist, the cost factor is quite low. Direct operating cost compare favorably with existing large wind tunnels.

Further work is being done to investigate the difference between free-air testing and wind-tunnel testing. But it is believed that the unusual flow field associated with all VTOL/STOL aircraft can only be duplicated in a free air facility with no wall restraint or in a very large wind tunnel where the effects of walls are negligible.

References

[1] Grey, Cecil Harrington, *An Investigation of the Fundamental Parameters which Govern the Aerodynamics of Various Wing-Propeller Combinations Related to Vectored Slipstream Aircraft*, Princeton Report 437, October 1958.

[2] Hazen, D. C., Lehnert, R. F., and Payne, H. E., *A Preliminary Evaluation of the Use of an Airship as a Test Vehicle for VTOL-STOL Aircraft Models*, Princeton Aero Report 520, August 1960.

[3] Payne, H. E., and Cromwell, C. H., *A Stability Analysis of Tile Wing Aircraft (Experimental)*, Princeton Report 478, May 1960.

[4] Payne, H. E., *Propeller Effects on the Stability and Control of VTOL Aircraft*, Aero/Space Engineering, Vol. 19, No. 3, pp. 48–52, March 1959.

[5] Yaggy, Paul F., and Rogallo, Vernon, *A Wind-Tunnel Investigation of Three Propellers Through an Angle of Attack Range from 0° to 85°*, NASA TND-318, May 1960.

An Authorized Binding for *Aerospace Engineering*

Arrangements have been made by the Institute of the Aerospace Sciences for members and subscribers to have their magazines bound carefully and economically. Simply write for details to:

Publishers' Authorized
Bindery Service Ltd.
430 West Erie St.
Chicago 10, Ill.

LONG RANGE INPUT / 1794

News of the recapture of Condé from the Austrians was sped to the French Revolutionary Convention at Paris in a matter of minutes via Claude Chappe's amazing télégraphe aérienne, or relay aerial telegraph, Sept. 1, 1794. A new era in rapid communications had begun.

Today, instantaneous and completely reliable Electronic Communications insure the immediate and continuous interchange of intelligence throughout the Free World. ECI is proud of its initiative and responsibilities in the design, development and manufacture of high precision electronic equipment to the critical specifications required in various aerospace and surface roles vital to our National Defense and to scientific achievement. An example is ALRI—Airborne Long Range Input—a program where ECI communications and data link equipment fill an integral and essential requirement in linking USAF's advanced early warning system to SAGE—our continental defense network.

System
Development
Communications
Data Link
Countermeasures
Computers
Actuators

ELECTRONIC COMMUNICATIONS, INC.
St. Petersburg, Florida

RESEARCH DIVISION
Timonium (Baltimore), Maryland

ADVANCED TECHNOLOGY CORPORATION (ADTEC)
Santa Barbara, California

REGIONAL OFFICES: Washington, D.C., Teterboro, N.J., Boston, Mass., Dayton, O., Dallas, Tex., No. Hollywood, Calif.

Industry Research Management (Continued from page 25)

very specialization of the modern scientist tends to reduce his effectiveness unless he has ample opportunity to exchange ideas and review his work with colleagues. Opportunity to continue education is another requisite in the environment, particularly for the researcher who has not yet received his Ph.D. While environment can be analyzed and described under specific headings, in the final analysis the most important criterion is the spirit which prevails among the researchers. The spirit, I believe, derives from the leadership afforded by the director and the collective capability of the staff.

Research management in the older aerospace industry firms must pass through a transition from the earlier period when engineering also was research, to the newer state when emphasis must be given to basic research. The transition involves some hurdles. Some status values in engineering will become subordinated. Budgets will be redistributed. Empires will shrink. Terms will assume new definitions. Innovations in job classifications and salary scales will be reconciled. Public relations will turn the warm light of fame on new (and younger) faces. New and strange technologies will move into the center of activity. Organization lines will be bent.

The new look in aerospace research presents a financial crisis for the company required to conform to government-set standards for profit in a defense industry. If research is not done, the firm goes out of business, at least as a prime contractor. If enough research is funded from company money to avoid product obsolescence, the firm loses money. The escape from this trap appears to be a greatly expanded research business for customer firms. Expanding the research function to provide for contracted activity increases the planning and coordination needs; however, the basic problems of research management do not change.

The Work Ahead

While the days ahead in aerospace research management will bring continued frustration and hard work, the potential of our industry is so great that the rewards most certainly will justify the effort needed to solve the research management problems now before us. Although engineering may be the most difficult group to become convinced of the importance of basic research, the capability and versatility of the aerospace engineering organizations will ultimately be the critically essential ingredient needed to translate the fruits of research to products and services. While difficult and numerous, the goals of research management are within reach and finite. Higher authority must be convinced of the necessity of specified responsibility, authority, capability, and support proportionate with the results expected. In some firms higher authority must be convinced that the research function provides one of the strongest available means of avoiding product obsolescence, and that basic research plays a vital role in the overall research function. The establishment and maintenance of research goals require an authoritative outline, regularly brought up to date, of company long-range plans. The research director must have the opportunity to review research results periodically for top management, and to participate in the integration of technical advances into long-range company plans as the feed-back phase of planning.

From knowledge of company long-range plans the research director forms research programs and individual projects by which the company plans are given required scientific support. The success of the program depends largely on the director's strength, which derives from his personal capability and institutional strength—i.e., responsibility, authority, capability, and support.

The success of research management also depends on the ability to lead the scientific staff. The research goals may be reached only by the discovery of ways to reconcile the divergence between company goals and individual scientist professional goals.[6] The goals of scientists are strongly influenced by inward orientations, professional interests, and the desire for autonomy and independence. The scientist seeks these goals in industry within the environment of the company organization which seeks to place its workers in positions of dependence and subordination.[6] The orientation of the scientist may sometimes act as a deterrent in obtaining higher management approval for costly equipment, support, and travel. Research management must reorient the scientist and act as a buffer between research and the other functions of the company.[6] The reorientation of the scientist involves sensitive values. Knowledge of the company, its functions and plans, discussed by top management, goes far in giving the scientist the ingredients for his own reorientation. Considering the stakes and investment, top management can ill afford to allow its senior scientists to remain uninfluenced by company goals. The scientist has undergone many years of self-discipline while mastering difficult scholarly goals. He knows that his scholarship ha required high intellectual capacity. He knows that the world has acknowledged the vital necessity of scientific progress, and he carries this knowledge with him as he takes up his professional work. It is little wonder that status in relation to other scientists ranks high in his values. For reasons well established in his mind he recognizes no technical authority above that of his scientific colleagues.

Particularly in the transient phase of research growth in a company, research management is under heavy pressure by the corporation to give greater emphasis to development. Yet it is in the early growth period when most care should be given to research organization, scientific programs, and recruiting. Research management must find acceptable compromises in the degree to which the staff is engaged in development and project consultant work.

The discovery by research management of the happy compromise in imposing executive authority normal in business firms in contrast to allowing autonomy and independence is probably best found in a mixture of sanctions and rewards. Scientists resent nonprofessional supervision, and therefore the transition from professional to company interest along the management line of authority is a sensitive factor in gaining compliance with company regulations. Because the scientist knows that he can find another job—perhaps at higher pay—research executive control poses new requirements. Research management needs new organizational principles and a specialized concept of group management involving new kinds of men in new kinds of work, with new kinds of very expensive equipment. In the new organization provision must be made for indoctrinating the scientist and adjusting the industrial environment to research work. The creative power of the scientist's mind is a valuable asset to both society and industry. It should not be deleteriously affected by a hostile environment. The problems of adjustment can be solved.

Conclusions

The results of a recent study of research management at Columbia University[7] provide an outline for summing up this discussion. Research management work falls into this pattern:

(1) Participation in the formulation of corporate long range goals.

(2) Conversion of corporate goals into research programs.

(3) Organization of the research function in a manner agreeable to higher corporate management and as required to execute programs.

(4) Definition of responsibilities and authority of each research organizational unit.

(5) Maintenance of respect, con-

THIS IS AN ENEMY BOMBER. NORTHROP BUILDS IT.

On a radar screen, the RP-76 target missile can look as big as the largest enemy bomber. Rocket powered, it flies faster than sound, operates above 70,000 feet. Yet this little giant is less than ten feet long, weighs just over 300 pounds, and parachutes down for re-use after completing its run. It is the heart of the Army's program for training the ground-to-air missile crews who guard our cities. The complete target and tracking system is made, managed and serviced for the Army by

RADIOPLANE
A DIVISION OF
NORTHROP

fidence, understanding, and communication between and within all areas.

(6) Formulation of administrative plans.

(7) Continual protection of the scientific environment.

(8) Interpret and convey research results to top management for action.

References

[1] Hickey, Albert E., Jr., *Basic Research: Should Industry Do More Of It?*, Harvard Business Review, Vol. 36, No. 4, July-Aug., 1958.

[2] Sibley, Alden K., and McNeice, William H., *The War Of Basic Research*, Army, Oct., 1959.

[3] Brozen, Yale, *Trends In Industrial R/D*, Journal of Business, University of Chicago, Aug., 1960.

[4] Gershenowitz, Harold, *Industrial Research Programs And Academic Research*, American Scientist, March, 1958.

[5] Brown, Harrison, Bonner, James, and Weir, John, *The Next Hundred Years;* The Viking Press, New York, 1957.

[6] Marcson, Simon, *The Scientist In American Industry*, Industrial Relations Section, Princeton University, 1960.

[7] Report of Oval Room Work Group, *Reconciling Professional And Personal Goals And Needs With Company Goals And Needs*, 11th Annual Industrial Research Conference, Columbia University, New York, Aug., 1960.

✦ ✦ ✦

Instrumentation Precision (Continued from page 31)

by the customer, in this case the Air Force Ballistic Missile Division and its technical program management team at the Space Technology Laboratories, was as illustrated by the Fig. 1. The performance value to be demonstrated on all PFRT, acceptance, and qualification tests was to be above the contractual minimum by 1 per cent or one standard deviation of the instrumentation error, whichever was less.

Our initial efforts on the development program were devoted to fabricating hardware to the initial designs, activating new facilities, hiring and training personnel, and getting to the point that the large thrust chambers would hold together a reasonable portion of the time. Little attention was given to the accuracy of the instrumentation until it became apparent that we would have difficulty in meeting the required performance on the engine. An error analysis was then made to determine the accuracy of performance measurements and to define the areas where improvement could be effected to the greatest advantage. This analysis included studying a large amount of calibration data, evaluation of redundant measurements of all critical parameters, and a comparison of performance figures obtained with the same thrust chambers using different test stands and different instrumentation systems. The results indicated that one standard deviation of our instrumentation error was ± 0.6 per cent. There was considerable uncertainty regarding the accuracy of measurement of the flow rate of liquid oxygen since there was no existing standard available to calibrate against at the flow rates with which we were concerned. Therefore, it was necessary to design and construct a standard. As a result of this and other improvements, we were able to provide an error analysis with sufficient substantiating data to effect an official change in the engine acceptance criteria. The instrumentation error to be allowed for above the contract minimum for performance demonstration was one standard deviation of ± 0.52 per cent. The average indicated performance of the engine was 1.1 per cent above the contract minimum. The repeatability of the test results including variations between engines and variations due to the instrumentation system was 0.38 per cent (1σ). Fig. 2 shows that under these conditions and on the basis of a normal distribution of test results only 5 per cent of the tests should be rejected as compared to almost 50 per cent rejection with a 1 per cent measuring system which we were assumed to have at the beginning of the program.

The economic benefits derived from the improvement in the accuracy of the performance measurements and the revision in the acceptance criteria based on this improvement were as follows: (1) with a 1 per cent measuring system, it would have required improving the engine performance by at least 1 per cent over the best available performing engine at that time to meet the requirements. It was estimated that the cost of developing an improved injector and thrust chamber assembly with the required performance would be at least $6 million; (2) with a 0.5 per cent measuring system that had not been fully demonstrated to be within this error bandwidth would have required an expenditure of at least $3 million to obtain a 0.5 per cent improvement in the performance of the engine.

The flow calibration facility mentioned above is a bonus benefit of this effort and is shown in Fig. 3. The story of the development of this flow standard is a subject of a separate paper.[2] This facility has the capability of calibrating flow meters with cryogenic as well as noncryogenic fluids at flow rates up to 1,200 lb./sec. with an accuracy better than 0.1 per cent. This is still the only facility with this capability in this country. National Bureau of Standards has flow standards for cryogenics only to 30 lbs./sec.

(2) Economic Aspects of Testing a Large Number of Solid Propellant Formulations With Minor Differences in Performance

To determine the performance indices of the many possible formulations of solid propellant ingredients and processing variables, it is necessary to discern performance changes of one pound-second per pound, or approximately 0.4 per cent. Two years ago, we were trying to do this with a 1 to 2 per cent measuring system, which at times required 20–40 tests per formulation to determine the average performance; and even so, the confidence level was frequently not very high. A concentrated program was established to improve both motor processing and test techniques. The areas of improvement were: (1) tighter controls on the propellant and motor processing variables; (2) improved scales for weighing the propellant; and (3) redesign of the test stand and instrumentation. The new test stands provide for precise

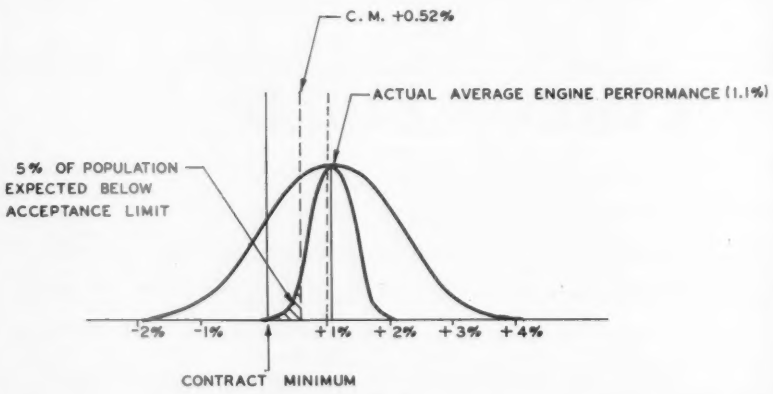

Fig. 2.

KEARFOTT developed and now produces precision floated gyros for the Atlas missile.

Engineers: *Kearfott offers challenging opportunities in advanced component and system development.*

KEARFOTT DIVISION
Little Falls, New Jersey

GENERAL PRECISION, INC.
Other Divisions: GPL, Librascope, Link

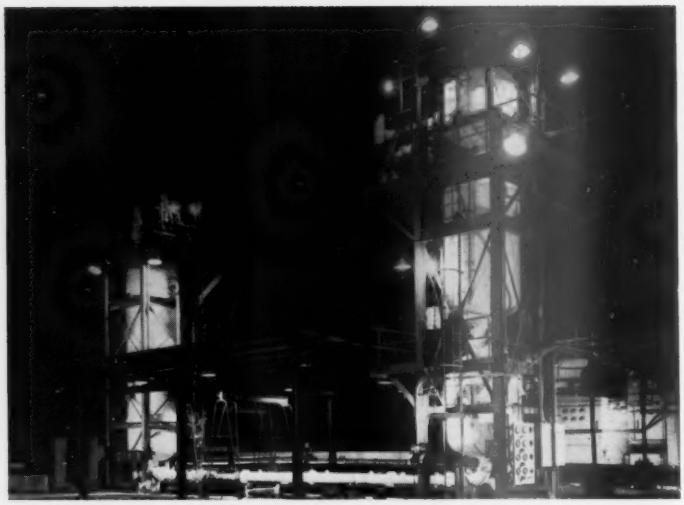

Fig. 3.

alignment of the motor axis with the thrust measuring system, in-place dead weight calibration for the complete assembly, and minimum restraint flexures for supporting the motor. The instrumentation recording method was changed from recording oscillographs to digital recording and integrating voltmeters. Test results are now repeatable to ± 0.1 per cent ($1\ \sigma$).

An estimate of the savings was obtained by comparing the number of tests conducted over an 8-month period prior to the accuracy improvement program to the number of tests for a similar period after accomplishment of the above changes and adjusting for an increase of 24 per cent in costs per test incumbent with the tighter control. An estimated savings of $750,000 a year has been realized at our present rate of testing in order to get information with the same confidence on the same number of propellant formulations.

(3) Economic Aspects of Statistically Demonstrating Performance Repeatability—Large Solid Engine for a Ballistic Missile

The original work statement for this engine required the demonstration of total impulse repeatability of ± 1 per cent at a confidence level of 95 per cent. This appears easy on the surface; however, an analysis of the number of tests required to demonstrate the specification requirements versus the product variability and instrumentation variability, the results of which are shown in Fig. 4, produces some startling results. Examination of these relationships show that with product variability of 0.75 per cent and measuring system repeatability of 0.75 per cent, 200 tests would be required on each configuration to demonstrate that the requirements had been met. At a cost of approximately $100,000 per test to provide the propellant, hardware, and associated test costs, the program could not afford this requirement. Therefore, a process control study determined that it was possible to maintain the product variability to ± 0.5 per cent. With this product variability it becomes almost an economic necessity to reduce the instrumentation variability from 0.75 per cent (50 tests required) to 0.50 per cent (28 tests required), and highly desirable to reduce the instrumentation variability to 0.25 per cent (16 tests required). The savings in reducing from a half per cent to a quarter per cent is approximately $1,000,000 per model. A more detailed presentation of this analysis can be found in Reference (3).

As a result of this analysis, the design target for the instrumentation system to be used to obtain the total impulse was established at 0.25 per cent, three standard deviations, and this target is presently being approached. Our error analysis of the thrust measurement indicated that one of the largest errors, for high thrust levels, is the possible error in the standards calibrated by the NBS. This results from the fact that the limit of the Bureau's dead weight calibrating capability at present is 111,000 pounds. The results of this analysis contributed to Congressional approval of funding to increase the Bureau's capability to 1.5 million pounds. The new facility to provide this capability is scheduled for completion in 1963.

By pointing out the economic advantages of increased precision, it is not intended to imply that all measurements need to be or should be made with the maximum possible precision. This would certainly be uneconomical since to obtain higher precision and/or accuracy requires greater care and attention to detail as well as more refined equipment. Therefore, it is necessary to analyze the effects of errors in the various measurements on the desired information in order to determine which

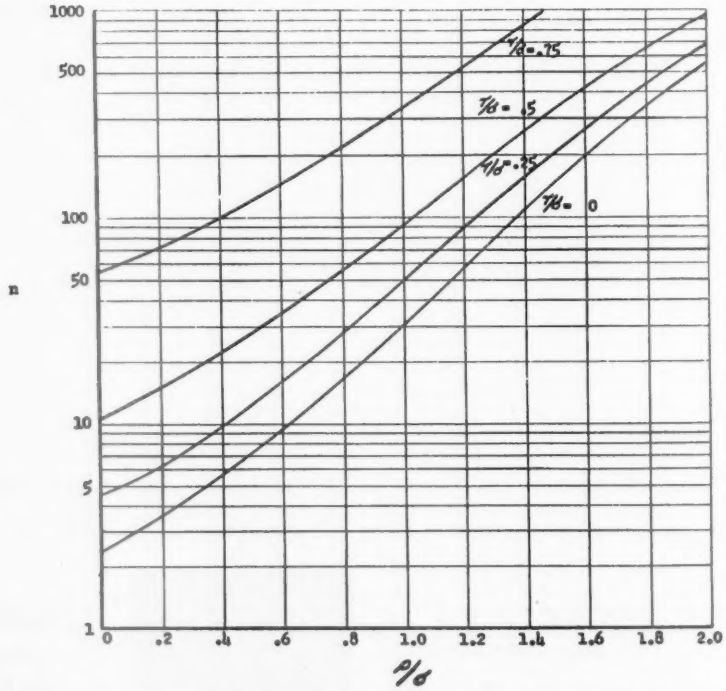

Fig. 4. Number of tests required for ratios of ρ/σ and τ/σ. Confidence level, 95%. n = sample size, ρ = instrumentation variability, σ = specification variability, τ = product variability.

of the measurements needs to be made at high accuracy. At Aerojet, we have divided the rocket measurements into 4 classes of different accuracy levels as a guide in putting the emphasis where it helps and avoiding unnecessary expenditures where they do not benefit us.

Applicability to the General Field of Space Vehicle Development

The discussion and examples above are drawn from experience in static testing of rocket propulsion systems. However, the principles apply to testing of any advanced complex system; and the problems are much more difficult when telemetering links are required, and when compromises in the performance of equipment are necessary to obtain the light weight and small sizes demanded for airborne and space applications.

The quality of most telemetered data has been poor relative to the quality of data obtained from static tests, primarily because of the compromises accepted in transducer characteristics to obtain high outputs with light weights. Very little information on propulsion system performance useful to designers has been obtained from internal measurements on flight tests. The present trend toward the use of low-level PCM telemetry systems is encouraging in this respect.

Recent Progress

In the past 5 years, the areas where considerable advances have been made in measurement precision and accuracy are:

(1) Application of digital recording devices in measuring systems and marrying these devices to digital computers (thus minimizing the manual handling of data) has resulted in a significant reduction in the number of errors, has provided much more data from each test in a usable form, and has made the test information available much sooner after a test.

(2) Development of transducers with much improved performance characteristics. Reference to the transducers as the weak link in measuring systems has become almost a cliché; and there is still work to be done but at present the primary limitations result more frequently from the method of application of the transducers than in the transducer characteristics themselves.

(3) Increased appreciation for, and use of, standards with a direct, traceable line to the accepted national standards for critical measurements.

Areas of Improvement

Some of the areas where effort is needed to improve the economics of testing are:

(1) Additional national standards—Two of these needed standards were mentioned in the examples discussed above, and there are others such as standards for microwave power,[4] and dynamic pressure and force.

(2) Nondestructive testing—As space vehicles become larger and achieve the reliability required for human occupancy, the economics of testing require further minimizing of the numbers of tests to achieve proven reliability. Further developments in the techniques and use of nondestructive testing are necessary.

(3) Data compression—A large part of the test data now taken is not used. Emphasis should be given to the design of data systems which report not all measurements, but only the deviation of measurements made from a predicted pattern of behavior. Increased accuracy may be achieved by a dynamic balance approach to measurements system design to provide data in terms of the deviation from a dynamic standard.

(4) A greater use should be made of specialists in measurement and instrumentation systems in determining the best methods to obtain critical test information in order to take advantage of recent advances in state-of-the-art. Hardware development engineers are inclined to specify the measurement methods to be used based on equipment and techniques which they have seen used in the past rather than stating the problem and leaving it to test specialists to determine the best method to apply. However, there is an insufficient supply of adequately trained engineers and scientists in the field of measurements, and a greater emphasis needs to be put forth in the training of qualified people, both by educational institutions and by industry.

(5) The performance requirements specified in procurement documents and the criteria for demonstrating fulfillment of these requirements have a very large effect on development program costs. Therefore, close attention to details to make sure that the specified requirements are realistic and no more stringent than is necessary for successful fulfillment of program objectives is very important, and requires continual surveillance to obtain optimum progress per dollar invested.

References

[1] *Development Problems in the Field of Measuring Techniques, 1959–1965*, Measurement Techniques (Soviet publication), Transl. and published by ISA.

[2] Deppe, G. R., *Report of D-6 Flow Calibration Facilities Test Results*, unpublished AGC paper.

[3] Dow, R. H., *The Cost of Instrumentation Error*, ISA 6th National Flight Test Symposium, April 1960.

[4] Wilson, L. B., *A New Space Age Challenge—Standards and Electronic Measurements*, 1960 Conf. on Standards and Electronic Measurements, June 22, 1960.

AEROPHYSICS AND SPACE PROPULSION

ARMOUR RESEARCH FOUNDATION offers exceptional opportunities for unusually qualified engineers and scientists to join our Fluid Dynamics Research staff. We are seeking engineers and scientists with advanced degrees, demonstrated creative ability and a minimum of five years of research experience to initiate and direct research programs in:

MAGNETOHYDRODYNAMICS
ELECTRIC PROPULSION
NUCLEAR PROPULSION
HEAT TRANSFER
MOLECULAR FLOW
HYPERVELOCITY

As a Foundation staff member there is opportunity to be associated with a mature independent research organization with a staff of over 600 engineers and scientists contributing to a wide variety of industrial and government research programs. Interested research workers please contact Dr. T. Paul Torda, Director of Fluid Dynamics and Systems Research, Department 2-S.

ARF

ARMOUR RESEARCH FOUNDATION
OF ILLINOIS INSTITUTE OF TECHNOLOGY
TECHNOLOGY CENTER, CHICAGO 16, ILL.

Hydrofoils (Continued from page 11)

very low speeds, conventional freighters, slow-speed tankers, and similar conventional forms are many times more efficient than any of the high-speed design forms. However, as the speed is increased, first the planing boat and then the hydrofoil craft become much more efficient.

This principle of the hydrofoil has been known as long as the principle of flight yet its application has been much slower. The hydrofoil craft was a high-speed form of surface vehicle that until recent technological advances could not show an economic advantage.

Another factor which has slowed the development of the hydrofoil is that its problems include complicated ones not answered by the usual techniques of subsonic aerodynamics or displacement ship hydromechanics. The successes that have been achieved have been the gradual ones in overcoming the special problems generated in application of known hydrodynamic and aeronautic techniques. The "hydronautic" success has been steadily improving our recognition, definition, and understanding of the areas peculiar to the hydrofoil development that are not already in the storehouse of knowledge of either discipline alone. Of course, merely uniting the conservative naval architect and the "wild blue yonder" aeronaut has not been spontaneous or without communication difficulty. Perhaps an important part has been the gradual increased interest of the aircraft industry as conventional aircraft orders decreased. Future development rests on the continued successful welding of the two arts and sciences and on the application of further effort to the peculiar problems of "hydronautics."

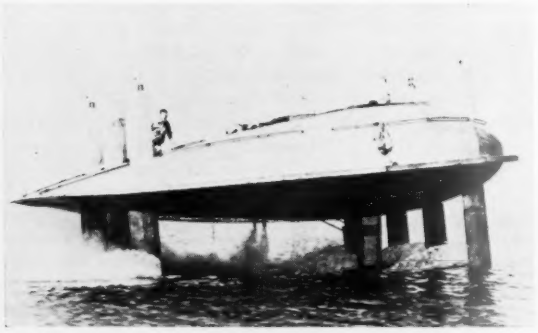

Fig. 3.

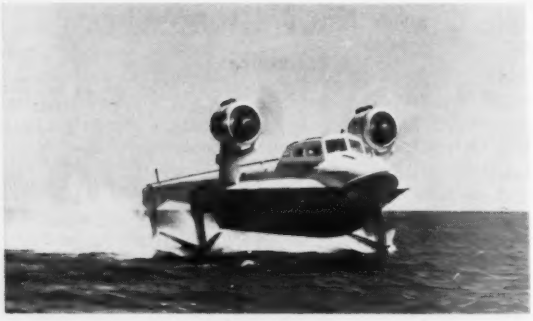

Fig. 4.

Fig. 5.

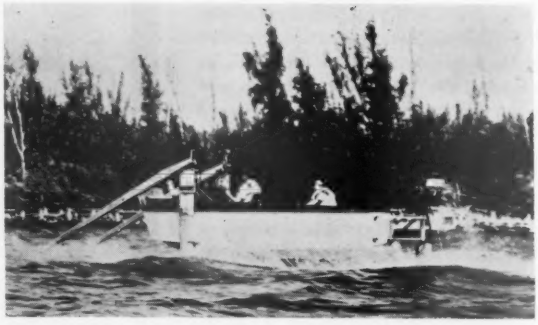

Fig. 6.

Brief History of the U.S. Navy Hydrofoil Program

The historical development of experimental hydrofoil craft has been previously reported, notably in references 1 and 2. Little has been published in summary of the U.S. Navy's program of hydrofoil development. The following paragraphs give a brief history and describe some of the experimental craft.

The Navy Department, through the Bureau of Ships and the Office of Naval Research, with assistance from the then Bureau of Aeronautics, initiated a joint program in 1947 to develop the hydrofoil principle and determine its usefulness. In the initial phases of the program, theoretical studies were undertaken with major emphasis on design characteristics such as pressure distribution on foils, turbulence, and cavitation, and on the problems of maneuvering and control. In addition, a number of hydrofoil craft design studies were started. Beginning in 1951, these basic studies were conducted at a more accelerated rate, and additional investigations of lift, drag, stability, minimum-weight high-strength structures, and propulsion systems were undertaken. Construction began in 1952 on three test craft designed to evaluate some of the basic hydrofoil principles. Feasibility studies of larger craft were initiated, and theoretical

work was concentrated in areas of electronic control systems and height-sensing devices.

The first of the hydrofoil test craft to be completed was the HC-4, or Lantern (Fig. 3), developed by Hydrofoil Corp., Annapolis, Md. The principal characteristics of this craft were as follows: length 36 ft., beam 22 ft., displacement 22,200 lbs., and speed 18 knots. Developed under the direction of Dr. Vannevar Bush, it was one of the first craft to employ fully submerged foils with an associated autopilot control system. The HC-4 was beset by numerous difficulties, not the least of which was its lack of power.

At about the same time, a second craft, designated the XCH-4 (Fig. 4), was completed by the Dynamic Development Corp. The principal characteristics of this craft were: length 54 ft., beam 19 ft., displacement 16,500 lbs., and speed 75 knots. The foil system consisted of an airplane or conventional system with two foils forward in a split arrangement and a single foil aft. The two forward foils were of a V-type ladder configuration which carried the major portion of the load. The single after foil was fully submerged. Power was provided by two 450-hp. aircraft engines with air propellers mounted on top of a seaplane-type hull. Problems developed in the design and location of the after submerged foil. Successful flights were made, and a speed of 75 knots was attained in smooth water.

The third in this first series of test craft was completed in 1953 by Baker Manufacturing Co., Evansville, Wis., and was named High Pockets (Fig. 5). The principal characteristics of this craft were: length 24 ft., beam $10^1/_2$ ft., displacement 6,000 lbs., and speed 35 knots. A system of four separate surface-piercing V-foils was used, one at each corner, and the angle on the foils was set at 45 deg. The craft had good seakeeping qualities, and successful trials were conducted in 5- and 6-ft. seaways off Pensacola, Fla. Power was provided by a 125-hp. Chrysler Crown engine.

In 1953 a study was undertaken to determine the applicability of hydrofoils to small landing craft. As a result, several small test craft were built to further develop and test some of the concepts the studies had engendered. The first of these craft, developed by Miami Shipbuilding Corp., Miami, Fla., was 20 ft. in length, had a $5^1/_2$-ft. beam, and displaced 2,600 lbs. (Fig. 6). It utilized retractable submerged foils. Control of the foil in response to changes in position relative to the water surface was provided by floats attached to arms extended ahead of the bow. The end of the arms at the boat were mechanically linked to the foils. This craft proved to be fairly successful in both stability and control and attained a speed of 23 knots.

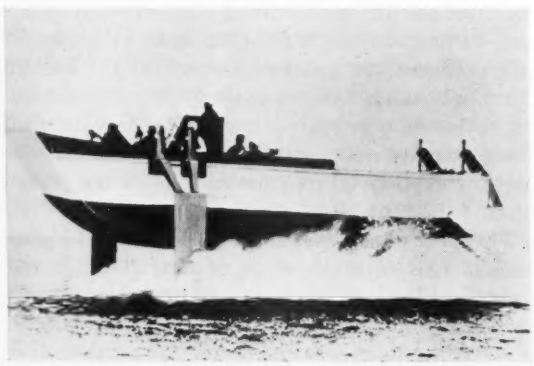

Fig. 7.

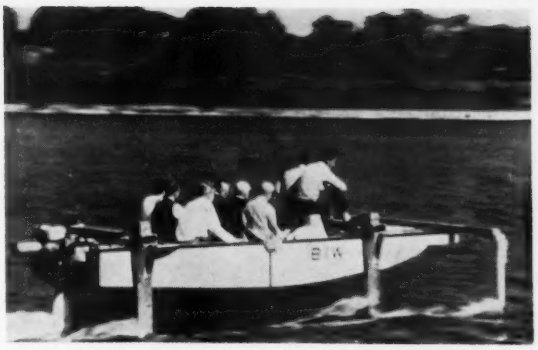

Fig. 8.

Fig. 9.

During the following 2 years, design and construction of two larger amphibious-type landing craft were undertaken. One of these was completed and tested in 1957. It was called Halobates (Fig. 7), and it remains the largest hydrofoil test craft the United States has operated to date. It is 45 ft. 9 in. long, has a 12-ft. beam, displaces 31,000 lbs., and has a 630-hp. engine. Originally the boat had the same type of mechanical feelers forward as did the preceding 20-ft. test craft. These feelers were relatively large and proved too cumbersome, although quite successful. An electrical sensing system was developed and installed in place of the feelers, but this system was only partially successful. The second of the large hydrofoil landing craft has not yet been completed. It will be fitted with surface-piercing, V-type foils.

In 1955, at the same time the landing craft studies were being conducted, another craft (Fig. 8) was built and tested by Gibbs & Cox, Inc., New York. It was 20 ft. in length, 5 ft. in beam, displaced about

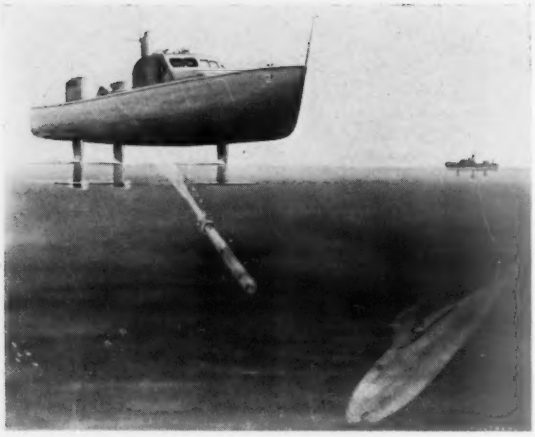

Fig. 10.

1,800 lbs., and was powered with a 22-hp. outboard motor. This test craft was very active in the mid-fifties. Fitted with fully submerged foils that could be located at various positions fore and aft, it was utilized to test methods of autopilot control. Experimentation with this craft resulted in the development of an electronic device for measuring the distance to the water's surface and using this information in the foil control system.

As a result of this development, a second test craft, Sea Legs (Fig. 9), was built. This craft has been the most successful submerged-foil craft built to date. It is 29 ft. in length, 8 ft. in beam, and displaces 11,000 lbs. Powered by a 210-hp. engine, the craft has attained a maximum speed of 31 knots. Its main support—a large, controllable, submerged foil—is aft, and a small foil to control the pitch is located forward. This craft has excellent sea-keeping qualities and has been run through 4- and 5-ft. waves in both following and ahead seas with no loss in stability or control.

In 1958, the evaluations of both Sea Legs and Halobates were completed, and studies of the use of hydrofoil-equipped, antisubmarine patrol craft were initiated. In addition, research work began on the use of titanium in foils, gas turbines for power, and right-angle drives for large power transmission.

In 1959, the U.S. Navy recommended to Congress that the Fiscal Year 1960 Shipbuilding Program include a hydrofoil craft whose mission would be to conduct antisubmarine patrols in harbors, harbor approaches, and coastal waters. Congress authorized construction and appropriated funds. The preliminary design work, which had started in 1958, was completed by the Bureau of Ships in February 1959. The final contract for completing the construction plans and building the craft was awarded to the Boeing Aircraft Co. in June 1960, with delivery to be made late in 1962.

The patrol craft, hydrofoil, designated PC(H) (Fig. 10), will be the first operational military hydrofoil craft designed by and built for the U. S. Navy. It provides in a small, relatively inexpensive surface ship an attack capability against high-speed submarines. The submarine-detection capabilities—a retractable, active, low-frequency sonar and a lightweight, variable-depth sonar—will be employed in a "grasshopper" search and attack technique. Search will be conducted at low speed. After search of an area, the PC(H) will proceed foilborne at high speed to a new area or attack using torpedoes. The craft will be capable of more than 40 knots in water whose roughness would normally limit the speed of existing patrol craft to 15 knots or less. The military requirement for the ability to maintain high sea speed in rough seas on any heading has dictated a submerged foil and autopilot arrangement.

The submerged foil configuration and control is based on the system successfully used on the test craft Sea Legs. Foil retraction will enable the craft to operate in shallow waters if required. The craft will be 110 ft. in length and 31 ft. in beam. The draft will be 15 ft. 5 in. with foils down, 4 ft. 4 in. with foils retracted, and 6 ft. 7 in. while flying. The full-load displacement is 110 tons.

The PC(H) has a dual propulsion system. The main propulsion engines for foilborne operation are two gas turbines each rated at 3,100 s.hp. Power from the turbines is transmitted through two right-angle drives to propulsion nacelles at the intersection of the submerged aft foil and the struts. A propeller is located at each end of the propulsion nacelle, making a total of four propellers for foilborne operation. The propulsion system for hullborne operation is a 600-s.hp. diesel engine connected through a right-angle drive to a single propeller in a nacelle which is retracted at take-off to reduce drag. Speed is 12 knots in the displacement condition and 40–50 knots while flying.

Description of Hydrofoil Craft Design Features

Design features of a typical contemporary hydrofoil craft can be visualized by following a routine flight.

When the craft is at rest, the only problem is that the floating body remain upright. While this problem is routine to the average naval architect, we take time to mention it since the technology of hydrofoil design requires the techniques of both the naval architect and the aeronautical engineer, and, in our zeal to promote the union, the basic principles of either science are apt to be overlooked. Assured that our boat has its beam properly proportioned and its center of gravity low enough to provide good static stability and a good range of stability in the heeled condition, let us examine some of the particulars of the boat itself.

The most peculiar feature of the craft is the presence of foils with the shape of aircraft wings but much smaller. The foils are freshly cleaned, and they are smooth and fair. We may observe protective coatings and perhaps, in addition, a system of cathodic protection to prevent the accumulation of

fouling and pitting so that unacceptable roughness cannot develop between the rather frequent cleanings.

The hull will use the highest strength-to-weight ratio material available, and will save weight in terms of plates, shapes, and fastening methods to develop the full strength of the assembly. In the bottom and the bow, greater plate thickness and more stiffening have been used so that the hull can withstand the slamming loads of landing and wave encounter.

In the engine compartment, there will be either lightweight internal combustion engines or gas turbines converted from aircraft use for marine application. High power is required for high speed, and these boats depend for their advantage on speed. A more conventional power plant of modest size and high efficiency, such as a diesel, is provided for in-port maneuvering and for low-speed cruising in the hullborne condition. Another item of interest will be the gearing for either right-angled drive or inclined shafting since the power of the engines in the hull must be transmitted to propellers that must remain with good submergence even when the boat is flying at its greatest height.

Most of the equipment such as chairs, eating facilities, plumbing, and general furnishing is very similar to that found in aircraft, again to keep down weight.

When under way and preparing for flight, the cruising engine is secured and its propeller is probably retracted from the water altogether. In a well-designed boat, no unnecessary item is in the water and there is an absolute minimum number of struts or protuberances intersecting the water surface.

The size of the hull and its take-off speed dictate the shape of the hull. The designer faces a distinct hump in the drag curve when he tries to drive the foils, struts, and hull through the water at take-off speed. He has found that, although he has plenty of power in his engines, he has sorely taxed the available margin of thrust in his propulsion system. Thus, he has had to expend considerable effort to reduce hull drag to a minimum. Unless special devices such as auxiliary foils, ladder foils, or some type of retractable flaps are used, the take-off speed of such a boat is about one half of the top speed. A very large boat with moderate top speed will probably employ hull lines that are quite conventional (about destroyer-style) for operating in a speed-length regime where displacement-type operation is an advantage. If, however, the boat is smaller, or if the top speed is much higher, we will find a planing-type hull, with perhaps a little more deadrise than would be normal to cut down on impact loads on the bottom. It will also be noticeable that the topside of the boat is much cleaner aerodynamically than most other boats. At top speed the air drag of the hull can be a noticeable part of the total drag unless particular pains are taken to present a minimum drag in the air stream.

As the boat increases speed and the hull starts to rise from the water, the designer is concerned with stability and control. At the instant the hull leaves the water, the foils carry the weight of the boat at the minimum possible flying speed, and the greatest steady-state lift coefficient is reached. Unless sufficient margin of area or of available lift coefficient is available, seas or winds may cause difficulty (Fig. 11) since the hull no longer can provide a transverse or longitudinal righting moment. At this instant, the differential flaps or, in the case of surface-piercing foils, the outboard reserves of area provide the only restoring forces and are likely to be taxed to their limit if a minimum drag system has been used. In this condition the main engines develop virtually all their available thrust. The absolute value of drag at this condition is at a maximum value that will not again be equalled until the craft has attained nearly its top speed. In all probability, unless the added complication of controllable pitch propellers has been incorporated in the design, the propellers are running well off their most desirable design points, and the lower propulsive coefficient adds to the criticality of the situation.

At speeds just above take-off, the smooth ride is a new sensation in water travel. Small waves will pass practically unnoticed, and the largest ones will be negotiated with relative ease and minimum vertical acceleration. How is this possible? The craft we are riding, in the above description, is one equipped with fully submerged foils and an autopilot control system. This is capable of measuring the distance of the boat from the water and being adjusted to smooth wave-height response. There is also sufficient control surface either as flaps or as fully rotable foils so that for the most violent corrections needed there is neither cavitation nor gross separation of flow.

There must be a reasonable balance between stability of the foil system and its controllability or

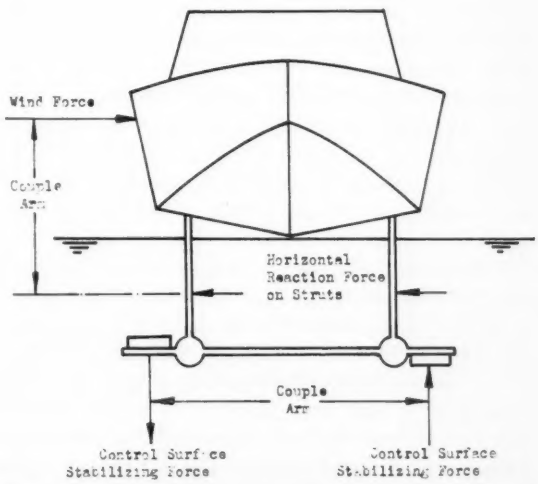

Fig. 11. Control surface moment and heeling moment after take-off and loss of hydrostatic righting moment.

agility. This reasonable balance is not a simple thing to determine even for aircraft, where long experience with this problem exists. If it is more important to remain nearly in steady flight than to make quick changes the balance should tend toward providing a conservative margin of stability. On the other hand, if it is necessary to provide a great deal of controllability or quick maneuver, then a lesser margin of stability is better. In hydrofoil craft, it appears that, for relatively slow speeds (40–50 knots) where a maximum degree of seakeeping is desired, rapid system response is advantageous. For very high speed craft, where limitations in usable values of vertical acceleration govern and "contouring" waves is impractical (Fig. 12), a level flight path must be maintained and the largest amount of pitch stabilization should be provided.

The foil plans of all the hydrofoil boats constructed up to the present time present a confusing array of foil arrangements. All of these schemes, however, may be classified in two ways: (1) whether the lifting surface pierces the water surface or is submerged at all times and (2) by the longitudinal distribution of the foil area in the canard, tandem, or airplane type (Fig. 13).

Characteristically, the airplane configuration can be made more inherently stable than the tandem or canard, while the canard system can be made more controllable or agile. Thus, for maximum following of seaways at moderate speeds, the canard configuration is considered desirable; while for the level flight required in very high speed craft, the airplane configuration is probably better.

For optimum distribution of foil loading, the center of gravity of the craft should be near the center of area of the foil system. The location of heavy weights tends aft in a canard and forward in an airplane configuration. Therefore, characteristic types of internal arrangements correspond to the foil configuration selected.

If a boat is equipped with surface-piercing foils, the previous description of take-off and flying does not apply since there are several differences. First, we shall probably notice no abrupt change in flying characteristics during and after take-off. This is principally due to the fact that the surface-piercing foil does not change lift coefficient radically and hence does not change induced drag, a function of lift-coefficient squared.

The surface-piercing or area-stabilized systems have the foils essentially fixed in attitude with respect to the hull and depend upon variations in area of foil in the water to supply added lift as needed. The lift coefficient remains substantially constant. This capability is built into the system by the use of dihedral foils or by multiple small foils arranged ladderwise to provide variation of lift with immersion. In effect, the foils perform the dual function of sensing the required lift correction and providing it. Submerged foils, on the other hand, depend upon control surfaces or change in angle of attack of the entire foil to change the lift coefficient and lift force. The submerged foil system has no height sensitivity built in so it must be supplied separately Then the foil control system may be made to respond to other quantities than height alone. Craft attitude and accelerations may also be sensed and used as control inputs in order to obtain a truly stabilized or controlled "ride."

Various sensing devices for submerged foil systems have been tried. One of the simplest was the Hook system in which the water surface ahead of the craft was "felt" by floats on the ends of long arms ahead and on each side of the craft. The wave heights thus anticipated were mechanically transmitted through a relatively simple linkage system to the foils, which were rotated to provide the needed change in lift. Other sensors including electrical probes, velocity and static pressure taps, and sonic altimeters have been proposed. The most successful sensor to date has been that installed in "Sea Legs," the 5-ton research craft that has operated in the open ocean in moderate seas without incident.

The fundamental difference in craft control stems from the sensor position in relation to the craft. Early in the research effort it was realized that spatial anticipation by the sensor could improve craft performance by providing lead time. Several craft that had zero anticipation have operated successfully, either by the use of computing devices to predict the wave action based on observed values or because the response time of the craft was so short that even corrections applied after the fact kept the craft in a reasonable flight attitude. Just how much improvement in performance can be achieved by the use of spatial anticipation is not clear at present. Suffice it to say that, at least in one case, the difference between anticipation and the lack of it was the difference between a highly successful hydrofoil craft and a marginal one.

Another significant difference between surface-piercing and submerged systems will be the quality of the ride when fully foilborne. In the boat with surface-piercing foils of normal design, every change in the water surface is transmitted to the boat as a change in lift force because of the change in wetted foil area. Also, in a boat with surface-piercing foils, the performance in a head sea is noticeably different from that in a following sea. In the crest of a following sea, the orbital velocity of the waves reduces the the effective angle of attack and reduces the relative fluid velocity. For a given ship speed, considerable change in either area of foil or lift coefficient is required to sustain flying equilibrium. Since the geometry of the surface-piercing foil system prohibits a very large range of total lift variation, a following sea can stall such a boat and cause it to come down on the hull. Since the water particle velocity is a specific independent quantity, very high boat speed can

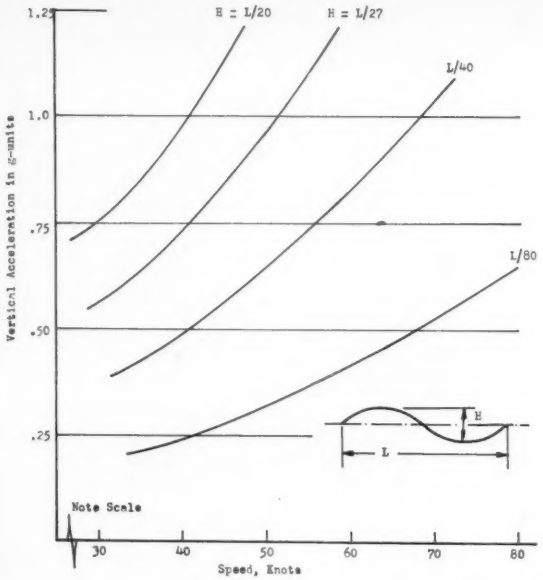

Fig. 12. Vertical accelerations implied by "contour flying" regular surface waves illustrated for the case with $L_w^0 = 400$ ft.

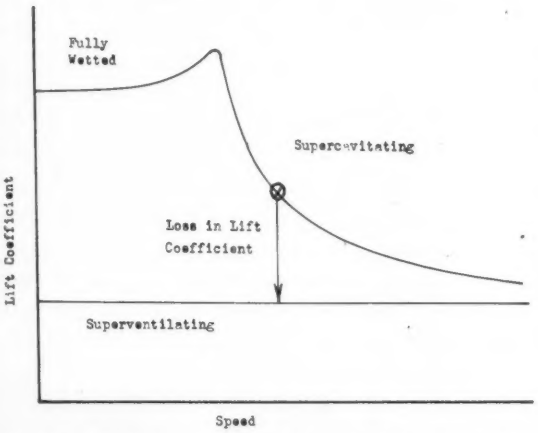

Fig. 15. Loss in lift coefficient due to transition from supercavitating to superventilating operating conditions.[3]

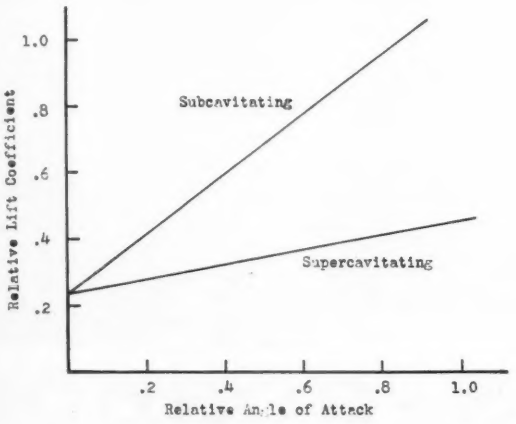

Fig. 16.

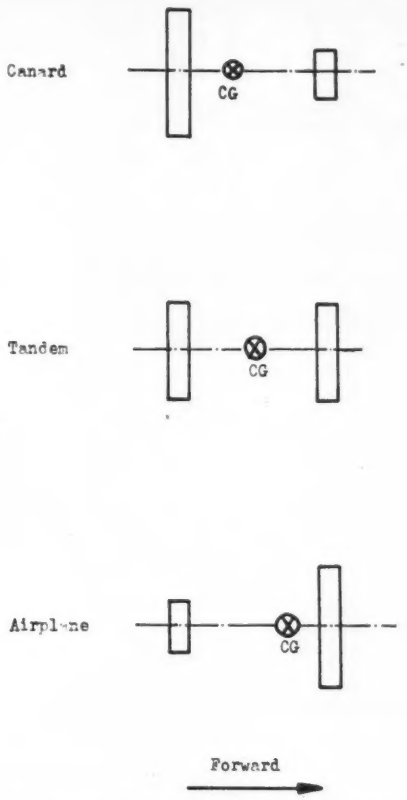

Fig. 13. Longitudinal distribution of hydrofoil area.

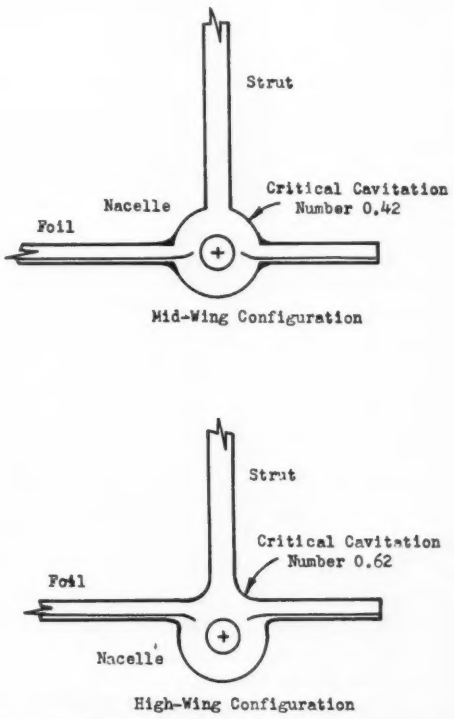

Fig. 14. Cavitation number and critical location at foil, nacelle, and strut intersection.

DOME and CLOSURE FORGINGS

speed solid-propellant missile capabilities

FORGED

OUT OF HIGH-STRENGTH STEELS AND TITANIUM ALLOYS

Dome and closure components, forged and machined by Wyman-Gordon in both low-alloy, high-strength steels and all-beta Titanium—have contributed measurably to our present status in solid-fuel missile development. Research is continuing for the purpose of adapting new materials to these applications. Wyman-Gordon engineer-metallurgists are available to counsel on all phases of forging such critical-service parts. Their assistance can help extend ultimate-strength limits of your space designs.

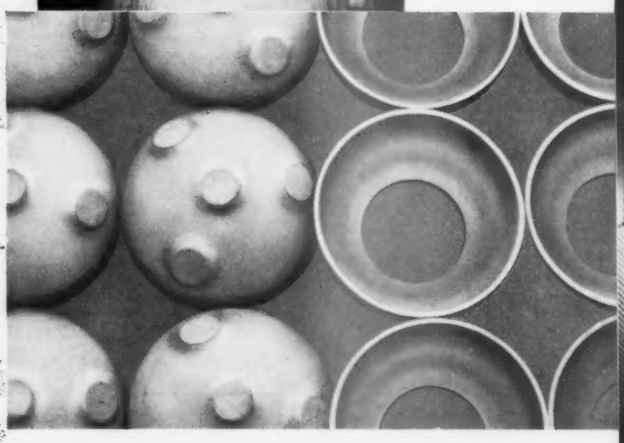

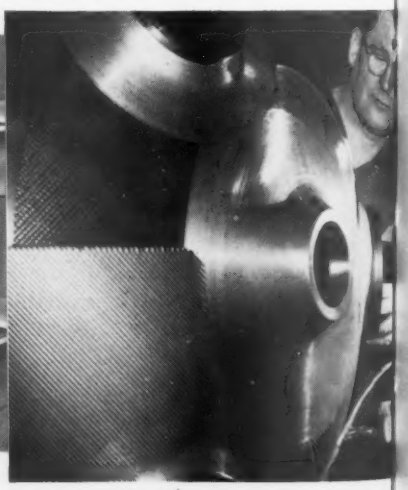

EST. 1883

WYMAN-GORDON

FORGINGS

of Aluminum Magnesium Steel Titanium . . . and Beryllium Molybdenum Columbium and other uncommon m

HARVEY ILLINOIS WORCESTER MASSACHUSETTS DETROIT MI

GRAFTON MASSACHUSETTS LOS ANGELES CALIFORNIA PALO ALTO CALIFORNIA FORT WORTH

reduce its effect to a minimum. On the other hand, with surface-piercing foils, very high boat speeds make accelerations in the head sea condition excessive. Thus, surface-piercing foil craft seem to be limited to lesser sea conditions than submerged-foil craft. Some operational results confirm this. Ladder foil configurations which increase the available area-change tend to improve this situation. For these stabilized configurations, the foils and the center of gravity of the craft must be so arranged as to provide positive stability in all planes of motion.

Hydrofoil craft with surface-piercing foils or the fully wetted type have a common stability problem—redundancy of control. It has been observed that craft that rely on the same control surface or on the same area-change to make corrections to both list and trim or to both list and heave have exhibited lack of reliable control in heavy seas. On the other hand, the best performers have been those which have surfaces that independently control list, or those that have more than one pair of surfaces contributing to list control. It is believed that this problem arises from an occasional coupling of motions in pitch, heave, and roll which may call on one surface to apply corrections which overload the surface and cause loss of lift.

Model Testing

In addition to design studies and calculations for the features mentioned above, a complex system such as a hydrofoil with its intersections, nacelles. and surface-piercing effects requires a final clean-up in a model basin to ensure minimum drag of the assembly. While many of the tricks of aerodynamics such as fillets and fairings can be used directly, one must remember that water has some particular differences in properties that may alter drag significantly. For example, Fig. 14 shows two versions of a foil-nacelle-strut intersection. Aerodynamic experience indicated that the high wing configuration would be better, but after considerable work on fillets and fairings it was found that the midwing version reduced drag by over 25 per cent at designed speed. The cause was cavitation in the upper intersection. This example is recited not as design guidance but as a warning that blind use of aerodynamic experience may lead to trouble in hydrofoils. Similar caution applies to consequences of the much greater density of the liquid medium. Dynamic pressures and their related forces are directly influenced.

Future Development of Hydrofoils

Today hydrofoil development stands at the crossroads. Current technology is adequate for the large and fast craft now being built. Two examples are the PC(H) and the craft being built for the Maritime Administration. This same technology is not adequate for larger, faster craft. An intensive research and development effort may lead successful hydrofoil development through areas now unexplored. The absence of constructive design guidance will limit the performance of future designs.

Table 1. Preliminary Drag Analysis of a Subcavitating and a Supercavitating Hydrofoil Design

(Based on a Ship Speed Ratio of About 1.5)

Drag Item	Ratio of Subcavitating Drag / Supercavitating Drag
Section drag All underwater items	1.7
Cavity drag All underwater items	0
Induced drag Lifting surfaces	1.3
Spray formation Struts	0.65
Interference Filleted intersections	1.8
Air drag Hull and structure	0.25
Total drag	0.65

Total drag ratio, 0.65, is also equal to the ratio of L/D supercavitating/L/D subcavitating for equal-weight ship designs.

The Navy Department is supporting a continuing research and development program whose overall objective includes establishing the technology required for higher performance designs. The problems associated with future development are in areas of hydromechanics, machinery and propulsion, structures, and autopilot control.

Hydromechanics

At the speed of present hydrofoil craft, the lifting surfaces, controls, and struts generally perform as predicted by the techniques of subsonic aerodynamics. It is desired to investigate the possibility of the operation of a hydrofoil craft at higher speeds. A natural barrier exists which is difficult to overcome at speeds greater than 45–50 knots. This barrier is the result of the tendency of the liquid to cavitate.

One approach to forestall this problem is the utilization of foil sections with nearly uniform chordwise pressure distribution in order to delay the onset of cavitation. Further investigation of this approach is necessary, especially behavior in a seaway. It should be noted, however, that the increase in speed made possible by this approach will not be large.

The destructive effects of partial and intermittent cavitation are so severe that it does not seem practical to consider this type of operation over any prolonged period in a hydrofoil.

The alternative to limiting the speed for hydrofoils to subcavitating designs and accepting the inherent size limitation is to design for supercavitation. In this condition, the wedge-shaped foil creates a bubble that encompasses the entire upper surface of the foil. The bubble collapses downstream and does not damage the foil. There are numerous advantages to this method of operation, as well as many disadvantages. One obvious advantage is the possibility of very high speeds. Another is the

possibility of larger craft without unwieldy foil geometry. The disadvantages are manifold.

The structural problem of designing the thin sharp foil required for supercavitation is an imposing one with existing materials for use in salt water.

The basic question of drag and attendant power required makes the practical consideration of such craft an economic problem of the balance of need against cost of operation.

Table 1 shows a preliminary drag analysis of two high-speed boats. One of these has a speed at the limit of subcavitation while the other is well into supercavitation. The lift-to-drag and speed ratios show that the supercavitating craft will require about $2^1/_4$ times as much power. Modern high-power lightweight engines make such craft feasible but do not necessarily make them economical and desirable.

The problem of control of supercavitating foils may be even more critical. Because the foil is operating near the free surface, there is a reasonable expectation that the cavity, at the vapor pressure of water, will communicate with the atmosphere either down a strut or through a trailing vortex. When this happens, the foil is no longer supercavitating but is superventilated and the cavity pressure equals the atmospheric. Fig. 15 illustrates the precipitous drop in lift occurring when this happens.

The rate-of-change of lift coefficient is an important control parameter. Fig. 16 shows the change of lift of a supercavitating foil with change of angle of attack as compared with a subcavitating foil. Here we see that major changes in angle of attack or effective camber will give only moderate changes in lift. It also suggests that a very low cruising lift coefficient (angle of attack) or larger-than-normal area will be required to supply a large enough range of lift forces for control. The use of large angles of attack incurs high drag penalties for supercavitating foils (Fig. 17). Fortunately, control by the use of flaps will considerably reduce these drag penalties.

These properties are not a complete argument against the feasibility of supercavitating foil design. The extremely high speeds, by the square-law of lift require much smaller changes in lift coefficient to produce the required control forces.

Existence of the cavity raises the question of flap effectiveness. Since the upper surface of the foil to its trailing edge and beyond is in a cavity, deflecting a flap into this region is fruitless. Some scheme such as that illustrated by Fig. 18 seems necessary to control supercavitating foils with the attendant drag penalty of a partially deflected flap in a cruising condition.

Even though all of the above are conquered, there remains the question of system stability. A subcavitating foil has a weak but welcome loss of lift as the free surface is approached, giving it a slight degree of heave and pitch stability. On the other hand, from theoretical studies it appears that a supercavitating foil has an increase in lift as the surface is approached, warning of a potential divergence in pitch and instability in heave.

While it is too early to assess accurately the factors mentioned above, it would appear that intentional ventilation will be preferred even though it is less efficient than supercavitation. Ventilation suggests more reliable lift characteristics, as well as the possibility of using intentional ventilation to give better moderate-speed cruising characteristics and controlled transition from subcavitating conditions.

The U.S. Navy research and development program includes an attempt to classify a series of transcavitating, supercavitating, and superventilating foil sections. Since such information is not now available as are data on subcavitating foils, the approach will be sort out the most promising sections and test them in model scale. The ones which prove to be best will then be completely characterized to provide design data. Closely connected with the selection of foil section is the means of changing lift for control. A series of flaps and possibly other types of control surfaces will be characterized in association with the preferred foil profiles.

Because the question of superventilation appears to be so vital, effort will be directed toward studies, both theoretical and experimental, to understand the phenomenon of natural ventilation, and to determine the possibilities and requirements associated with forced ventilation. The technique of forced

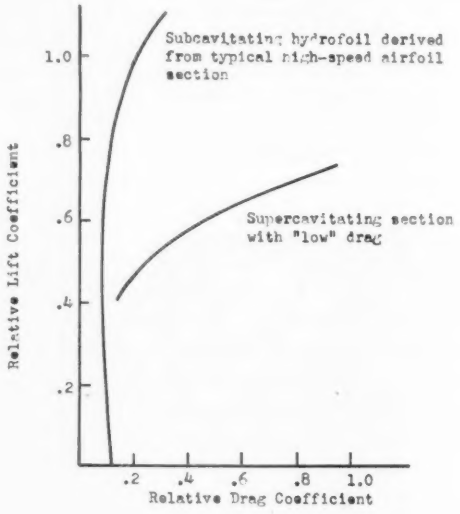

Fig. 17.

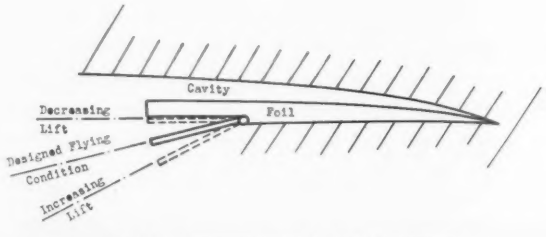

Fig. 18. Supercavitating foil with flap control.

ventilation may also prove of value in experimental work. By artificially inducing cavities, test work may be performed in relatively low-speed hydrodynamic test facilities at cavitation numbers equivalent to full scale and high speed.

Machinery and Propulsion

Larger hydrofoil craft and higher speed will require comparable increases in power. In order to provide a reasonable payload, high performance engines must be developed which are characterized by a low weight to horsepower ratio, a low specific fuel rate, and a high power output. Most marine engines are not capable of meeting all of these requirements, and "marinization" of the aircraft industry's gas turbines seems to be a fruitful approach. Such a choice does not solve all of the problems because operating an aircraft-type engine in a marine environment presents additional difficulties. These include corrosion, life expectancy, and reliability. This adaptation of aircraft-type engines to marine use is currently under way.

A related problem must be recognized—the transmission of power. The practice of using right-angle drive systems for transmission of power from the engines to the propeller in the water may not be possible in larger craft. The current program calls for studies of improved right-angle drives and other means of powering the larger hydrofoil craft.

Structures

As in the aircraft industry, structure weight is a critical problem. Each pound saved in the basic craft can be utilized as payload for sensor systems, weapon systems, or fuel. Studies and research must be conducted in order that the best of the aircraft and marine technology unite to produce a minimum-weight, high-strength hull.

One of the critical areas will be in the design and construction of the foils themselves. Supporting several hundred tons on stilt-like struts presents a problem in static considerations alone. Add to this the effect of dynamic loads due to turning and that resulting from the action of a heavy seaway, and the structural design problem becomes a formidable one.

The optimum material for foils is being sought. It will have the necessary high elastic limit and be relatively resistant to corrosion and erosion. This material must be easy to fabricate and must possess the properties of good weldability, high impact resistance, notch toughness, and high endurance limit.

The problem of hydrofoil failure due to fatigue is critical. The foil must be highly stressed to ensure minimum weight. The dynamic nature of the load requires that the joints, intersections, and areas of high stress concentration must be thoroughly investigated. Fatigue information is being obtained on complete foil and strut assemblies to ensure maximum safety and extended life of the foil system.

The problems of fouling, corrosion, and erosion of foils will undergo investigation. At the higher speeds contemplated, erosion will be a serious problem, and tests of materials in high-velocity flow are to be made. Cleanliness of the foils is a hydrodynamic must; consequently, the means of preventing corrosion and fouling of the foils requires careful consideration. Since usual coatings are difficult to keep on surfaces at high speeds, other means of prevention, such as electrical and sonic methods, are being investigated.

Stability and Control

As hydrofoil size and speed increase, the problems of control increase Some of the aspects of the control problem were mentioned during the discussion of hydrodynamic problems. The problem of inherent stability was not discussed, but this is in part hydrodynamic. The submerged-foil system has shown the greatest potential for development of all-weather flying capability. But the submerged-foil system, subcavitating or supercavitating, is not blessed with an inherent heave or pitch stability margin. The submerged-foil system hydrofoil craft therefore must fly under the continuous automatic supervision of an autopilot. To the naval architect, this has some of the unpleasant tolling of requiring all course-keeping by gyropilot.

A great burden of reliability is placed on autopilot design and dynamic range of operation. As previously stressed, high sustained sea-speed is required in all possible sea states. The very large dynamic loads possible in this dense medium prohibit overcontrol and require supervised performance during take-off, maneuvering, and landing.

New Development Craft

The Navy plans to build two test craft. The first will be a small 15–20-ton craft designed for supercavitating operation up to about 90 knots. It will be utilized to verify theories and model tests under actual operating conditions. The second craft is to be a ship of 250–300 tons originally fitted with subcavitating foils for test and evaluation of larger hydrofoil ships. It will have the necessary arrangements, hull strength, and power to accommodate a future installation of supercavitating foils.

Conclusions

Hydrofoil development requires contributions from the aircraft and shipbuilding industries, the aeronautical engineer, and the naval architect. The successful future hydrofoil ship will require the solution of many problems associated with higher speed and larger size.

The hydrofoil ship shows promise of a bright future in both military and commercial applications. Today we stand at the crossroads. One direction is

toward limited, small-craft application, and the other leads toward larger, high-speed ships. The next 2 or 3 years of research and development will determine what this future will be. It is hoped that this paper, in presenting some of the Navy's past and future efforts, as well as areas of known difficulties, may foster creative effort toward the successful development of the hydrofoil.

References

[1] Buermann, T. M., Leehey, P., and Stilwell, J. J., *An Appraisal of Hydrofoil Supported Craft*, Trans., Soc. Naval Arch. & Mar. Engrs., vol. 61, pp. 242–264 (discussion pp. 265–279), 1953.

[2] Crewe, P. R., *The Hydrofoil Boat; Its History and Future Prospects*, Trans., Inst. Naval Arch., 1958.

[3] Christopher, K. W., and Johnson, V. E., *Experimental Investigation of Aspect Ratio 1 Supercavitating Hydrofoils at Speeds up to 185 Feet Per Second*, NASA TN D-187, 1960.

✦ ✦ ✦

Moving Shocks (Continued from page 17)

$$Q_{mn}(t) = \iint_A p(x, y, t)\, \psi_{mn}(x, y)\, dA. \qquad (6)$$

The general solution of Eq. (4) may then be written as

$$q_{mn}(t) = A_{mn} \sin \omega_{mn} t + B_{mn} \cos \omega_{mn} t + r_{mn}(t) \qquad (7a)$$

$$M\omega_{mn}\Phi_{mn} \cdot r_{mn}(t) = \int_0^t Q_{mn}(\tau) \sin \omega_{mn}(t - \tau)\, d\tau \qquad (7b)$$

The constants A_{mn}, B_{mn} may be obtained from the modal initial conditions, so that in view of Eqs. (6) and (7), the response of the plate may then be expressed by Eq. (3), in conjunction with

$$q_{mn}(t) = \frac{\dot{q}_{mn}(0)}{\omega_{mn}} \sin \omega_{mn} t + q_{mn}(0) \cos \omega_{mn} t + \frac{1}{M\omega_{mn}\Phi_{mn}} \int_0^t d\tau \sin \omega_{mn}(t - \tau) \iint_A dA \times p(x, y, \tau)\psi_{mn}(x, y) \qquad (8)$$

Pressure Discontinuities on Rectangular Plates

In general, when studying the responses of typical structural elements one does well to begin with rectangular plates. Such plate shapes are the most common encountered in practice, and besides, they lend themselves most readily to mathematical analysis.

The pressure loading $p(x, y, t)$ acting on a plate which is exposed to a moving shock must be evaluated before the plate response can be determined from Eq. (8). For a straight shock front the pressure distribution on a rectangular plate at any time t may be visualized by means of Fig. 1. In actual shocks the pressures do not change very much outside the shock front, so that one may assume constant pressures of different magnitudes to prevail over the two regions into which the plate is divided by the shock front. One of these values of pressure may be taken as datum—i.e., zero—for the sake of convenience. The effect of this constant uniform pressure can be taken into account separately, by superposition, if one should wish to do so.

Let the constant pressure difference across the shock be denoted by p, and let $s = -\tan \phi$, where ϕ denotes the angle between the straight shock front and a plate edge of length a, as shown in Fig. 1. Further, let $d(t)$ denote the distance, measured along the edge $y = 0$, from the corner subject to the pressure p to where the shock front intersects this edge. As evident from the figure, the surface subject to p is a triangle for $sd \leq b$ and a trapezoid for $sd \geq b$ (b is the length of the edges parallel to the y-axis). Thus, one should obtain somewhat different analytic forms for $p(x, y, t)$ and $Q_{mn}(t)$ for these two conditions.

The pressure loading may be expressed as

$$p(x, y, t) = \begin{cases} p, & x + y/s < d \\ 0, & x + y/s > d \end{cases} \qquad (9)$$

where both d and s may be functions of time in the most general case. From Eq. (6) one may then obtain the generalized forces as

$$\frac{Q_{mn}(t)}{p} = \int_0^{\mu} dy \int_0^{d - y/s} dx \cdot \psi_{mn}(x, y)$$

$$\mu = \begin{cases} d, & sd \leq b \text{ (Case I of Fig. 1)} \\ b, & sd \geq b \text{ (Case II of Fig. 1)} \end{cases} \qquad (10)$$

These relations apply, of course, only for $d < a$. The condition where $d > a$, shown as Case III of Fig. 1, may be reduced to Case I (by superposition of a uniform pressure) and hence need not be considered separately.

The integrations indicated in Eq. (10) cannot be carried out specifically until the eigenfunctions ψ_{mn} are specified. These, in turn, depend on the boundary conditions, and one must therefore state boundary conditions before continuing.

Rectangular Plates on Simple Supports

(1) General

In order to carry the analysis further, it is convenient to consider the plates as simply supported. This assumption leads to analytical simplicity and permits one to arrive at some conclusions relatively directly. Since boundary conditions have relatively little effect for all but the lowest few modes,[10] these conclusions apply at least approximately for the higher modes of all plates, regardless of the boundary conditions.

The eigenfunctions, natural frequencies, and modal masses [Eq. (5)] applicable to rectangular plates on simple supports are given by

$$\left.\begin{aligned} \psi_{mn}(x, y) &= \sin(m\pi x/a)\sin(n\pi y/b) \\ \omega_{mn} &= \pi^2\sqrt{D/M}\,(m^2/a^2 + n^2/b^2) \\ \Phi_{mn} &= ab/4 \end{aligned}\right\} \quad (11)$$

if the coordinate system is chosen as indicated in Fig. 1. By substituting Eqs. (11) into Eq. (12) one obtains that for $sd \leq b$,

$$\frac{mn\pi^2 Q_{mn}}{abp} = \begin{cases} 1 + \dfrac{\alpha^2}{1-\alpha^2}\cos\dfrac{m\pi ds}{b} - \dfrac{1}{1-\alpha^2}\cos\dfrac{m\pi d}{a} & \alpha \neq 1 \\ 1 - \cos\dfrac{m\pi d}{a} - \dfrac{m\pi d}{2\alpha}\sin\dfrac{m\pi d}{a} & \alpha = 1 \end{cases} \quad (12)$$

and for $sd \geq b$,

$$\frac{mn\pi^2 Q_{mn}}{abp} = \begin{cases} 1 + (-1)^{n+1} - \dfrac{1}{1-\alpha^2}\cos\dfrac{m\pi d}{a} + \dfrac{(-1)^n}{1-\alpha^2}\cos\left(d - \dfrac{b}{s}\right)\dfrac{m\pi}{a} & \alpha \neq 1 \\ 1 + (-1)^{n+1} - \dfrac{n\pi}{2}\sin\dfrac{m\pi d}{a} & \alpha = 1 \end{cases} \quad (13)$$

where

$$a \equiv mb/nas \quad (14)$$

The foregoing expressions must be substituted into Eq. (7b) if one wishes to compute the modal response. Of course, now one must know the time dependence of s and d before one can carry out the indicated integration with respect to τ.

The problem of the response of simply supported rectangular plates to moving pressure discontinuities is thus solved, at least in principle. The only difficulties that remain are those encountered in carrying out the indicated integrations and those of interpreting the mathematical results in terms of physical concepts.

In the following sections the results developed so far are applied to special cases of particular interest. These were chosen because of their practical importance and because their relative simplicity gives one an insight into the physical phenomena without the encumbrance of excessive algebra.

(2) *Shocks Parallel to a Pair of Edges*

The previous results become somewhat more tractable for special cases where the shock fronts are always parallel to a pair of plate edges. For such shock fronts $\phi = \pi/2$, $s = \tan\phi$ is infinite, and $\alpha = 0$ according to Eq. (14). Then $sd \geq b$ for any finite value of d, so that Case II of Fig. 1 applies. Of the four expressions of Eqs. (12) and (13), only the first of Eq. (13) applies here, and this reduces to

$$\frac{mn\pi^2 Q_{mn}(t)}{2\,abp} = \begin{cases} 1 - \cos[m\pi d(t)/a] & n \text{ odd} \\ 0 & n \text{ even} \end{cases} \quad (15)$$

In view of the foregoing relation one may write Eq. (7b) for the special cases presently under consideration as

$$r_{mn}(t) = N_{mn}\, J_{mn}(t) \quad (16)$$

where

$$N_{mn} = \begin{cases} 8p/mn\pi^2 M\omega_{mn}^2 & n \text{ odd} \\ 0 & n \text{ even} \end{cases} \quad (17)$$

$$J_{mn}(t) = \omega_{mn}\int_0^t \left[1 - \cos\frac{m\pi d(\tau)}{a}\right] \times \sin\omega_{mn}(t-\tau)\, d\tau \quad (18)$$

(2a) *Shock Moving at Constant Velocity*

In order to compute the response of a plate to a shock front moving at constant velocity v in the x-direction (Fig. 1) and always remaining parallel to the edges of length b, one may set $d(t) = vt$ in Eq. (18). The result obtained may be expressed as

$$J_{mn}(t) = \begin{cases} 1 + \dfrac{1}{1-c_{mn}^2}\left[c_{mn}^2\cos(\omega_{mn}t) - \cos(c_{mn}\omega_{mn}t)\right] & c_{mn} \neq 1 \\ 1 - \cos(\omega_{mn}t) - (1/2)(\omega_{mn}t)\sin(\omega_{mn}t) & c_{mn} = 1 \end{cases} \quad (19)$$

in terms of the ratio

$$c_{mn} \equiv v/(a\omega_{mn}/m\pi) \quad (20)$$

The term appearing in the denominator of Eq. (20) represents the x-ward velocity of propagation of a (m, n)-mode flexural wave; hence, c_{mn} is the ratio of the shock velocity to the modal wave velocity. One may observe that Eq. (19) represents an oscillation of limited amplitude for $c_{mn} \neq 1$:

$$|J_{mn}(t)| \leq \begin{cases} (1 - c_{mn}^2)^{-1} & c_{mn} < 1 \\ c_{mn}^2\,(c_{mn}^2 - 1)^{-1} & c_{mn} > 1 \end{cases} \quad (21)$$

but represents an oscillation with ever-increasing amplitude for $c_{mn} = 1$.

If $c_{mn} = 1$, the shock travels with a velocity which is equal to that of a flexural wave of the mn mode, giving rise to an effect which is similar to the coincidence phenomenon observed in studies of sound transmission through walls. As usually understood, coincidence refers to a matching between a bending wavelength (or velocity) of a structure and a trace wavelength (or velocity) of a pressure wave incident on that structure, so that the pressure and velocity fluctuations are in phase over some portion of the structure surface. The pressure field is considered to be sinusoidal in space and time, and the area over which the pressure and velocity fluctuations are in phase is independent of frequency. In the present case there occurs a matching of velocities, but the pressure is not sinusoidal and the area of coincidence

does depend on frequency (and, in fact, is not stationary on the structure), as is discussed subsequently.

One may visualize that the first crossing of a plate edge by the pressure increase causes a small disturbance to emanate from that edge. This disturbance gives rise to flexural waves of all frequencies, which propagate at different velocities (proportional to the square root of frequency). If the shock front moves with the same velocity as one of these bending wave components, it continues to feed energy into this component (since pressure and velocity then are in phase over the front-most half wavelength), while no net energy input occurs behind this front-most half wavelength. The area over which the effective excitation acts is proportional to the wavelength, or inversely proportional to the mode number; the area of excitation is thus inversely proportional to mode number n. This fact accounts for the more rapid decrease in modal amplitude with mode number here than in the more commonly considered coincidence problems.

The previous physical interpretation also accounts for the limits on the amplitudes associated with modes which are not in coincidence, as apparent from Eq. (21), in that it shows that modes whose velocities match the shock velocity less closely are excited less because the corresponding bending waves coincide less with the exciting field.

The foregoing equations can obviously represent the motion of the plate only as long as the pressure discontinuity is located on it, that is, for $0 < t < a/v$. After the discontinuity has moved off the plate, the plate is subject only to a steady uniform pressure p and executes free oscillations about a new equilibrium position. The displacement of this new position of equilibrium from the original one corresponds to the static plate deflection under a steady pressure p and may be expressed in terms of Eq. (3) if $q_{mn}(t)$ is replaced by

$$\bar{q}_{mn}(t) = \frac{Q_{mn}}{M\Phi_{mn}\omega_{mn}^2} = \begin{cases} \dfrac{16p}{\pi^2 M_{mn}\ \omega_{mn}^2} \equiv 2N_{mn} & m, n \text{ both odd} \\ 0 & \text{otherwise} \end{cases} \tag{22}$$

Eq. (22) is obtained by deleting the time derivative of Eq. (4), and by setting $d(t) = a$ in Eq. (15).

The amplitudes of the free oscillations depend on the new "initial" conditions, which correspond to $t = a/v$. If W_{mn} denotes the new initial modal displacement and $\dot{W}_{mn}$ the new initial modal velocity, as found from Eqs. (8) and (22), the amplitude A_{mn} of the residual free oscillation may be determined from

$$A_{mn}^2 = W_{mn}^2 + (\dot{W}_{mn}/\omega_{mn})^2 \tag{23}$$

For the commonly encountered condition where the plate is at rest before the shock enters upon it the foregoing yields

$$\left(\frac{A}{N_{mn}}\right)^2 = \begin{cases} 2(c_{mn}^2 - 1)^{-2}\{c_{mn}^2(c_{mn}^2 - 2)[1 + \cos(m\pi/c_{mn})] + 2\} & m \text{ even} \\ 2c_{mn}^4(c_{mn}^2 - 1)^2\{1 + \cos(m\pi/c_{mn})\} & m \text{ odd} \end{cases} \Bigg\} c_{mn} \neq 1$$
$$\begin{cases} (m\pi/2)^2 + 4 & m \text{ even} \\ (m\pi/2)^2 & m \text{ odd} \end{cases} \Bigg\} c_{mn} = 1 \tag{24}$$

with N_{mn} as defined in Eq. (17).

(2b) Sinusoidally Oscillating Shock

The position of a shock oscillating sinusoidally about some mean location $x = C$ on the plate may be expressed as

$$d(t) = C + H \sin \omega t \tag{25}$$

where H denotes the excursion and ω the circular frequency of the oscillation. Substitution of this into Eq. (18) results in

$$J_{mn}(t) = 1 - \cos(\omega_{mn}t) - F_{mn}(t) \tag{26}$$

$$F_{mn}(t) = \omega_{mn}\int_0^t \cos[(m\pi C/a) + (m\pi H/a)\sin\omega\tau]\sin\omega_{mn}(t-\tau)d\tau \tag{27}$$

However, this expression describes the motion resulting both from a sudden application of the pressure p over $0 < x < C$ at time $t = 0$ and from the sinusoidal oscillation of the shock front at $t > 0$. If one wishes to separate the two effects, one may compute the effect of the suddenly applied steady pressure by setting $d(t) = C$ in Eq. (18) and obtain the effect of only the shock oscillation by subtraction. The suddenly applied steady pressure results in oscillations described by

$$J_{mn_s}(t) = [1 - \cos(m\pi C/a)](1 - \cos\omega_{mn}t) \tag{28}$$

so that the plate motion due to only the shock oscillations may be obtained from

$$J_{mn_{osc}}(t) = J_{mn}(t) - J_{mn_s}(t) = [\cos(m\pi C/a)](1 - \cos\omega_{mn}t) - F_{mn}(t) \tag{29}$$

The integration indicated in Eq. (27) must still be carried out. General closed expressions for the integral are not available, but fortunately one can introduce approximations which permit some useful information to be extracted from the results obtained so far. One may observe (from an appropriate graph, for example) that for $\mu < \pi/2$:

$$\left.\begin{aligned} \sin(\mu\sin z) &\backsimeq \sin\mu\sin z \\ \cos(\mu\sin z) &\backsimeq (1/2)(1 + \cos\mu) + (1/2)(1 - \cos\mu)\cos 2z \end{aligned}\right\} \tag{30}$$

The approximation is better for smaller values of μ; the aforementioned upper limit set on μ excludes exact functions having more dips (i.e., maximums and minimums) than can be represented by the approximations.

If one uses the approximations of Eqs. (30) in Eq. (27) one may perform the integration and obtain the contribution of the shock oscillation from Eq. (29) as

$$J_{mn_{osc}}(t) \approx \frac{1}{2}\left(\cos\frac{m\pi C}{a}\right)\left(1 - \cos\frac{m\pi H}{a}\right) \times (1 - \cos\omega_{mn}t - 2R_{mn}) + \left(\sin\frac{m\pi C}{a}\right)\left(\sin\frac{m\pi H}{a}\right) S_{mn} \quad (31)$$

where

$$R_{mn}(t) \equiv \begin{cases} (4\omega^2/\omega_{mn}^2 - 1)^{-1}[\cos(\omega_{mn}t) - \cos 2\omega t] & \omega_{mn} \neq 2\omega \\ (1/2)(\omega_{mn}t)\sin(\omega_{mn}t) & \omega_{mn} = 2\omega \end{cases}$$

$$S_{mn}(t) \equiv \begin{cases} (\omega^2/\omega_{mn}^2 - 1)^{-1}[\omega\sin(\omega_{mn}t) - \omega_{mn}\sin\omega t] & \omega_{mn} \neq \omega \\ (1/2)[\sin(\omega_{mn}t) - (\omega_{mn}t)\cos(\omega_{mn}t)] & \omega_{mn} = \omega \end{cases} \quad (32)$$

Since μ of Eq. (30) corresponds to $m\pi H/a$, the foregoing results apply only for $H < a/2m$; that is for excursions H which are smaller than a quarter of the length of an m-mode wave (in the x-direction). The approximation may thus be expected to give good results except for the highest plate modes, provided that the shock excursions are small.

An examination of the result of Eqs. (31) and (32) leads one to some rather interesting conclusions. First, one may verify that $J_{mn_{osc}} = 0$ for $H = 0$, as one might expect. [$J_{mn_{osc}}$ as given by Eq. (31) vanishes identically also for $H = 2\lambda a/m$, where λ is any integer, but the result applies only for $H < a/2m$.]

Eqs. (31) and (32) indicate that for $\omega \neq \omega_{mn}$, $\omega_{mn}/2$, the plate response is made up of a combination of sinusoids only. The amplitudes are limited, since one may readily show that

$$(1/2)\left|1 - \cos\omega_{mn}t - 2R_{mn}\right| \leq (4\omega^2/\omega_{mn}^2 + 1)/\left|4\omega^2/\omega_{mn}^2 - 1\right|$$
$$\left|S_{mn}\right| \leq \left|\omega/\omega_{mn} - 1\right|^{-1} \quad (33)$$

for all values of t.

On the other hand, if $\omega = \omega_{mn}$ then $S_{mn}(t)$ oscillates with ever-increasing amplitude, and the same is true of $R_{mn}(t)$ if $\omega = \omega_{mn}/2$. These two conditions thus correspond to resonances—i.e., to driving the system at one of its natural frequencies. The two resonances for each mode indicated by the mathematical result may be explained physically by reference to Fig. 2. If one visualizes the pressure distribution in terms of a uniform steady pressure and a time-varying pressure component as indicated, the plate response depends on the time-varying component only. This gives rise to a net normal force ΔF (per unit width in the y-direction) and a net moment ΔM about $x = C$. In the figure the instantaneous shock excursion is shown as $\Delta x = H\sin\omega t$; then

$$\left.\begin{aligned} \Delta F &= p\Delta x = pH\sin\omega t \\ \Delta M &= \int_0^{\Delta x} px\,dx = (1/2)\,pH^2\sin^2\omega t = \\ &\qquad (1/4)\,pH^2(1 - \cos 2\omega t) \end{aligned}\right\} \quad (34)$$

Thus, with $\omega = \omega_{mn}$ the panel is at resonance with the oscillating force and with $\omega = \omega_{mn}/2$ the panel is at resonance with the oscillating moment.

It is of interest to note that one or the other of these plate resonances may be suppressed for certain values of C/a. As evident from Eq. (31), the moment resonance associated with R_{mn} is suppressed for $mC/a = (1/2) + \lambda$ and the force resonance associated with S_{mn} is suppressed for $mC/a = \lambda$, where λ is any positive integer or zero. The physical explanation of this may be illustrated most conveniently for the special case where $C = a/2$. In this case moment resonances are absent if $m/2 = (1/2) + \lambda$ (or $m = 1 + 2\lambda$) and force resonances are absent if $m/2 = \lambda$ (or $m = 2\lambda$). This agrees with the well established fact that because of symmetry conditions forces applied at the plate center can excite only the odd-numbered modes and moments only the even-numbered modes. Thus in general the suppression of resonances can be associated with a mismatching of the symmetries of the driving phenomena and of the mode-shapes in the vicinity of the $x = C$ position.

(3) *Inclusion of Damping Effects*

The effects of damping have been omitted until now in order to facilitate the analysis. This omission results in no appreciable error for systems in which damping is not too great and for conditions where damping effects do not predominate. In general, damping predominates only for systems excited at resonance or with trace-matching, where analysis leads to infinite amplitudes if damping is neglected.

In the previously treated problem where trace-matching is important the analysis predicts no infinite amplitudes because of the limited time during which the excitation acts. Hence the analysis in which damping is neglected may still be used to obtain conservative results for plates excited by uniformly moving shocks. On the other hand, the previous analysis does result in infinite amplitudes for plates excited at resonance by oscillating shocks; hence here one must account for the effect of damping in order to obtain reasonable results.

Announcing . . .

INTERNATIONAL AEROSPACE ABSTRACTS
PUBLISHED BY THE INSTITUTE OF THE AEROSPACE SCIENCES, INC.
CO-SPONSORED BY THE NATIONAL SCIENCE FOUNDATION
AND THE AIR FORCE OFFICE OF SCIENTIFIC RESEARCH

INTERNATIONAL AEROSPACE ABSTRACTS

First issue
January 1961

A monthly service providing fast, comprehensive coverage of the world's aerospace literature

Each monthly issue of *International Aerospace Abstracts* brings you abstracts of hundreds of the latest reports, periodical articles, meeting papers, and books—selected on the basis of their importance to aerospace technology. Coverage is world-wide. Convenient subject arrangement permits rapid location of topics of interest, and an author index in each issue gives further access. This new monthly combines, in improved format, the abstracts and book sections formerly carried in *Aerospace Engineering*.

SUPPORTED by the NATIONAL SCIENCE FOUNDATION and the AIR FORCE OFFICE OF SCIENTIFIC RESEARCH

DESIGNED EXPRESSLY FOR THE ENGINEER AND SCIENTIST

PROMPT ☆ SELECTIVE ☆ INFORMATIVE ☆ TIME-SAVING ☆ EXPANDED COVERAGE

Access to original publications is provided through the facilities of The IAS Library at National Headquarters in New York.

A separate index volume is being planned for yearly publication.

Subscription Information (Domestic and Foreign)

Basic Rate:	$60 per year
IAS Corporate Member Rate:	$40 per year
Individual IAS Member Rate:	$20 per year

An Individual IAS Member may subscribe at the special rate of $20 per year only if he signs an agreement certifying that the copies are for his personal use.

(*Subscriptions are written on a calendar year basis.*)

Prices of the Annual Index Volume will be announced later.

SEND IN YOUR SUBSCRIPTION ORDER NOW

INSTITUTE OF THE AEROSPACE SCIENCES 2 East 64th Street / New York 21, N.Y.

Damping in linear systems executing sinusoidal oscillations may conveniently be described mathematically in terms of complex stiffnesses. For the present purposes one may replace the real stiffness D in Eq. (1) by the complex quantity $D(1 + i\eta)$ if one lets $u = U(x, y)e^{i\omega t}$, $p(x, y, t) = P(x, y)e^{i\omega t}$ and employs the usual convention of complex notation.[11] The ratio η of the imaginary to the real part of the stiffness is known as the damping factor; it is equal to the reciprocal of the system "Q" or quality factor and may have any frequency dependence whatsoever.[12] The commonly discussed case of viscous damping—i.e., that corresponding to a damping force proportional to velocity—may be obtained by setting $\eta = \beta/M\omega$, where β is the usual viscous damping coefficient.

If one expands $U(x, y)$ and $P(x, y)$ in a normal mode series one finds from the now modified Eq. (1) that the series coefficients are related as

$$U_{mn}\,[(1 + i\eta)\omega_{mn}^2 - \omega^2] = P_{mn}/M \qquad (35)$$

At resonance of the m,n-mode the exciting frequency ω is equal to the natural frequency ω_{mn}; the U_{mn} corresponding to the resonant mode predominates, and in view of the foregoing,

$$U(x, y) \approx U_{mn}\,\psi_{mn} \approx \psi_{mn}\,P_{mn}/M\eta\omega_{mn}^2 \qquad (36)$$

Note that the previous discussion implies separability of the time and space dependence of the pressure function $p(x, y, t)$ and that this separability does not exist for moving shocks in general. However, for oscillating shocks one may obtain a good approximation by replacing the actual pressure distribution by a *separable* one in accordance with Fig. 2 and Eqs. (34).

Thus, one may approximate the force-resonance condition encountered with shocks moving parallel to a pair of edges by means of a timewise sinusoidally oscillating force with the space dependence

$$P_F(x, y) \approx \begin{cases} p & C - H/2 < x < C + H/2 \\ 0 & \text{otherwise} \end{cases} \qquad (37)$$

Similarly, one may approximate the moment-resonance condition with an oscillating force having the space dependence

$$P_M(x, y) \approx \begin{cases} -p/2 & C - \mathrm{H} < x < C \\ +p/2 & C < x < C + H \\ 0 & \text{otherwise} \end{cases} \qquad (38)$$

By use of the orthogonality condition for the normal modes one may establish that the coefficients P_{mn} of the normal mode series for $p(x, y)$ must obey

$$P_{mn}\Phi_{mn} = \iint_A \psi_{mn}\,dA \qquad (39)$$

with Φ_{mn} as defined in Eq. (5). The coefficients corresponding to the foregoing equivalent loadings then are found, for $H \ll a/m$, to be given by

AERO / THERMODYNAMICIST
PH.D.

Immediate research position available for senior scientist with specific experience and interest in Hypersonic Boundary Layer Theory and Separated Flows; Chemical Kinetics and Non-Equilibrium Hypersonic Flows.

This position offers exceptional opportunity for personal and professional advancement in a small, expanding research organization.

Please address inquiries to
Mr. D. L. Smelser
ELECTRO-OPTICAL SYSTEMS, INC.
125 North Vinedo Avenue, Pasadena, California

$$\begin{aligned} P_{mn_P} &\approx (4/n\pi)(1 - \cos n\pi) \times (H/a)p \sin (m\pi C/a) \\ P_{mn_M} &\approx (2m/n)(1 - \cos n\pi) \times (H/a)^2 p \cos (m\pi C/a) \end{aligned} \qquad (40)$$

where the first applies for the force, the second for the moment condition, of course.

The foregoing, in conjunction with Eqs. (36) and (11), then suffice to establish the resonant response of the simply supported rectangular plates subject to oscillating shocks.

Conclusions

It was demonstrated that trace-matching is the mechanism of prime importance in determining the response of plates to uniformly moving shocks. Large responses are obtained in those modes for which trace-matching or near trace-matching occurs. In the example of shocks moving parallel to a pair of edges (of length b) of a simply supported rectangular plate, which was examined in detail, trace-matching occurs for modes for which

$$v = a\omega_{mn}/m\pi = (m\pi/a) \times [1 + (an/bm)^2]\sqrt{D/M} \qquad (41)$$

as may be found from Eqs. (20) and (11). The smallest value of v for which trace-matching can occur corresponds to $n = 1$, $m = a/b$, and is given by

$$v_{cr} = (2\pi/b)\sqrt{D/M} \qquad (42)$$

Thus, for shock velocities somewhat below the critical velocity v_{cr} no trace-matching can occur. On the other hand, for velocities greater than v_{cr} it is very likely that Eq. (41) will be at least approximately satisfied for some combination of m and n, so that large amplitudes will result for the corresponding mode.

Similarly, it was found that the response of plates to oscillating shocks is dominated by the phenomena of moment and force resonance. Large amplitudes occur only when the frequency ω of the shock oscillation is equal or nearly equal to one of the natural frequencies of the plate. For the aforementioned

example discussed in detail in the present paper, resonances occur for

$$\omega = \omega_{mn} \text{ or } \omega_{mn}/2$$

$$\omega_{mn} = \pi^2\sqrt{D/M}(m^2/a^2 + n^2/b^2) \quad (43)$$

Again, no resonances can occur for $\omega < \omega_{11}/2$, but resonances are likely to occur in some mode when $\omega > \omega_{11}/2$.

Thus one may avoid resonances in panels of flight vehicles by adjusting v_{cr} and $\omega_{11}/2$ to sufficiently high values, depending on the excitation. Large values of v_{cr} and $\omega_{11}/2$ require panels that are stiff and light, and have small edge lengths. These requirements may be realized in practice, for example by structures made of honeycomb with closely spaced reinforcing beams. One may note from Eq. (42) that only the length of the edge parallel to the shock front determines v_{cr}, hence the desirability of close spacing of stringers or other reinforcing elements at least in that direction is evident.

It appears from Eqs. (16), (17), and (24), that the modal displacement responses of the plates considered are in general inversely proportional to $Mmn\omega_{mn}^2$ and that the same proportionality applies also to the plate motion after passage of a uniformly moving shock. Similarly, Eq. (36) shows that the amplitudes of resonant plate oscillations are inversely proportional to $M\omega_{mn}^2$. Once more, a similar sort of proportionality may be deduced from the results for plates excited by randomly moving shocks.[13] Since velocity response is proportional to displacement response times frequency, and since stress response is essentially proportional to velocity response,[14] the velocity and stress responses may be readily determined, and one may now draw the following conclusions.

The magnitudes of the modal plate responses are dependent essentially only on the corresponding natural frequencies (for plates of the same mass per unit surface), in addition to the trace-matching and resonance phenomena. This means if two different panels of the same surface density resonate or trace-match with a given input at a given frequency, their response amplitudes at that frequency will be the same although the two panels may be oscillating in different modes. Thus, if one cannot raise the fundamental frequency and critical velocity of a design exposed to a reasonably wide spectrum of excitations sufficiently to avoid all resonances and trace-matching, one can essentially reduce the plate responses only by increasing the plate density and/or the damping. Essentially, increases in damping reduce the responses at resonances, whereas increases in density reduce the responses off resonance.

References

[1] Ellinwood, J. W., Trilling, L., and White, J. F., *Shock-Wave Oscillations in Supersonic Flow*, WADC TN 57-409, Dec. 1957.

[2] Dyer, I., Franken, P. A., Ungar, E. E., *Noise Environments of Flight Vehicles*, Noise Control, Vol. 6, No. 1, pp. 31–40, 51, Jan.–Feb. 1960.

[3] Daniels, L. E., and Yoshihara, H., *The Effects of the Upstream Influence of a Shock Wave at Supersonic Speeds in the Presence of a Separated Boundary Layer*, WADC TR 54-31, Jan. 1954.

[4] Rubin, E. S., and Kerwin, E. M., Jr., *Proceedings of IX International Congress of Applied Mechanics*, Brussels, pp. 373–386, 1956.

[5] *Handbook of Noise Control*, Harris, C. (Ed.), McGraw-Hill Book Co., Inc., New York, 1957; Chap. 33, by von Gierke, H. E.

[6] Struble, R. A., Stewart, C. E., Brown, E. A., and Ritter, A., *Theoretical Investigations of Sonic Boom Phenomena*, WADC TR 57-412, Aug. 1957.

[7] Shapiro, A. H., *The Dynamics and Thermodynamics of Compressible Fluid Flow;* Ronald Press Co., New York, 1953.

[8] Hammit, A. G., *The Interaction of Shock Waves and Turbulent Boundary Layers*, Journal of the Aeronautical Sciences, Vol. 25, No. 6, pp. 345–356, 1958.

[9] Timoshenko, S., *Vibration Problems in Engineering* (2nd Ed.), p. 422; D. Van Nostrand Co., Inc., New York.

[10] Ungar, E. E., *Free Oscillations of Edge Connected Simply Supported Plate Systems*, Paper No. Go-WA-112, ASME Winter Annual Meeting, Nov. 27–Dec. 2, 1960. (To appear in Trans. of Amer. Soc. Mech. Engrs. Series B.

[11] Morse, P. M., *Vibration and Sound;* McGraw-Hill Book Co., Inc., New York, 1948.

[12] Ruzicka, J. (Ed.), *Structural Damping*, ASME, New York, 1959; Sections 1, 3.

[13] Ungar, E. E., *Response of Plates to Moving Shocks*, WADD TR 60-445, May, 1960.

[14] Ungar, E. E., *Maximum Stresses in Plates Vibrating at Resonance*, Bolt Beranek and Newman Inc., Report No. 724, Feb. 1960. (To appear in Trans. of Amer. Soc. Mech. Engrs. Series B.)

✦ ✦ ✦

Pilot Control (Continued from page 21)

from the center of the earth to the station and the ferry vehicle, respectively.

In order to include, in the equations of motion, the apparent gravity effect due to the earth's gravitational field acting on the ferry and the station, the equations describing the relations between the vehicles were simplified by a mathematical derivation similar to the one used by Hord.[4] The equation of motion when referenced to inertial coordinates with the original at the center of the earth are given as:

$$\ddot{\bar{\sigma}} = (\bar{F}/m) - (GM/\sigma^3)\bar{\sigma} \quad (1)$$

where

$$\bar{\sigma} = \bar{\rho} + \bar{R} \quad (2)$$

and $(GM/\sigma^3)\bar{\sigma}$ = gravitational acceleration; $\bar{F}/m$ = acceleration due to the remaining forces. In order to obtain R as a function of the forces and the station distance ρ, Eq. (2) was substituted in Eq. (1). Assuming that there are no forces on the station other than the gravity force, the resultant equation can be expanded in a Taylor series. By retaining only the lower order terms and assuming that $R \ll \rho$ the resulting equation obtained is

$$\ddot{\bar{R}} = (\bar{F}/m) - (GM/\rho^3)[\bar{R} - 3(\bar{\rho}\cdot\bar{R}/\rho^2)\bar{\rho}] \quad (3)$$

In order to simplify this equation, the orbit of the space station is assumed to be in the $X_I - Z_I$ plane, therefore

$$\bar{\rho} = \bar{\imath}\rho_{X_I} + \bar{k}\rho_{Z_I} \tag{4}$$

$$\bar{R} = \bar{\imath}X + \bar{\jmath}Y + \bar{k}Z \tag{5}$$

$$\bar{F} = \bar{\imath}F_{X_I} + \bar{\jmath}F_{Y_I} + \bar{k}F_{Z_I} \tag{6}$$

By substituting Eqs. (4), (5), and (6) in Eq. (3) the component accelerations are

$$\ddot{X} = \frac{F_{X_I}}{m} - \frac{GM}{\bar{\rho}^3}\left[X_I - \frac{3(\rho_{X_I}X_I + \rho_{Z_I}Z_I)}{\rho^2}\,\rho_{X_I}\right] \tag{7}$$

$$\ddot{Y} = (F_{Y_I}/m) - (GM/\rho^3)Y_I \tag{8}$$

$$\ddot{Z} = \frac{F_{Z_I}}{m} - \frac{GM}{\rho^3}\left[Z_I - \frac{3(\rho_{X_I}X_I + \rho_{Z_I}Z_I)}{\rho^2}\,\rho_{Z_I}\right] \tag{9}$$

In Eqs. (7) to (9) the gravitational accelerations are given as functions of the distances $\bar{R}$ and $\bar{\rho}$. Since ρ is related to the space station orbit only, it is a function of time and can be readily obtained from any assumed orbit. Of the forces applied to the vehicle, it is assumed that thrust is the only important one.

In order to solve Eqs. (7) to (9) it is necessary to resolve the thrusting forces into the inertial axis system. These forces are obtained from the body forces by means of the conventional Euler angle conversions

$$\begin{Bmatrix} F_{X_I} \\ F_{Y_I} \\ F_{Z_I} \end{Bmatrix} = \begin{bmatrix} \cos\psi\cos\theta & \cos\psi\sin\theta\sin\phi - \sin\psi\cos\phi & \cos\psi\sin\theta\cos\phi + \sin\psi\sin\phi \\ \sin\psi\cos\theta & \sin\psi\sin\theta\sin\phi + \cos\psi\cos\phi & \sin\psi\sin\theta\cos\phi - \cos\psi\sin\phi \\ -\sin\theta & \cos\theta\sin\phi & \cos\theta\cos\phi \end{bmatrix} \begin{Bmatrix} F_x \\ F_y \\ F_z \end{Bmatrix} \tag{10}$$

Thus it is possible once a station orbit is assumed to solve the resulting eqs. (7) to (9) and to obtain the relative distance, $\bar{R}$. It has been assumed that the spacecraft used as the ferry vehicle will have the capabilities of performing re-entry and landing maneuvers. Such a vehicle is assumed to have a single rocket engine alined with its x-body axis. Therefore, the forces F_y and F_z can be neglected in Eq. (10).

In order to obtain the Euler angles, the rotational accelerations of the body axes must be computed. These are

$$\dot{p} = (M_1/I_x) - [(I_z - I_y)/I_x]qr - K(M_1p/I_x) \tag{11}$$

$$\dot{q} = M_2/I_y - [(I_x - I_y)/I_y]\,pr - K(M_2q/I_y) + T\epsilon b/I_y \tag{12}$$

$$\dot{r} = M_3/I_z - [(I_y - I_x)/I_z]pq - K(M_3r/I_z) + T\epsilon b/I_z \tag{13}$$

The terms M_1, M_2, and M_3 represent pure couples. The second terms represent inertia coupling. For the problem herein it was assumed that $I_z = I_y$, which eliminates the inertia coupling term from Eq. (11). The third terms are the artificial damping produced by a feedback system where K is the system gain, the quantity I/KM represents the time constant τ of the damped system response. The remaining terms in Eqs. (12) and (13) are the thrust-misalignment terms, where ϵ is the thrust-misalignment angle, and b is the moment arm.

The body rates can be computed by integrating these acceleration equations, and the rate expressions can be used to define the Euler angle rates given by

$$\dot{\psi} = (q\sin\phi + r\cos\phi)/\cos\theta \tag{14}$$

$$\dot{\theta} = q\cos\phi - r\sin\phi \tag{15}$$

$$\dot{\phi} = p + \dot{\psi}\sin\theta \tag{16}$$

These equations can be integrated to obtain the Euler angles.

The relation of the ferry vehicle and the space station in both spherical and Cartesian coordinate systems is shown in Fig. 2. Also shown in this figure are the Euler angles of the vehicle. From Fig. 2 it can be seen that

$$\beta = \tan^{-1}(Y_I/X_I) \tag{17}$$

$$\alpha = \tan^{-1}(Z_I/\sqrt{X_I^2 + Y_I^2}) \tag{18}$$

$$R = \sqrt{X_I^2 + Y_I^2 + Z_I^2} \tag{19}$$

The rates of change of these quantities with respect

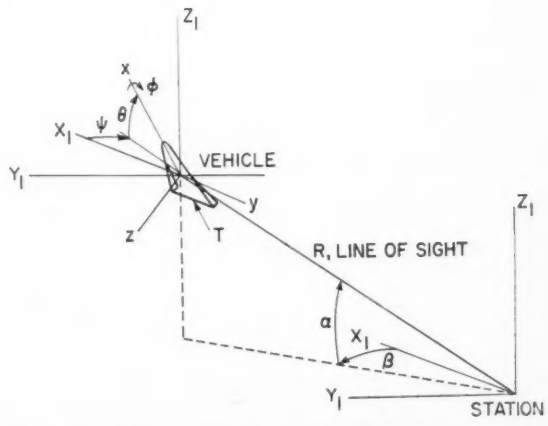

Fig. 2. Line-of-sight and Euler-angle relations between the rendezvous vehicle and the space station.

to time are obtained by differentiation and substitution of the spherical conversions

$$X_I = R \cos \alpha \cos \beta \tag{20}$$

$$Y_I = R \cos \alpha \sin \beta \tag{21}$$

$$X_I = R \sin \alpha \tag{22}$$

which yield

$$\dot{\alpha} = \frac{\dot{Z}_I}{R} \cos \alpha - \frac{\sin \alpha}{R} (\dot{X}_I \cos \beta + \dot{Y}_I \sin \beta) \tag{23}$$

$$\dot{\beta} = (\dot{Y}_I \cos \beta - \dot{X}_I \sin \beta)/R \cos \alpha \tag{24}$$

$$\dot{R} = \dot{Z}_I \sin \alpha + \cos \alpha(\dot{X}_I \cos \beta + \dot{Y}_I \sin \beta) \tag{25}$$

These relations were used to obtain the values of α, $\dot{\alpha}$, β, $\dot{\beta}$, R, and $\dot{R}$ for display to the pilot in the analog simulation.

Rendezvous Terminal-Phase Conditions

To simplify the required guidance for a pilot to effect rendezvous, a constant line-of-sight approach technique was used in the present study. Certain penalties in fuel will occur in using this technique, since a straight line-of-sight approach must be controlled against curving effects caused by different gravitational forces on the two vehicles.

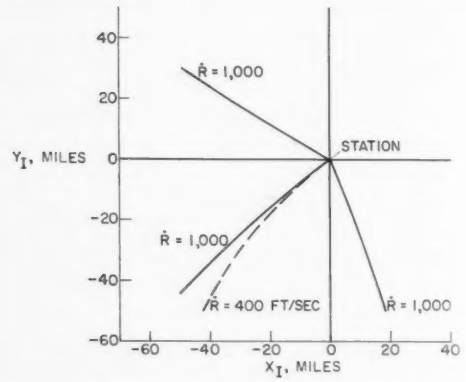

Fig. 3. Free-fall approach trajectories for coplanar orbits with an inertially fixed axis system.

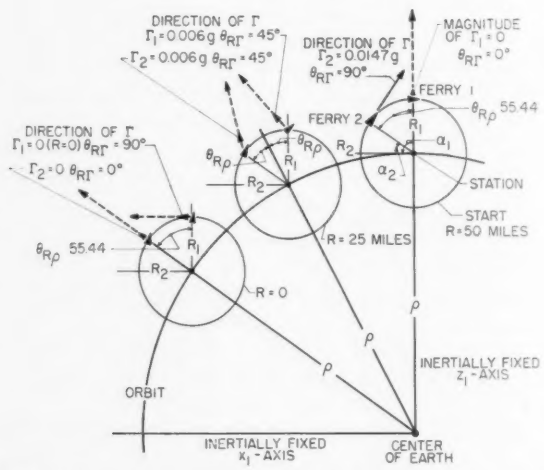

Fig. 4. Variation of apparent gravity effect on ferry as a function of R and sin $\Theta_{R\Gamma}$.

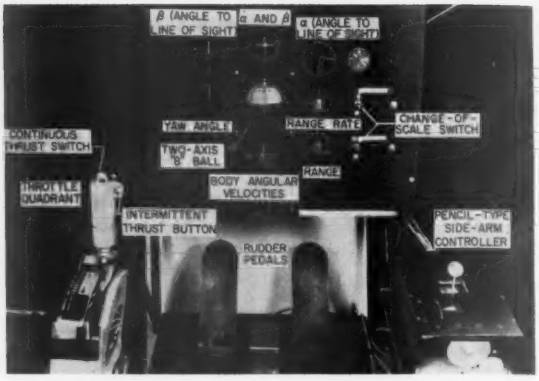

Fig. 5. Photograph of cockpit display and controls.

Two analytical rendezvous studies made by Hord[4] and Eggleston[1] can be used to show that the penalty in fuel due to using this guidance technique is small. The results of reference 1 show that the closure rates at the terminal rendezvous phase for typical launch techniques will be higher than 400 ft./sec. Coplanar results of reference 1, plotted on an inertially fixed axis system, are shown in Fig. 3 for sample conditions of 1,000 ft./sec., and 400 ft./sec. closure rates. The curves describe the path the ferry vehicle would make relative to the station on a coasting trajectory that terminates at the space station. As shown, the constant line-of-sight approach would not vary significantly from the curved paths out to 50 miles range.

Hord[4] describes the effect of the different orbits of the two vehicles as an apparent gravitational force on the ferry. Fig. 4 shows the apparent gravitational vectors and "g" values for two extreme constant line-of-sight approaches. It can be seen that a normal component exists so as to curve the relative flight path. For a 50-mile rendezvous that occurs as the space station traverses 54.44° of a 300-mile orbit, the maximum fuel penalty would be realized, and is on the order of 1/4 per cent of vehicle mass. Rendezvous maneuvers in the present study were completed within this orbital angle. The use of a constant line-of-sight approach to simplify the guidance therefore does not produce a significant fuel penalty.

Description of the Rendezvous Simulator

Assumed Vehicle Characteristics

The type of vehicle assumed in a rendezvous simulation study will result in variations in the requirements for controls, piloting techniques, and instrumentation. For the simulation in the present study a vehicle was assumed with a mass distribution to give a moment of inertia about the x-axis $^1/_{10}$ that of the y and z axes. The vehicle had a single main

thrusting engine having multistart capability with the nozzle 11 ft. aft of the c.g., producing thrust levels up to 0.4g. The pilot's throttle control allowed a proportional selection of thrust, with detents at 0.1g, 0.2g, 0.3g, and 0.4g (full throttle). Either continuous or on-off thrusting could be selected by the pilot at a desired g level.

Pilot controls commanded pure rotational jet-reaction couples for attitude control of the ferry vehicle. The maximum control moments gave angular accelerations of 2.8° per sec.^{2} in yaw, 2.3° per sec.^{2} in pitch, and 4.5° per sec.^{2} in roll. The attitude-control moments could be either linear with control movement or on-off.

Artificial damping was provided for the ferry vehicle by control-loop feedbacks which produced reaction torques proportional to body rates. This artificial damping caused angular velocities to decrease exponentially with a time constant ranging from 2 sec. for heavy damping to 10 sec. for light damping. Zero damping was also investigated.

Rocket misalinement effects, producing disturbing moments up to 90 per cent of control capabilities in yaw and pitch at the 0.1g level were simulated by canting the rocket thrust angle ϵ up to 2.8° relative to the $x - y$ and $x - z$ planes.

Instruments and Controls

Fig. 5 is a photograph of the simulator cockpit with pilot's instruments and controls. Dialed instrument displays were generally used rather than scope displays because of their reliability in actual use and the fact that these instruments may be adapted to other phases of a space mission.

To establish a constant line-of-sight approach, the attitude of the vehicle and the elevation and azimuth headings of the station relative to a fixed inertial reference must be displayed to the pilot. A two-axis "8-ball" instrument to show pitch and roll and a dialed instrument to show yaw were used for attitude information. Attitude-rate information was supplied by a triple-needled instrument in the lower center of the panel. Elevation angle α and azimuth angle β were displayed by separate instrument dials on the top of the panel. The angular rates $\dot{\alpha}$ and $\dot{\beta}$ were displayed on one instrument having a 1-milliradian per sec. scale. The pilot could read and maintain these rates to within ± 0.1 milliradian per sec. Range and range-rate information was displayed on dialed instruments that had scale switches. Full-scale readings were 50 miles range and 900 ft./sec. range rate on high scale, with 5 miles and 90 ft./sec. when switched, to low scale.

The α and β instruments were used during part of the rendezvous investigation to display $(\theta - \alpha)$ and $(\beta + \psi)$, automatically, thus permitting rapid determination of the vehicle thrust axis relative to the line of sight.

The attitude controls of the vehicle consisted of a pencil-type side-arm controller and rudder pedals. The throttle quadrant on the left allowed the pilot, to select desired thrust levels (0.1g, 0.2g, 0.3g, and 0.4g) and firing switches to either fire continuous thrust or intermittent thrust at the selected thrust levels.

Rendezvous Technique

As previously mentioned, the procedure used by the pilot was to establish and hold a constant line-of-sight approach to the space station, braking as range decreased to bring range and range rate to zero simultaneously. The single-rocket engine that was assumed for the ferry vehicle required that the attitude of the vehicle be controlled so as to point the thrust vector in the proper direction. The technique used by the pilot can be shown by referring to Fig. 2, which depicts typical initial conditions for rendezvous, the vehicle is ahead, above, and to the left of the station. In order to effect closure, the ferry must have less speed in the $X_I - Z_I$ plane than the station. Since the single-rocket engine thrusts rearward, the elevation and azimuth angles are described from the station so that when the vehicle attitude ψ equals $-\beta$, and $\theta = \alpha$, the rocket points

Table 1. Initial Conditions for Rendezvous Cases Investigated

Case number	α, deg	β, deg	$\dot{\alpha}$, deg/sec	$\dot{\beta}$, deg/sec	R, miles	$\dot{R}$, ft/sec	Uncontrolled miss distance, miles	ΔV_N, initial velocity correction, ft/sec
1	45	0	0.0284	0	30	-495	5	79
2	0	-22	0	-.0540	50	-435	29	249.0
3	20	40	-.0482	0	10	-317	1.5	45
4	-20	-15	-.0423	-.0315	50	-875	14	243.0
5	20	-10	-.06	-.0111	30	-705	7	173
6	20	20	.0775	.0858	30	-4.3	----	-----

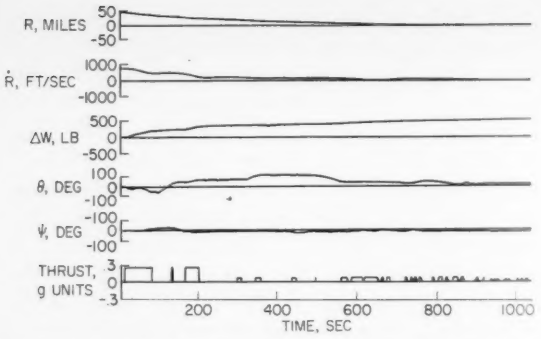

Fig. 6. Time history of a typical rendezvous made with conditions of case 4.

directly at the station. If there is a negative elevation-angle rate, $\dot{\alpha}$, thrust must be applied upward to arrest this rate. To maintain the rate of closure while correcting for $\dot{\alpha}$, this thrusting must be made 90° to the line of sight to the station. The vehicle must therefore be oriented with attitude angles that match $\psi = -\beta$, and $\theta = \alpha + 90°$, and thrust applied until $\dot{\alpha}$ goes to zero. In a similar manner, out-of-plane velocities producing $\dot{\beta}$ could be arrested holding $\theta = 0°$ and $\psi = -\beta \pm 90°$. Under most conditions at the start of terminal rendezvous both $\dot{\alpha}$ and $\dot{\beta}$ would exist. In such a noncoplanar case, both components can be corrected simultaneously by orienting the vehicle normal to the line of sight with a thrust component to arrest both $\dot{\alpha}$ and $\dot{\beta}$.

Braking is accomplished by bringing $\theta = \alpha$ and $\psi = -\beta$ and firing to achieve the proper $\dot{R}$. Simultaneous braking and correcting line-of-sight angular rates can be done in a similar manner to that described in the previous paragraph.

When the instruments presented $(\beta + \psi)$ instead of β, and $(\theta - \alpha)$ instead of α, the pilot's task was simplified; to correct for a negative $\dot{\alpha}$, he would yaw to bring the $(\beta + \psi)$ needle to zero and pitch upward to bring the $(\theta - \alpha)$ needle to 90°. For pure braking, both of these instruments would read zero to point the thrust axis toward the station.

Simultaneous corrections to the line-of-sight rates $\dot{\alpha}$ and $\dot{\beta}$ can be made by yawing to bring $(\beta + \psi)$ to 90° and then pitching so that the $(\theta - \alpha)$ needle reads

$$\tan^{-1}(\dot{\alpha}/|\dot{\beta}|)$$

However, as can be seen in Fig. 2, with this procedure the trigonometric relations result in a thrust component along the line of sight which may be undesirably large when α and $\dot{\alpha}$ are large. In an actual space rendezvous the pilot would initially align the X_I-axis within a few degrees of the line of sight and this thrust component along the line of sight would be negligible. In this study the initial position of the X_I-axis was not taken along the line of sight, but rather was taken as horizontal because it was desired to have gravity and noncoplanar effects accurately simulated.

Rendezvous Initial Conditions

Six sets of initial conditons, or cases, representing direct-launch trajectories,[1] with guidance errors, were used in making the present study. The conditions of the six cases are listed in Table 1, along with the approximate miss distances that would occur if no corrections were made, and the initial velocity increments ΔV required to arrest the angular velocity of the line of sight. Case 6 was a special case where near-orbital speed with no appreciable relative velocity toward the station existed. In this case the pilot had to initiate a closure rate by firing toward the station. The same technique as in the other cases was then followed to effect rendezvous.

Control During Rendezvous

Typical Rendezvous

Fig. 6 presents a typical rendezvous made by a pilot with the conditions of case 4 showing a time history of range (R), range rate ($\dot{R}$), retrofuel used (ΔW), pitch (θ), yaw (ψ), and thrust (T). It can be seen that the pilot chose to reduce the closing speed by about half during the first portion of the run, thrusting at the relatively high level of $0.2g$ for the first 200 seconds. About two-thirds of the total rocket fuel weight ΔW used for the rendezvous was used during this period (attitude-control fuel is not included in Fig. 6). At the same time, the attitude of the ferry in pitch and yaw was controlled so as to utilize this initial thrust to bring the line-of-sight angular rates to zero, placing the vehicle on a collision course toward the station. Since the vehicle dynamics included some damping and had no disturbing torques due to rocket misalignment, the attitude-control inputs were generally the same over the entire run. After obtaining a course of intercept, Fig. 6 shows that the pilot chose to retard the linear throttle control to about one-third the initial setting, and then followed a consistent pattern of orienting the main rocket and firing thrust by pressing the throttle button to maintain the collision course and reduce the speed of closure. The number of steps in the thrust trace and the number of control inputs to yaw and pitch are a measure of the frequency of corrections to line-of-sight and range rates considered necessary by the pilot. The consistent manner that X_I and Y_I approached zero, and the fact that R and $\dot{R}$ became zero simultaneously, indicated that the rendezvous was successful.

Effect of Damper Failure and Thrust Misalignment

To illustrate how a successful rendezvous would be possible with damper failure or with large misalignment torques, runs were made under these conditions and are presented in Figs. 7 and 8, respec-

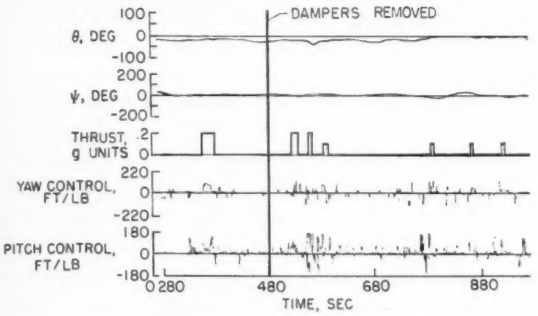

Fig. 7. Time history of a rendezvous showing the effect of damper failure.

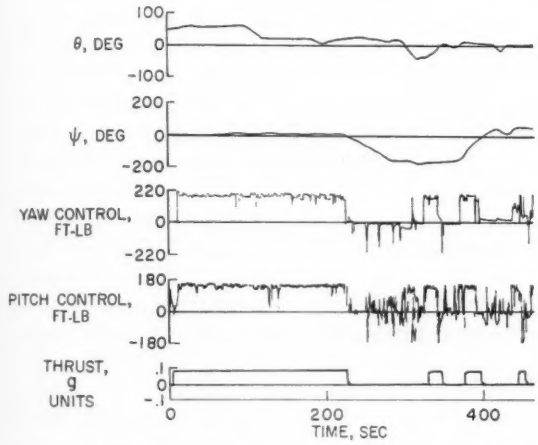

Fig. 8. Time history of a rendezvous showing the effect of misalignment torque.

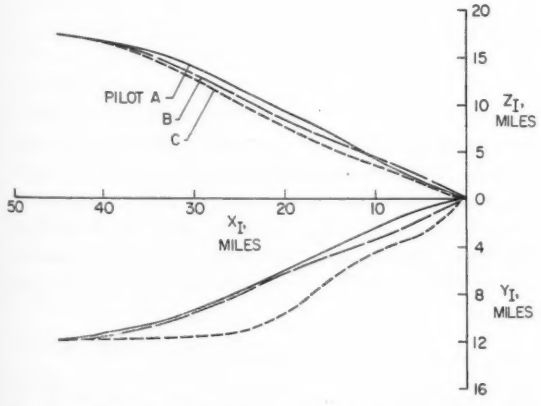

Fig. 9. Position trajectories for rendezvous conditions of case 4.

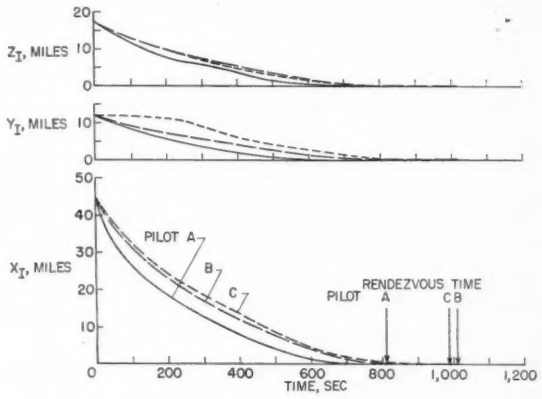

Fig. 10. Position-time trajectories for rendezvous conditions of case 4.

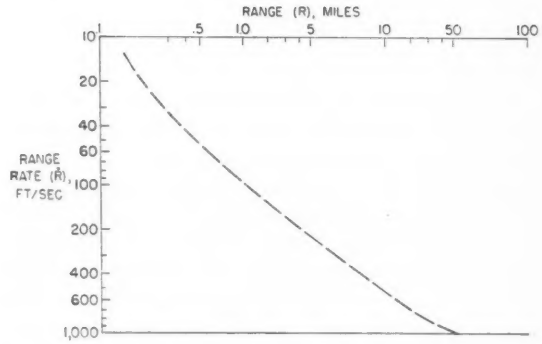

Fig. 11. Schedule of range vs. range rate used for pilot-controlled rendezvous.

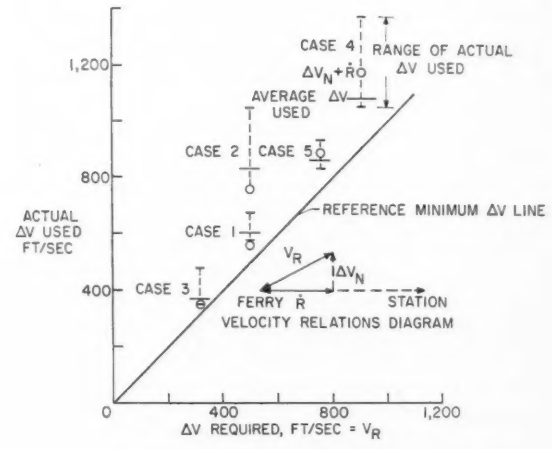

Fig. 12. Actual velocity vs. velocity required.

tively. In Fig. 7, heavy artificial damping with a 2-sec. time constant was removed 480 sec. after *lock-on* without causing undue trouble other than a slightly increased work load. No thrust misalignment was present for the run shown in Fig. 7. Although the pilots concur that the present system could be controlled without damping if other conditions were not too severe, nevertheless their comments indicate that some damping is desirable. In Fig. 8 a comparison between similar runs shows the effect of relatively high thrust misalignment torques. The run in Fig. 8 had damping, and the main rocket was misaligned so as to produce a disturbing torque equal to 90 per cent of the total attitude-control capability in pitch and yaw at the 0.1g thrust level used. It can be seen in Fig. 8 that the pilot had to control the vehicle about a new attitude-trim position equal to 90 per cent of control travel while firing thrust. Even under this extreme condition, rendezvous was successful. The pilot had the advantage of firing bursts at low thrust levels so as to identify disturbing torques and making anticipatory corrections during later bursts.

Pilots' Control Techniques

Fig. 9 presents the position of Y_I and Z_I plotted against X_I defining the space trails for three pilots flying case 4. It can be seen that except for the Y_I position of pilot C, the pilots tended to follow similar paths in space. This indicates that generally it took them about the same length of time to interpret the initial conditions and make the necessary corrections to get on a collision course; throughout the investigation the three pilots used essentially the same techniques to make spatial corrections and control the vehicle to the target.

Fig. 10, on the other hand, shows how the time of run can vary by referring the same quantities in Fig. 9 to the scale of time. Pilot A effected rendezvous in 800 sec. compared to about 1,000 for pilots B and C. This run for case 4 had damping and no misalignment, which made it an easy condition to control. When more stringent conditions existed, however, the variations in time to rendezvous were even more pronounced. Each pilot's control technique had a specific effect on time. For example, a minimum-fuel rendezvous would reduce initial velocity to near zero before obtaining a collision course, and rendezvous time would approach infinity, but if a minimum-time rendezvous is desired, initial velocity would be preserved or even increased while obtaining a collision course, and braking would be done just prior to contact. All this emphasizes that during intercept the pilots' energy- and time-management techniques differ, and that if time to rendezvous is important, then further information must be presented to the pilot.

Fig. 11 shows a suggested range—range-rate schedule for a single-rocket rendezvous vehicle made up by the pilots during the tests and shown as points joined by a dashed line. This range—range-rate schedule matches, approximately, a constant acceleration of 0.018g. This information was presented to the pilots in the form of a table, and proved helpful for monitoring these two variables during the present study so that the time to rendezvous could be controlled commensurate with adequate control of the vehicle. This schedule was especially useful in the final 10 miles, or in the presence of low thrust or large misalignment torques. This schedule would vary if more than one rocket (normal thrust) was provided. In order to get on schedule, initial thrusting of at least 0.2g was used by the pilots, and after acquiring a collision course, lower thrust levels were used. Braking was made in steps, with time between these step thrusts for the pilot to monitor the instruments and orient the vehicle. This procedure was found to be very satisfactory.

Some runs were made with the initial conditions of case 5 wherein a small constant acceleration of 0.05g was utilized from the start, requiring thrust for 82 per cent of the maneuver. This control procedure was found to be very difficult primarily because the instrument that presented $\dot{\alpha}$ and $\dot{\beta}$ to the pilot was against the stop during a large part of the run. This instrument had a maximum range of $\pm 0.057°$ per sec. Some runs were successfully completed when the computer operator verbally relayed the values of $\dot{\alpha}$ and $\dot{\beta}$ to the pilot while they were off scale. This result indicates that a rendezvous with constant, low acceleration might be completed if the instrument displaying $\dot{\alpha}$ and $\dot{\beta}$ had adequate range.

Fuel Requirements

Fig. 12 shows a comparison of the velocity used (ΔV) for each rendezvous case with the minimum required for that case. This is representative of the fuel requirements during the terminal phase of rendezvous. The absolute minimum ΔV is calcuated by assuming that a single burst of thrust would be used to decrease the relative velocity between the station and vehicle to near zero, leaving an infinitesimal velocity in the proper direction for closure. This velocity requirement is shown as V_R on the velocity diagram in Fig. 12 and is the vector sum of ΔV_N and $\dot{R}$. This type of procedure would make the time to rendezvous approach infinity. The ΔV required to effect rendezvous by the constant line-of-sight approach method would be the algebraic sum, $\Delta V_N + \dot{R}$; this is represented by circles in Fig. 12 for each case investigated. Actual fuel used was recorded and ΔV used was calculated by the relation:

$$\Delta V = -I_{sp} g \log_e [1 - (W_P/W_0)]$$

where a specific impulse I_{sp} of 230 sec. was assumed, and initial weight W_0 was 4,000 lbs. The study indicates that the pilot was able to use ΔV on an average within 20 per cent of the theoretical minimum. An exception was case 2, with a relatively

large range of 50 miles and only 435 ft./sec. closure rate $\dot{R}$. This $\dot{R}$ would match about 15 miles range on the schedule shown in Fig. 11, so the pilots tended to increase the closure rate to effect rendezvous sooner, thus using a larger ΔV. Case 4 represents an initial condition where a high $\dot{R}$ and ΔV_N existed. Under these conditions the pilots corrected ΔV_N and reduced $\dot{R}$ simultaneously, which resulted in the average ΔV used being less than the normal procedure of first establishing a constant line-of-sight approach without changing R.

Rendezvous With Elliptical Orbits

Another series of special runs was made to study the effects due to the station being in an elliptical orbit on the ability to rendezvous. The initial conditions for the vehicle relative to the station were the same as for case 4, but the station orbit was elliptical with a 100-mile perigee and a 500-mile apogee. Rendezvous maneuvers were begun with the station at apogee. As was indicated by the previous discussion, the apparent gravity effects are independent of the type of orbit of the space station, therefore no particular difficulties would be expected for the case of an elliptic orbit. This was proved to be true as no difficulties were encountered by the pilots in controlling rendezvous.

Line-of-Sight Rates

Present day airborne radar equipment may be expected to have angular rate inaccuracies of up to ± 1 milliradian/sec. This information was not available at the start of the study, and the accuracy assumed was 1 milliradian in $\dot{\alpha}$ and $\dot{\beta}$ for full-scale instrument deflections, with the pilot capable of controlling to ± 0.1 milliradian if desired. These extremely good instrument readings are desirable early in the terminal phase for optimum fuel economy, and point up the need for further research to improve the inputs to these instruments. Improved airborne radar and signal smoothing, or such techniques as optical tracking units to supplement the electronic data, would provide the improved accuracy required.

It should be pointed out that in the early stages of rendezvous the pilot would have time to supplement radar rate values with optical sighting to improve the accuracy of the information. As range decreases to under 10 miles the small errors in normal velocity are not expected to affect significantly the results of this study.

Conclusions

The results of the present investigation of the terminal phase of a satellite rendezvous using a single-rocket engine and attitude controls led to the following conclusions:

(1) All pilots were able to control the terminal phase of rendezvous with the equipment assumed.

(2) The following information is required on the pilots' instrument display:

(a) Elevation and azimuth line-of-sight angles and rates.

(b) Range and range rate.

(c) Vehicle attitude relative to the line of sight and the attitude rates.

(3) The fuel used by the pilot to control the terminal phase of rendezvous is within 20 per cent of the theoretical minimum required.

(4) A single-rocket engine with multistart capabilities and a single thrust level ($0.1g$) or preferably two levels ($0.1g$ and $0.2g$) is sufficient for the terminal phase of rendezvous.

(5) Vehicle attitude damping is desirable but not essential for the terminal phase of rendezvous.

(6) Thrust misalignments, within the vehicle attitude control capabilities, can be handled by a pilot without appreciable changes in the fuel used.

References

[1] Eggleston, John M., and Beck, Harold D., *A Study of the Positions and Velocities of a Space Station and a Ferry Vehicle During Rendezvous and Return*, NASA TR R-87.

[2] Wolowicz, Chester H., Drake, Hubert M., and Videan, Edward N., *Simulator Investigation of Controls and Display Required for Terminal Phase of Coplanar Orbital Rendezvous*, NASA TN D-511.

[3] Levin, E., and Ward, J., *Manned Control of Orbital Rendezvous*, Rand Corp., Oct. 1959.

[4] Hord, Richard A., *Relative Motion in the Terminal Phase of Interception of a Satellite or a Ballistic Missile*, NACA TN 4399, 1958.

✦ ✦ ✦

Meteorological Satellite Systems

(Continued from page ?3)

are obvious in this and other Tiros photo mosaics of cloud systems over large areas.

Although meteorological satellites so far are best known for their cloud photographs and infrared measurements, they have several other capabilities of importance in research and applied meteorology. Among those presently known are measurements of:

(1) Mean temperatures of the clear air column.

(2) Temperature of the visible surface—cloud tops, ground or ocean surface.

(3) Various radiation values, solar and terrestrial, for studies of earth's heat budget and basic mechanism of the "heat engine" that produces weather and climate.

(4) Precipitation areas, ice and snow covers.

(5) Vertical distribution of ozone, water vapor, carbon dioxide (narrow-band emission), and certain other constituents of the atmosphere.

(6) Unique features of clouds useful in early detection of incipient severe storm developments (Fig. 2).

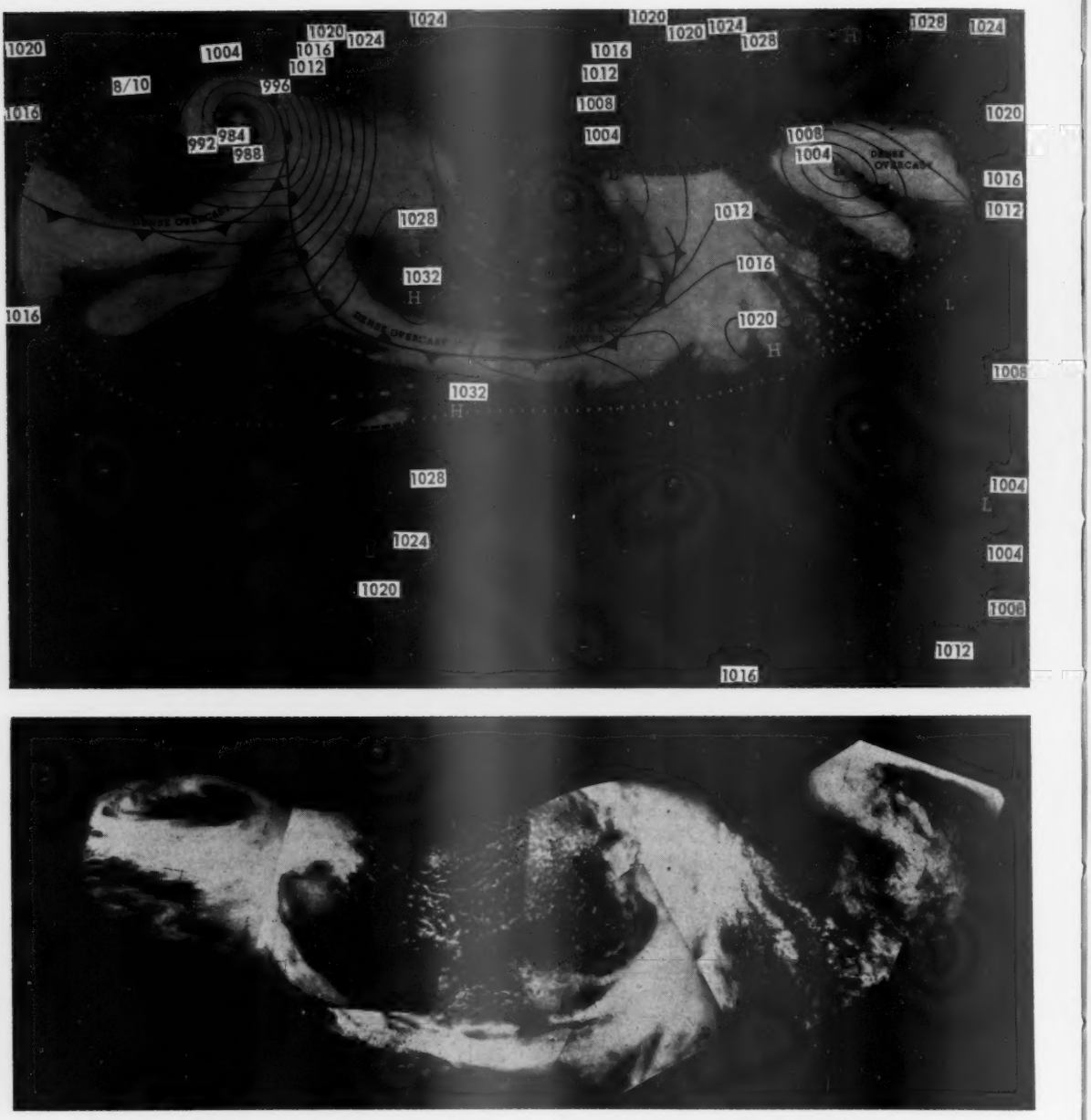

Fig. 1. Pacific storm family observed by Tiros I, May 19–20, 1960 (after Oliver[6]). (*Top*) Experimental cloud depiction chart prepared from Tiros pictures superimposed on NAWAC 0000Z map analysis of May 20, 1960. (*Bottom*) Actual Tiros photographs taken on May 20, 1960.

Research results already obtained from Tiros experimental satellites suggest that future studies based on data from advanced operational types will bring major changes in meteorological theory, knowledge, and techniques. Probably these will lead to refinements in design of sensors and new capabilities not given in the foregoing list. Some of the data will be useful mostly for research, but much will have immediate applications in daily weather services. The volume of material for study and the potentialities for research in detail are immense, and much will be suitable for more or less independent studies. For these purposes satellite data will be distributed widely for research in universities and other private institutions, as well as in the several interested Government agencies. Fig. 3 shows the main channels for flow of satellite data to research and service users.

Results So Far

Fritz, Kaplan, Stroud, Wexler, and others have published recent papers relating to Explorer VII and Tiros I.[1–4] Ultimately, important advances in meteorological knowledge will doubtless come from the data of radiation phenomena, but the Tiros cloud photographs have already added directly to knowledge of certain broad features of storms and much more can be inferred indirectly about air masses, jet streams, and other conditions in the atmosphere

of importance in aeronautics and general weather forecasting. Photo mosaics of clouds over large areas give an outline of the broad-scale weather analysis; in fact, clouds represent "nature's own weather map." Principal fronts and changes in weather are associated with clouds. Consequently, cloud maps identify the main features of weather analysis. Where the sky is cloudless, it usually means an expanse of stable air mass and absence of significant changes in weather.

Without repeating in detail the studies that are being presented currently in other technical papers, a brief account of some of the research conclusions and practical applications in aviation and other fields is offered here. The cloud mosaic shown in the lower part of Fig. 1 is made from 30 photographs transmitted during two orbits of Tiros I, May 19–20, 1960. With nothing more than this cloud map, it is possible to locate the cold and warm fronts and visualize the most likely path of the associated jet streams aloft. The upper part of the figure shows the cloud map after being rectified and superimposed on the system of fronts and isobars drawn from the relatively few reports from ships and islands in the North Pacific for the date concerned. Rectification of cloud photos is necessary to correct for distortion by the oblique angle at which the Tiros camera lens viewed portions of the area. Neither the cloud map nor the isobar and frontal map would be complete or accurate taken alone. This analysis based on the two supplementary sources of data bears striking resemblance to the classical Norwegian model of the structure of moving cyclones as published by J. Bjerknes, T. Bergeron, and others from their studies beginning about 1915. Other features of significance to the aviator and the mariner can be deduced from analyses such as this. Naturally, the greater the accuracy in mapping the air mass and frontal for-

Fig. 2. Quadrilateral cloud formation (*lower left*) precedent to tornadoes in central Oklahoma, May 19, 1960.

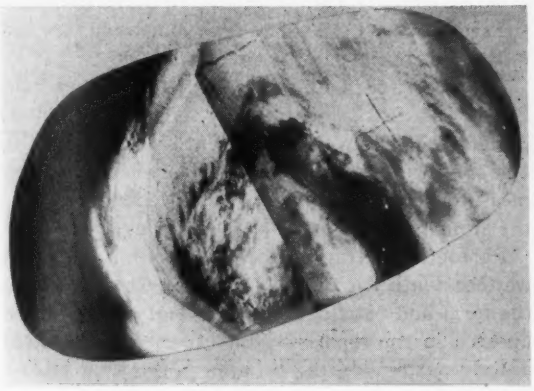

Fig. 4. Tiros I photographic mosaic from orbit 731, at about 2000 hours, Z,[9] May 21, 1960.

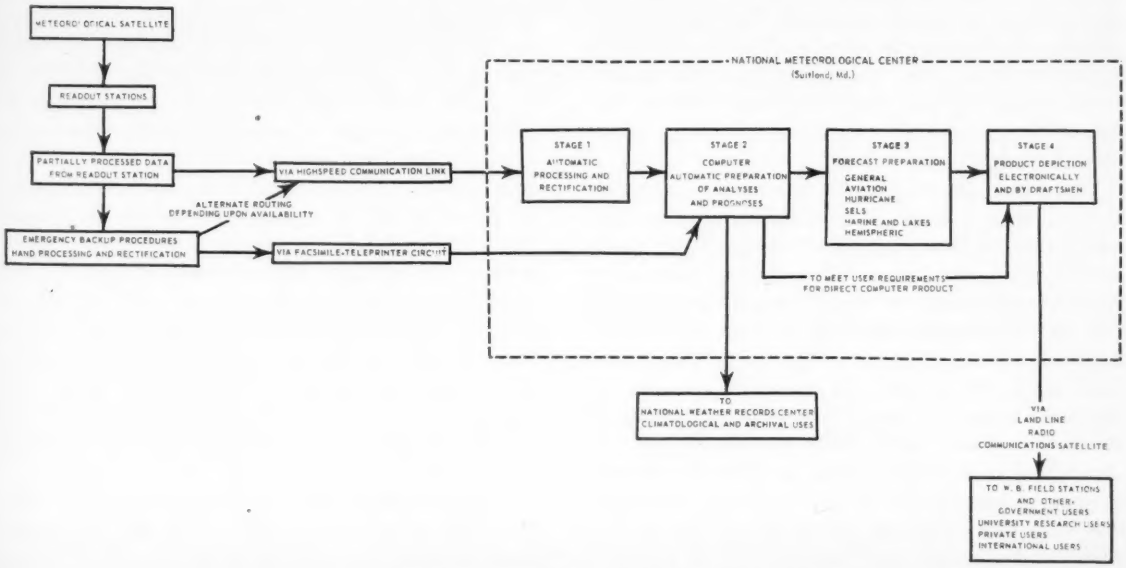
METEOROLOGICAL SATELLITE
READOUT STATIONS
PARTIALLY PROCESSED DATA FROM READOUT STATION
VIA HIGHSPEED COMMUNICATION LINK
ALTERNATE ROUTING DEPENDING UPON AVAILABILITY
EMERGENCY BACKUP PROCEDURES HAND PROCESSING AND RECTIFICATION
VIA FACSIMILE-TELEPRINTER CIRCUIT
NATIONAL METEOROLOGICAL CENTER
(Suitland, Md.)
STAGE 1 AUTOMATIC PROCESSING AND RECTIFICATION
STAGE 2 COMPUTER AUTOMATIC PREPARATION OF ANALYSES AND PROGNOSES
STAGE 3 FORECAST PREPARATION GENERAL AVIATION HURRICANE SELS MARINE AND LAKES HEMISPHERIC
STAGE 4 PRODUCT DEPICTION ELECTRONICALLY AND BY DRAFTSMEN
TO MEET USER REQUIREMENTS FOR DIRECT COMPUTER PRODUCT
TO NATIONAL WEATHER RECORDS CENTER CLIMATOLOGICAL AND ARCHIVAL USES
VIA LAND LINE RADIO COMMUNICATIONS SATELLITE
TO W. B. FIELD STATIONS AND OTHER GOVERNMENT USERS UNIVERSITY RESEARCH USERS PRIVATE USERS INTERNATIONAL USERS

Fig. 3. Flow chart—utilization of meteorological satellite data.

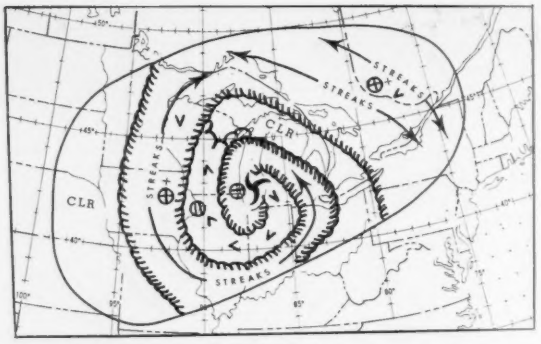

Fig. 5. Rectified neph-analysis[9] based on Fig. 4.

mations, the more complete and reliable the forecasts made therefrom.

Of significance also are the cloud masses arrayed in more or less orderly fashion in the wake of the cold front over the ocean. These masses are too large for their dimensions to be determined in eye observations by an observer on a single ship and too small to be recognized for what they are in the reports from the synoptic network where their dimensions are lost in the wide open spaces between stations.

In other Tiros photographs, the jet stream over the Andes was clearly identified by its associated cloud pattern. This gave information not usually available for air navigation in the region where upper air measurements by balloons or other soundings from the ground are few or altogether lacking.

Photographs transmitted from orbits over the western South Pacific and the Indian Ocean revealed the form and extent of typhoons not otherwise delineated in the reports. Still other photos showed orderly patterns in the spiraling winds that stream into gigantic cyclones over the Pacific. Some of these cyclones are much greater in extent and better organized than heretofore supposed. There are evidences of secondary cyclones, anticyclones, and small-scale atmospheric waves along frontal surfaces which doubtless affect weather in flight operations, terminal landings and many other local weather conditions of concern to commerce, industry, recreational interests, and so on.

Other examples of the very numerous and noteworthy features seen in Tiros photographs are the two or more vortexes in cyclones evidenced by cloud arrays in circumstances where sparse barometric data indicated only one vortex; narrow cloud strips like that paralleling the Gulf Stream for several hundred miles; cloudless strips as pictured over Madagascar in an otherwise overcast sky covering the entire region; a complex family of cyclones over the Indian Ocean; alternating "streets" of cumulus clouds and clear strips in cold, unstable air masses; irregular fields of sea ice in the Gulf of St. Lawrence and snow fields covering the mountain tops in the Alps, the Andes, and the Himalayas.

For research, the foregoing phenomena and many others suggested in Tiros photographs offer excellent material. What are the causes and significance of the elongated cloud masses of some 30 to 50 miles in length shown in Fig. 1? Their typical shapes seem to occur more frequently than would be expected at random. Do some of the cloud cells have the characteristics of Bénard cells and, if so, why? What is the explanation for the orderly arrangement of cloud systems, and how may these be used in improving the techniques for weather forecasting? Further studies should bring out relationships between features of the spiral bands in cyclones and the stage of development of the vortex and its accompanying storm. Quite possibly new knowledge of atmospheric hydrodynamics will be gained and applied to methods of weather prediction by numerical process under continuous development in the Numerical Weather Prediction establishment in Suitland, Md. Studies of some of these subjects and also of the general field of radiation measurements by satellites are cited in the references at the end of this paper. These subjects relate to the earth's heat budget, the general circulation of the atmosphere and the fundamentals on which weather forecasting in quantitative terms must be based.

Turning to questions relating to research in mesometeorology and severe local storms, can tornado-breeding conditions be detected in unique characteristics of precedent clouds photographed by satellite? Only further research can determine whether the case shown in Fig. 2 is a rarity or is illustrative of various storm "signatures" by which their development may be recognized in early stages. Obviously, this capability would be of great value not only in predicting but also in speedy modification of the storm if that ultimately becomes practicable.

Data Transmission and Utilization

The general steps and channels for transmission and processing of meteorological satellite data from its receipt by read-out stations to its final utilization by public and private users is sketched in Fig. 3. New ways for depicting essential features in weather analysis are under development. Undoubtedly, transmission of maps, diagrams, and photographs by facsimile will be an important means for getting the results of satellite output into the hands of users with minimum delay. It now appears that in most cases the finished product can be transmitted by facsimile to field weather offices within five or six hours of the time the raw data are sent by the satellite. This will be somewhat speedier than the present interval between hour of standard synoptic weather observations all over the globe and issuance of maps based on these reports.

As in all general meteorological systems, the satellite program is an interagency operation and depends much on interdepartmental cooperation. Responsibility for research and development of

meteorological satellites in their experimental stages is vested in the National Aeronautics and Space Administration (NASA). Other agencies including the military departments, the Weather Bureau and several university and private research laboratories have worked closely with NASA in these developments. The Weather Bureau's expanded program in this field has been funded almost entirely by NASA up to the present time.

Plans for programing satellites that have reached the stage of regular service performance are now under development. Since the output of operating satellites will have immediate and far-reaching uses in the national meteorological service of the Weather Bureau and since satellite data will find greatest immediate value in its role with global synoptic weather data from all sources now processed in the National Meteorological Center and used in numerical weather prediction, the Weather Bureau hopes to have responsibility for operational satellite data-processing and utilization. Preliminary plans for this have been prepared and are now under interdepartmental consideration.

Fig. 4 shows a mosaic of Tiros photographs of storm clouds over central North America on May 16, 1960. The cloud chart or neph-analysis obtained from this mosaic is reproduced in Fig. 5. Neph-analysis is one of the forms in which weather intelligence from satellites can be transmitted to field forecasting stations and other meteorological offices and to users who find the cloud analysis valuable in their forecasting. A study of Fig. 5 shows that the passing weather in any locality within the analysis area is much more understandable when the patterns and formations are shown in more detail than is possible with use of regular synoptic reports only.

Important steps in the central processing of satellite data are the rectification of cloud photographs so that they faithfully present a plan view and are accurately positioned geographically and in relation to other synoptic weather parameters, and their integration into the three-dimensional depiction of atmospheric conditions in an analysis based on all available synoptic reports. Provision is made for these steps in the proposed operating plans.

The communications facilities for transmission of weather reports are already extensive but they are far short of "requirements." Communications satellites appear to be peculiarly suited to the problems of exchange of meteorological data. In general, the main meteorological centers everywhere need representative reports from other weather stations practically everywhere, particularly for air traffic scheduled to every country on earth. In plans for advanced types of satellites like the Nimbus and Aeros series[12, 13] there should be provisions for communications relays by satellites, thus speeding up exchange of weather reports and synoptic analyses and relieving radio and cable channels of some of the increasing load of meteorological communications. References 10, 12 describe some of the features of Nimbus and Aeros satellites. Essentially the Nimbus series is visualized for launching into polar orbits at distances approximately 600 miles from earth.

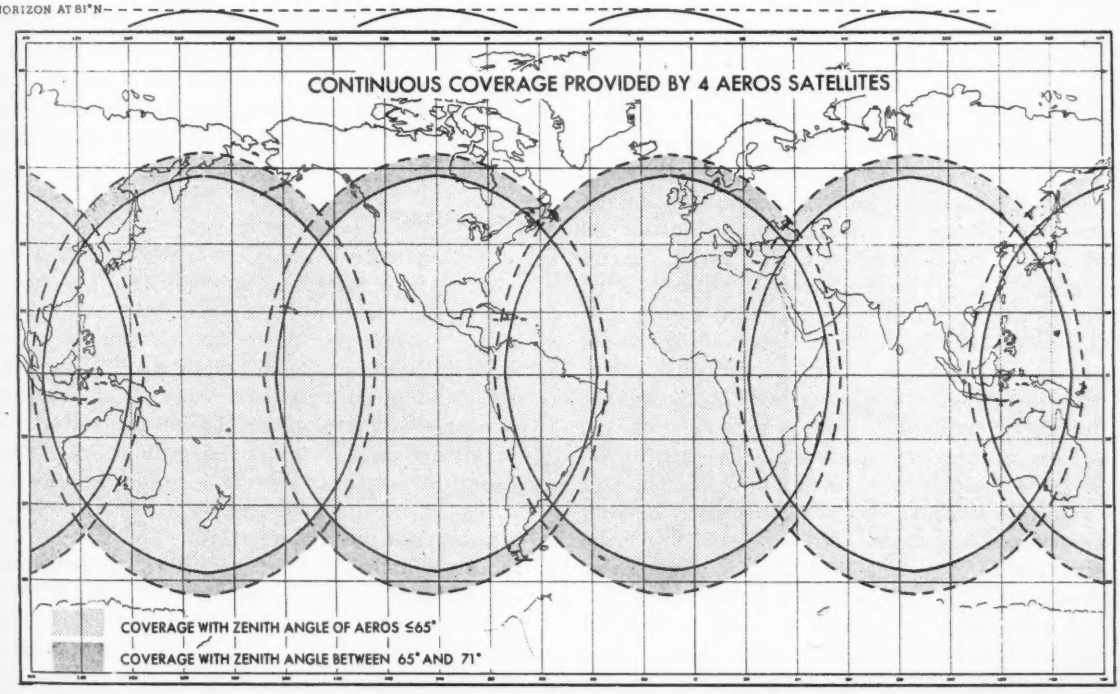
HORIZON AT 81°N
CONTINUOUS COVERAGE PROVIDED BY 4 AEROS SATELLITES
COVERAGE WITH ZENITH ANGLE OF AEROS ≤65°
COVERAGE WITH ZENITH ANGLE BETWEEN 65° AND 71°

Fig. 6.

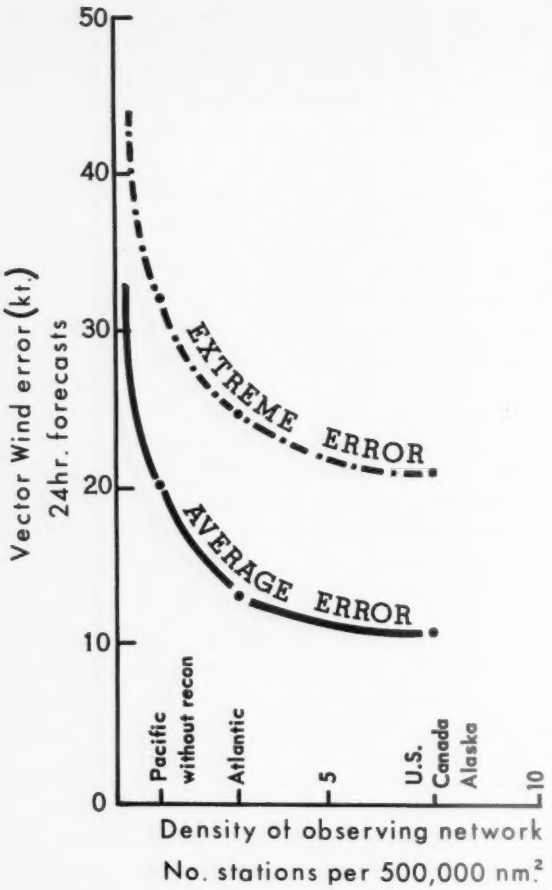

Fig. 7. Forecast errors proportional to sparsity of data[7] (for general wind velocities aloft).

In order to provide observations of every area at least four times daily, two Nimbus satellites would be in orbit at all times. The Aeros series is proposed for equatorial orbit at distances about 19,400 miles above earth. This would give each Aeros satellite an angular velocity equal to that of the earth and thus keep the satellite "hovering" over the same point. With four Aeros satellites in orbit at all times, the continuous coverage shown in Fig. 6 would be given. Instrumentation of Nimbus and Aeros satellites would give improved outputs of cloud photographs, radiation measurements, communications relays, and eventually other parameters listed in an earlier paragraph.

Satellite programs implied in preceding paragraphs are directed primarily toward improvements in the methods of weather forecasting. The loss in accuracy of forecasts in proportion to sparsity of data required for daily weather maps to show analysis of initial conditions as the basis for forecasting is indicated in Fig. 7. This illustrates the rapid loss in accuracy of wind forecasts when the reporting network falls below an average of three well-spaced stations for every 500,000 square miles. This minimum figure for network density applies only to broad-scale wind forecasts and not to detailed local forecasts for which much closer spacing of stations is necessary. Data from satellites will fill the gaps in many regions where more stations are impracticable.

Meteorological records contain many instances of severe storms and destructive hurricanes which could not be forecast in definite terms because the location, configuration and intensity of the storm were unknown. Synoptic reports from the storm area were too few and too irregularly spaced for satisfactory analysis, and consequently there were insufficient data on which to base definite forecasts. Among the many examples are Hurricanes Ione (1955), Audrey (1957), and Donna (1960) whose position, course, and shape of the central vortex were uncertain during part of their life. Such uncertainties are even more frequent with typhoons in the Pacific and cyclones in the Indian Ocean where these storms sometimes reach intensities exceeding most hurricanes. Satellites with their possibilities for complete cloud map coverage of storm areas will remove much of the uncertainty about the position of the center and extent of the destructive winds. Losses in life and property can thus be reduced to the minimum.

In summarizing some of the plans and possibilities of meteorological satellites it is not suggested that all meteorological problems can thus be solved. Atmospheric measurements by other means that give observations not within the capabilities of satellites will still be necessary. Moreover, there are meteorological problems other than the sparsity of basic data that await solution. Among these are the need for communications to transmit and disseminate essential data, maps, and forecasts speedily; imperfections in present techniques for quantitative analysis and prediction; and limitations in present means for "display" or visualization in needed detail of the current atmospheric conditions. But the first step is to obtain sufficient basic data. Satellite systems will go far in correcting the present serious gaps.

Conclusions

The Explorer VII and Tiros satellites have shown that this new source of atmospheric observations and measurements will contribute greatly to knowledge of storm systems, air masses, and fronts, as well as give basic data on radiation and other phenomena that must be understood if the general circulation and its resulting changes in weather and climate are to be analyzed and predicted quantitatively. Although satellites cannot be expected to satisfy all remaining requirements for atmospheric data, they can directly or indirectly give much of the information now lost in the gaps in existing synoptic weather and upper air sounding networks. They are uniquely suited to contribute to comprehensive coverage of weather conditions which the national weather bureau of every modern country seeks to provide for its citizens. In effect, satellites view

"nature's weather map" and picture much of the daily weather of interest to almost every person and business activity. Although many problems remain, the advantages and benefits of information provided by meteorological satellites are likely to lead to national and international support for the launching and maintenance of satellite systems.

Research possibilities from satellite data are relatively unproved but are certainly of great significance. Evidence supports the view that major advances in meteorological theory and understanding of the general circulation and its secondary systems, large and not so large, will come eventually in no small measure as the result of data provided by satellites.

References

[1] Fritz, S., and Wexler, H., *Cloud Pictures from Satellite Tiros I*, Monthly Weather Review, Vol. 88, No. 3, pp. 79–87, Mar. 1960.

[2] Wexler, H., and Fritz, S., *Tiros Reveals Cloud Formations*, Science, Vol. 131, No. 3415, pp. 1708–1710, June 10, 1960.

[3] Hanel, R. A., and Stroud, W. G., *Infrared Imaging from Satellites*, Journal of Motion Picture and Television Engineers, Vol. 69, pp. 25–26, 1960.

[4] Kaplan, Lewis D., *Inferences of Atmospheric Structure from Remote Radiation Measurements*, Journal of the Optical Society of America, Vol. 49, pp. 1004–1007.

[5] Wark, D. Q., *On Indirect Temperature Soundings of the Stratosphere from Satellites*, Journal of Geophysical Research, Vol. 66, No. 1.

[6] Oliver, V. J., *Tiros Pictures a Pacific Frontal Storm*, Weatherwise, Vol. 13, No. 5, Oct. 1960 (front cover, inside).

[7] Staff, Meteorological Satellite Lab., U.S. Weather Bureau, *Some Meteorological Results from Tiros-I*, Report to NASA, U.S. Weather Bureau, 1960.

[8] Ludlum, *Tiros I Concludes Mission; Tiros II Readied*, Weatherwise, Vol. 13, No. 4, pp. 159–161, 180.

[9] Staff, Office of Forecast Development, *Depiction of Satellite Cloud Observations for Facsimile Transmission*, OFDEV Report, No. 1, U.S. Weather Bureau, Washington, D.C., Dec. 1960.

[10] Panel Report, *A National Plan for Common System of Meteorological Observation Satellites*, U.S. Weather Bureau, Washington, D.C., Oct. 1960.

[11] Panel Report, *Plan for Meeting Meteorological Observation Requirements Over Sparse Data Regions*, Technical Planning Study No. 1, U.S. Weather Bureau, Washington, D.C., June 1960.

[12] Staff, Report on NASA, *Industry Program Plans Conference*, pp. 74–76 (Aeros Satellite), July 28–29, 1960, Supt. of Docs., Washington, D.C.

[13] U.S. Senate Hearings Before NASA Subcommittee of Committee on Aeronautical and Space Sciences, *Scientific and Technical Aspects of NASA Program*, 86th Congress, 2nd Session, on H.R. 10,809, Part II, pp. 643–668, June 30, 1960.

✦ ✦ ✦

Creep in Cylindrical Shells (Continued from page 27)

performed to ascertain the degree and region of agreement.

To employ this method of approach, the analytical method is developed and inherent limitations are discussed. Next, existing test data are summarized, a test-theory comparison is performed, and discrepancies between results are rationalized. Theoretically predicted biaxial creep strengths of typical aircraft materials for which no pertinent test data are available are then reported, as are the analytical and experimental complexities introduced by time-varying loads and temperatures. Design considerations are then briefly examined. Based upon these results, conclusions regarding the current state of the art are drawn, and specific recommendations are made for studies which would serve to extend and refine presently used methods of analysis, provide unknown material property data, and yield practical design information.

Method of Analysis

Consideration of equilibrium conditions of the vessel shown in Fig. 1 yields the following expressions relating applied pressure p, instantaneous radius $\dot{a}$, instantaneous thickness $\dot{t}$, and instantaneous stress $\dot{\sigma}$:

$$\dot{\sigma}_c = p\dot{a}/\dot{t} \qquad \dot{\sigma}_e = \dot{\sigma}_c/2 \qquad \dot{\sigma}_r \simeq 0 \qquad (1)$$

Theories of creep in the presence of combined stresses have been formulated by various investigators.[2–6] Basically, these theories are an extension of the theory of plastic flow and utilize the following assumptions:

(1) The material is homogeneous and isotropic.

(2) Creep deformations occur at constant volume.

(3) Mohr's three principal strain circles are geometrically similar to Mohr's three principal stress circles.

(4) The principal shear creep strain rates are proportional to the principal shear stresses.

(5) A universal relation exists among stress, creep strain, time, and temperature and is valid for all states of stress.

(6) The elastic and thermal strains are small in comparison to the creep strains and hence are neglected.

From assumptions (2) and (4), Nadai[6] obtains the following creep relationships in terms of the true principal stresses and strains:

$$\left.\begin{aligned} d\dot{\epsilon}_1/d\theta &= C_{cp}[2\dot{\sigma}_1 - \dot{\sigma}_2 - \dot{\sigma}_3] \\ d\dot{\epsilon}_2/d\theta &= C_{cp}[2\dot{\sigma}_2 - \dot{\sigma}_3 - \dot{\sigma}_1] \\ d\dot{\epsilon}_3/d\theta &= C_{cp}[2\dot{\sigma}_3 - \dot{\sigma}_1 - \dot{\sigma}_2] \end{aligned}\right\} \qquad (2)$$

where C_{cp} is a function of strain, stress, time, and temperature.

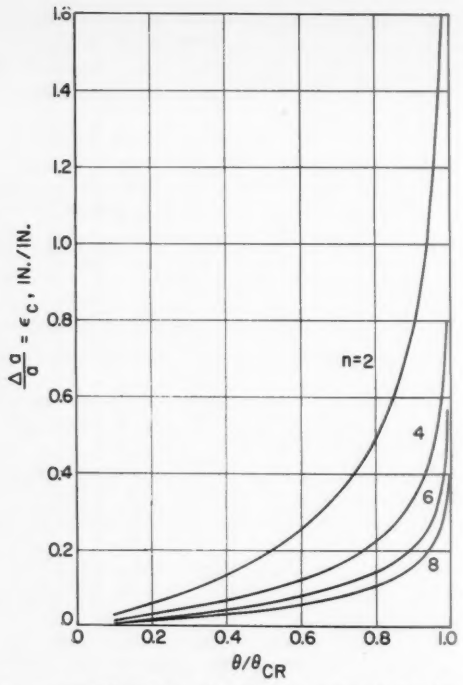

Fig. 2. Theoretical variation of hoop creep strain with time for pressurized cylinders.

In accordance with assumption (5), a universal relationship of the following form exists:

$$d\bar{\epsilon}_{cp}/d\theta = f(\bar{\sigma}_{cp}, \theta, T) \tag{3}$$

where $\bar{\epsilon}_{cp}$ and $\bar{\sigma}_{cp}$ are the effective creep strain and stress, respectively.

By use of the distortion energy theory, expressions relating the true principal stresses and strains to the effective stresses and strains are derivable. This results in

$$\bar{\sigma} = 1/\sqrt{2} \times \sqrt{(\dot{\sigma}_1 - \dot{\sigma}_2)^2 + (\dot{\sigma}_2 - \dot{\sigma}_3)^2 + (\dot{\sigma}_3 - \dot{\sigma}_1)^2} \tag{4}$$

$$d\bar{\epsilon}/d\theta = \sqrt{2}/3 \times \sqrt{\left(\frac{d\dot{\epsilon}_1}{d\theta} - \frac{d\dot{\epsilon}_2}{d\theta}\right)^2 + \left(\frac{d\dot{\epsilon}_2}{d\theta} - \frac{d\dot{\epsilon}_3}{d\theta}\right)^2 + \left(\frac{d\dot{\epsilon}_3}{d\theta} - \frac{d\dot{\epsilon}_1}{d\theta}\right)^2} \tag{5}$$

For the uniaxial case, $\dot{\sigma}_1 = \dot{\sigma}$, $\dot{\sigma}_2 = \dot{\sigma}_3 = 0$, $d\dot{\epsilon}_1/d\theta = d\dot{\epsilon}/d\theta$, and $d\dot{\epsilon}_2/d\theta = d\dot{\epsilon}_3/d\theta = -(1/2)(d\dot{\epsilon}/d\theta)$. Substituting these relations into Eqs. (4) and (5) yields

$$\bar{\sigma}_1 = \dot{\sigma}$$
$$d\bar{\epsilon}/d\theta = d\dot{\epsilon}/d\theta$$

Thus, the creep law derived from uniaxial creep tests is identical to that given by Eq. (3). Further, since Eq. (2) is also valid for a uniaxial creep test, C_{cp} can be found by substituting the values of the uniaxial stresses and strains. This results in

$$C_{cp} = \frac{1}{2\dot{\sigma}}\frac{d\dot{\epsilon}}{d\theta} = \frac{1}{2\bar{\sigma}}\frac{d\bar{\epsilon}}{d\theta} \tag{6}$$

and, from Eq. (3), using the results of Eq. (6),

$$C_{cp} = [f(\bar{\sigma}, \theta, T)]/2\bar{\sigma} \tag{7}$$

If a creep law[7] of the form

$$d\dot{\epsilon}_{cp}/d\theta = B\dot{\sigma}^n \tag{8}$$

is assumed, where B and n are functions of temperature only, then, with the aid of Eq. (7), C_{cp} becomes

$$C_{cp} = B\bar{\sigma}^n/2\bar{\sigma} = B\bar{\sigma}^{(n-1)}/2 \tag{9}$$

Introducing Eq. (4) into Eq. (9) yields

$$C_{cp} = [B/2^{(n+1)/2}]\,[(\dot{\sigma}_1 - \dot{\sigma}_2)^2 + (\dot{\sigma}_2 - \dot{\sigma}_3)^2 + (\dot{\sigma}_3 - \dot{\sigma}_1)^2]^{(n-1)/2} \tag{10}$$

These creep laws are identical to those proposed by Marin.[5] However, in this development it was unnecessary to assume that the creep rate or stresses were constant. Thus, it appears reasonable to assume that these relations will remain valid for time-dependent stress conditions.

Substituting the expressions for the instantaneous stresses set forth in Eq. (1) into Eq. (2), and employing the value of C_{cp} as given by Eq. (10), yields

$$\left.\begin{aligned} d\dot{\epsilon}_c/d\theta &= B/2^{(n+1)/2}\,(3/2)^{(n+1)/2}\,\dot{\sigma}_c^{\,n} \\ d\dot{\epsilon}_1/d\theta &= 0 \\ d\dot{\epsilon}_r/d\theta &= -(d\dot{\epsilon}_c/d\theta) \end{aligned}\right\} \tag{11}$$

Thus the axial strain is zero. For small values of creep strain, the true stress and strain are approximately equal to the conventional values. Hence, with the aid of Eq. (8) and the relationships following Eq. (5), Eq. (11) yields the ratio of $\dot{\epsilon}_c$ to $\dot{\epsilon}$, at the same stress and time, to be

$$\dot{\epsilon}_c/\dot{\epsilon} = \epsilon_c/\epsilon = (\sqrt{3}/2)^{n+1} \tag{12}$$

Now by definition, the true strains are given in

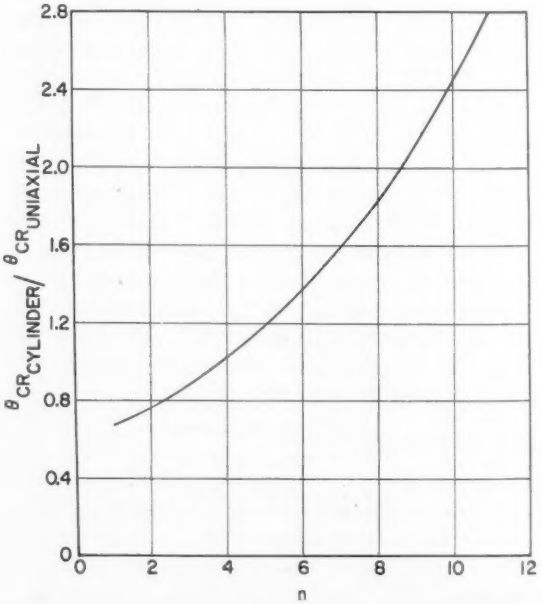

Fig. 3. Ratio of theoretical cylinder and uniaxial creep-rupture times as a function of n.

terms of the conventional strains as

$$\left.\begin{aligned} \dot{\epsilon}_c &= \ln(1 + \epsilon_c) = \ln \dot{a}/a \\ \dot{\epsilon}_t &= \ln(1 + \epsilon_t) \\ \dot{\epsilon}_r &= \ln(1 + \epsilon_r) = \ln \dot{t}/t \end{aligned}\right\} \qquad (13)$$

Eliminating $\dot{t}$ and $\dot{a}$ from Eq. (1) by the use of Eq. (13) results in

$$\dot{\sigma}_c = \frac{p\dot{a}}{\dot{t}} = \frac{pa}{t}\left(\frac{e^{\dot{\epsilon}_c}}{e^{\dot{\epsilon}_r}}\right) = \sigma_c e^{\dot{\epsilon}_c - \dot{\epsilon}_r} \qquad (14)$$

Further, eliminating $\dot{\sigma}_c$ from the first Eqs. (11), with the aid of Eq. (14), and noting that $d\dot{\epsilon}_r/d\theta = -d\dot{\epsilon}_c/d\theta$ from the third of Eqs. (11), yields

$$\frac{d\dot{\epsilon}_c}{d\theta} = \frac{B}{2^{(n+1)/2}}(3/2)^{(n+1)/2}(\sigma_c)^n e^{2\dot{\epsilon}_c n} \qquad (15)$$

Separating variables in Eq. (15), and integrating and employing the initial condition that $\dot{\epsilon}_c$ at $\theta = 0$ is $(\dot{\epsilon}_c)_{\theta=0}$, results in

$$\theta = [2^n/3^{(n+1)/2}(\sigma_c)^n nB][e^{-2n\dot{\epsilon}_c} - e^{-2n(\dot{\epsilon}_c)_{\theta=0}} \qquad (16)$$

Assuming that $(\dot{\epsilon}_c)_{\theta=0}$ is equal to zero in Eq. (16) gives

$$\theta = [2^n/3^{(n+1)/2}(\sigma_c)^n nB][1 - e^{-2n\dot{\epsilon}_c}] \qquad (17)$$

The condition for creep rupture is that the cylinder thickness approach zero, which is expressible as

$$\epsilon_r = \Delta t/t = -1$$

that is, the change in thickness is equal in magnitude and opposite in sign to the original thickness. Thus, from the last of Eqs. (13),

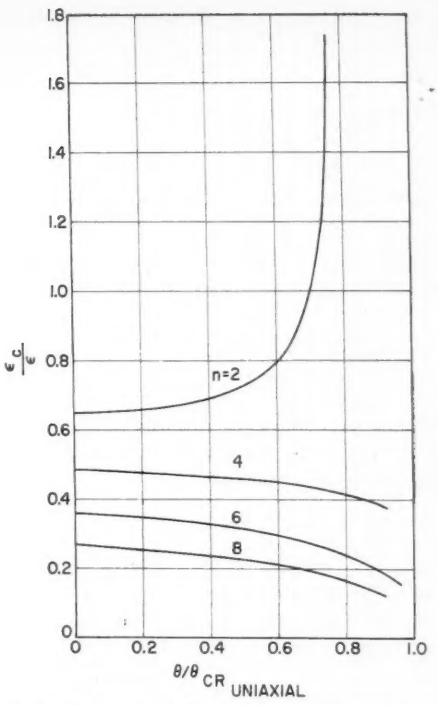

Fig. 4. Variation of ϵ_c/ϵ with time for various values of n.

$$\dot{\epsilon}_r = \ln(1 + \epsilon_r) = \ln 0$$

and therefore $\epsilon_r \to -\infty$.

With the aid of the last of Eqs. (11), $\dot{\epsilon}_c = -\dot{\epsilon}_r$, hence $\dot{\epsilon}_c \to \infty$. Thus, equating $\dot{\epsilon}_c$ to ∞ in Eq. (17) results in a critical rupture time of

Table 1. Test-Theory Comparison of Time to Creep Rupture[1]

Specimen Type[2]	Minimum Wall[3] (in.)	Internal Pressure (psi)	Stress[4] (psi)	Test Rupture Time (hours)	Theoretical Rupture Time (hours)
Steel A[5] tube	0.156	9,600	56,750	Short time	
	0.168	6,800	37,100	36.1	
	0.167	5,800	37,800	112.4	
	0.161	4,800	27,400	744.2	204.7
	0.168	4,000	21,800	2,969.8	1,246
	0.167	3,600	19,750	5,682.0	2,848
	0.159	3,100	17,950	10,591.0	6,052
Steel B[6] tube	0.152	5,400	32,800	13.2	
	0.152	4,400	26,750	64.8	249.2
	0.149	3,700	23,000	399.4	801
	0.156	2,850	16,850	2,851.2	9,968
Steel C[7] bar			27,000	144.8	$n = 7.83$
			25,000	203.8	
			23,000	449.8	
			21,600	793.8	
			18,000	2,566.5	
			16,500	8,930.7	
			15,000	Still running	
			13,500	Still running	

[1] Data from reference 9, material A-210 steel, temperature 850°F.
[2] Tubes were 2 in. O.D. by 0.15 in. min. wall. Bars were 0.505 in. diam. standard specimens.
[3] Min. wall = average of min. wall thickness measured at both ends of specimen.
[4] Tube stresses were calculated using the formula

$$\text{stress} = \frac{\text{pressure} \times (\text{I.D.} + \text{O.D.})}{4 \times \text{min. wall thickness}}$$

[5] Hot finish only.
[6] Normalized at 1,650°F.
[7] One-half hour 1,300°F. furnace cooled.

$$\theta_{cr} = \frac{2^n}{3^{(n+1)/2}(\sigma_c)^n nB} = (2/\sqrt{3})^{n+1}\,[1/2nB(pa/t)^n] \tag{18}$$

or, from Eq. (15),

$$\theta_{cr} = 1/2^n(d\dot{\epsilon}_c/d\theta)_{\theta=0} \tag{19}$$

where $(d\dot{\epsilon}_c/d\theta)_{\theta=0}$ is the creep rate at time equal to zero.

Substituting Eq. (18) into Eq. (17) yields an expression for the creep curve in the form

$$\theta = \theta_{cr}[1 - e^{-2n\dot{\epsilon}c}] \tag{20}$$

or

$$\theta = \theta_{cr}[1 - (a/\dot{a})^{2n}] \tag{21}$$

However, $a/\dot{a} = (1 - \epsilon_c)$ from the first of Eqs. (13). Substituting this relation into Eq. (21), and rearranging terms, results in

$$\epsilon_c = [1 - (\theta/\theta_{cr})]^{-(1/2n)} - 1 \tag{22}$$

Eq. (22) is plotted in Fig. 2 for various assumed values of the exponent n.

Adopting the same method of approach,[8] the uniaxial critical time is

$$\theta_{cr} = 1/n\ B\sigma^n \tag{23}$$

A similar relationship, for the biaxial case, is given by Eq. (18). Hence, the ratio of the critical times to rupture for the cylinder and uniaxial loading conditions, and for the same value of initial stress, becomes

$$\frac{\theta_{cr\ \text{cylinder}}}{\theta_{cr\ \text{uniaxial}}} = \frac{1}{2}\left(\frac{2}{\sqrt{3}}\right)^{n+1} \tag{24}$$

This relation is depicted in Fig. 3. The results shown there reveal that for $n \geq 4$, the rupture time of the cylinder is greater than that of the uniaxially loaded member, whereas for values of $n < 4$, the reverse is true.

To compare the theoretical creep strains for uniaxial and biaxial loading conditions, at the same time and nominal stress, divide Eq. (22) by

$$\epsilon_{cp} = [1 - (\theta/\theta_{cr})]^{1/n} - 1 \tag{25}$$

and substitute for θ_{cr} from Eq. (24) to yield

$$\epsilon_c/\epsilon_{cp} = \frac{[1 - 2\,(\sqrt{3}/2)^{n+1}\,(\theta/\theta_{cr_u})]^{-(1/2n)} - 1}{[1 - (\theta/\theta_{cr_u})]^{-1/n} - 1} \tag{26}$$

The variation of the nominal creep strain ratios ϵ_c/ϵ_{cp} with nondimensional time θ/θ_{cr_u}, as given by Eq. (26), is shown in Fig. 4. For large values of n, the hoop creep strain is always less than the creep strain for the same uniaxial stress; lower values of n result in strain ratios initially less than one, but, for greater time ratios, the hoop strain exceeds the corresponding value of uniaxial strain.

Test-Theory Comparisons

The validity of the theory proposed to calculate creep rupture can be substantiated only by comparison with test. A limited amount of test data is reported in references 9–13 for the creep rupture

Table 2. Test-Theory Comparison of Time to Creep Rupture[1]

Specimen Type[2]	Minimum Wall[3] (in.)	Internal Pressure (psi)	Stress[4] (psi)	Test Rupture Time (hours)	Theoretical Rupture Time (hours)
Steel A[5] tube	0.159	8,000	46,300	Short time	
	0.157	5,000	29,350	8.0	
	0.163	4,410	24,850	28.0	
	0.161	3,700	21,150	98.8	
	0.166	3,150	17,950	327.7	190.6
	0.170	2,750	14,800	711.9	541.2
	0.161	2,100	12,000	2,404.0	1,623.6
	0.161	1,700	9,700	6,661.3	5,043.0
Steel B[6] tube	0.156	5,000	29,550	1.4	
	0.157	2,500	14,650	197.8	565.8
	0.157	2,000	11,750	483.6	1,845
	0.154	1,650	9,900	1,287.2	4,551
	0.154	1,500	9,000	2,951.3	7,380
Steel C[7] bar			20,000	20.4	$n = 5.27$
			18,000	87.3	
			16,800	235.6	
			12,800	983.1	
			10,500	2,384.0	
			8,500	8,261.0	
			7,500	Still running	

[1] Data from reference 9, material A-210 steel, temperature 950°F.
[2] Tubes were 2 in. O.D. by 0.15 in. min. wall. Bars were 0.505 in. diam. standard specimens.
[3] Min. wall = average of min. wall thickness measured at both ends of specimen.
[4] Tube stresses were calculated using the formula

$$\text{stress} = \frac{\text{pressure} \times (\text{I.D.} + \text{O.D.})}{4 \times \text{min. wall thickness}}$$

[5] Hot finish only.
[6] Normalized at 1,650°F.
[7] One-half hour 1,300°F. furnace cooled.

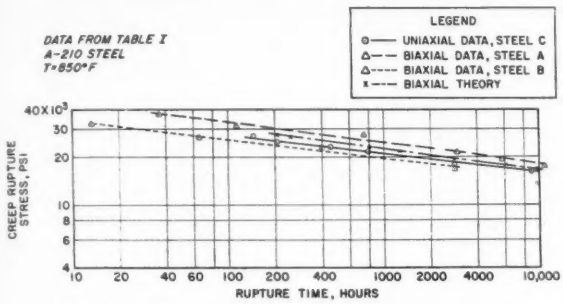

Fig. 5. Test-theory comparison of time to creep rupture.

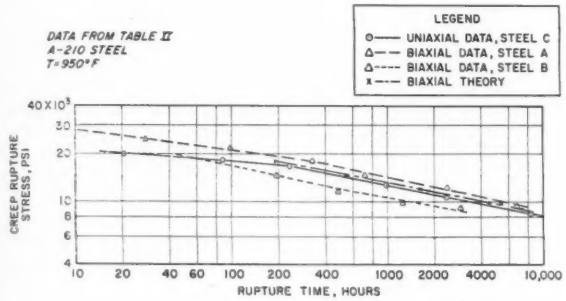

Fig. 6.

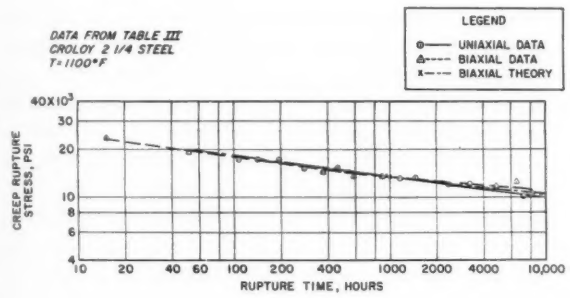

Fig. 7.

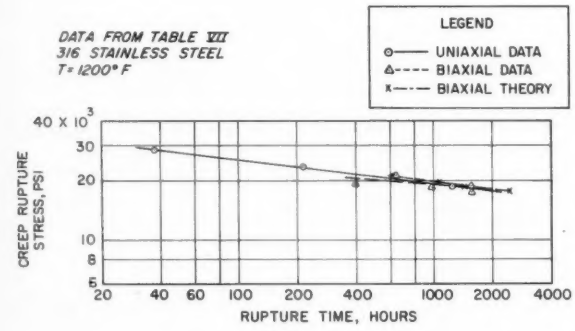

Fig. 11

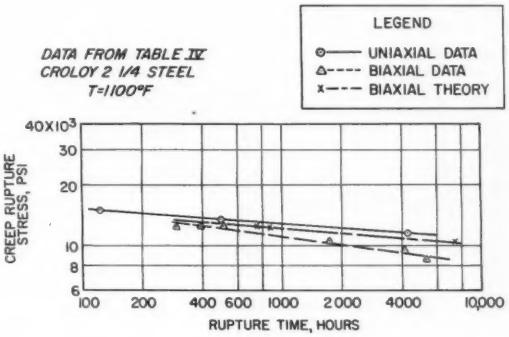

Fig. 8.

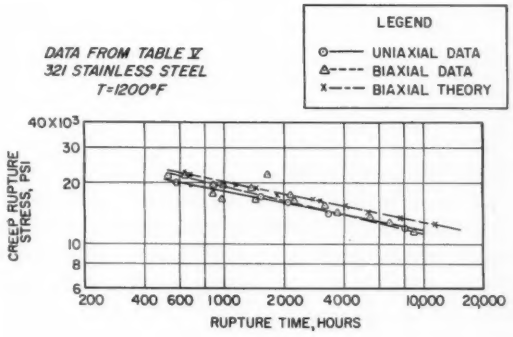

Fig. 9.

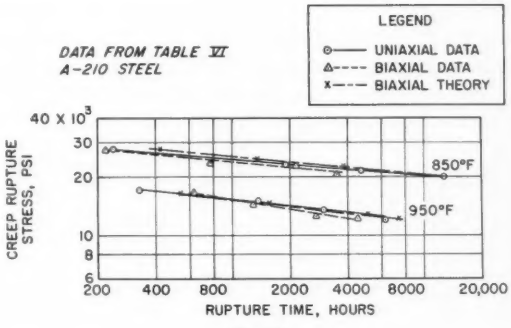

Fig. 10.

Figs. 5–11. Test-theory comparison of time to creep rupture.

Table 3. Test-Theory Comparison of Time to Creep Rupture[1]

Specimen Type[2]	Minimum Wall (in.)	Internal Pressure (psi)	Stress[3] (psi)	Test Rupture Time (hours)	Theoretical Rupture Time (hours)
Tube, Heat No. 924[4]	0.209	5,570	23,850	15	
	0.212	4,680	19,650	51	58
	0.205	3,340	14,550	372	544
	0.216	3,300	13,550	580	1,000
	0.205	3,120	13,600	858	955
	0.206	2,600	11,250	4,348	3,950
	0.208	2,770	11,900	4,786	3,200
	0.202	2,800	12,400	6,422	2,130
	0.203	2,280	10,050	7,928	9,450
Bar, Heat No. 924			17,000	107	$n = 5$
			17,000	140	
			17,000	191	
			15,000	281	
			15,000	458	
			13,000	1,175	
			13,000	1,486	
			12,000	2,363	
			12,000	3,255	
			10,000	7,179	
			10,500	7,788	

[1] Data from reference 10, material croloy 2-1/4, temperature 1,100°F.
[2] Tubes were 2 in. O.D. by 0.203 in. min. wall. Bars were 0.250 in. diam. standard specimens.
[3] Tube stresses were calculated using the formula

$$\text{stress} = \frac{\text{pressure} \times (\text{I.D.} + \text{O.D.})}{4 \times \text{min. wall thickness}}$$

[4] Furnace cooled to room temperature.

of thick-walled cylinders used for high-pressure, high-temperature piping.

The specimens tested in reference 9 were fabricated from ASTM A-210-46 steel, with an outside cylinder diameter of 2 in. and a wall thickness of 0.150 in. The internal pressures resulted in a stress range of approximately 10,000 to 40,000 lbs./sq.in., the test temperatures were 850° and 950°F., and the rupture times were between 10 and 10,000 hours. The detailed data are set forth in Tables 1 and 2.

The uniaxial creep-rupture strength of the material was included; the minimum creep rate of the material was not. Hence the theoretical results of reference 8, as given by Eq. (23), were used to approximate the exponent n directly from the creep-rupture test data. In this manner, the value of the material constant B need not be calculated. Eq. (24) was then used to predict the rupture time for the cylinder, and the comparison with test for the two temperature levels is shown in Figs. 5 and 6. The theoretical creep-rupture stress, as presented, was based upon the mean cylinder diameter.

Although the material used for both the uniaxial and cylindrical specimens conformed to the same specification, they were obtained from different heats and heat-treatment cycles. A portion of the discrepancy between theory and test may be attributed to this source, inasmuch as the creep behavior is greatly affected by the metallurgical structure of the material.

Test-theory comparisons were performed in a similar fashion for the experimental results presented

Table 4. Test-Theory Comparison of Time to Creep Rupture[1]

Specimen Type[2]	Minimum Wall (in.)	Internal Pressure (psi)	Stress[3] (psi)	Test Rupture Time (hours)	Theoretical Rupture Time (hours)
Tube, Heat No. H19131[4]	0.560	7,470	12,800	394	750
	0.574	7,670	12,800	507	750
	0.574	6,030	10,050	1,744	7,200
	0.561	5,600	9,550	4,098	
	0.572	5,130	8,600	5,314	
	0.432	5,300	12,650	299	865
Bar, Heat No. H19131			15,000	121	$n = 1.56$
			13,500	498	
			11,500	4,267	

[1] Data from reference 10, material croloy 2-1/4, temperature 1,100°F.
[2] Tubes were 2 1/2 in. O.D. by 0.570 in. min. wall. Bars were 0.503 in. diam. standard specimens.
[3] Tube stresses were calculated using the formula

$$\text{stress} = \frac{\text{pressure} \times (\text{I.D.} + \text{O.D.})}{4 \times \text{min. wall thickness}}$$

[4] One hour 1,550°F.; 25°F. per hour furnace cooled to 1,200°F.

Table 5. Test-Theory Comparison of Time to Creep Rupture[1]

Specimen Type[2]	Minimum Wall (in.)	Internal Pressure (psi)	Stress[3] (psi)	Test Rupture Time (hours)	Theoretical Rupture Time (hours)
Tube, Heat No. 20526[4]	0.514	15,000	21,675	527	680
	0.508	12,780	18,700	1,393	1,430
	0.515	11,120	16,050	2,279	3,060
	0.514	10,490	15,150	3,199	4,080
	0.514	9,870	14,250	3,683	5,250
	0.511	9,190	13,350	5,389	7,560
	0.511	8,580	12,470	6,675	11,200
	0.507	7,910	11,600	8,972	
	0.467	13,950	22,000	646	630
	0.373	9,360	19,700	879	1,120
	0.246	5,110	17,600	871	1,870
	0.154	2,850	16,500	945	2,800
	0.468	14,000	22,000	1,663	630
	0.374	9,430	19,700	972	1,120
	0.251	5,230	17,600	2,115	1,870
	0.157	2,880	16,500	1,452	2,800
Bar, Heat No. 20526			20,000	572	$n = 8.33$
			17,000	1,517	
			16,000	2,098	
			14,000	3,317	
			12,000	7,999	

[1] Data from reference 10, material 321 stainless steel, temperature 1,200°F.
[2] Tubes one through eight were 2 in. O.D. by 0.512 in. min. wall. Bars were 0.320 in. diam. standard specimens.
[3] Tube stresses were calculated using the formula

$$\text{stress} = \frac{\text{pressure} \times (\text{I.D.} + \text{O.D.})}{4 \times \text{min. wall thickness}}$$

[4] One-half hour, 1,900°F. water quench.

in references 10 and 11. Tables 3–6 present the data obtained from reference 10; Table 7 lists the results given in reference 11. Figs. 7–11 depict the test-theory comparisons obtained. The value of the exponent n employed in each analysis is listed in the appropriate table.

The results obtained, as shown graphically in Figs. 5–11, indicate a reasonable agreement between test and theoretically predicted time to stress rupture. This agreement is seen to be better for the higher tube radius to thickness ratios tested. One explanation for this is that, as the wall thickness decreases, the stress gradient across the thickness is diminished and a more nearly two-dimensional state of stress is brought into being. Such stress systems are in closer agreement to those employed in the analytical development, and some improvement between test and theory may be attributable to this factor.

Thus it is seen that the actual value of the stress

Table 6. Test-Theory Comparison of Time to Creep Rupture[1]

Temperature (°F.)	Specimen Type[2]	Minimum Wall (in.)	Internal Pressure (psi)	Stress[3] (psi)	Test Rupture Time (hours)	Theoretical Rupture Time (hours)
850	Tube, Heat No. T1088[4]	0.466	17,590	27,800	220	420
		0.375	11,960	24,800	768	1,350
		0.249	6,570	22,200	2,221	3,780
		0.156	3,630	20,800	3,551	12,300
	Bar, Heat No. T1088			28,000	238	$n = 7.83$
				23,000	1,988	
				21,500	4,772	
				20,000	12,801	
950	Tube, Heat No. T1088	0.462	10,030	16,500	622	540
		0.377	6,980	14,600	1,290	1,530
		0.250	3,820	12,900	2,734	5,150
		0.156	2,110	12,100	4,472	7,380
	Bar, Heat No. T1088			17,000	330	$n = 5.27$
				15,000	1,388	
				13,500	2,998	
				12,000	6,228	

[1] Data from reference 10, material SA-210 steel, temperature 850° and 950°F.
[2] Bars were 0.321 in. diam. standard specimens.
[3] Tube stresses were calculated using the formula

$$\text{stress} = \frac{\text{pressure} \times (\text{I.D.} + \text{O.D.})}{4 \times \text{min. wall thickness}}$$

[4] One-half hour 1,650°F., air cooled to below 400°F.; one-half hour 1,300°F., air cooled to room temperature.

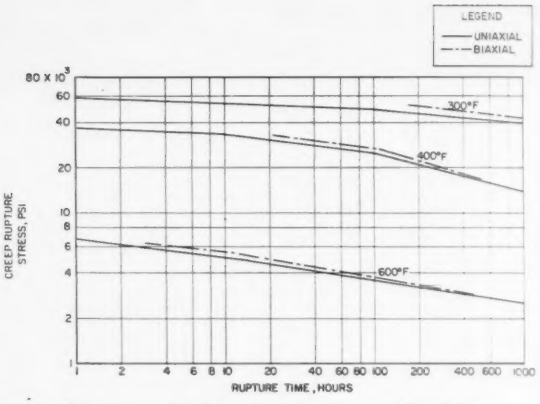

Fig. 12. Predicted biaxial creep strength of 2014-T6.

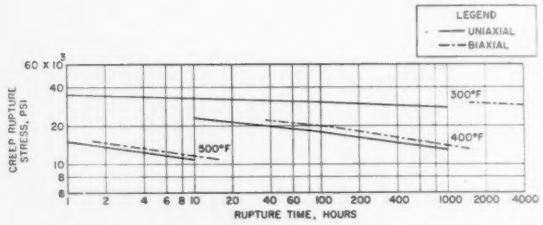

Fig. 13. Predicted biaxial creep strength of 6061-T6.

at rupture is not well known. Fortunately, however, for the parameter range of interest to the aircraft designer, the degree of this uncertainty will be less as the radius to thickness ratio approaches the values encountered in design. Finally, it should be noted that the differences between test and theory lie, for the most part, within the scatter band of the test results obtained.

Predicted Biaxial Creep Strengths

It has been noted that there is a particular lack of experimental data on the biaxial creep-rupture strength of materials common to aircraft construction. For this reason, typical data will be predicted on the basis of available uniaxial experimental results. In this way, significant shortcomings either of the method of analysis or of these materials may be uncovered in an approximate manner. The analytical investigations and tests necessary to determine the exact extent of such shortcomings may then be delineated.

Table 8 lists the materials for which this approach has been adopted, as well as the range of temperatures, stresses, and failure times portrayed. This table also provides a listing of the references from which the basic data were abstracted, and the diagrams in which the comparisons between uniaxial and biaxial creep-rupture strengths are displayed.

Examination of these diagrams (Figs. 12–16) allows certain general observations to be made. First, for low temperatures, the predicted biaxial creep strength exceeds the experimental uniaxial creep strength. Indeed, for those temperatures at which a material barely undergoes creep deformation, the method of analysis employed would indicate inordinately high rupture times. This result is compatible with the creep law assumed in the analysis [see Eq. (8)]. As the temperature levels are increased, the relative strength under biaxial loading decreases with respect to the uniaxial creep resistance of the material. This condition arises, primarily, from strain softening of the material at high temperatures, and this effect is manifest by reduced values of the exponent of the true stress-time strain relation. A specific example of this phenomenon is illustrated in Fig. 16 for annealed 316 stainless steel.

Further, with regard to Fig. 16, additional complexities are noticeable in the temperature range between 1,100° and 1,500°F. For the exposure times at these temperatures, certain metallurgical changes are likely, giving rise to the results shown. A brief discussion of such changes is included in the following two sections.

Some final remarks on the creep strength of notched specimens will now be made. Fig. 17 presents certain of the results of uniaxial stress-rupture studies[14] on A-286 steel at 1,200°F. Also depicted in this diagram are the predicted notched biaxial creep strengths. A study of these data indicates that the percentage reduction in the time to failure is greater for the notched biaxial specimens than for the unnotched. Thus, based upon the extremely limited amount of data, the effect of notches on pressurized components is likely to be more severe than on components fabricated of the same material but subject to uniaxial creep stresses only.

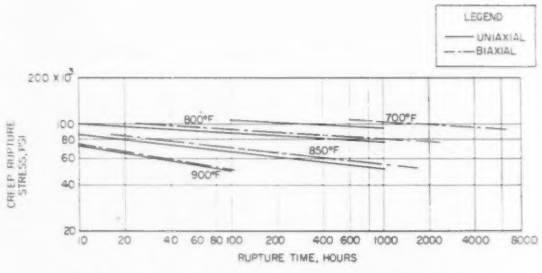

Fig. 14. Predicted biaxial creep strength of 6AL-4V.

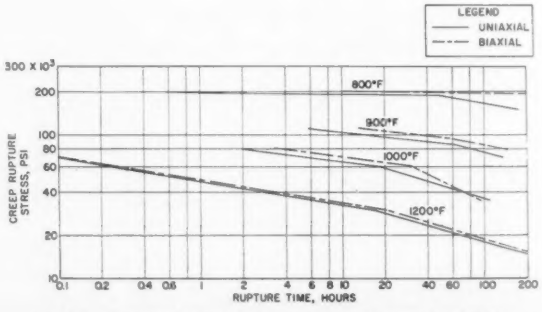

Fig. 15. Predicted biaxial creep strength of extra hard 301.

Complexities Introduced by Intermittent Conditions

The vessels for which the analysis presented was undertaken rarely operate under conditions of constant stress and temperature. To predict failure by test under the actually experienced intermittent stress and temperature conditions, however, would be both expensive and time consuming, and the duplication of all actual operating conditions would be impractical. Therefore, methods should be devised which will yield a safe prediction of failure based on relatively simple constant temperature and stress applications.

Methods currently available for this purpose were reviewed by Padlog and Schnitt,[15] who drew the following salient conclusions:

(1) The creep properties of aluminum alloys are not greatly affected by the application of intermittent temperature-constant stress, or in-phase cycles of intermittent stress and temperature, if the deformation and rupture characteristics are compared with constant-load isothermal creep for net time under load.

(2) Based upon the net time criterion, accelerated creep and earlier rupture are experienced when the material is subjected to intermittent stress at constant temperature, or to out-of-phase combined cycles of load and temperature.

These factors give rise to a certain amount of analytical difficulty. However, additional difficulties are encountered from the metallurgical changes promoted by exposure to transient conditions. A partial listing of such factors, and an explanation of each, is presented here. (Note that these factors have a weakening effect on the material and, in

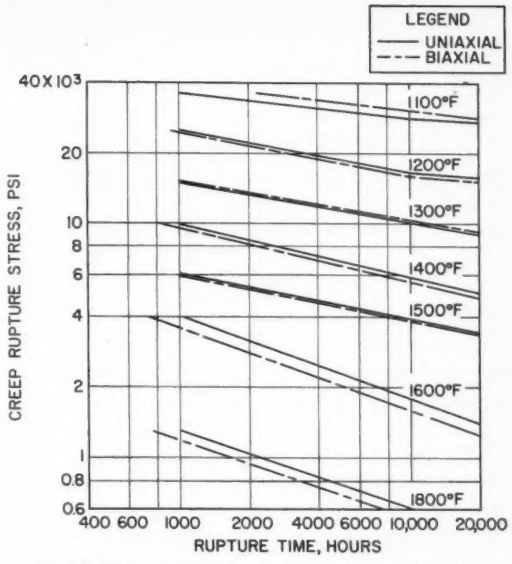

Fig. 16. Predicted biaxial creep strength of annealed 316.

Table 7. Test-Theory Comparison of Time to Creep Rupture[1]

Specimen Type[2]	Wall Thickness (in.)	Internal Pressure (psi)	Stress[3] (psi)	Test Rupture Time (hours)	Theoretical Rupture Time (hours)
Tube[4]	0.284	15,000	19,600	400	1,080
	0.287	14,000	18,200	970	1,570
	0.303	13,400	17,500	1,590	2,430
	0.375	24,000	21,000	639	610
	0.375	21,000	18,250	1,550	1,460
Bar			23,400	213	$n = 6.29$
			18,300	1,248	
			28,300	37.5	
			15,300	>620	
			10,450	>868	
			11,450	>10,200	

[1] Data from reference 11, material 316 stainless steel, temperature 1,200°F.
[2] Tubes were $1^1/_8$ in. O.D. by 0.284 min. wall. Bars were 0.505 in. diam. standard specimens.
[3] Tube stresses were calculated using the formula

$$\text{stress} = \frac{\text{pressure} \times (\text{I.D.} + \text{O.D.})}{4 \times \text{min. wall thickness}}$$

[4] Two hours 1,950°F., water quench.

Table 8. Predicted Biaxial Creep Strength Materials

Material	Temperature (°F.)	Stress Range (ksi)	Rupture Time Range (hours)	Data Source	Fig.
2014-T6	300–600	2.5–60	1–1,000	Unpublished Alcoa data	12
6061-T6	300–500	10–35	1–1,500	Unpublished Alcoa data	13
6Al-4V	700–900	50–110	10–5,000	*Compilation of Available Information on Ti-6Al-4V Alloy*, Titanium Metallurgical Lab. Memo. 97, Feb. 1958	14
301-extra hard	800–1200	15–200	0.1–1,000	*Properties of Certain Cold-Rolled Austenitic Stainless Sheet Steel*, DMIC Report 113	15
316-annealed	1,100–1,800	1–40	700–20,000	Allegheny Ludlum Steel Corp. data sheets	16

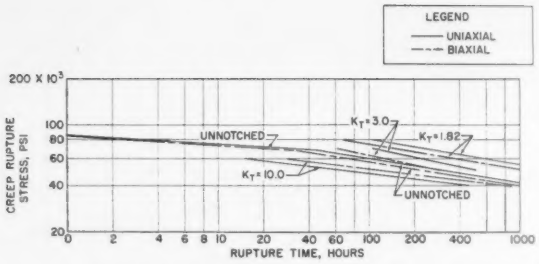

Fig. 17. Predicted biaxial creep strength of notched and unnotched A-286 at 1,200°F.

general, result in earlier failures than those predictable.)

Overaging

When load-carrying capacity is critically dependent upon a precipitation-hardened heat-treat condition, high sensitivity to time at temperature results. It has been conclusively demonstrated[15] that the greatest errors in predicting the time to failure exist when the component has been exposed to more time at temperature than accounted for, and that these errors increase with increasing temperatures.

Loss in Ductility

Where loss in rupture ductility results from exposure to cyclic load, fracture occurs prematurely and creep acceleration may be experienced as the result of the formation of microcracks.

Relaxation and Recrystallization

During the load-off or temperature-off portion of the cycle, the material may revert to its original state through the medium of recrystallization or relaxation. This condition is commonly termed *recovery*. Upon reapplication of load or temperature, the creep rate will be greater than that experienced previously.

Intergranular Oxidation or Corrosion

This factor intensifies the thermal cycling effect by the formation of surface notches which propagate across the section, yielding reduced ductility and accelerated failure.

Design Considerations

These considerations will be presented in two parts. The first reports the analytical procedures for calculating the rupture time and required tank wall thickness for a specific, but simplified, problem. The second discusses, in a general manner, the design complexities introduced by practical problems and suggests methods for their solution.

Eq. (24) relates the time to failure for a pressurized cylinder to that of a uniaxial specimen fabricated of the same material and tested at the same temperature. If it is further assumed that this relation is valid for fractures which occur at fractions of the theoretical value, the procedure for calculating the rupture time of a cylinder is as follows:

(1) Calculate the initial hoop stress $\sigma_c (\sigma_c = pa/t)$.

(2) Determine the time to rupture $\theta_{\sigma_{\text{uniaxial}}}$ from a conventional creep-rupture test for a stress equal to σ_c.

(3) Compute the time to rupture for the cylinder using Eq. (24).

Note that this approach is based on the premise that failure, for both the cylinder and the uniaxial specimen, occurs at the same percentage of the theoretical creep-rupture time.

The required cylinder wall thickness, for a given design life and constant pressure and temperature, may be obtained from Eqs. (18), (19), and (24) by the following procedure:

(1) Calculate $\theta_{\sigma_{\text{uniaxial}}}$ from Eq. (24).

(2) Determine the allowable stress σ_c for the critical uniaxial time from conventional, uniaxial creep-rupture data.

(3) Compute the required cylinder wall thickness from $t_{\text{req.}} = pa/\sigma_c$.

This analysis is based on the assumption that, if Eq. (23) correctly predicts the time to creep rupture for the uniaxial specimen, then Eq. (18) or (19) correctly predicts the rupture time of the cylinder. In addition, the method presumes that the exponent n is the only significant material parameter relating uniaxial creep rupture to stress rupture under combined stresses.

As already noted, the analytical approach is applicable, in the strictest sense, to isothermal steady-load creep. Attempts have been made to extend these relations to intermittent conditions by replacing the steady load with a periodic function of definite form. The ability to correlate such extensions with test data has been limited primarily because intermittent creep depends on the condition of the material and on the previous history of applied loads and temperatures, as well as on the present operating temperature and stress level. Also, as was implied previously, intermittent loading normally accelerates metallurgical changes, and such conditions add to the complexity of the problem.

Another of the problems encountered in design is that occasioned by the local stress discontinuities existing in the region of the head to shell juncture. While the tank heads do not experience the full magnitude of the cylinder temperature rise, for elliptical heads the stress levels are greatest in this area. Thus it is possible that local bulging due to creep may be encountered if the temperature and time at temperature are sufficiently high. If the region is in compression, as is the case for elliptical heads of moderate aspect ratio, then the phenomenon of creep buckling may be experienced. On the other hand, for peak tensile areas, the rate of creep is rapidly increased inasmuch as the creep rate is exponentially related to the stress level, and early failure due to creep rupture may result. This prob-

lem requires experimental checking before a decision regarding its importance can be made.

An additional problem which demands consideration is the effect of stress concentrations such as welding, reinforcing rings, etc., on the magnitude of creep deformations at failure. Recent creep deformation studies[15] applied to airframe design indicate that failure at extremely small overall creep strains is possible for structures with stress concentrations of this type. Creep deformation limits for pressure vessels are likely to be even more stringent in view of the nature of failure due to crack propagation.

Further, the effect of operating propellant tanks at elevated temperatures capable of initiating creep is that accelerated corrosion and stress-corrosion rates can occur. The importance of these factors is a function of the life expectancy of the tanks. For nonexpendable aircraft, these conditions may well specify the type of material to be employed in the tank construction. Although the creep strains per flight may be small, the accumulated creep strains from many flights can become significant. Accompanying these strains are residual stresses which remain and continue to increase throughout the tank life. Thus, if the contained propellants or the atmosphere in which the tank operates is corrosive, these effects must be suitably accounted for in the design.

The incremental amounts of creep experienced during each cycle of loading may be manifest in another combined failure mechanism—namely, that due to creep fatigue—and this is particularly applicable to that portion of the tank wall not wetted by fuel. The simultaneous introduction of cyclic thermal and mechanical stresses when the wall temperatures are sufficient to initiate creep will propagate creep fatigue. At present, no method capable of predicting failure under these conditions exists, nor are the test data necessary to verify any proposed theory available.

Conclusions and Recommendations

This paper has reviewed the design implications of creep in pressurized cylindrical shells. In general, it has been found that there is a negligible amount of the elevated temperature experimental information necessary for verification of the proposed theory.

To extend and refine existing methods of analysis, the following recommendations for future studies are made.

The proposed method for the prediction of creep in integral pressure vessels has been shown to provide relatively good agreement with the limited test results available. This method should therefore be further verified by the performance of tests on tank structures in an environment in which creep is experienced. Such tests should determine burst pressure, time to failure, and strain at failure for various materials, types of construction, and temperature levels. A comparison of the test data with those predicted by theory should then be made. If reasonable agreement is not obtained, the theory should be modified to predict the experimental results more accurately. It is expected that these modifications would be empirical at first, and then based upon more complicated theoretical formulations of the problem. In particular, the effects of notches, welds, and rivet holes on the creep strain at failure should be ascertained.

Further studies, both experimental and analytical, should be directed toward determining the effect of thermal stresses upon the amount of creep experienced in a pressurized vessel. The importance of this aspect of strength analysis has been indicated by the magnitude of thermal stress experienced by aerodynamically heated integral fuel tanks.[1]

Upon completion of a flight, a system of residual stresses may be introduced by the creep strains experienced. Inasmuch as these strains are cumulative, buckling or permanent distortions may eventually result and impair tank operation after sufficient numbers of flight cycles. Thus, methods for the prediction of the residual stresses arising from creep are required for the estimation of incipient failure times.

To limit the number of tests, as well as reduce the time required to perform these tests, efforts should be directed toward determining load-temperature histories which are accelerated representations of the actual environmental conditions. These test environments should conservatively simulate the actual operational conditions and their effects on pressure vessel strength. The degree of conservatism in this method of approach should be determined by testing.

Additional study recommendations have been briefly presented in the report section dealing with design considerations, and as such will not be repeated here. Finally, while no specific recommendations regarding the metallurgical processes attendant upon creep are proposed, it is recognized that it is impossible to be completely divorced from such processes. Indeed, studies on this level may be the only way to provide a complete understanding of the problem at hand.

References

[1] Rattinger, I., and Gallagher, R. H., *An Investigation and Design Study for Fuel Stowage in High-Performance Aircraft*, WADC TR-59-18, May 1959.

[2] Narasimhamurthy, P., *An Analytical Investigation of Creep Under Combined Loadings*, Aircraft Engineering, Vol. 29, No. 345. Nov. 1957.

[3] Marin, J., and Pao, Y. H., *A Theory for Combined Creep Stress-Strain Relations for Materials with Different Properties in Tension and Compression*, Proc. of 1st U.S. National Congress of Applied Mechanics, June 1951.

[4] Pao, Y. H., and Marin, J., *An Analytical Theory of the Creep Deformation of Materials*, Journal of Applied Mechanics, Vol. 20, June 1953, pp. 245–252.

[5] Marin, J., *Engineering Materials;* Prentice-Hall, Inc., New York, 1952.

[6] Nadai, A., *Theory of Flow and Fracture of Solids;* McGraw-Hill Book Co., Inc., New York, 1950.

[7] Saks, H., Wiseman, C. D., Sherby, O. D., and Dorn, J. E., *Effect of Stress on Creep at High Temperatures,* Journal of Applied Mechanics, Vol. 24, June 1957, pp. 207–213.

[8] Hoff, N. J., *The Necking and the Rupture of Rods Subjected to Constant Tensile Loads,* Journal of Applied Mechanics, Vol. 20, March 1953, pp. 105–108.

[9] Kooistra, L. F., Blaser, R. U., and Tucker, J. T., Jr., *High Temperature Stress Rupture Testing of Tubular Specimens,* Trans. of ASME, Vol. 74, 1952, pp. 783–792.

[10] Tucker, J. T., Jr., Coulter, E. E., and Kooistra, L. F., *Effect of Wall Thickness on Stress Rupture Life of Tubular Specimens,* ASME Paper No. 59-MET-11, 1959.

[11] Davis, E. H., *Creep Rupture Tests for Design of High Pressure Steam Equipment,* ASME Paper 59-MET-14, 1959.

[12] Voorhees, H. R., Sliepcevich, C. M., and Freeman, J. W., *Thick-Walled Pressure Vessels,* Industrial and Chemical Engineering, Vol. 48, No. 5, 1956, pp. 872–881.

[13] Kennedy, C. R., Douglas, B. A., and Harns, W., *Multi-Axial Creep Studies on Inconel at 1500°F,* Trans. of ASME, Vol. 81, 1959, pp. 599–609.

[14] Voorhees, H. R., and Freeman, J. W., *Sixth Progress Report to Materials Laboratory, WADC, on Notch Sensitivity of Aircraft Structural and Engine Alloys,* Univ. of Michigan Report No. 2475-20-P, Jan. 1958.

[15] Padlog, J., and Schnitt, A., *A Study of Creep, Creep-Fatigue, and Thermal-Stress-Fatigue in Airframes Subject to Aerodynamic Heating,* WADC TR No. 58-294, July 1958.

✦ ✦ ✦

Base Flow (Continued from page 29)

At low-pressure levels, it is clearly seen that the flow in the center of the missile base proceeds smoothly downstream. In this operating range, the nozzle exhausts act as ejectors and force atmospheric air from the outside into the base region (Fig. 2).

At high altitudes, the flow pattern is drastically changed. A part of the exhaust gases no longer proceeds in the direction of the main rocket exhaust but flows backward toward the base and from there in a four-spoke fashion radially outward into the atmosphere (Fig. 3).

The cause for the observed phenomena can be readily understood when the rocket exhaust jet boundaries are considered. At low altitudes—for instance, at 10,000 ft.—the rockets exhaust downstream without interference and, as expected, produce some ejector effect (Fig. 4). At high altitudes, the exhaust jets expand to the lower atmospheric pressure and, consequently, impinge upon each other (see contours for 50,000 and 100,000 ft. in Fig. 4). Because of jet interaction and the formation of shock waves and the resulting pressure rise, some exhaust gases in the mixing zone are forced back toward the base, producing a flow pattern as shown schematically in Fig. 5. At sufficiently high altitudes, the jet expansion becomes so large that the center base area is completely enclosed by the exhaust jets forming a confined space. This space is then vented to the surrounding atmosphere only through the gaps between the rockets.

(2) Pressure Distribution Over Base

The pressure over the base of the model was surveyed and some results are given in Fig. 6 for various test altitudes. At the low altitude of approximately 61,000 ft., the base pressure is nearly uniform, with only a slight pressure rise at the base center. The slight pressure rise indicates that only a slight interference between the individual exhaust jets occurs. At higher altitudes, the center pressure rises rapidly. For example, at 72,000 ft. altitude, the center pressure is approximately 1.25 times the external atmospheric pressure; at 88,000 ft., the pressure is 2.8 times the external pressure. It is obvious that the high pressure in the base center forces some exhaust gas to flow through the gaps between the rockets to the outside (Figs. 3 and 5). The exhaust velocity between the individual rockets reaches sonic speed since the pressure ratio of 2.8, observed at the test altitude of 88,000 ft., is definitely above the critical pressure ratio of 1.77 for choked flow with $\gamma = 1.20$.

As soon as critical conditions are reached, further increases of the altitude will have no effect on the pressure distribution in the base area because of the choking phenomenon. To show this relationship, peak base pressure and ambient pressure are plotted in Fig. 7 as ratios of the rocket chamber pressure. For altitudes up to approximately 60,000 ft. (hot rocket chamber pressure of 500 psi), the pressure in the confined space is nearly equal to the pressure in the surrounding air. At an altitude of approximately 80,000 ft., the pressure ratios reach critical values. Above 80,000 ft. up to outer space (absolute vacuum), the pressure between the rockets retains a constant value. At these high altitudes, the supercritical pressure ratio forces the air to stream outward at sonic velocities through the gaps between the rockets.

A comparison of some hot rocket and cold rocket models is also shown in Fig. 7. The correlation between the cold-flow and the hot-flow test results is very good, indicating that, when the correct simulation laws are applied to cold-flow tests, reliable information on the flow parameters of hot rocket exhausts can be obtained.

(3) Heat Flux Into the Base Surfaces

The hot rocket exhaust gases forced back toward the missile base produce high-pressure flux into the base area. The heat flux is very intense at high altitudes where the backflow and outward radial flow reach sonic velocities. Hot rocket tests were conducted which, at high altitudes, resulted in the heat flux pattern presented in Fig. 8. It was found that in the center base area, particularly at the fully choked conditions at 100,000 ft. altitude, a seriously

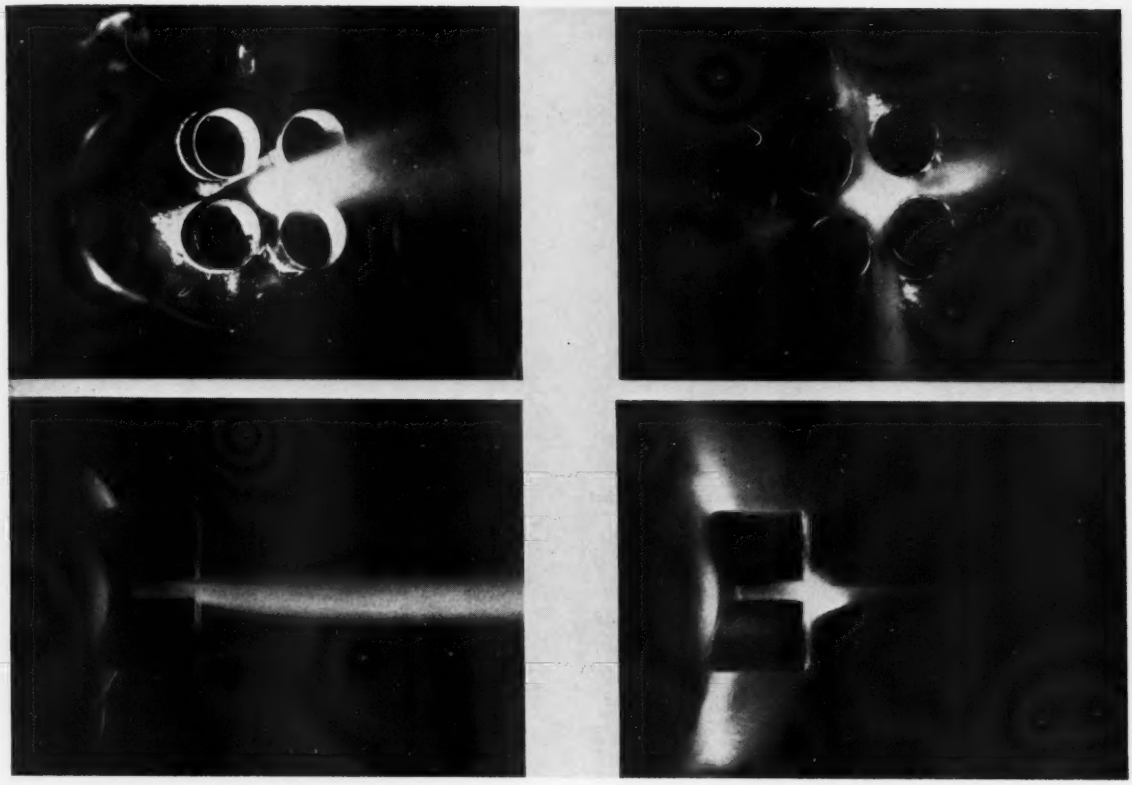

Fig. 2 (*left*). Four-nozzle configuration (cold air) at low altitude. Fig. 3 (*right*). Four-nozzle configuration (cold air) at high altitude.

high heat flux occurs which, however, quickly disappears as soon as the exhaust backflow passes through the gap between the rockets.

(4) One Rocket Not Firing

The results of special cold and hot model tests indicated conclusively that the high heat flux into the missile base is caused not by radiation from the luminous hot exhaust gases but by the backflow of the rocket exhaust gases transmitting heat into the base, primarily by high-velocity convection. In these experiments, one of the rocket exhausts was inoperative so that exhaust gases were discharged only through three of the four nozzles. Under these conditions, the confinement of the gases in the space in between the rocket exhausts is greatly reduced because the exhaust gases can now discharge not only through the narrow gaps between the rockets but also across the inoperative rocket. As expected, the pressure build-up in the base center does not occur, and, consequently, the heat flux into the base is very much lower. The maximum heat flux is not

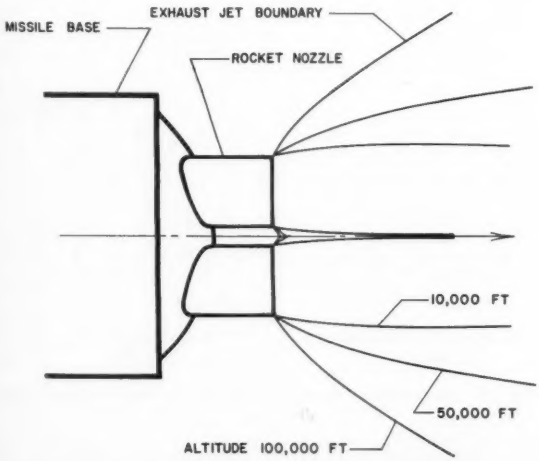

Fig. 4. Rocket jet boundaries at various altitudes.

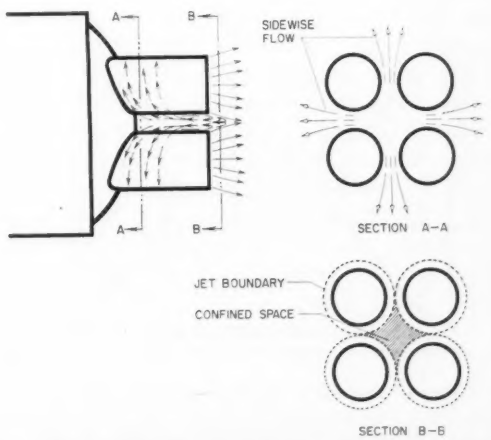

Fig. 5. Sidewise flow and confined space between rocket exhausts.

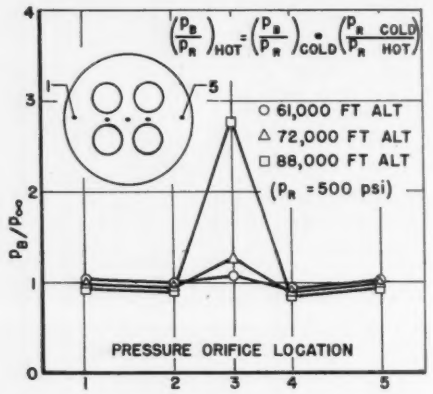

Fig. 6. Base pressure distribution at various altitudes corrected to hot flow conditions.

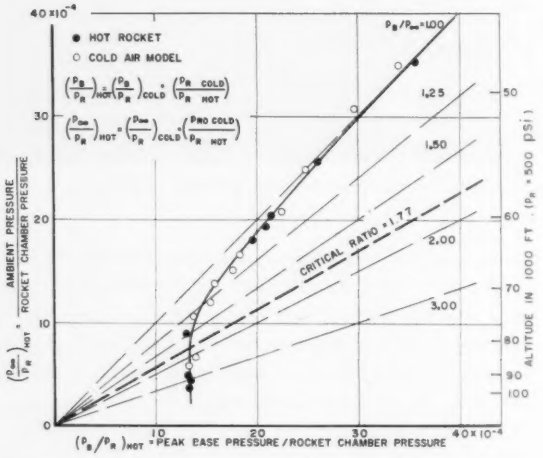
HOT ROCKET
COLD AIR MODEL
$\left(\frac{p_B}{p_R}\right)_{HOT} = \left(\frac{p_B}{p_R}\right)_{COLD} \left(\frac{p_R\ COLD}{p_R\ HOT}\right)$
$\left(\frac{p_\infty}{p_R}\right)_{HOT} = \left(\frac{p_\infty}{p_R}\right)_{COLD} \left(\frac{p_{R\infty}\ COLD}{p_R\ HOT}\right)$
p_B/p_∞ = 1.00
1.25
1.50
CRITICAL RATIO = 1.77
2.00
3.00
$\left(\frac{p_\infty}{p_R}\right)_{HOT}$ = AMBIENT PRESSURE / ROCKET CHAMBER PRESSURE
ALTITUDE IN 1000 FT (p_R = 500 psi)
$(p_B/p_R)_{HOT}$ = PEAK BASE PRESSURE / ROCKET CHAMBER PRESSURE

Fig. 7. Peak base pressure ratio as a function of ambient pressure ratio for hot rocket model and cold air rocket model.

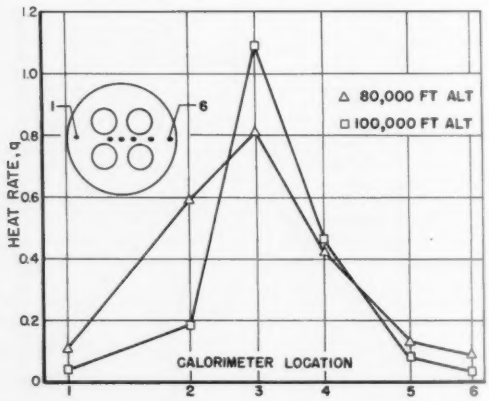

Fig. 8. Heat flux at missile base at various altitudes.

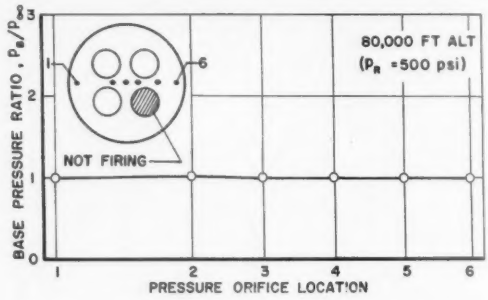

Fig. 9. Base pressure distribution with only three rockets firing.

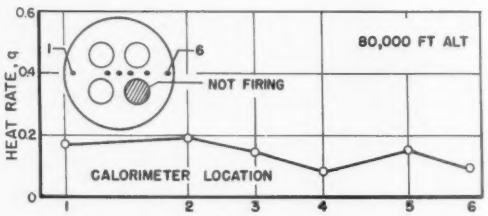

Fig. 10. Heat flux at missile base with only three rockets firing.

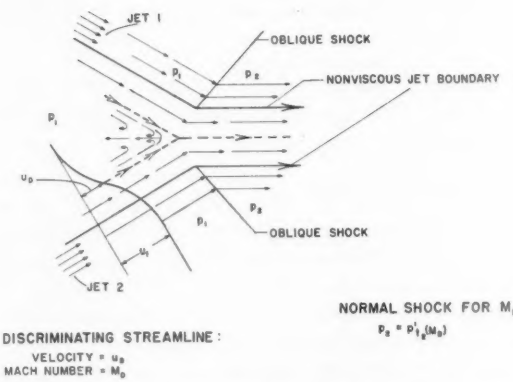

Fig. 11. Sketch of flow pattern for two jets impinging upon each other.

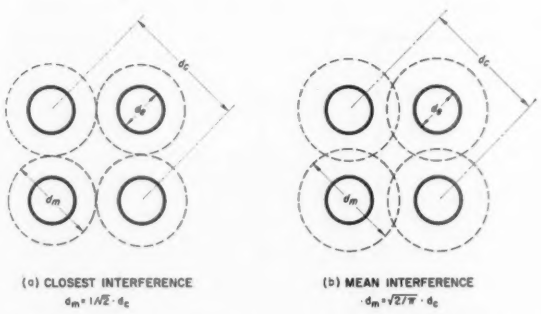

Fig. 12. Comparison of different assumptions for effective interference diameter d_m.

larger than 17 per cent of the peak flux occurring with all four nozzles operating (Figs. 9 and 10).

In summary, the cold-flow experiments indicated that a drastic reversal of the base flow pattern occurs in the operation of ring cluster nozzles. At low altitudes, cold air (ambient) will be forced into the base, producing cooling effects. At high altitudes, hot exhaust gases are forced back toward the base, discharging radially outward. Whereas in the first case a cooling effect of the base is produced because of the base flow, a severe heating of the base occurs when at high altitude the exhaust gases proceed toward the base and outward with sonic and supersonic velocities. For each cluster-nozzle configuration, a critical altitude exists at which the reversal from cold air inflow to hot exhaust gas backflow into the base area occurs. At another characteristic altitude, the hot exhaust radial outflow reaches choking conditions so that above this altitude, up into outer space, the base flow characteristics remain unchanged.

In Section II some theoretical calculations are presented which were used to determine the critical altitudes for base flow reversal, as well as for the conditions producing choking of the exhaust flow.

(II) Method of Calculation of Exhaust Flow Parameters

(1) Exhaust Contours

The exhaust contours of the individual jets were determined according to the approximate method developed by E. K. Latvala.[2] Experiments have shown that this approximate method indicates reasonably well the exhaust contour of rocket exhausts over a wide range of Mach number, nozzle area ratio, and nozzle exit angle.

(2) Base Pressure

The base pressure was determined according to the theory of Korst and Chow.[3] This method is based on an approximate calculation of the velocity profile for the mixing zone of a supersonic exhaust jet discharging into still air. This method is derived for two-dimensional flow. However, it is expected that a reasonably close approximation can also be obtained in axially symmetric cases in which the radius of the exhaust jet does not differ greatly from the radius of the nozzle exit. Since primarily only the overall trends of the flow pattern and the critical altitudes for cluster nozzles will be determined, the above simplification should be satisfactory.

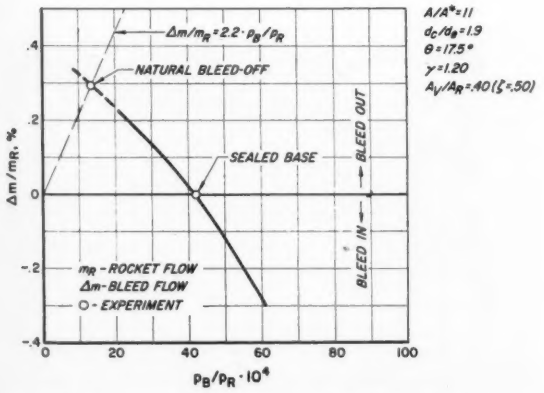

Fig. 13. Comparison between experiment and theory for four-nozzle cluster (choked base vent).

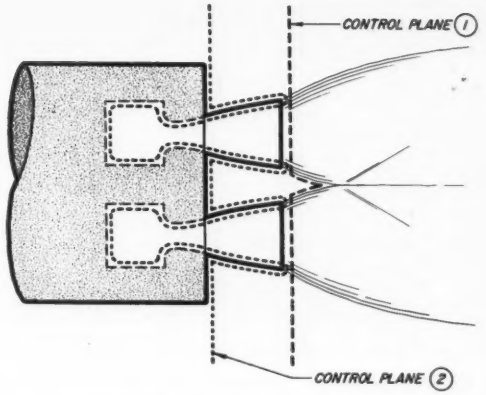

Fig. 14. Control planes for thrust determination by use of momentum equations.

The method of Korst determines the velocity profile in the mixing layer:

$$u/u_1 = (1/2)(1 + \text{erf}\ \eta)$$

where

$$\text{erf}\ \eta = \frac{2}{\sqrt{\pi}} \int_0^\eta e^{-\beta^2}\, d\beta$$

At the impingement of two jets, an oblique shock is produced. The intensity of this shock wave is determined from the flow conditions in the main jet—that is, at the boundary of the mixing layer. A discriminating streamline can be determined from the requirement that the flow along this streamline can build up a pressure equal to the pressure behind the oblique shock in the main stream, by forming first a normal shock, followed by isentropic subsonic compression to velocity zero. The flow farther inward from this discriminating streamline will be capable of proceeding downstream in the main exhaust. The flow outward from the discriminating streamline, however, can build up pressures which are smaller than the pressure downstream of the oblique shock and which, consequently, must turn back toward the base (Fig. 11). The velocity and pressure along the discriminating streamline and the amount of flow turning back toward the base are determined by means of charts provided in reference 3.

In the case of a cluster-nozzle exhaust, the exhaust gases impinge upon each other along an intersection line which is similar to the intersection of two cones. Along the intersection line, the impingement angle

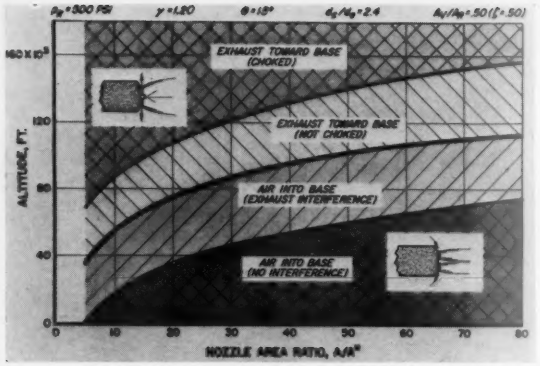
EXHAUST TOWARD BASE (CHOKED)
EXHAUST TOWARD BASE (NOT CHOKED)
AIR INTO BASE (EXHAUST INTERFERENCE)
AIR INTO BASE (NO INTERFERENCE)
ALTITUDE, FT.
NOZZLE AREA RATIO, A/A*

Fig. 15. Regions of exhaust patterns for four-nozzle cluster as function of nozzle area ratio.

varies, and consequently the discriminating streamline also shifts position. In order to simplify the calculations, the assumption was made that one characteristic impingement point exists which controls the entire flow pattern. This characteristic impingement point was selected as the point where the rocket exhausts are closest to each other—that is, the point where the impingement angle has its maximum value (Fig. 12a). As an alternative, it was also considered that the planes of the actual intersection were converted into circular intersections with a constant impingement angle in such a manner that the area described by the straight intersection lines and that described by the circles are equal (Fig. 12b). From model tests it was found that the first assumption yields closer correlation—that is, the largest impingement angle occurring between the jets appears to control the flow. Unless otherwise stated, all the results presented in the following paragraphs and figures referred to are based on this assumption. It should be noted that the alternate assumption will yield somewhat smaller base pressures and, therefore, shift the critical altitudes slightly to higher altitudes.

The method for calculating the base pressure makes use of the fact that the base pressure is determined by the mixing profile occurring in the boundary zone of the jet. The theory in its simplest form assumes that the mixing layer starts with thickness zero at the nozzle exit. This assumption is definitely not correct in actual flow since in the exhaust nozzle a boundary layer builds up along the internal nozzle walls so that a low-energy layer similar to a mixing layer already exits at the nozzle exit. In order to take this effect into consideration, the effective starting point of the mixing layer was assumed to be located not at the nozzle exit but at a certain distance upstream. This distance was determined from tests with typical configurations; in these cases the total momentum deficiency thickness of the nozzle boundary layer was made equal to the momentum deficiency of a fictitious turbulent mixing layer with the starting point upstream of the nozzle exit. As a further simplification, it was assumed in the following calculations that the upstream shift of the effective starting point of the turbulent mixing zone was equal for all nozzle configurations considered—that is,

$$\Delta x/d_e = 1.4\,[1 - (1/\sqrt{A/A^*})]$$

This assumption is naturally not correct. However, it is expected that sufficiently accurate results can be obtained with this extremely simplified assumption since only approximate values of base pressure and trends for the characteristic altitudes are determined in this report.

The following equations were used in the calculations.

Mass flow per unit width between outer edge of the mixing layer and a streamline:

$$G = I_1\left[\frac{1 - (u_1/u_{1max})^2}{\sigma}\right](\rho_1 u_1)\,(x + \Delta x)$$

The velocity u_1 is the undisturbed velocity outside of the mixing layer and is a direct function of the isentropic expansion of the exhaust gas from the chamber pressure p_R to the base pressure p_B.

Mass flow to be removed (per unit width) between the outside of the jet and the discriminating streamline:

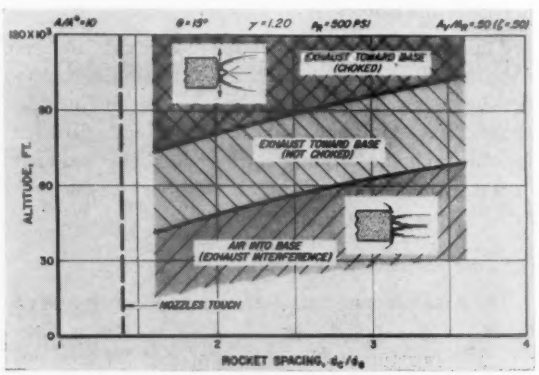

Fig. 16. Regions of exhaust patterns for four-nozzle cluster as function of rocket spacing.

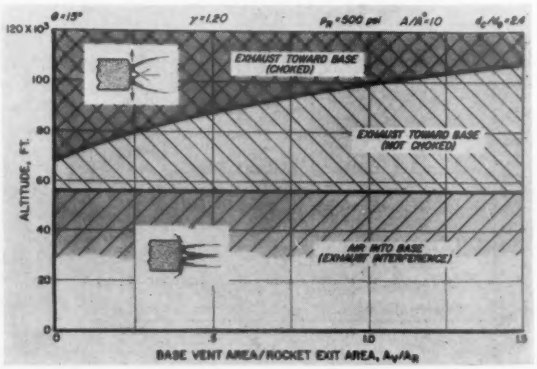
EXHAUST TOWARD BASE (CHOKED)
EXHAUST TOWARD BASE (NOT CHOKED)
AIR INTO BASE (EXHAUST INTERFERENCE)
ALTITUDE, FT.
BASE VENT AREA/ROCKET EXIT AREA, A_v/A_R

Fig. 17. Regions of exhaust patterns for four-nozzle cluster as function of base vent area.

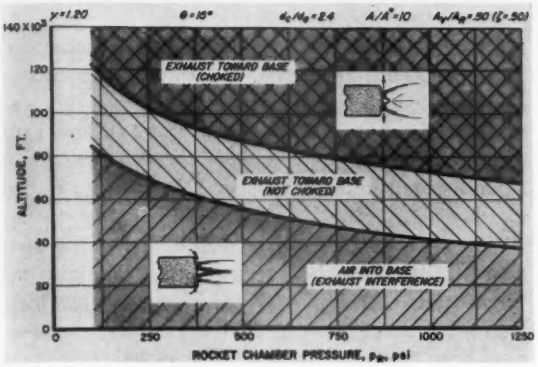
EXHAUST TOWARD BASE (CHOKED)
EXHAUST TOWARD BASE (NOT CHOKED)
AIR INTO BASE (EXHAUST INTERFERENCE)
ALTITUDE, FT.
ROCKET CHAMBER PRESSURE, p_R, psi

Fig. 18. Regions of exhaust patterns for four-nozzle cluster as function of rocket chamber pressure.

$$\Delta G = (I_{1_D} - I_{1_j}) \left[\frac{1 - (u_1/u_{1_{max}})^2}{\sigma} \right] (\rho_1 u_1)(x + \Delta x)$$

The values I_1 and I_{1_j} are listed in the charts of reference 3.

Total mass flow removed (4 rockets):

$$\Delta m = (\Delta G)L$$

$$= \pi (I_{1_D} - I_{1_j}) \times \left[\frac{1 - (u_1/u_{1_{max}})^2}{\sigma} \right] (\rho_1 u_1) \left(\frac{d_m}{d_e} \right) \left(\frac{x + \Delta x}{d_e} \right) d_e^2$$

Relative mass flow removal ratio:

$$\Delta m/m_R = (I_{1_D} - I_{1_j}) \times \left[\frac{1 - (u_1/u_{1_{max}})^2}{\sigma} \right] \left(\frac{\rho_1 u_1}{(\rho_1 u)_e} \right) \left(\frac{d_m}{d_e} \right) \left(\frac{x + \Delta x}{d_e} \right)$$

Assuming various values for the base pressure p_B, the free jet velocity u_1 and the mass flow removal $\Delta m/m_R$ can be determined. For a typical example, the obtained mass flow removal curve is represented in Fig. 13. The larger the mass flow removal from the base area, the smaller the base pressure p_B in the confined area between the exhaust jets. At very low base pressures, the theory of reference 3 becomes unreliable. In this region, the curve was extrapolated as indicated in Fig. 13.

(3) Mass Flow Through Base Vent Area

The mass flow for choked flow through the vent area A_V can be obtained from simple calculations:

$$\Delta m/m_R = \left(\frac{\zeta A_V}{A_R} \right) \left(\frac{A_e}{A^*} \right)_R \left(\frac{p_B}{p_R} \right)$$

where ζ is the flow coefficient of the bleed flow through the vent area. In view of the very uneven distribution and the extensive turning of the flow from an axial to a radial direction, the flow coefficient was assumed to be $\zeta = 0.5$ for all configurations investigated. For the case represented in Fig. 13, the relationship for the bleed flow is then

$$\Delta m/m_R = 0.5 \times 0.40 \times 11 \, (p_B/p_R) = 2.2 \, (p_B/p_R)$$

The bleed flow curve according to this equation is a straight line which intersects with the characteristic mixing flow curve at a point of mass flow removal $\Delta m/m_R = 0.29$ per cent and a base pressure ratio of $p_B/p_R = 13.5 \times 10^{-4}$. The agreement with the experiments is extremely good. However, it should be noted that this case was selected as one of the reference cases used for determining the flow coefficient ζ and the effective impingement point of the jets.

Various values for the base vent area A_V/A_R were introduced into the calculation presented in the following figures. In the case of those curves for which the rocket spacing ratio d_c/d_e was varied, the base vent area was varied directly proportionally to the confined area between the rockets in the exit plane—that is,

$$A_V/A_R \sim (2/\pi)(d_c/d_e)^2 - 1$$

(4) Thrust Increase

It is remarkable that a thrust increase is produced by the increase of the base pressure, even though part of the rocket exhaust flow is not discharged in the normal downstream direction but is turned in the opposite direction toward the base. Calculations based on the application of the momentum balance between the two reference planes (shown in Fig. 14) indicate that the relative thrust increase in case of true radial discharge of the rocket bleed flow in vacuum is

$$\frac{\Delta T}{T_R} = \left(\frac{1}{4_{c_T}} \right) \frac{P_B}{P_R} \left(\frac{A_e}{A^*} \right)_R \left[\frac{2}{\pi} \left(\frac{d_c}{d_e} \right)^2 - 1 \right]$$

(5) Heat Transfer in the Base Area

In the case of turbulent flow which can reasonably be expected in the base area, the heat flux per unit area q will be proportional to the pressure to the 0.8th power. This is true both for the conditions at the stagnation point as well as for the conditions

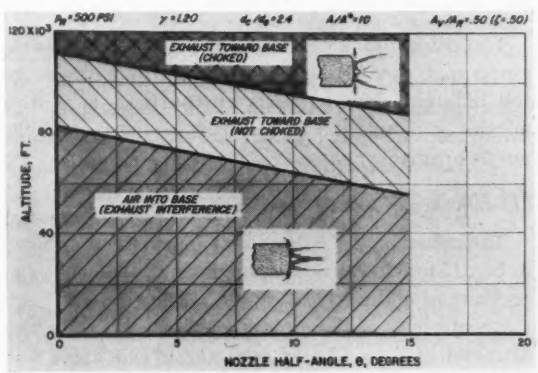
EXHAUST TOWARD BASE (CHOKED)
EXHAUST TOWARD BASE (NOT CHOKED)
AIR INTO BASE (EXHAUST INTERFERENCE)
ALTITUDE, FT.
NOZZLE HALF-ANGLE, θ, DEGREES

Fig. 19. Regions of exhaust patterns for four-nozzle cluster as function of nozzle exit angle.

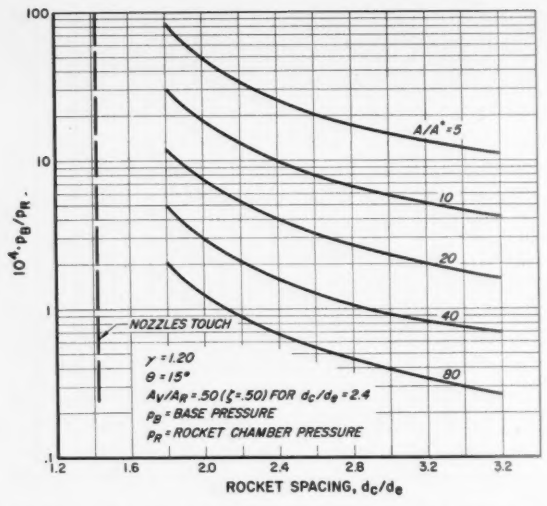

Fig. 20. Base pressure ratio for four-nozzle cluster (choked base vent). (a) As function of nozzle area ratio and rocket spacing.

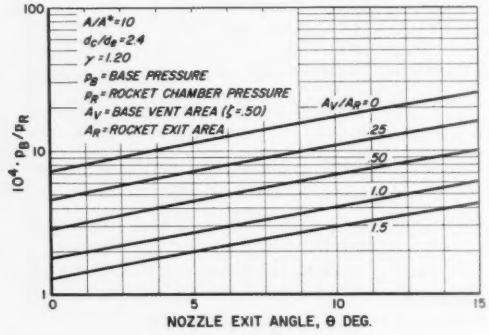

Fig. 20 Concluded. (b) As function of base vent area and nozzle exit angle.

at the throat areas with sonic velocities. The pressure term is the only remaining factor when the total temperature is the same and when the overall geometry of the rockets and the base is similar. In order to indicate the relative magnitude of the heat flux, the values of $q/p^{0.8}$ have been calculated and plotted in the following figures with respect to an arbitrarily selected reference point.

(III) Altitude Ranges for Various Base Flow Patterns

The calculations described in the preceding paragraph were used to determine the altitude ranges for the different flow patterns at the base of cluster nozzles as a function of the base geometry and the nozzle operating characteristics.

(1) *Influence of Nozzle Area Ratio*

The influence of the nozzle expansion ratio is shown in Fig. 15 for cluster nozzles operating with a chamber pressure of 500 psi ($\gamma = 1.20$). The circle through the centerlines of the nozzles was assumed to have a diameter of $d_c = (2.4)\ d_e$, the nozzle exit angle $\theta = 15°$, and the total vent area of the base to the surrounding atmosphere $A_V/A_R = 0.50$ with $\zeta = 0.50$.

First, the altitudes are indicated at which the individual nozzles begin to interfere with each other. At the selected geometry, this condition occurs at sea level at a nozzle area ratio of 5 and shifts to an altitude of approximately 35,000 ft. at an area ratio of 20. At altitudes below this line, air will be drawn from the outside over the base into the rocket exhaust.

When the altitude is increased above this first characteristic line, the interference of the individual exhaust jets causes a rise of the base pressure which, in turn, results in a reduction of the flow of atmospheric air into the base area. At a definite critical altitude, the interference between the individual exhaust jets and the base pressure rise becomes so large that the flow of atmospheric air into the base is completely stopped. At altitudes above this critical line, backflow of hot rocket exhaust gases toward the base is developed. This critical altitude line is located, for instance, at 35,000 ft. at an area ratio of 5, rises to 56,000 ft. at an area ratio of 10, and to 75,000 ft. at an area ratio of 20, etc.

If the altitude is further increased, the backflow of hot gases toward the base gains intensity until finally the base vent area is choked. At altitudes above this critical line to outer space, unchanged base pressure and backflow conditions exist. The altitude line for choked vent flow is located at 68,000 ft. for a nozzle expansion ratio of 5, at 87,000 ft. for an expansion ratio of 10, and at 107,000 ft. for a ratio of 20, etc.

In summary, it can be stated that for all nozzle clusters of the indicated geometry, the different flow patterns described occur through the altitude scale—that is, altitude regions with atmospheric air flow into the base as well as altitude regions with reversed exhaust gas flow toward the base. The characteristic altitudes rapidly increase when the nozzle expansion ratio is increased at otherwise unchanged geometry and operation parameters.

(2) *Influence of Other Cluster-Nozzle Parameters*

In the same manner as for the nozzle area ratio, the influence of other typical cluster-nozzle parameters was examined with respect to the critical altitudes at which inflow of atmospheric air into the base area stops and backflow of hot exhaust gases toward the missile base starts. Also, the altitudes at which the backflow reaches choking conditions in the vent areas were determined.

It was found that increasing the spacing of the individual nozzles (Fig. 16) and increasing the vent area (Fig. 17) lead to an increase of the critical altitudes. On the other hand, increase in the rocket chamber pressure (Fig. 18) and in the nozzle exit angle (Fig. 19) leads to rapid lowering of the critical altitude lines. For example, at a rocket chamber pressure of 1,000 psi, the critical altitude line between inflow of atmospheric air and backflow of hot exhaust gases is shifted to an altitude as low as

41,000 ft., and choked bleed flow conditions occur at an altitude of 73,000 ft.

These graphs make it possible to estimate, for a wide range of cluster-nozzle parameters, the altitudes at which inflow of atmospheric air into the base area occurs, as well as the altitudes at which recirculation of hot exhaust gases and choked conditions in the base vent areas are produced.

(IV) Base-Pressure Ratio, Heat Flux Into the Base, and Thrust Increment

(1) Base-Pressure Ratio

In a more general form, the results of the preceding calculations can be presented as ratios of the base pressure versus the rocket chamber pressure for the various parameters involved. Because of the special significance of the base flow pattern with choked-exhaust backflow, the base-pressure ratios for choked base vent conditions are shown in Figs. 20a and 20b. For a wide range of the cluster parameters—such as nozzle expansion ratio, rocket spacing, nozzle exit angle, and base vent area—the base-pressure ratio can be determined from these figures and the critical altitudes calculated.

(2) Heat Flux Into the Base

With the base pressure known and altitudes assumed high enough to establish choked flow conditions, the heat flux into the base can be estimated as shown previously in Sect. II, 5 (Figs. 21a and 21b). It is apparent that for close rocket spacing d_c/d_e = 1.8 and small nozzle area ratio of 5—for instance, the heat flux into the base is five times larger than that which occurred under the reference conditions. Taking into account, moreover, that at reference conditions heat flux values of 50 B.t.u./ft.^{2}/sec. and even more have been measured, it is apparent that, for such a geometry, the protection of the base area against excessive heating presents a serious problem.

(3) Base-Thrust Increment

In addition to the detrimental effects of the interference of the individual exhaust jets on backflow and base heating, the interference of the jets increases the total thrust of the cluster-nozzle arrangement. The exhaust interference produces higher base pressures and, consequently, thrust increments as indicated in Sect. II, 4. For some typical arrangements, the base thrust increment in relationship to the total rocket thrust is shown in Figs. 22a and 22b. For average venting of the base area (A_V/A_R = 0.50), thrust increments of 0.3 to 0.6 per cent are produced for area ratios varying from 5 to 20. If the base vent area is decreased and the nozzle exit angle increased, the thrust increment rises to approximately one per cent for a typical arrangement with a nozzle expansion ratio of 10. Although these thrust values are generally of no great significance,

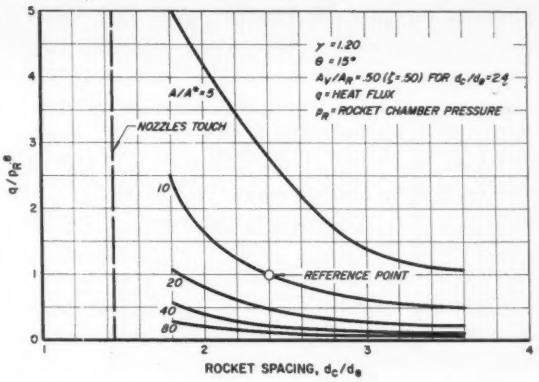

Fig. 21. Heat flux into base for four-nozzle cluster (choked base vent). (a) As function of nozzle area ratio and rocket spacing.

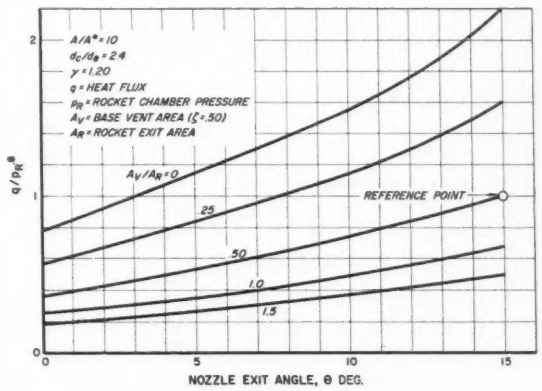

Fig. 21 Concluded. (b) As function of base vent area.

they nevertheless represent a beneficial effect large enough to merit consideration.

(4) Thrust Increments of Base Shrouds

Thrust increments several times larger can be produced by adding a cluster shroud than with plain cluster bases. At the same time, the heat flux into the base can be substantially reduced.

By adding a suitable shroud, the same interference is produced at the shroud walls as at the impingement line of adjacent rocket exhausts. When, for the benefit of simplicity of the theoretical calculation, a square shroud is assumed, the thrust increments are four times as large as indicated for the case without shroud and a vent area of A_V/A_R = 0. The equalization of the pressure in the shroud area (Fig. 23) eliminates the strong detrimental backflow of hot exhaust gases toward the missile base.

Some tentative calculations were conducted for various area ratios and rocket spacing (Fig. 24). It is shown that the thrust increases in vacuum, estimated by the preceding theory, are of the order of 4 to 8 per cent for nozzle expansion ratios of 5. Such values of thrust increments definitely deserve a more detailed consideration.

It should be kept in mind that experimental verification of the previous theoretical results is

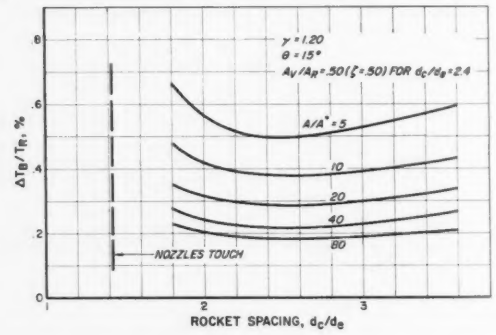

Fig. 22. Base thrust increment for four-nozzle cluster in vacuum (a) As function of nozzle area ratio and rocket spacing.

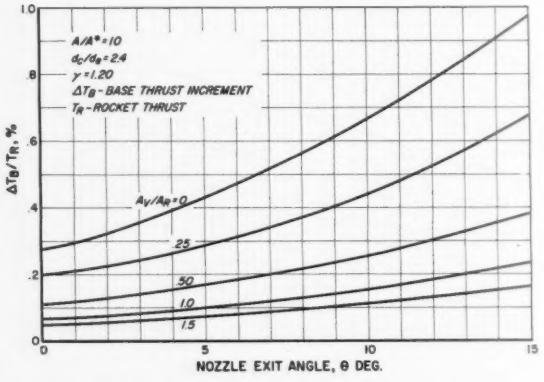

Fig. 22 Concluded. (b) As function of base area vent and nozzle exit angle.

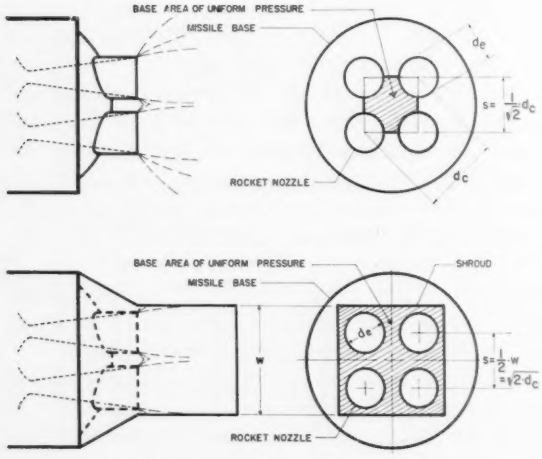

Fig. 23. Sketch of base without and with shroud. (Top) Missile base without shroud showing area of uniform base pressure. (Bottom) Missile base with square shroud.

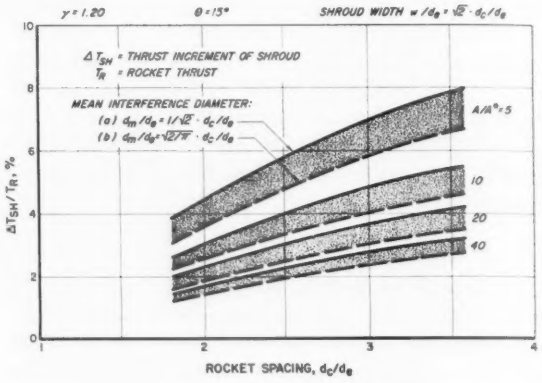

Fig. 24. Shroud-thrust increment for four-nozzle cluster as function of nozzle area ratio and rocket spacing (in vacuum).

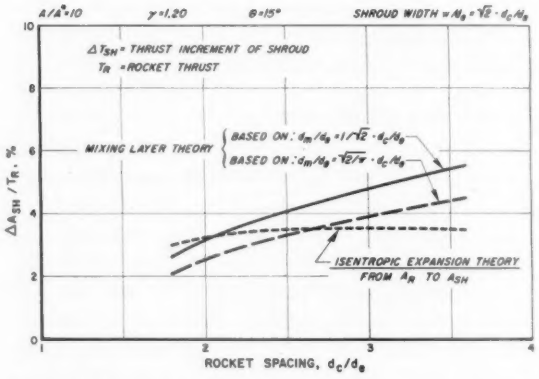
A/A* = 10
γ = 1.20
θ = 15°
SHROUD WIDTH w/de = √2 · dc/de
ΔTSH = THRUST INCREMENT OF SHROUD
TR = ROCKET THRUST
MIXING LAYER THEORY
BASED ON: dm/de = 1/√2 · dc/de
BASED ON: dm/de = √2/π · dc/de
ISENTROPIC EXPANSION THEORY FROM AR TO ASH
ΔASH/TR, %
ROCKET SPACING, dc/de

Fig. 25. Comparison for shroud-thrust increments of four-nozzle cluster calculated with different theoretical assumptions (in vacuum)

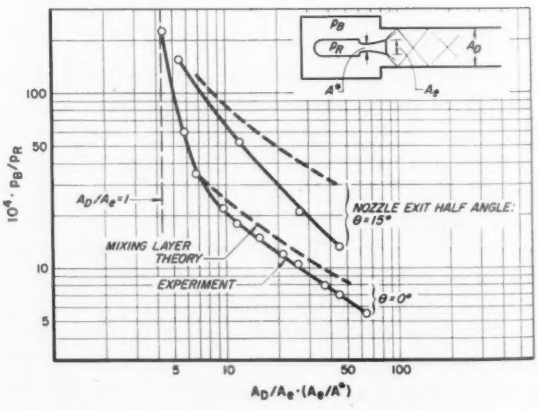

Fig. 26. Comparison between theory and experiment for single-nozzle exhaust diffuser (see reference 5 for experiments).

known only for a few cases with the small rocket spacing of approximately $d_c/d_e = 2$. The thrust increments associated with rocket spacing of $d_c/d_e = 3$ and above are greatly extrapolated so that the thrust increments in this range may have been overestimated. In order to obtain a lower limit for the thrust increments, completely independent calculations were conducted based on the results of a large number of tests with both full-scale and model rockets exhausting into exhaust diffusers.[4] These test results indicate that the base pressure is approximately equal or somewhat larger than the pressures which correspond to one-dimensional isentropic expansion of the rocket exhaust gases from the chamber to the area of the exhaust shroud. For cluster rockets with area ratio of 10, the thrust increments caused by the addition of shrouds have been calculated on the basis of the mixing layer theory discussed above and on the basis of the one-dimensional isentropic expansion theory which is believed to be conservative (Fig. 25). It is apparent that, with either assumption, thrust increments of significant magnitude are obtained. However, depending upon the extrapolation method applied, there is a noticeable difference between the results obtained. Further experiments are being conducted to obtain more precise information on the attainable thrust increments of shrouded cluster nozzles.

(5) Comparison Between Theory and Experiments for Single Nozzles With Shroud

Since no systematic experimental results are available at the present time to check the theoretical calculations, a test series with single-nozzle exhausts surrounded by a circular shroud is cited here. These experiments with nozzles having an expansion ratio $A/A^* = 4.23$ were conducted to obtain information on exhaust diffuser effectiveness.[5] The base pressures were calculated according to the method of Sect. II, 2, of this report for nozzle exit angles of $\theta = 0°$ and $\theta = 15°$. The results indicate good agreement between theory and experiments for the nozzle exit angle $\theta = 0°$ (Fig. 26). At $\theta = 15°$, the curves deviate from each other with increasing exhaust diffuser diameter. Based on these experiments, the preceding calculations for cluster nozzles and shrouds may be expected to indicate with sufficient accuracy the trends of the effects investigated.

(V) Conclusion

(1) Model experiments and theoretical calculations show that with ring cluster nozzles several different base flow patterns exist which vary in type with altitude. In the low-altitude range, atmospheric air is sucked into the base area, producing a cooling effect at the base. At high altitudes, the interference among the individual nozzle exhausts forces hot gases to flow backward toward the base, causing high heat flux into the vehicle base. At sufficiently high altitudes, the base area is completely enclosed by the strongly expanding exhaust jets, and, because of choking, the backflow pattern as well as the heat flux into the base remain unchanged above the critical altitude up into the outer space.*

(2) For several cluster-rocket geometry-and-operation parameters, the altitude ranges for the different base flow patterns of ring cluster nozzles are determined by calculations. In particular, the critical altitudes for flow reversal from atmospheric air flowing into the base to hot exhaust gases flowing back toward the base are determined.

It is shown that for each ring cluster-nozzle arrangement such a critical altitude exists. The critical altitude moves upward to higher altitudes when the expansion ratio of the nozzles is increased, when the chamber pressure is reduced, and when the rocket spacing is increased.

(3) Comparative values for the heat flux into the vehicle base are determined.

(4) The backflow of hot exhaust gases toward the base, occurring at high altitudes, produces small thrust increments which have been calculated and presented in graphs.

(5) By addition of a suitable shroud around the rocket exhausts, noticeable thrust increases can be obtained as shown by theoretical calculations and some exploratory experiments. Also, the base heating should be significantly reduced by a shroud because of the absence of large pressure differences which could lead to large recirculating velocities under the shroud.

References

[1] Goethert, B. H., and Barnes, L. T., *Some Studies of the Flow Pattern at the Base of Missiles with Rocket Exhaust Jets*, AEDC-TR-58-12. (Originally published in Oct. 1958, to be reissued as unclassified and nonproprietary.)

[2] Latvala, E. K., *Spreading of Rocket Exhaust Jets at High Altitudes*, AEDC-TR-59-11, June 1959.

[3] Korst, H. H., and Chow, W. L., *Compressible Non-Isoenergetic Two-Dimensional Turbulent ($P_{r_t} = 1$) Jet Mixing at Constant Pressure*, Univ. of Illinois, Engineering Experiment Station, ME Tech. Note 392-4, Jan. 1959.

[4] Barton, D. L., and Taylor, D., *An Investigation of Ejectors Without Induced Flow—Phase I*, AEDC-TN-59-145, AD 229860, Dec. 1959.

[5] Foster, R. M., *The Supersonic Diffuser and Its Application to Altitude Testing of Captive Rocket Engines*, AFFTC-TR-60-1, Jan. 1960.

* The influence of altitude on base heating is very different for straight-line arrangements of the rocket nozzles (the Atlas configuration, for example). In the case of these configurations, the base heating is mainly produced by afterburning of fuel-rich exhaust gases in the atmospheric air. Consequently, the most severe heating problem of such configurations occurs at *low and medium altitudes*. At high altitudes, the base heating problem is greatly reduced or entirely eliminated because of lack of atmospheric oxygen and therefore nonexistence of afterburning.

IAS PAPERS

Twenty-Ninth Annual Meeting, New York, January 23-25, 1961*

IAS MEMBER PRICE—$0.50, NONMEMBER PRICE—$1.00

61-1 Sandwich Construction for Primary Structure of Ballistic Missiles and Space Vehicles—Ralph F. Foral

61-2 Design Procedures for Structures Under Non-uniform Temperature Distribution. I. Axial Loads and Bending Moments—B. E. Gatewood and R. W. Gehring

61-3 Experimental Investigation of Lithium Hydride and Water Absorbers as Possible Heat-sink Materials for Hypersonic and Reentry Vehicles—R. O. Hickel, R. P. Cochran, C. R. Morse and R. P. Dengler

61-4 Optimum Design of Integral Fuselage Propellant Tanks for Use in High Performance Aircraft—Ivan Rattinger, Alexander Krivetsky and Richard H. Gallagher

61-5 Change of Satellite Orbit Plane by Aerodynamic Maneuvering—Howard S. London

61-6 Determination of the Lift or Drag Program that Minimizes Re-entry Heating with Acceleration or Range Constraints Using a Steepest Descent Computation Procedure—A. E. Bryson, W. F. Denham, F. J. Carroll and K. Mikami

61-7 Variation of Parameters for Near Circular and Low Inclination Orbits—Samuel Pines

61-8 Asymptotic Expansions of the Solutions of the Equations of Motion in the Earth-Moon Space—A. Zukerman

61-9 Guidance Error Analysis of Satellite Trajectories—Harold S. Braham and Lionel J. Skidmore

61-10 Preliminary Comparison of Air and Ground Launching of Satellite Rendezvous Vehicles—T. N. Edelbaum

61-11 Analysis of the Vertical Floating (Hydra) Launch of Rocket Vehicles—J. E. Draim and C. E. Stalzer

61-12 Corrosion Problems Encountered in Silo Storage of Missiles—Leo E. Gatzek

61-13 Thermal Stresses in the Bending of Ogival Shells—C. N. De Silva

61-14 Stresses and Deformations of the Thin-walled Pressurized Torus—Peter F. Jordan

61-15 General Formulas for Influence Coefficients for Thin Spherical Shells—Nicholas J. Hoff

61-16 A Criterion for Dynamic Buckling of Shallow Shells under Uniform Impulsive Loading—John S. Humphreys and Sol R. Bodner

61-17 On the Design of Hypersonic Aircraft—Hans Multhopp

61-18 Space Cooling Procedures—Martin Macklin

61-19 General Considerations for Satellite Attitude Control Systems—John S. White and James S. Pappas

61-20 Liquid Behavior in a Zero-G Field—Ta Li

61-21 Application of Inequality Constraints to Variational Problems of Lifting Re-entry—Ely S. Levinsky

61-22 On the PLK Method and the Supersonic Blunt Body Problem—Roberto Vaglio-Laurin

61-23 Viscous and Inviscid Non-equilibrium Gas Flows—Robert J. Whalen

61-24 Elements of Solar Collector Design—D. L. Dresser

61-25 Variation of Rotor Dynamic Response by Self-contained Mechanical Feedback—G. J. Sissingh

61-26 Helicopter Tire Design to Control Mechanical Instability—Robert Jones

61-27 Future Performance Capabilities of Rotary Wing VTOL Aircraft—Paul J. Carpenter

61-28 An Experimental Investigation of Stall Flutter—Norman D. Ham

61-29 An Investigation of Improved Flying Qualities for Tandem Rotor Helicopters—John A. DeTore

61-30 Bending Vibrations of a Perforated Grain Solid Propellant Rocket During Powered Flight—Sidney Birnbaum

61-31 Unsteady Aerodynamic Forces on Slender Supersonic Aircraft With Flexible Wings and Bodies—John E. Yates and E. F. E. Zeijdel

61-32 The Response of Linear Systems to Inhomogeneous Random Excitation—M. Botman

61-33 Development of a Quasi-Steady Approach to Flutter and Correlation of Quasi-Steady and Kernel Function Flutter Analyses—S. I. Gravitz, W. R. Laidlaw, W. W. Bryce and R. E. Cooper

61-34 Propeller-Nacelle Whirl Flutter—John C. Houbolt and Wilmer H. Reed, III

61-35 Trajectory Considerations for Circumlunar Missions—William H. Michael Jr., and Jack W. Crenshaw

61-36 The Trajectories and Some Practical Guidance Considerations for Rendezvous and Return—John M. Eggleston

61-37 Pilot Control of Rendezvous—M. C. Kurbjun, R. F. Brissenden, E. C. Foudriat and B. B. Burton

61-38 Project Transit, Earth and Aerospace Navigational Satellite System—John D. Nicolaides

61-39 New Developments in the Design of Model Reference Adaptive Control Systems—P. V. Osburn, H. P. Whitaker and A. Kezer

61-40 The Electrical Properties of the Air Around a Reentering Missile or Spacecraft—Glen F. Pippert and S. Edelberg

61-41 The Hydrodynamic Characteristics of High Speed Hydrofoils—Virgil E. Johnson, Jr., and Marshall P. Tulin

61-42 Aircraft Techniques Applied to Submarines—Joseph D. Malloy

61-43 Hydrodynamic Factors in Submarine Design and Their Relationship to Aerodynamics—Robert K. McCandliss

61-44 Hydrofoils at the Crossroads—J. J. Stilwell, P. W. Nelson and W. R. Porter

61-45 Some Design Problems of Hovercraft—R. Stanton Jones

61-46 A Conceptual Nuclear Propulsion System For Ground Effect Machines—J. C. Westmoreland, J. B. Dee and J. E. Loos

61-47 GEM Design Philosophy for an Over-Water, Over-Ice Vehicle—Olle Ljungstrom

61-48 Ground Effect Machine Propulsion System Design Consideration—L. W. Norman

61-49 A Study of Manned Nuclear-Rocket Missions to Mars—S. C. Himmel, J. F. Dugan, Jr., R. W. Luidens and R. J. Weber

61-50 Combustion Instability in Liquid Propellant Rockets—A Review—R. B. Lawhead

61-51 Launch-Vehicle Recovery Techniques—C. A. Lysdale

61-52 Propulsion Systems for Laminar Flow Aircraft—J. W. Connors, W. Pfenninger and C. B. Smith

61-53 Helicopter Instrument Certification—H. H. Hermes and Charles M. Seibel

61-54 East Coast FAA Helicopter Operations—Frederick Freeman

61-55 Development of Navy Helicopter Instrumentation—L. S. Guarino

61-56 Army-Navy Instrumentation Program—Rotary Wing Phase—Neil E. Welter

61-57 The Application of Satellites for Commercial Communication Purposes—Leonard Jaffe

61-58 Commercial Applications of Satellite Boosters—Beardsley Graham

61-59 The Satellite Vehicle for Communications—H. M. Wittner and W. J. Roths

61-60 Study of VTOL Control Requirements During Hovering and Low-Speed Flight Under IFR Conditions—W. J. Klinar and S. J. Craig

61-61 Aerodynamics of Deflected Slipstreams—A. Sowyrda

61-62 A New Look at V/STOL Flying Qualities—R. C. A'Harrah and S. F. Kwiatkowski

61-63 Flight Test Experience With the XV-3 Low-Disc-Loading V/STOL Aircraft—C. E. Davis and R. L. Lichten

61-64 Nuclear Rocket Stages Increase Saturn's Payload Capability—Willis Y. Jordan, Jr., Donald R. Saxton, and Paul G. Thomas

61-65 Kiwi-A: The First Rocket Reactor Experiment—R. E. Schreiber

61-66 Nuclear Electric Power for Space Missions—Terry W. Koerner and John J. Paulson

61-67 Safety Considerations for Nuclear Power in Aerospace—Joseph A. Connor, Jr.

61-68 The Geocorona—Herbert Friedman

61-69 Preliminary Stability, Control and Handling Criteria for Ground Effect Machines (GEMS)—N. K. Walker

61-70 An Approach to the Operational Features Desirable in a Militarily Acceptable GEM—P. G. Fielding

61-71 Basic Principles of the Stability of Peripheral Jet Ground Effect Machines—Michael C. Eames

61-72 Experimental Research on the Cesium Thermionic Converter—N. S. Rasor

61-73 Thermionic Conversion of Heat to Electricity—W. B. Nottingham, G. N. Hatsopoulos and E. N. Carabateas

61-74 The RIAS Enterprise—A Pattern for the Expansion of Basic Research in the Aerospace Industry—Welcome W. Bender

61-75 The Feasibility of a T.V. Satellite—Louis Pollack

61-76 Economics of Instrumentation Precision for Space Vehicle Development—V. R. Boulton

61-77 Navy Interest in Meteorological Satellites—John F. Tatom

61-78 Tektites and Natural Satellites of the Earth—John A. O'Keefe and Barbara Shute

61-79 Translational Characteristics of Ground Effect Machines—Winston W. Royce and Scott Rethorst

61-80 Design Selection and Performance of a Lifting Fan V/STOL Logistic Transport—E. Kazan and W. Berger

*See page 82 for another IAS publication available.

Order by number from: **Special Publications Dept., IAS, 2 E. 64th St., New York 21, N.Y.**

AEROSPACE ENGINEERING CATALOG

THE STANDARD BUYER'S GUIDE OF THE AEROSPACE INDUSTRY . . . SINCE 1944

If you have either hardware or special engineering and manufacturing capabilities you want the Aviation-Missile Planners and Contractors to know about, AEROSPACE ENGINEERING CATALOG is *the* medium tailored to do the job for you *every day of the year.*

7000 ANNUAL DISTRIBUTION

guaranteed circulation to Planners, Engineers and Purchasing Agents. . . with *constant* "referral readership" by 26,000 Planners and Buyers throughout Government and the Aerospace Industry.

Plan to print 7500 extra copies of your catalog for inclusion in this all-important 1961 issue of . . . AEROSPACE ENGINEERING CATALOG.

Publisher printed pages also available.

For all the facts, contact our nearest sales office listed on page 4.

AEROSPACE ENGINEERING CATALOG
— Established 1944 —
"The Official Buyers' Guide of the Aerospace Industry"

Personnel Opportunities

This section is for the use of individual members of the Institute seeking new connections and eligible organizations offering employment to specialists in the aerospace industry. Any member or eligible organization may have requirements listed without charge by writing to the Secretary of the Institute.

Wanted

Graduate Assistants—Staff Members—University of Kansas, Dept. of Aeronautical Engineering, Lawrence, Kan., has openings for Graduate Assistants and two full-time staff members between now and September 1961, to teach courses in aerodynamics (basic, theoretical, compressible flow, and hypersonics); mechanics of flight (including stability and control, aircraft design, and aircraft dynamics); aircraft structures; wind tunnel and other aeronautical laboratories. Salary and academic rank will depend upon education and experience. Write Ammon S. Andes, Chairman, giving training, teaching interest, starting rank and salary desired. Teaching load will be reduced when staff engages in research. Plans are complete for new building, money is partly appropriated.

101. Missiles Design Engineer—One of the country's leading companies seeks a creative preliminary design engineer with experience to participate and lead in the formulation of new concepts for systems design directed toward proposals. Advanced conceptual state-of-the-art thinking founded on broad base missile structure and design experience is required. Excellent career growth opportunity. Salary in five figures depending on background.

Available

999. British Aeronautical Engineer—Desires to work for United States firm in Europe, business aviation particularly. Twelve years' experience in aeronautical and consulting engineering. Qualified as designer and stressman; management trained at U.S. university; pilot's license. Résumé on request.

998. Aeronautical Engineer—M.S., with some 30 years' background in teaching, industry, and applied research; desires to continue working in the field of subsonic aerodynamics. Also interested in full- or part-time teaching of Russian language, or evaluating and translating scientific paper.

997. Consulting Management Engineer—M.S.M.E.; B.S.M.E.; age 37. Available as private consultant on PERT/PEP computerized management techniques. Successful direct industrial experience in development and application of PERT to portions of the Polaris program; developed new methods of introducing flexibility into cost and budget systems; specific, low-cost methods of adding cost to PERT/PEP. Experienced in solid rocket design, aircraft missile environmental control systems design and development, Air Force R&D management, and facilities planning and construction.

106. Senior Test Engineer—B.S. in A.E.; age 31. Nine years' experience in aerospace fields including design, flight test, and assignment as airborne launch engineer. Five years as flight test supervisor and aeromechanical supervisor participating in more than one hundred missile launchings of various types. Broad experience covering rockets, turbojets, ramjets, aerodynamics, structures, electronics, and parachute systems. Desires supervisory or staff position with a new and growing test organization located away from big cities in the western states. Résumé on request.

105. Aeronautical Engineer—B.A.E., M.S.E.; age 37. Seventeen years' experience in missile, airplane, helicopter, and VTOL aerodynamics. Eight years in development, four as project aerodynamicist; and nine in applied research and teaching in charge of prime sponsored programs. Desires responsible technical direction position in industrial or university research. Complete résumé on request.

104. Management Consultant—Specialist in systems management, analysis, and organization. Extensive background in corporation long range planning and diversification. Academic, industrial, and military background encompass M.S.A.E., M.B.A. candidate, USAF weapon system project officer, and 10 years experience in aerospace industry principally in the management of missile and space systems. Associate Fellow IAS, Senior Member IRE. Desires part time consulting activities. Fee schedule and résumé upon request.

103. Senior Mechanical Engineer—B.S. and M.S. in M.E., 17 years experience in design, specifications, with strong emphasis on heat transfer, thermal expansion for reliability. Heat exchanger calculation; forecasting schedules, administering funds, etc., on a project basis. Registered Professional Engineer in Massachusetts. Résumé on request.

102. Aeronautical Engineer—B.S. in M.E., M.S. in Aeronautics; age 30. Three years experience in research, system analysis for space application. Familiar with foreign markets and languages. Desires challenging position in international department, overseas assignment preferred. Résumé upon request.

100. Mathematician—Age 25; B.Sc.; good background in theoretical fluid mechanics and automatic computing; seeks position for September 1961. Full details on request.

The number preceding the notice represents the Box Number of the Institute of the Aerospace Sciences to which inquiries should be addressed.

A word about our Advertisers

The many companies whose advertising appears in this issue are interested in you and your work. They are anxious to let you know what they are doing to help you solve research and design problems in missile, rocket, air, and spacecraft projects.

AEROSPACE ENGINEERING'S advertising pages keep you posted on new and improved materials, components, services, and supplies useful to your professional work.

To request more information on any product or service advertised, may we suggest you write to the *advertiser* directly, at no obligation to you. It would be greatly appreciated if you would mention that you saw the ad in AEROSPACE ENGINEERING.

AEROSPACE ENGINEERING

2 E. 64th St., New York 21, N. Y.

Index to Advertisers

Aerospace Engineering Catalog..... 119

★AiResearch Mfg. Divs., The Garrett Corp..... 33
J. Walter Thompson Co.

American Machine & Foundry Co., Government Products Group..... 5
Cunningham & Walsh, Inc.

Armour Research Foundation..... 67
Roark and Colby Advertising, Inc.

Bendix Corp., The
Eclipse Pioneer Div.....54, 55
Red Bank Div..... 49
Scintilla Div..... 1
MacManus, John & Adams, Inc.

★Douglas Aircraft Co., Inc..... 37
J. Walter Thompson Co.

Eastman Kodak Co..... 35
The Rumrill Co., Inc.

Electronic Communications, Inc..... 61
Alfred L. Lino & Associates

Electronic Specialty Co..... 45
Wallis & Rice Advertising Agency

Electro-Optical Systems, Inc..... 83
Epic Advertising, Inc.

General Motors Corp., Harrison Radiator Div.....back cover
D. P. Brother & Company

Government Products Group, American Machine & Foundry Co... 5
Cunningham & Walsh, Inc.

International Aerospace Abstracts.... 82

Jet Propulsion Laboratory, California Institute of Technology..... 2, 41
Barton A. Stebbins Advertising

Kearfott Div., General Precision, Inc... 65
Gaynor & Ducas, Inc.

Lincoln Laboratory, Massachusetts Institute of Technology..... 53
Randolph Associates

Lockheed Aircraft Corp.
Burbank Division.....inside back cover
Missiles and Space Div..... 6, 7
Hal Stebbins, Inc.

Los Angeles Division of North American Aviation, Inc..... 57
Batten, Barton, Durstine & Osborne, Inc.

Northrop Corp., Radioplane Div..... 63
Doyle, Dane, Bernbach, Inc.

Rocketdyne Division of North American Aviation, Inc.....46, 47
Batten, Barton, Durstine & Osborne, Inc.

Space Technology Laboratories, Inc.....inside front cover
Gaynor & Ducas, Inc.

Sperry..... 43
Reach, McClinton & Co.

U.S. Naval Laboratories in California..... 39
M. Belmont Ver Standig, Inc.

United Technology Corp..... 8
Campbell-Ewald Co.

Wyman-Gordon Co..... 74
The Davis Press, Inc.

★ Specifications and further information on the missile, rocket, and aircraft products of these companies will be found in the 1960 AERO/SPACE ENGINEERING CATALOG

The only publication devoted exclusively to the aerospace industry, this CATALOG serves as a valuable buyers' and reference guide to sources and specifications on aircraft and missile parts and materials. It is distributed annually to Chief Engineers, Designers, Production Heads, and Purchasing Departments of all leading manufacturers of missiles, rockets, aircraft, and spacecraft, and their related components; Government Agencies; Research Organizations; etc.

Published Annually by

INSTITUTE OF THE AEROSPACE SCIENCES

2 East 64th Street • New York 21, N.Y.

NOW UNDER ONE ROOF AT LOCKHEED / BURBANK

Lockheed California Division has expanded its already great resources at Burbank. For it now encompasses, under one roof, the two vast worlds of Spacecraft and Aircraft.

This typifies Lockheed policy to steadily advance the state of the art through basic research in related and scientific fields.

Result? Now—more than ever—Lockheed offers Scientists and Engineers uncommon opportunities; equips them with every modern facility; gives them freedom to explore and express new ideas; makes possible greater individual recognition.

Now being designed and developed in Spacecraft and Aircraft are: Hypersonic interceptors; V/STOL; supersonic interceptors; limocopters; missiles; manned spacecraft; and satellites.

Scientists and Engineers of outstanding talent are now invited to participate in this new, dual enterprise. Immediate openings are available to: Aerodynamics engineers; thermodynamics engineers; dynamicists; electric research engineers; servosystem engineers; electronic systems engineers; biophysicists; infrared physicists; hydrodynamicists; ocean systems scientists; physio-psychological research specialists; mammalian culture research specialists; and radiation hazards specialists.

Write today to Mr. E. W. Des Lauriers, Manager Professional Placement Staff, Dept. 2603, 2415 N. Hollywood Way, Burbank, California.

LOCKHEED

CALIFORNIA DIVISION